RHODES UNIVERSITY

Where leaders learn

Towards an improved understanding of episodic benthic turbidity events (Benthic Nepheloid Layer) on the Eastern Agulhas Bank, South Africa.

Dissertation submitted in fulfilment of the requirements for the degree of

MASTER OF SCIENCE

of

RHODES UNIVERSITY

By

Brett Mordaunt Johnstone

G13J2290

Supervisors:

Prof. W.H.H Sauer (*Rhodes University*); Prof. M.J. Roberts (*Nelson Mandela University*)

Dr A. Shaw (*Skymat Ltd., Southampton, United Kingdom*)

June 2021

DECLARATION

I, Brett Mordaunt Johnstone, hereby declare that the work described in this thesis was carried out in the Department of Ichthyology and Fisheries Science, Rhodes University, under the supervision of Professor W.H.H Sauer and Professor M.J Roberts. This thesis's components comprise original work by the author and have not been submitted to any other university.

Signed: 

Date: 10/05/2022

ACKNOWLEDGEMENTS

Firstly, I would like to acknowledge my supervisors for their unwavering and continued support throughout the entire journey, during what has been an incredibly challenging time in my life. I want to emphasize their patience, understanding, and care during the tough times; without whom this would not be completed. So, thank you Prof Roberts and Prof Sauer, true greats of the game. Furthermore, I would like to thank Andrew Shaw for his mentorship, as well as his technical and conversational skills.

Furthermore, I would like to give a heartfelt thank you to the South African Squid Management Industrial Association (SASMIA) and Bayworld Centre of Research and Education (BCRE) for the monetary contribution which has allowed me to undertake this project. I am forever indebted to the trust you have placed in me. To the National Research Foundation (NRF), I must say a huge thank you to for covering my tuition and living costs over the past two years. Without either of these funders I would not have been able to participate and complete this fantastic study.

I would like to thank all of those from the Sustainable Oceans and Livelihoods through Increase Capacity in Ecosystem research (SOLSTICE) team. I feel very honoured and privileged to have been a part of this fantastic multi-disciplinary study, and for all the opportunities it has given me. To the people of the National Oceanography Centre in Southampton, England, for their hospitality, I would like to extend a huge thank you. Especially to Fatma Jebri for all her help, comments and motivation.

Thank you Jean Githaiga-Mwicigi for allowing and encouraging my position as an observer on the Scientific Squid Management Group, within the Department of Environment, Forestry and Fisheries over the past 5 years.

Finally, I would like to thank my parents for being with me through this journey. I would like to thank my sister for everything she has done for me and everything she has taught me despite her tender years. To my brother, we would not be here without you, so thank you for everything. Furthermore, I would like to thank Mary-Jane Paulsen for her devoted love and support, for being with me every step of the way. And last but not least, Samantha Mannheim, for being my Fish-Friend from day one.

DEDICATION

I would like to dedicate this thesis to my best friend, the bravest and strongest person I know:
My mother.

Without you, mum, I probably would have finished this years ago.

All jokes aside, I am so grateful you are still here with me to see me achieve my dream.

ABSTRACT

The harvest of *Loligo reynaudii,* or "chokka," represents a critical source of revenue and job creation in the historically impoverished Eastern Cape Province of South Africa. Due to the importance of visual stimuli in the reproductive processes, it has been hypothesized that a primary driver of successful reproduction is the clarity of the water column. The presence of increased particulate matter concentrations within the water column generates turbid conditions near the seafloor (visibility < 1m), that are proposed to restrict spawning activity. This benthic nepheloid layer (BNL) contains both organic and inorganic components, with the BNL intensity a function of bottom turbulence, substratum type, and detritus level. However, the spatial and temporal resolution of BNL intensity on the Eastern Agulhas Bank (EAB) and the environmental drivers thereof remain unknown. Here we show that benthic turbidity events are a common but highly variable occurrence on the EAB. Results from a 17-month time-series of *in-situ* and remote sensing data between 2002 – 2004 in Algoa Bay, supplemented by experiments in other bays important for spawning, show that turbid conditions existed for ~ 30 % of the sample period. Exploration of environmental drivers, including the influence of wind, altimeter-derived significant wave height (Hs), sea surface temperature (SST), and chlorophyll-a (Chl-a) concentrations indicate that BNL intensity does not conform to a "one-size-fits-all" approach. Rather, complex local hydrological and physiochemical parameters control the BNL characteristics on the EAB. Global warming is likely to increase the frequency and intensity of extreme westerly-wind and storm events, promoting BNL events on the Eastern Agulhas Bank and possibly causing a shift in the reproductive strategy of chokka squid to the cooler mid shelf region. This is likely to have consequences for both the species in terms of reproductive success and the fishery, which is concentrated on inshore spawning aggregations. Future research needs to quantify and characterize the constituents, source particles and spatial-temporal variability of BNL events in order to build a predictive capacity. Through incorporating the qualitative analysis of the dynamics of nepheloid layers on the EAB into Regional Oceanographic Models (ROMS), General Linear Models (GLM) and particle distribution models such as DELFT-3D, it is possible to move toward predicting the timing and intensity of these events.

Keywords: Benthic Nepheloid Layer, Turbidity, Loligo reynaudii, Fisheries, Oceanography, Remote Sensing, Altimetry, Climate Change

TABLE OF CONTENTS

DECLARATION 2
ACKNOWLEDGEMENTS 3
DEDICATION 5
ABSTRACT 6
TABLE OF CONTENTS 7
LIST OF FIGURES 10
LIST OF TABLES 14
CHAPTER 1 15
1.1 Background 15
1.2 The South African chokka industry 19
1.3 Chokka reproductive strategies 21
1.4 Relationship between chokka and the environment 24
1.5 Aims 30
1.6 Study Approach 31
CHAPTER 2 32
2.1 Review of oceanography and meteorology of the Eastern Agulhas Bank 32
2.1.1 The Agulhas Bank 34
2.1.2 The Agulhas Current and the Eastern Agulhas Bank 35
2.1.3 Upwelling and Primary Productivity 36
2.2 Nepheloid Layers 43
2.2.1 Definitions 43
2.2.2 Ecological impacts of nepheloid layers 46
2.2.3 Global distribution of nepheloid layers 48
2.2.4 Measuring suspended particulate matter (SPM) 51
2.2.5 Nepheloid layer studies in South Africa 53
CHAPTER 3 56
3.1 Study Area 56
3.1.1 The Eastern Agulhas Bank 56
3.1.2 Algoa Bay 58
3.1.3 St Francis Bay 59

3.1.4 Oubos 59
3.2 Algoa Bay Time-Series Experiment 60
3.2.1 Relationship between underwater visibility and turbidity 60
3.2.2 Turbidity 61
3.2.3 Temperature 62
3.3 Wind 63
3.4 Extended-Bay-Experiments 63
3.4.1 November Closed-Season Study, 2002 64
3.4.2 November Closed-Season Study, 2003 64
3.5 Hydrographic Survey 64
3.6 Remote Sensing Data 65
3.6.1 Sea Surface Temperature (SST) 65
3.6.2 Ocean Colour: Chlorophyll-a 66
3.6.3 Altimeter-derived significant wave height (Hs) 67
3.7: Data Analysis 69
CHAPTER 4 70
4.1 Defining underwater visibility, NTUs, and cleaning the *in-situ* mooring data 70
4.1.1 Relationship between underwater visibility and turbidity 70
4.1.2 Data quality corrections of benthic turbidity 72
4.2 The Algoa Bay Time Series Experiment 74
4.2.1 Benthic Turbidity in Algoa Bay 76
4.2.2 Bottom Temperature in Algoa Bay 80
4.2.3 Relationship Between Bottom Temperature and Turbidity 83
4.3 Wind 85
4.4 Altimeter-derived Significant Wave Height (Hs) and Benthic Turbidity Events on the EAB 88
4.5 Extended-Bay-Experiments (EBE) 95
4.5.1 Extended-Bay-Experiment, November 2002 95
4.5.2 Extended-Bay-Experiment, November 2003 109
4.5.3 Highlights of the Extended-Bay-Experiments 114
CHAPTER 5 115
Algoa Bay Time-series Experiment 116
(i) Benthic Turbidity 116
(ii) Bottom Temperature 118

(iii) Wind 120
Extended-Bay-Experiments (EBE) 122
Mechanisms responsible for BNL dynamics 123
(i) Fragmentation of BNL into 'patches' 124
(ii) Resuspension events/Wave-induced turbidity 126
(iii) Temperature-Turbidity Interface 128
Climate change and fisheries management 129
Conclusions and future research 132
List of References: 137
APPENDIX A: 152
APPENDIX B: 15268
APPENDIX C: 15270
APPENDIX D: 15273

LIST OF FIGURES

Fig. 1.1: Annual catch abundance (kg) of the commercially important chokka squid as landed by the hand-jig fishery from 1985 – 2018. The red bars denote years of meagre catches, including the marked drop in catches in 1992, 2001, 2013. Commercial jig catch data are from the South African Bureau of Standards as provide by the industry for the period 1985 – 2006 and the National Regulator for Compulsory Standards from 2007 to 2018 (DFFE, 2020).

Fig. 1.2: (a) Demersal distribution (dots) from DFFE research trawls of adult (females >18 cm; males > 25 cm) chokka on the west coast and the Agulhas Bank of South Africa, (b) chokka biomass on the west coast extends as far as Southern Angola, although the biomass here is lower compared to the Agulhas Bank, (c) commercial hand-jig fishing positions (dots) for chokka indicate commonly used spawning sites traversing the nearshore (< 70 m) coastal region of the Eastern Agulhas Bank. Taken directly from Roberts et al. (2012).

Fig. 2.1: The complexity and variability in the marine environment around South Africa is partly due to the (a) latitude and associated weather and (b) the influence of two contrasting boundary currents, namely the cold Benguela Current on the west coast and the warm Agulhas Current on the east coast. Highlighted in this figure are the complex oceanographic features associated with South Africa. The red box denotes the Eastern Agulhas Bank, and the focus of this study. Adapted from Roberts (2005).

Fig 3.1: Schematic highlighting the variable oceanography of the Eastern Agulhas Bank (A) in comparison to the broadening bathymetry of the Agulhas Bank south-west of Port Alfred (B). The location of Algoa Bay (red), St Francis Bay (green) and Oubos (yellow) mooring locations are evident in both A & B. Schematic A highlights the locations of divergent and wind-induced upwelling hotspots on the EAB in relation to the in-situ instrumentation and weather stations (pink). The dominant south-westerly swells direction is also highlighted in reference to the prominent headlands of the bays on the EAB, namely; Cape St Francis (CSF), Cape Recife (CR) and Cape Padrone (PR). The red line on the left-hand side of **Fig. 3.1 (A)** highlights the location of the hydrographic cruise sampled in November, 2002.

Fig. 3.2: Map showing the position of the Algoa Bay mooring in relation to the prominent headland, Cape Recife, as well as the dominant direction of south-western swell, bathymetry and potential for refraction of swell, wave height and wave period around the point. Other prominent features such as Cape Padrone, Bird Island, Riy Bank and St Croix Island are shown too. Note the convergence of the bathymetric lines near the Cape Recife pinnacle, as well as the position of the Cape Recife temperature recorder (Grey dot).

Fig. 4.1: The frequency of occurrence of underwater visibility (m) based on diver observations (n = 170) between 1992-1999 at the DFFE Monitoring Mooring in St Francis Bay, an important chokka squid spawning ground.

Fig. 4.2: Relationship between benthic turbidity (NTU) and underwater visibility (m) as ascertained through *in-situ* observations by divers. The non-linear relationship is given by the equation f(x), for n = 33. The left panel (1) highlights the relationship between OBS output in mV, comparative Nephelometric Turbidity Units (NTU), and bottom visibility from the study conducted by Dorfler (2002) on bottom turbidity in St Francis Bay between 1999 - 2001. This was incorporated into this study as the same instruments and techniques were used to analyse benthic turbidity. The right panel (2) highlights the

relationship between NTU and bottom visibility as ascertained during the deployment period of this study.

Fig. 4.3: The process of turbidity (NTU) data correction for instances of biofouling during deployment of optical sensors in Algoa Bay, from November 2002 to March 2004. The grey lines demarcate raw bottom turbidity readings, whilst the black lines show corrected bottom turbidity values. The vertical, red-dashed line indicates the date at which a service dive was undertaken.

Fig 4.4: Time-series of variables turbidity (NTU) and temperature (°C) collected in Algoa Bay, at a depth of 25 m, throughout the 17-month study period (08/11/2002 - 12/03/2004). The most significant gap in the data between 21/12/2003 - 08/02/2004 occurred as a result of instrument failure. The green dotted line demarcates turbidity values representative of 1 m of visibility or less. Green boxes denote the 3-Bay & 4-Bay studies of 2002 & 2003, respectively.

Fig. 4.5: Monthly percentage occurrence of benthic turbidity readings (NTU) in the western sector of Algoa Bay over a 17-month sample period between November 2002 and March 2004. The white bars are representative of good underwater visibility, or '*Clear*' conditions (< 5 NTU). The black bars indicate near- '*Black-Out*' turbid conditions on the seafloor (NTU > 15) whilst the grey bars, denoting NTU values of between 5 – 15 NTU, are expressive of periods of elevated concentrations of particulate matter in suspension within the water column, known as '*Turbid*' conditions.

Fig. 4.6: Climatology of benthic turbidity (NTU) in the western sector of Algoa Bay throughout the 17-month sampling period (November 2002 - March 2004). The pie charts indicate the percentage occurrence of turbidity readings. The seasonal sample size (n) is given below each seasonal chart. The white segments are representative of good underwater visibility, or '*Clear'* conditions (< 5 NTU). The black segments indicate '*Black-Out'* turbid conditions on the seafloor (NTU > 15) whilst the grey segments, denoting NTU values of between 5 – 15 NTU, are expressive of periods of elevated concentrations of particulate matter in suspension within the water column, known as '*Turbid*' conditions.

Fig. 4.7: Average daily bottom temperature (A) and monthly averages of bottom temperature in Algoa Bay. The red-dotted line in A and B denote the average bottom temperature over the time-series of 17.64 °C. The blue-dotted lines in (A) indicate standard deviation from the mean, equal to ± 2.78 °C. The error bars in (B) show monthly variation from the mean.

Fig. 4.8: Seasonal average in bottom temperatures (°C) recorded in Algoa Bay between November 2002 and March 2004. Error-bars denote standard deviation from the mean whilst the number of samples (n) are provided in each bar. Red dotted-line shows average bottom temperature throughout the sample period, *17.64 ± 2.78 °C.*

Fig. 4.9: Total percentage occurrence and monthly percentage occurrence of benthic temperatures found in Algoa Bay over the course of 17-months from November 2002 – March 2004. Seasonal percentage occurrence is calculated from 10 238 hourly measurements of bottom temperature (°C).

Fig. 4.10: The relationship between bottom temperature (°C) and episodic benthic turbidity events (NTU) in Algoa Bay. The left-sided panels (A & C) highlight incidents where bottom turbidity events occur in the absence of temperature fluctuations (i.e., upwelling). The right-sided panels (B) highlight occurrences of benthic turbidity events coinciding with the phenomenon of upwelling and when upwelling occurs

without a subsequent increase in benthic turbidity (D). The above figures were extracted from **Fig. C1**, **Fig. C3**, **Fig. C11** and **Fig. C5**.

Fig. 4.11: Monthly mean of bottom temperature (°C) and turbidity (NTU) collected over 17-months from November 2002 - March 2004. Error bars represent standard deviation from the monthly mean. Monthly sample size (n) is apparent above the respective monthly bar. Red-dotted lines denote the average across the timeseries, 17.64 °C and 4.16 NTU, respectively.

Fig. 4.12: Daily averages of Meridional (North/South, V) and Zonal (West/East, U) velocity components over a 17-month time frame from November 2002 - March 2004 at PE International Airport. A seven-day running mean is plotted in red.

Fig. 4.13: Wind Rose highlights wind speed and direction from Port Elizabeth Weather Station (*0035209B1, 63 m above sea level*) between November 2002 and March 2004 (A). Seasonal wind roses are given in B – E. Colour bands indicate wind speed ranges in $m.s^{-1}$. Values around the concentric circles show the percentage of time wind is blowing towards a particular direction, with the longest spikes highlighting the wind direction with the greatest frequency. Wind direction is measured relative to true north.

Fig. 4.14: Spatial - temporal regression analysis between geographically assimilated observations of Hs (m) and benthic turbidity (NTU on the Eastern Agulhas Bank (24 – 28 °E). The geographically partitioned satellite passes are shown in A – E, namely; (A) Algoa Bay, (B) Cape Padrone, (C) Cape Recife, (D) St Francis Bay and (E) Oubos. The results from the regression analysis for Cape Recife as well as the timeseries of Hs recorded for the Cape Recife location are seen at (F) and (G), respectively. Coastal bathymetry is represented by the red, magenta and black lines, denoting the 30 m, 200 m and 2000m isobaths, respectively. Port Alfred (PA), Algoa Bay (ALB, red dot), St Francis Bay (SFB, green dot) and Oubos (OU, yellow dot) are shown.

Fig. 4.15: Monthly climatology of altimeter-derived significant wave height (Hs; m) for Cape Recife (A) and the greater Eastern Agulhas Bank (B). Error bars denote standard deviation from the mean whilst the values within the bars highlight the number of Hs counts per month.

Fig. 4.16: Seasonal climatology of altimeter-derived significant wave height (Hs) for Cape Recife (A) and the entire Eastern Agulhas Bank (B). Error bars denote standard deviation from the mean whilst the values within the bars highlight the number of Hs counts per season.

Fig. 4.17: Representation of the overall wave state as measurements of significant wave height (Hs) on the Eastern Agulhas Bank from data taken from the ESA CCI Sea State L3 Altimetry Product. The data was aggregated into 0.2 km bins and all passes were sampled to highlight the variability of wave conditions experienced on the Agulhas Bank. The inshore coastal zone (3 – 10 km) was compared to the mid-shelf (43 – 50km) as well as the coastal shelf (0 -50km). Distances (km) represent the proximity of the measurement to the coast.

Fig. 4.18: Extended Bay Study of November 2002 displaying hourly observations of bottom temperature (°C, red line) and turbidity (NTU, black line) at three locations traversing the Eastern Agulhas Bank, namely; Algoa Bay (top), St Francis Bay (middle) and Oubos (bottom). Periods of interest discussed in this section are highlighted in the blue dashed-boxes labelled A – D. The green-dashed vertical lines

represent dates between which data were omitted from the study due to biofouling (Algoa Bay) and instrument reaching saturation point (Oubos). No measurements of the benthic environment occurred in St Francis Bay after the 11 December 2002. No adjustments were made to the St Francis Bay turbidity data.

Fig 4.19: Altimeter-derived measurements of significant wave height (Hs, m) for the 2002 Extended-Bay-Experiment. Satellite paths represented here are those closest to the in-situ mooring as described in Chapter 3.

Fig 4.20: Daily OSTIA L3 SST images highlighting the intensity of upwelling on the EAB in the vicinity of the Port Alfred Upwelling Cell (A). A complementary 9-Day composite image of primary productivity (chl-a, $mg.m^{-3}$) on the EAB from the 16 – 22 November 2002 (B). Note the high productivity emanating from Port Alfred and within Algoa Bay.

Fig 4.21: Daily OSTIA L3 SST images highlighting the intensity of upwelling on the EAB (A). (B) a complementary 9-Day composite image of primary productivity (chl-a, $mg.m^{-3}$) on the EAB from the 06 – 14 December 2002 (B). Note the high productivity (as a result of upwelling) in Algoa Bay and St Francis.

Fig. 4.22: Transect of surface to bottom temperature (°C) at six sampling stations during the bi-annual demersal surveys conducted by DFFE on board the 'FRS AFRICANA,' cruise #171, between October – November 2002. This transect was sampled on the 28th of November, 2002.

Fig. 4.23: Transect of surface to bottom turbidity (NTU) at six sampling stations during the bi-annual demersal surveys conducted by DFFE on board the 'FRS AFRICANA,' cruise #171, between October – November 2002. This transect was sampled on the 28th of November, 2002. Note that the CTD stopped ~10 m from the benthos.

Fig. 4.24: Transect of surface to bottom fluorescence at six sampling stations during the bi-annual demersal surveys conducted by DFFE on board the 'FRS AFRICANA,' cruise #171, between October – November 2002. This transect was sampled on the 28th of November, 2002. Note that the lowest values for fluorescence are located inshore near the most intense BNL expression. In contrast, the highest fluorescent values are located further offshore.

Fig. 4.25: Transect of surface to bottom oxygen at six sampling stations during the bi-annual demersal surveys conducted by DFFE on board the 'FRS AFRICANA,' cruise #171, between October – November 2002. This transect was sampled on the 28th of November, 2002. Note that the lowest values for oxygen are located inshore near the most intense BNL expression.

Fig. 4.26: Transect of surface to bottom salinity at six sampling stations during the bi-annual demersal surveys conducted by DFFE on board the 'FRS AFRICANA,' cruise #171, between October – November 2002. This transect was sampled on the 28th of November, 2002.

Fig. 4.27: Extended Bay Experiment of November 2003 displaying hourly observations of bottom temperature (°C, red line), surface temperature at Mangold's Pool (°C, blue dotted line), and turbidity (NTU, black line) at Algoa Bay (top), St Francis Bay (bottom). Periods of interest discussed in this section are highlighted in the grey dashed-boxes labelled E – G.

Fig 4.28: Altimeter-derived measurements of significant wave height (Hs, m) for the 2003 Extended-Bay-Experiment. The figure is divided geographically into satellite paths which are closest to the in-situ mooring using the methods described in Chapter 3.

LIST OF TABLES

Table 1: Summary of spatial-temporal linear regression analysis between altimeter-derived measurements of significant wave height (Hs) and optically-derived measurements of benthic turbidity (NTU). Individual satellite altimeter missions were assimilated based on the ground tracks geographical proximity to one another and the specific sites of interest traversing the Eastern Agulhas Bank (24 – 28 ° E). Regression analysis was performed between spatially aggregated satellite passes and four classifications of temporal means of benthic turbidity surrounding the timing of the satellite pass, namely, Hourly, 6-Hour Mean, 12-Hour Mean, and 24-Hour Mean. The Cape Recife 12-hour NTU mean, highlighted in bold, is used in this study.

CHAPTER 1
Introduction

1.1 Background

The harvest of *Loligo reynaudii* d'Orbigny (1839-41), locally referred to as "chokka," represents the most important cephalopod and third-largest commercial fishery in South Africa (Augustyn et al., 1992a; Cochrane et al., 2014). Since the early 1980s, the coastal hand-jig fishing industry has developed to represent a critical source of revenue and job creation in the historically impoverished Eastern Cape province of South Africa (Augustyn, 1991; Cochrane et al., 2014). The chokka fishery, as with other cephalopod fisheries around the globe (Arkhipkin et al., 2015; Rodhouse et al., 2014), is plagued by inconsistent catch on both annual and intra-annual time scales (Augustyn, 1991; Glazer and Butterworth, 2006; Roel and Butterworth, 2000; Roel, 1998). The variability in apparent abundance (catch) suggests that both the environmental perturbations and the associated cephalopod population responses tend to be distinct and, at times, temporary.

The rapid growth of the commercial chokka fishery from small ski-boats to larger, live-a-board freezer vessels saw an upsurge in reliance of the local workforce on the squid fishery for economic growth and job creation. The fishery now comprises a fleet of ~ 136 boats, encompassing ~ 2 451 fishers supporting an estimated ~ 20 000 people, in what is South Africa's most labour-intensive fishery (Cochrane et al., 2014). Individual chokka fishermen are considered casual employees (Hara, 2009), and their wage structure is principled on a 'pay-per-catch' basis. The going rate is at an average of R5 /kg, with little change over the last decade (Hara, 2009). There is no salary retainer for fishermen involved in the fishery; therefore, periods of "low-to-no" catch mean periods of "low-to-no" income (Cochrane et al., 2014; Roel et al., 2000). The financial pressure brought about by low catches results in an increase in local crime rates (Roel et al., 1998; Roel and Butterworth, 2000). The variability in catch-related income induces socio-economic hardships on the fishers, local communities, industry, and resource

managers alike (Agnew et al., 2002; Cochrane et al., 2014; Hara, 2009; Hill and Agnew, 2002; Popova et al., 2016).

Cephalopods respond to environmental variability either actively, passively, or through a combination of both. Active responses include migrating to areas of more favourable environmental conditions to feed or spawn (Arkhipkin et al., 2015). In contrast, passive responses include differential growth, maturation, and reproductive strategies according to and in conjunction with fluctuating environmental conditions (Brierly et al., 1995; Pierce et al., 2008, 1994). The short life-span and high turnover of generations coupled with differential growth, maturation and spawning strategies is what enables cephalopods to overcome short-term environmental variability (Caddy and Rodhouse, 1998; Rodhouse et al., 2014). However, a tipping point in cephalopod population dynamics may be reached when unfavourable environmental conditions coincide with the overexploitation of the species.

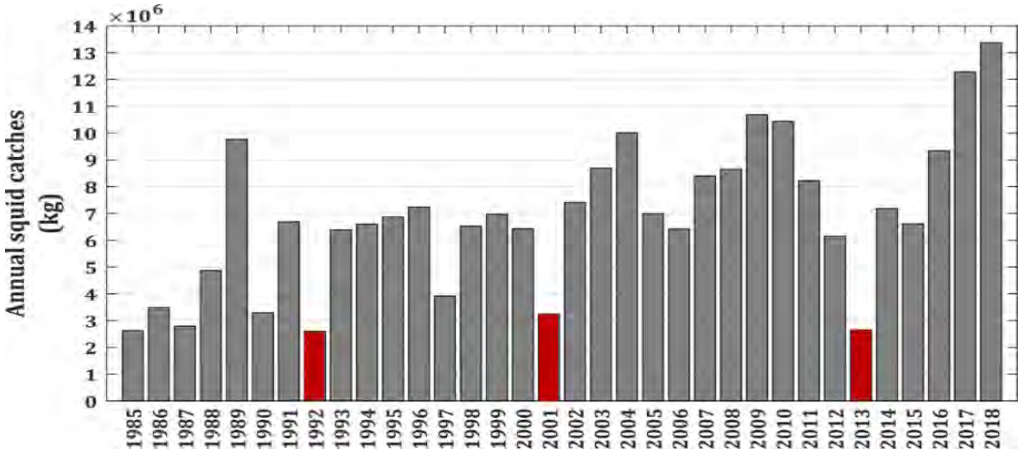

Fig. 1.1: Annual catch abundance (kg) of the commercially important chokka squid as landed by the hand-jig fishery from 1985 – 2018. The red bars denote years of meagre catches, including the marked drop in catches in 1992, 2001, 2013. Commercial jig catch data are from the South African Bureau of Standards as provide by the industry for the

Unpredictable catch presents a severe risk to the sustainability and resilience of the chokka industry. Annual catch demonstrates significant variability over the past 30 years, with apparent abundance fluctuating between 6 000 and 12 000 tonnes per annum (**Fig. 1.1**; DFFE 2020).

Monthly and even daily catch variability is linked to short-term deviations in spawning behaviour in response to abrupt changes in oceanographic conditions (Roberts and Van Den Berg, 2002; Sauer et al., 1992). Annual variability in squid catch may be due to reduced or diverse recruitment into the fishery as a result of the interplay between localized and large-scale environmental forcing mechanisms (Lipiński et al., 2020; Roberts and Van Den Berg, 2002). The alarming "crash" in annual catches in 2013 (**Fig. 1.1**), and the resultant socio-economic consequences on the local fishing community, has led to the need to re-examine the relationship between apparent abundance (catch) and environmental variability in the chokka industry.

Chokka populations are known to form nearshore (< 70 m) spawning aggregations along South Africa's southeast coast (Augustyn, 1991; Roberts et al., 2012), utilizing an environmental niche where conditions are optimal for reproductive success (Oosthuizen and Roberts, 2009; Roberts, 2005, 1998). Although deeper spawning is known to occur toward the edge of the continental shelf (< 270 m, Oosthuizen and Roberts, 2009; Roberts et al., 2012), the coastal jig-fishery primarily targets chokka on the inner-shelf of the Eastern Agulhas Bank (EAB) during spawning aggregations (Augustyn, 1991; Augustyn et al., 1992; Cochrane et al., 2014, DFFE, 2020). Ultimately, inshore catch, and therefore fishermen's income, is concomitant to the formation, quantity, and duration of these nearshore spawning aggregations (Cochrane et al., 2014; Lipiński et al., 2016; Roel et al., 2000; Sauer et al., 1997, 1992).

It is widely accepted by both industry and scientists alike that environmental variability strongly influences chokka spawning aggregations (Roberts, 2005; Roberts and Sauer, 1994; Roel et al., 1998; Sauer et al., 1991). There have been several studies highlighting the sensitivity of spawning aggregations of chokka to environmental perturbations, some of which include the effects of; water temperature (Downey, 2009; Joyner, 2016; Sauer et al., 1991; Singh et al., 2009), wind-driven upwelling (Melo and Sauer, 2007; Sauer et al., 1992), predators (Lipinski and Soule, 2007; Smale et al., 2001), sea swell state (Augustyn et al., 1994; Sauer et al., 2000, 1992a), and physical oceanographic forcing (Githaiga-Mwicigi, 2012; Joyner, 2016; Roberts, 2005, 1998b; Roberts and Sauer, 1994; Schön et al., 2002).

Initial observations by divers on SCUBA of a dense layer of particulate matter limiting visibility over important squid spawning sites brought about the hypothesis that benthic turbidity may be an essential environmental variable influencing spawning behaviour and, consequently, catch abundance (Roberts and Sauer, 1994). Furthermore, local fishermen have long made the association between 'Coca-Cola' coloured water, i.e., turbid water and poor catches (Roberts, pers. comm).

In its simplest form, turbidity is an apparent optical measurement used to describe Suspended Particulate Matter (SPM) concentration within a parcel of water. Turbidity is proportional to the concentration of SPM and, consequently, inversely proportional to the optical/visual clarity of the water column (Agrawal, 2004; McCave, 2019). The concentration of SPM into a distinctive layer within a water medium exhibiting variable light attenuation characteristics is termed a Nepheloid Layer (Boss et al., 2015). Nepheloid Layers' characteristics depend on the physical composition of SPM, water column turbulence, resuspension of sediments, and position relative to the seafloor. The characteristics of nepheloid layers will be discussed in further detail in Chapter 2.

The reliance of cephalopods on visual cues in the courting and reproductive process suggests that chokka require clear, non-turbid, and sufficiently illuminated waters to successfully detect and communicate with potential mates (Hanlon, 1998; Hanlon et al., 1994; Sauer et al., 1997a). Prolonged periods of poor visibility restricting spawning processes can have detrimental consequences to not only catch but overall future recruitment into the fishery (Dorfler, 2002; Roberts, 1998), as spawning chokka are forced out of the favourable inshore spawning grounds (Martins et al., 2010; Melo and Sauer, 2007; Roberts et al., 2012; Smith et al., 2013). Therefore, benthic turbidity, and the resultant Benthic Nepheloid Layer (BNL), is considered an important and understudied factor influencing catch and recruitment into the fishery and is central to the theme of this thesis.

1.2 The South African chokka industry

Adult populations of commercially viable chokka are distributed on the continental shelf from the lower reaches of Angola to Port Alfred on the eastern extreme of the Agulhas Bank (**Fig. 1.2b**). The accumulative results of decades of demersal trawl surveys highlight the widespread distribution of *L. reynaudii* (**Fig. 1.2b**.; Roberts et al., 2012).

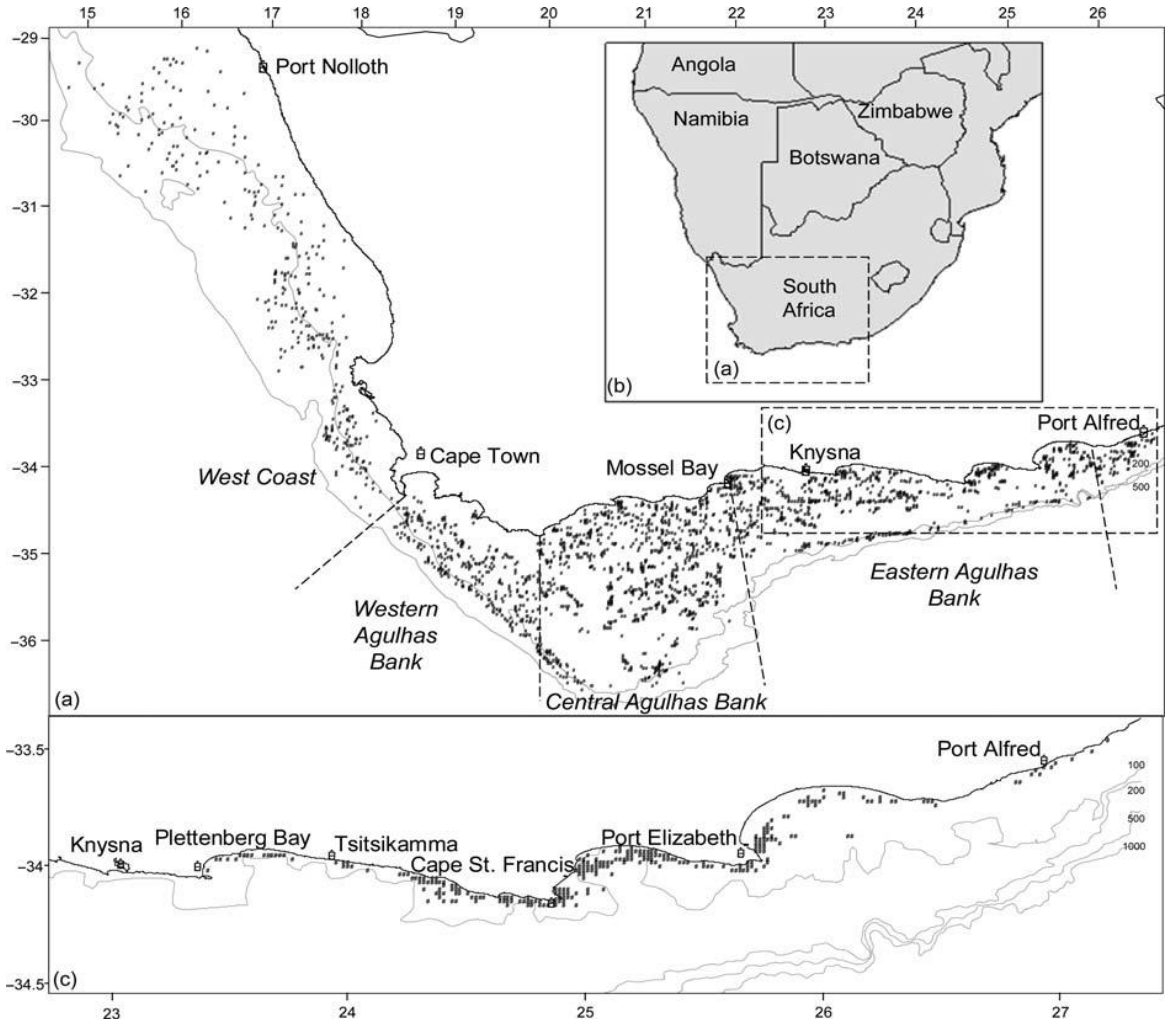

Fig. 1.2: (a) Demersal distribution (dots) from DFFE research trawls of adult (females >18 cm; males > 25 cm) chokka on the west coast and the Agulhas Bank of South Africa, (b) chokka biomass on the west coast extends as far as Southern Angola, although the biomass here is lower compared to the Agulhas Bank, (c) commercial hand-jig fishing positions (dots) for chokka indicate commonly used spawning sites traversing the nearshore (< 70 m) coastal region of the Eastern Agulhas Bank. Taken directly from Roberts et al. (2012).

Although initially caught as bycatch within the hake (*Merluccius capensis*) and sole (*Austroglossus pectoralis/microlepis*) bottom-trawl fisheries (Augustyn, 1990; Augustyn et al., 1994; Roel et al., 2000, 1998), the high export value of chokka prompted substantial commercial advances in the jig industry in the early 1980's (Cochrane et al., 2014; Roel et al., 2011). There are five other species of cephalopods caught as bycatch in the demersal trawl fisheries around the southern African waters (**Fig. 1.2a**). These five species include one other *Loliginid* species (*Uroteuthis duvauceli*), three species of *Ommastrephids* (*Todarodes angelonsis, Todaropsis eblanae, and Ommastrephes bartramii),* and a singular *Thysanoteuthid* (*Thysanoteuthis rhombus*) (DFFE, 2020). However, the low export value of these species has undermined the need for targeted, industrialized fishing such as that seen for the chokka fishery traversing the southeast coast of South Africa.

Currently, the industry exports ~ 99 % of total landings, fetching annual foreign revenue equating to ~ R500 000 000 (Crookes and Brenner, 2016) from nations in the European Union, e.g., Spain and Italy (Cochrane et al., 2014; Paterson et al., 2010). In addition, between 200 – 500 tonnes are caught annually as bycatch in the demersal trawl fisheries (DFFE, 2020;Hanan, 1998; Roel, 1998). Artisanal fishing for cephalopods is prevalent along the southern African stretch of coastline (Crookes and Brenner, 2016). For example, in southern Angola (**Fig. 1.2a**), artisanal fishers catch chokka in the nearshore coastal zone using rafts, hand-lines, and homemade jigs (Cochrane et al., 2014; Lipiński et al., 2016; Van Der Vyver et al., 2016).

The commercial fishing fleet operates out of St Francis Bay and Port Elizabeth ports, intersecting the main fishing grounds for the species (**Fig. 1.2a**; 23 – 28 °E). The highest spawning intensity lies between Knysna (~ 23° E) and Port Alfred (~ 27° E), based on geographical data on fishing positions and accumulative results of egg-biomass research surveys (**Fig. 1.2c**; DFFE, 2020; Roberts et al., 2012). Good commercial catches are known to occur within the log-spiral-shaped bays amidst the immediate vicinity of chokka spawning sites (Sauer et al., 1991). More recent technological advances (including drogues and multiple anchors) have allowed for targeted harvesting of spawning and feeding aggregations further offshore (DFFE, 2020). The prevalence of offshore spawning challenges the traditional view of the life history characteristics of chokka,

particularly around the importance of the inshore (< 70 m) versus offshore (> 70 m) spawning grounds (Roberts et al., 2012, Cochrane et al., 2014).

The geographical limits that are depicted in **Fig. 1.2.** should not be seen as definitive, as the demersal trawl surveys target hake and do not accurately reflect the entire spatial and temporal extent of the chokka life cycle (Roberts et al., 2012). The results from more recent bottom trawl surveys show egg beds and aggregations at depths of ~ 270 m near the edge of the Agulhas Bank (DFFE, 2020; Roberts et al., 2012). Despite the clear evidence of trans-shelf spawning, the presence of higher biomass (82 %) of benthic squid eggs in the shallower, nearshore environment compared to the deeper outer-shelf (18 %), further cements the importance of nearshore spawning to the commercial chokka industry (Roberts et al., 2012).

The active targeting of spawning populations presents the risk of the selective removal of genetic and phenotypic variability due to selective fishing pressure. Concern regarding the impact of targeting spawning aggregations of squid on population genetic diversity has been raised for chokka (Augustyn et al., 1994), as well as other *Loliginid* species (e.g., Moltschaniwskyj et al., 2007). However, it has been argued that quantifying the impact of targeting spawning aggregations on a population level is complicated in *Loliginid* species based on the extended spawning season, variable rates of growth, maturation, and migration (Pecl et al., 2004). In addition, the relationship between chokka spawning-stock biomass and recruitment, which is essentially the following year's spawning biomass (Lipiński et al., 2020), is poorly understood.

1.3 Chokka reproductive strategies

The commercially important chokka is one of the best-studied *Loliginids* in the world (Arkhipkin et al., 2015). The process of courtship, mating, formation, and disintegration of spawning aggregations of chokka have been extensively reviewed in the literature (Augustyn, 1991, 1990; Blackburn et al., 1998; Hanlon et al., 2002, 1994; Lipiński et al., 2016; Melo and Sauer, 2007; Roberts et al., 2012; Roberts and Sauer, 1994; Sauer et al., 1992, 1997; Smale et al., 2001).

There is a relative degree of conformity regarding the breeding biology of *Loliginid* squid. Similarities between *Loliginid* populations include a 'seasonal' breeding cycle, patterns of migration between feeding and spawning grounds, and a well-defined geographical area for spawning (Pierce et al., 2008). Communal spawning areas, or "arenas", involve individual squid congregating and mating on mass (Shashar and Hanlon, 2013). An early and well-accepted hypothesis from research into the species distribution on the continental shelf suggests that chokka evolved to utilize an environmental niche on the EAB (24 - 28° E), where temperature (~ 12 – 17 °C) and dissolved oxygen levels (~ 3 – 5 ml L^{-1}) are optimal for egg and larval development (**Fig. 1.2c**; Augustyn, 1990; Roberts, 2005). The use of warm inshore areas for spawning is a common trait among *Loliginid* squid species. For example, *L. vulgaris*, *L. chinensis*, *L. duvauceli,* and *L. pealei* are all known to be serial inshore spawners (Arkhipkin et al., 2015; Roberts et al., 2012; Shashar and Hanlon, 2013).

Chokka populations spawn predominantly in the summer months (November to January), with a secondary, less pronounced spawning season evident in autumn leading into winter (March to July). Characterized by rapid growth, short-life span (1 - 1.5 years), and iteroparous spawning behaviour, chokka are susceptible to environmental perturbations at all life history stages (Lipiński et al., 2020; Ané Oosthuizen et al., 2002; Segawa, 1995; Steer et al., 2002; Villanueva, 2000). It is on the nearshore spawning grounds that the complex reproductive strategy of chokka has been studied, either through direct observations (e.g., SCUBA and acoustic telemetry) or through biological studies through which inferences on the reproductive process have been made (e.g., Augustyn, 1990; Sato et al., 2019). The re-use of spawning sites both annually and intra-annually further highlight the importance of the nearshore spawning grounds to the chokka population (**Fig. 1.2c**; Downey, 2009; Olyott et al., 2007; Roberts et al., 2012; Singh et al., 2009).

The actual mating and courtship process for *Loliginid* species suggests that spawning success is primarily visually orientated and dependent on body patterns (Hanlon, 1998). The term 'body pattern' is a reference to the overall physical appearance of a cephalopod at any moment and is made up of a combination of one or more of the following characteristics; posture, movement or

locomotory function, and chromatic (i.e., colour) variability (Hanlon et al., 1994; York and Bartol, 2016). Chromatic body patterns include the absorption and scatter of light via pigmented granules in the skin, known as chromatophores (Hanlon et al., 2002, 1994). Cephalopods actively control the neurologically operated chromatophilic pigments in its skin, using them in courtship displays or camouflage in both inter-and-intraspecies interactions (Hanlon et al., 2002, 1994; Lipiński et al., 2016).

An Ethogram is a catalogue of species-specific body patterns, interactions, and behaviour that describes the communication between cephalopods and the biotic and abiotic environment (Hanlon and Messenger, 1996). Hanlon et al. (1994) described an Ethogram with twenty-three chromatic components, three postural components, and nine locomotor components of body positioning for *L. reynaudii*, further highlighting the importance of visual stimuli in the reproductive process. The vast majority of the chromatic components were expressed during intra-specific behaviours (i.e., agonistic behaviour amongst males, courtship, mating) and, to a lesser extent, during interactions with fishes and predators (Hanlon et al., 1994; Sauer et al., 1997). For example, when stressed, chokka neurologically activate and expand its chromatophores, resulting in a reddish-brown overall colour (Hanlon et al., 1994; Smale et al., 2001). Relaxation or retraction of the chromatophores results in the animals' white, transparent, or translucent appearance (Hanlon et al., 1994).

The choreography of the chokka ‘nuptial dance,’ described in detail by Sauer et al. (1997), highlights the complexity of the reproductive strategy on the environmentally variable nearshore spawning grounds. Chokka aggregate into large arenas of spawning adults at various stages of maturity, during which they form breeding pairs (Sauer et al., 1997). There is a high degree of male-to-male agnostic behaviour in competition for females (Sauer et al., 1997). Visual stimuli brought about by chromatophilic pigments in the skin are crucial for conferring an advantage over other males as well as warning off predators (Sauer et al., 1997, 1992). The longevity of spawning aggregations, where chokka is available to the fishery, is subject to optimal environmental conditions suitable for the full aggregation and courtship process.

1.4 Relationship between chokka and the environment

The ability to manage catch and improve forecast accuracy through a greater understanding of the environmental drivers behind catch variability has been the emphasis of scientific discourse on *L. reynaudii* over the last few decades (Arkhipkin et al., 2015; Blackburn et al., 1998; Downey-Breedt et al., 2016; Lipiński et al., 2020; Martins et al., 2010; Oosthuizen et al., 2002; Peterson and Hutchings, 1995; Roberts, 1998; Roberts et al., 2012; Sauer and Lipiński, 1991; Sauer et al., 1997, 1992). It is evident from the variability in catch statistics in cephalopods globally that apparent abundance is strongly influenced by both local and large-scale environmental forcing mechanisms at all life history stages (Arkhipkin et al., 2015).

The early life history characteristics within the phylum Mollusca are unusual, owing to a feeding strategy that alternates between exogenous and endogenous food sources (Martins et al., 2010). From both biotic and abiotic factors; temperature, food, and predation are likely the most critical components affecting paralarvae survival (Augustyn et al., 1992, Oosthuizen and Roberts, 2009). Studies on the distribution of paralarvae post-hatching have found that paralarvae distribution depends mainly on the physical forcing of the Agulhas Current as well as food availability (Roberts and Van Den Berg, 2002). However, the post-hatching life history of chokka paralarvae are understudied and not well understood.

The greatest concentration of available food resources for squid paralarvae, which are strongly dependent on copepods (Olyott et al., 2007), is found southwest of the main spawning grounds in a quasi-permanent area of upwelling known as the 'Cold-Ridge' (Roberts and Van Den Berg, 2002). The 'Cold-Ridge' is an elongated oceanographic feature of increased primary productivity, and subsequently, squid food abundance, due to the upward doming of the thermocline, which brings cold, nutrient-rich waters to the surface of the central Agulhas Bank (Roberts, 2005). The hypothesis is that squid paralarvae hatched on the EAB will be passively transported by the Agulhas Current towards the copepod-maximum centered around the 'Cold-Ridge,' forming what is known as the 'Western-Transport Hypothesis' (WTH) (Roberts, 2005). The WTH is important because it serves as a bridge to explain the variability in geographical

locations between the main spawning grounds and the main nursery areas/feeding grounds for chokka (**Fig. 1.2a-c**; Roberts, 2005). Furthermore, patterns of sex-related size-class distribution of chokka over the continental shelf reinforce the notion that chokka squid migrate to and from the main feeding areas and the favourable nearshore spawning grounds (**Fig. 1.2c;** Lipiński et al., 2016; Lipinski and Soule, 2007; Naud et al., 2016).

Due to the complexity within *Loliginid* reproductive strategies, finding a single environmental factor that influences squid spawning is confounded by the myriad of possible effects on different aspects of the short life history (Boyle et al., 1995; Caddy and Rodhouse, 1998). In the chokka industry, disruption to nearshore spawning aggregations result in lower catch rates. Optimal conditions for spawning and aggregation behaviour include bottom currents of low-to-zero velocity as well as low levels of benthic turbidity; a function of swell-induced turbulence, substratum type and detritus level (Dorfler, 2002). Chokka spawning behaviour has been noted to differ between diurnal and nocturnal states (Sauer et al., 1997). Resultantly, light availability has been marked as an abiotic disturbance to the formation and duration of spawning aggregations due to the importance of visual stimuli in the reproductive process (Roberts, 1998).

Chokka spawn mainly through daylight hours (Sauer et al., 1992). Results from acoustic experiments show that chokka aggregations dissolve at dusk with the movement of chokka out of the inshore spawning grounds (Downey et al., 2010; Jackson et al., 2005; Sauer et al., 1997). The reduction in light may be responsible for the disruption to spawning, as chromatophilic communication relies on the ability of squid spawning aggregations to see one another. Resultantly, the chokka fishery use bright lights in an attempt to either (a) enhance chromatophilic communication despite the reduction in natural light or (b) enhance and concentrate otherwise dispersed feeding behaviour (Sauer et al, 1995). Similarly, video observations revealed that the eastern American *L. opalescens* does not aggregate at night in the absence of artificial lighting (Forsythe et al., 2004). Other *loliginid* squids such as *L. opalescens* and *Sepioteuthis sepiodea* are daytime spawners who favour warm water environments (Hanlon and Messenger, 1996).

Temperature is seen as one of the primary abiotic factors that influence the timing of spawning, hatching, growth, maturation, and feeding patterns of cephalopods (Boletzky, 1994; Pierce et al., 2004; Villanueva, 2000). Temperature has been shown to have an effect on squid metabolism, ovary development and species distribution in many cephalopods globally (Oosthuizen et al., 2002; Oosthuizen and Roberts, 2009; Pierce et al., 2004). Furthermore, it has been suggested that temperature plays a vital role in the reproductive cycle, particularly the initiation and termination of spawning aggregations (Roberts and Sauer, 1994). Augustyn (1990) was the first to propose sea temperature as an important factor influencing the abundance of chokka on the nearshore spawning grounds. A host of studies have since focused on the potential 'holy-grail' of chokka variability, sea temperature (e.g., Augustyn, 1990; Cochrane et al., 2009; Hobday et al., 2016; Joyner, 2016; Lipiński et al., 2016; Martins et al., 2010a; Sauer et al., 1992).

Early experiments on the effect of water temperature on embryonic development suggested that chokka egg mortality occurred at temperatures outside of the optimal environmental range (Augustyn, 1990). Laboratory studies demonstrated high (> 50%) incidences of embryonic abnormalities occurred at temperatures less than 12 °C and higher than 17 °C (Oosthuizen et al., 2002). These initial studies suggested that based on temperature, the reproductive success of chokka was confined to the nearshore spawning sites on the EAB. However, results from demersal trawl surveys (Augustyn et al., 1992, 1994; Roberts and Sauer, 1994; Augustyn and Roel, 1998; Roberts et al., 2002) and hydroacoustic evidence of mid-shelf spawning (Roberts et al., 2002), questioned the viability and prominence of mid-shelf spawning. This led to a conceptual model of the spawning process, which included environmental variables thought to either instigate or terminate chokka reproductive behaviour, namely; temperature, turbidity, currents, and waves (Roberts, 1998). Although at the time, the exact interplay between the variables and catch remained elusive.

To resolve the temperature conundrum, Oosthuizen and Roberts (2009) undertook *in-situ* experiments where chokka egg strands were exposed to mid-shelf temperature ranges (8.2 – 13.7 °C) and found that embryonic abnormalities (0.45 %) differ markedly from the laboratory experiments (> 50 %). More recently, studies have shown that mid-shelf spawning is indeed

viable (Roberts et al., 2012). It is clear from the temperature regime that chokka spawn in two very contrasting environments, namely, the variable nearshore spawning grounds (13 – 17 °C) and the more stable, colder mid-shelf region (9 – 11 °C).

Chokka spawning on the Agulhas Bank mid-shelf results in asynchronous rates of hatching amongst the population (Roberts et al., 2012), which is advantageous by offsetting adverse conditions on the more favoured nearshore spawning grounds. Furthermore, lower temperatures result in the slower utilization of yolk, providing more time for developing predatory skills (Martins et al., 2010). In the species *L. vulgaris*, low temperatures result in hatchings growing larger and for longer than under optimal temperature conditions (Villanueva et al., 2003). The slower yolk utilization allows for greater size at hatching and provides the paralarvae with a competitive advantage due to increased swimming power, food-searching capabilities, and predator avoidance (Villanueva et al., 2003). Furthermore, larger hatchlings are also less vulnerable to starvation, meaning they are more likely to reach the primary feeding grounds than their smaller counterparts (Roberts et al., 2012; Vidal et al., 2006).

It has been postulated that chokka spawn in two such contrasting environments as a diversified response to the species' reproductive strategy. Due to the variable nature of environmental conditions on the shallow more sheltered nearshore spawning grounds, chokka migrate between the nearshore and mid-shelf areas as a diversified aspect of the life cycle, protecting the population against anomalously poor environmental conditions. Alternatively, frequent benthic warm-water intrusions emanating from the coast due to westerly-wind driven downwelling might expand the optimal spawning habitat (i.e., temperature) and therefore promote spawning on the mid-shelf (Roberts et al., 2012). Downwelling of warmer surface waters has been shown to extend as deep as 120 m and as far as 20 km offshore (Oosthuizen and Roberts, 2009). The presence of intermittent warm water intrusions onto the mid-shelf make spawning and egg development possible for chokka in environments previously thought to be too cold for spawning (Oosthuizen and Roberts, 2009; Roberts and Sauer, 1994).

From a behavioural perspective, the fact that chokka spawn in two such contrasting environments may be because it is (a) forced behaviour, or (b) it is an aspect of a diversified life-history strategy that strengthens recruitment into the fishery. For the former, Roberts and Sauer (1994) and Dorfler (2002) postulated that benthic turbidity events on the nearshore spawning grounds may deter spawning aggregations from using the preferred warmer water environment by disrupting intraspecific courtship behaviour so forcing the aggregation down the continental shelf to clearer, colder waters of the mid-shelf where they become largely unavailable to the depth-limited jig-fishery (Roberts, 1998). For the latter, deep-to-mid-shelf spawning may be an evolutionary trait brought about by the need to encounter a more suitable survival window of food and currents which motivates the need for delayed hatching and slower growth rates in an otherwise variable oceanic shelf environment such as that on the EAB. A quantitative study on the effects of the environment on chokka catches suggested that benthic turbidity is the single most important variable influencing apparent chokka abundance, i.e., catch rates (Schön et al., 2002).

The 'Temperature/Turbidity Spawning Strategy' is a thought experiment that explains chokka spawning in such contrasting environments (Roberts, unpublished). The primary motivation for spawning is to take advantage of the optimal temperature range found on the nearshore spawning grounds for egg and larval development (Roberts, 2005). In instances where benthic turbidity events persist, spawning aggregations of chokka squid are forced out of the favourable nearshore spawning grounds and onto the mid-shelf, where they become unavailable to the depth limited hand-jig fishery, resulting in lower catch rates. It is important to note that the Temperature/Turbidity Spawning Strategy does not act alone in affecting catch rates, as other environmental forcing mechanisms may influence reproductive behaviour. Consequently, even when temperatures are optimal and water clarity is high, chokka catches may be low. The interplay between 'clean-and-clear' and turbid conditions highlights the complexity regarding fleshing out the relationship between temperature and turbidity, and ultimately, chokka catch.

To further explore the relationship between benthic turbidity events and catch, a four-year pilot study was initiated in 1999 on benthic turbidity events traversing the primary spawning grounds

of chokka (Dorfler, 2002). Initial results from this four-year study highlighted the variability of turbid conditions across the Agulhas Bank. Turbidity in the surface layers was found to increase in intensity away from the coast, with a maximum Surface Nepheloid Layer (SNL) found on the central Agulhas Bank. Benthic turbidity events and the subsequent Benthic Nepheloid Layer (BNL) were shown to occur anywhere along the coastline. However, the BNL was more intense inshore of the 100 m isobath and within sheltered bays of the EAB. The BNL was associated with warmer waters > 12 ℃, with the greatest intensity closest to the seabed. Within the embayment's, Dorfler (2002) showed that turbidity was closely correlated to bottom temperature, with a deepening of the thermocline increasing the concentration of the BNL.

1.5 Aims

The uncertainty associated with catch variability induces socio-economic hardships on local fishers, industry, and resource managers alike. This problem will likely manifest itself further, considering the uncertainty of future climate change. Therefore, the relationship between apparent chokka abundance and the environmental drivers thereof must be holistically unpacked to move towards marine resource resilience in the Anthropocene. Episodic benthic turbidity, and the resultant benthic nepheloid layer (BNL), is a significant factor influencing intra-specific communication critical to the formation of spawning aggregations, and ultimately, catch and recruitment into the fishery. The role of this thesis is to couple physical *in-situ* observations and remote sensing techniques to elucidate further the complex relationship between the environment and benthic turbidity events on the EAB.

This study aims to answer the following questions:

1) How does ***benthic turbidity relate to underwater visibility*****?**

2) What is the ***frequency and intensity*** of benthic turbidity events in Algoa Bay, a sheltered embayment of the EAB?

3) What is the ***spatial extent*** of turbidity across adjacent embayment's on the EAB?

4) What ***environmental parameters influence*** these benthic turbidity events**?**

1.6 Study Approach

The approach taken in this study is to analyze historical data on benthic turbidity on the EAB. The aims of this study were achieved through the qualitative analysis of a 17-month time series of benthic turbidity in Algoa Bay, a sheltered embayment on the EAB, between November 2002 and March 2004. The relationship between turbidity events and local and large-scale environmental forcing mechanisms was qualitatively assessed for any themes or patterns relating to the role of environmental variability on episodic benthic turbidity. In conjunction with the Algoa Bay Time-Series Experiment, the Extended Bay Experiments aimed to determine the spatial extent of turbidity events through historical data collected in adjacent bays, namely, Algoa Bay, St Francis Bay, Oyster Bay and Oubos. The Extended Bay Experiments were conducted during the annual October-November closed season in 2002 and 2003, respectively. Remote sensing techniques, including along-track altimetry, sea surface temperature, and primary productivity, will provide further in-depth analysis of benthic turbidity events concerning the overlying physical environment.

CHAPTER 2
Literature Review

The outline of the upcoming literature review begins with a brief synthesis of the variable oceanography of the Agulhas Bank. The literature review will then provide an introduction to nepheloid layer studies and dynamics applicable to this study.

2.1 Review of oceanography and meteorology of the Eastern Agulhas Bank

South Africa's coastline, nestled amongst some of the most dynamic and complex oceanographic conditions on the planet, stretches some ~ 2500 km from the desert border with Namibia on the western Atlantic to the eastern sub-tropical Mozambique border on the Indian Ocean (**Fig 2.1b**; Penven et al., 2001). The cold Benguela upwelling system dominates the west coast, while the oceanography of South Africa's east coast is strongly influenced by the warmer, faster flowing Agulhas Current (AC; **Fig 2.1b**; Lutjeharms, 2001).

The proximity of two such contrasting marine environments makes this region unique in oceanographic patterns, meteorology, and aquatic life. The AC is a well-formed western boundary current that transports warm Indian Ocean water poleward traversing the east coast of southern Africa (Schumann, 1987). Influenced by the larger circulation patterns of the wind-driven, anti-cyclonic gyre of the South Indian Ocean (**Fig 2.1a**; Lutjeharms, 2006), the AC and its role in regulating and modulating meso-to-global-scale environmental variability has been subject of increased scientific study of late (e.g. Beal and Elipot, 2016; De Ruijter et al., 2013; Elipot and Beal, 2018; Leber et al., 2017).

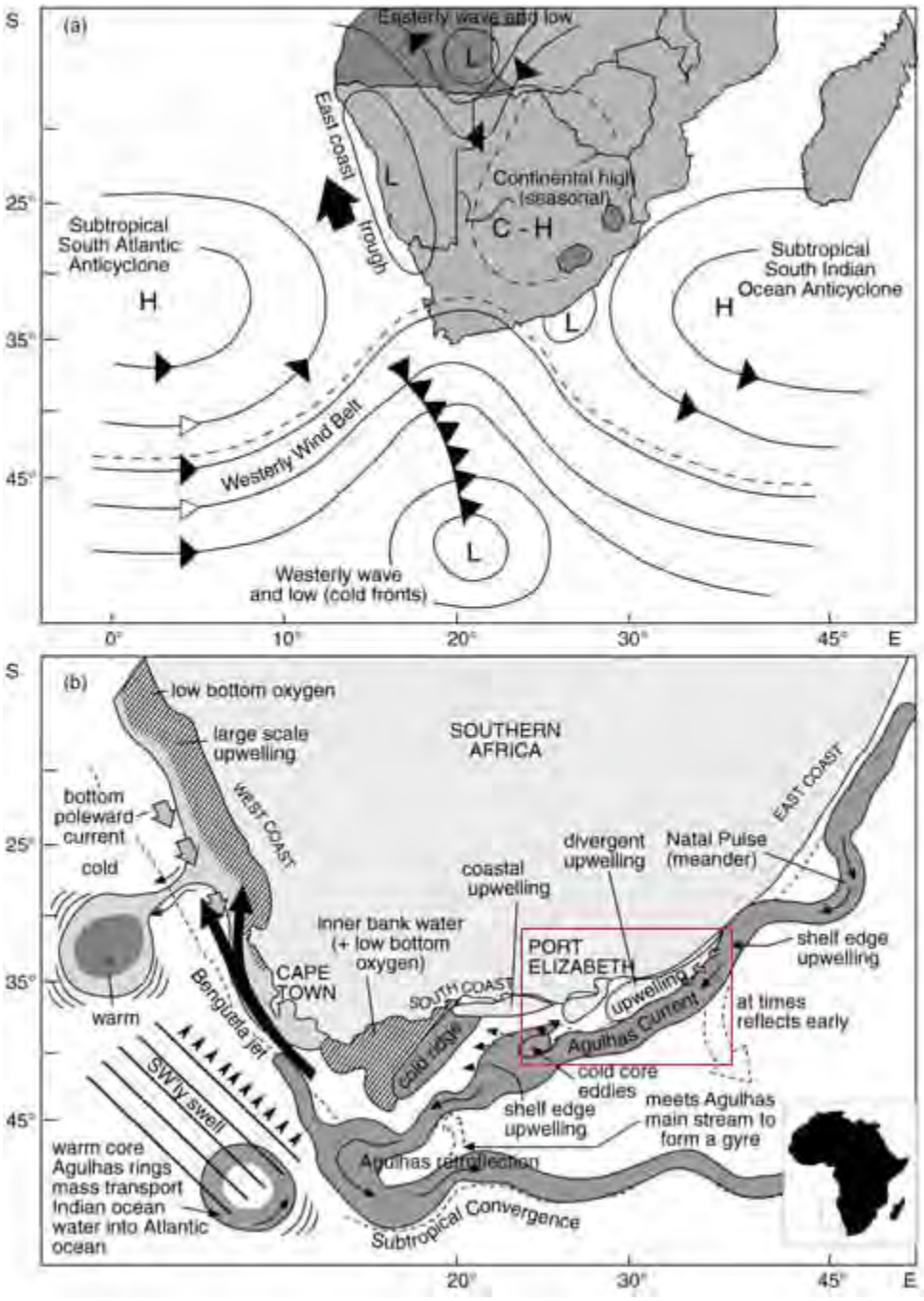

Fig. 2.1: The complexity and variability in the marine environment around South Africa is partly due to the (a) latitude and associated weather and (b) the influence of two contrasting boundary currents, namely the cold Benguela Current on the west coast and the warm Agulhas Current on the east coast. Highlighted in this figure are the complex oceanographic features associated with South Africa. The red box denotes the Eastern Agulhas Bank, and the focus of this study. Adapted from Roberts (2005).

2.1.1 The Agulhas Bank

The Agulhas Bank is an extension of the continental shelf of southern Africa that forms the central biomass region for chokka (Augustyn et al., 1994; Boyd and Shillington, 1994). The complexity and variability of Agulhas Bank processes can be attributed mainly to the interactions between meteorological forcing mechanisms (**Fig 2.1a;** high- and low-pressure systems) and the contrasting physical hydrography of the region (refer to **Fig 2.1b**). It has been suggested that the Agulhas Bank can be sub-divided into distinct geographical regions based on these differences (Probyn et al., 1994). However, the exact lines of division are largely subjective based on the author and choice of division, i.e., oceanography (Boyd and Shillington, 1994), wind field (Reason, 2001), rainfall (Rogers, 1971), and primary productivity (Probyn et al., 1994). A reasonable criterion for the delineating of the Agulhas Bank is the variable properties of the thermocline (Probyn et al., 1994). The depth and intensity of the thermocline and associated nutricline can have profound consequences on phytoplankton biomass and ultimately primary productivity on the Agulhas Bank as a whole (Carter et al., 1987; Largier and Swart, 1987).

This study is particularly interested in the Bank's region best associated with the chokka fishery, the EAB (**Fig 2.1, red box**). The EAB is defined in this study as the portion of the southeast coast from 24 – 28 ° E, extending to the outer limits of the squid fishery, the 200m isobath, ~ 36 ° E (Roberts et al., 2012). The EAB differs from the Central (22 - 24° E) and Western (18 – 22 ° E) sectors of the Agulhas Bank through increased intermittent coastal upwelling, which leads to irregular but highly productive coastal waters (Probyn et al., 1994). In addition, the oceanography of the EAB is markedly different from that further southwest on the Agulhas Bank (**Fig 2.1**).

2.1.2 The Agulhas Current and the Eastern Agulhas Bank

The warm, fast-moving (~2 m s^{-1}) Agulhas Current (AC) flows in a south-westerly direction, closely following the continental margin until it reaches the Agulhas Bank, which begins to widen south off Port Elizabeth (~ 27 °E, **Fig 2.1b**; Lutjeharms, 2006). At the southernmost tip of the Agulhas Bank, the AC undergoes a retroflection back into the Indian Ocean (De Ruijter et al., 2013). Thus, the AC can be seen as two distinct sections, each with a different set of characteristics.

The delineation between the two AC sub-regions is the altering bathymetry in the region of Cape Padrone, Port Elizabeth (~26.5 ° E). Unusual for a western boundary current (Lutjeharms, 2006), the upper part of the AC has its origins in the Mozambique channel and follows a relatively stable trajectory until it reaches Port Elizabeth (**Fig 2.1b**). The stability of the path is exempted only in the anonymously shallow region of the Natal Bight, which induces cyclogenesis crucial for the generation of many of the features of the AC, such as the Natal Pulse (De Ruijter et al., 2013) and Durban Eddies (Roberts and Nieuwenhuys, 2016). As the AC broadens in its trajectory from North to South, interactions between the current and the widening Agulhas Bank lead to AC early retroflection's, meanders, and cold-core eddies synonymous with the EAB region (Jackson et al., 2012; Largier and Swart, 1987; Lutjeharms, 2006; Swart and Largier, 1987; Weidberg et al., 2015).

The water masses across the Agulhas Bank tend to be highly stratified, with a well-developed thermocline. The hydrography of the EAB is notable by marked seasonal variability in thermal structures (Largier and Swart, 1987; Swart and Largier, 1987). The thermocline on the EAB is well defined close to the coast, decreasing in intensity further offshore (Schumann and Beekman, 1984). The strong thermocline in summer is linked to coastal shelf upwelling processes and increased photoperiod. In contrast, the dissolution of the thermocline in winter is attributed to increased vertical mixing due to storm events and increased westerly-components winds which drive swell (Probyn et al., 1994). The most notable feature of importance to this study is the

variable coastal upwelling and the associated implications for the chokka fishery. However, different mechanisms are responsible for the variability of temperature, and subsequently primary productivity structures, on the EAB (Probyn et al., 1994; Roberts, 2005).

2.1.3 Upwelling and Primary Productivity

Upwelling hotspots are of critical biological and economic importance in shelf systems globally where they occur (Beckley, 1983; Kainge et al., 2020; Russo et al., 2019). The re-use of chokka spawning sites on the EAB brought about the idea that the temperature structure of the favourable spawning grounds was responsible for the variability in chokka catches (Augustyn et al., 1994). Intermittent coastal upwelling resulting from strong easterly-component winds drives upwelling at prominent capes traversing the main spawning grounds for chokka squid. The upwelling events resulted in colder and generally clearer water being brought onto the nearshore spawning grounds (Roberts, 1998). The peak in frequency and intensity of these upwelling events coincide with the primary spawning season of chokka squid, namely, November through to February. As a result, the temperature structure of the nearshore spawning grounds has been seen to be central to chokka catch (Sauer et al., 1991).

Upwelling is the process by which cold, nutrient-rich water is brought up the water column due to replacement flow when the surface waters are forcibly moved offshore. Upwelling on the Agulhas Bank results in the movement of Indian Ocean Central Water (IOWC, 6 – 14 °C) onto the continental shelf, which enhances primary productivity in the euphotic zone down current from where it occurs (Probyn et al., 1994). For example, IOCW has been found at depths of 400 m off the continental shelf off Durban but has been found at depths of only 150 m off Port Elizabeth and the EAB (Goschen et al., 2015; Goschen and Schumann, 1988). Upwelling processes on the Agulhas Bank can be divided into two categories based on the principal driver of the process. Upwelling is driven by (i) mesoscale variability in the AC itself, which can induce instability in the current trajectory, as well as (ii) more localized upwelling in the coastal system as a result of dynamic wind forcing mechanisms.

2.1.3.1 Wind-induced coastal upwelling

A combination of both wind-induced upwelling, downwelling, and shelf-edge processes contribute to the variability in temperature structure seen on the Agulhas Bank (Leber et al., 2017). Wind stress is, therefore, one of the effective forcing mechanisms driving oceanic variability on the EAB (Malan et al., 2019). A wind with an easterly component drives coastal upwelling at prominent headlands or capes along the EAB through the process of Ekman transport, deflecting surface and near-surface water some 45° to the left of the wind direction in the Southern Hemisphere (Schumann, 2015; Schumann and Brink, 1990). Winds with a prominent easterly component are more prevalent in summer than in winter due to the movement of the South Atlantic high-pressure system (**Fig. 2.1a**; Probyn et al., 1994; Schumann, 2016).

In austral summer, the oceanic high-pressure cells dominate the wind-field, causing south-easterly winds on the west coast and north-easterly winds on the EAB due to the contracting of the westerly belt (**Fig. 2.1a**; Roberts, 2005). In austral winter, the westerly wind belt expands, moving cold-fronts and strong westerly-component winds to southern Africa (**Fig. 2.1a**; Roberts, 2005), resulting in large swells and storm events (Lutjeharms, 2006). Winds with an easterly component are the drivers of coastal upwelling on the EAB, in contrast, westerly-component winds reverse the upwelling process and move warmer surface waters back onto the shelf in a process known as downwelling. The transient intrusions of warmer and cooler waters seen on the mid-shelf result from the variable nature of dynamic upwelling experienced along this portion of the coast (Oosthuizen and Roberts,2009).

The dominant modes of wind stress along South Africa's southeast coast are strongly influenced by more extensive environmental forcing mechanisms, such as the El-Nino-Southern Oscillation (ENSO). ENSO is known to drive nearshore variability in sea surface temperatures along the east coast of South Africa by influencing wind-induced upwelling (Duncan et al., 2019). An El-Nino event is characterized by the movement of the South Atlantic High-Pressure system towards the equator. This leads to an increase in the dominant westerly-wind field and a weakening of the

easterly-component winds, which drive wind-induced upwelling events inshore of the Agulhas Current (Duncan et al., 2019). The La-Nina phase has the opposite effect, causing a poleward shift in the South Atlantic High-Pressure system, increasing westerly-component winds on the EAB (Duncan et al., 2019). In terms of larger environmental forcing mechanisms, high catches corresponded to exceptional coastal upwelling on the Agulhas Bank and a well-developed La-Nina event in the Pacific Ocean. Poor catches observed in the summers of 1987 and 1991/1992 corresponded to El-Nino phases (Roberts and Sauer, 1994). This emphasizes the often-intricate relationship between the environment and different aspects of chokka biology and life history characteristics pertaining to catch abundance.

Although largely understudied, the wave climate on the EAB is considered to be highly seasonal (MacLachlan, 1983). The dominant wave direction is southwest, with swells < 2 m occurring for 80 % of the time (MacLachlan, 1983). However, significant storm events in the Southern Ocean generate large swells of > 3 m that emanate from the southwest, mainly during the winter months due to the increased frequency of westerly component winds and storm events. The Council for Scientific and Industrial Research (CSIR, 1987), using wave-rider buoy data, showed that the wave climate near Algoa Bay in summer to be between 0.5 – 5 m, although 87 % of waves were found between 1 – 3 m. In winter, the number of wave events exceeding 2 m increased (CSIR, 1987), with winter waves ranging between 1.0 – 6.5 m at Cape Recife. Due to the log-spiral shaped nature of the bay in comparison to dominant wave direction, most of Algoa Bay is protected from these swells by the rocky headland at Cape Recife, despite some degree of refraction (Goschen and Schumann, 2011; Grundlingh and Rossouw, 1995; Hutchings et al., 2019).

2.1.3.2 Mesoscale features of the Agulhas Current

Following ten years of remote sensing satellite data on sea surface temperature (SST) and chlorophyll-a concentrations, a proxy for primary productivity, Lutjeharms et al. (1989) described shear features and boundary phenomena that pointed to meanders increasing in

amplitude south of Port Elizabeth. These features were shown to have a distinct effect on the temperature structure of the Agulhas Bank, particularly between Port Alfred and Port Elizabeth, through advection of cold water onto the continental shelf (Lutjeharms et al., 1989). The physical mechanisms by which temperature is controlled on the shelf is influenced by surface convergence or divergence as a result of Ekman transport (Malan et al., 2019, 2013).

These meanders follow similar cyclonic features to those studied in the Gulf Stream (Churchill and Milkowski, 1986) and the South Brazil Currents (Campos et al., 2000) and have been shown to have upwelling on the leading edge and a downwelling sector on the trailing edge of the meander. These frontal meanders are also present on the Agulhas Bank and are associated with warm water plumes at the trailing edge of the meander (Lutjeharms, 2006). The cyclonic nature of the meanders and the associated warm water plumes bring warm and cold water to the upper layers of the EAB (Lutjeharms, 2006) and support increased productivity and larval recruitment through upwelling-related retention of water masses and, subsequently, drift materials, such as SPM (Hutchings, 1994; Jackson et al., 2012). Such shelf-edge upwelling processes are associated with bottom stress on the AC that drives upslope Ekman veering of colder IOCW onto the shelf from below the shelf edge (Malan et al., 2019). The ability of these mesoscale features to transport bottom waters across the continental shelf onto the inshore edge of the AC is essential in priming the EAB for further coastal upwelling features (Goschen et al., 2015; Weidberg et al., 2015).

The most extensive and intensive of these meanders is the solitary Natal Pulse (**Fig. 2.1**). It is generally accepted that the Natal Pulse, which can have an offshore extent of between 30 – 300 km (Lutjeharms, 2006), are the dominant mode of variability in the trajectory of the AC (Malan et al., 2019). Instabilities in the bathymetry of the Natal Bight in conjunction with the presence of anti-cyclonic eddies are thought to be the reason behind the formation of the Natal Pulse, which then propagates south-westwards with the direction of the AC (Goschen et al., 2012a; Roberts and Nieuwenhuys, 2016; Tsugawa and Hasumi, 2010; Weidberg et al., 2015). The temporal frequency of this feature on the Agulhas Bank is not very well understood, but it is generally accepted to occur on average 1.6 - 1.7 times a year (Krug et al., 2014; Rouault et al.,

2010), but can range from zero to 5-6 times a year (Krug et al., 2014; Tsugawa and Hasumi, 2010). The meandering speed differs, but ranges from 10 km.day^{-1} to more than 60 km.day^{-1} (Krug et al., 2014).

In a study on the effects of solitary Natal Pulses on the variable oceanography of the EAB, Krug et al. (2014) noted that Natal Pulses have a residence time of 65 days on average and can impact the EAB for up to 110 days a year. The passing of a Natal Pulse resulted in variability in sea surface temperatures in Algoa Bay, a sub-embayment of the EAB (Goschen and Schumann,1988). Lutjeharms and Roberts (1988) described the presence of shelf-edge upwelling further north of Algoa Bay, in the region of Port Alfred, during one such meander. Furthermore, Schumann et al. (1988) noticed enhanced upwelling on the southern shorelines of prominent capes and headlands on the EAB during moments when easterly-component winds coincide with large AC meanders. More recently, Roberts et al. (2010) highlighted the presence of cold water associated with the Natal Pulse on the eastern side of Algoa Bay, while Goschen et al. (2015) provided empirical evidence of the enhancement of coastal upwelling systems on the EAB as a result of meanders in the Agulhas Current. The upwelling due to wind-forcing may operate on the dynamics already present on the continental shelf due to the forcing of the Agulhas Current (Goschen et al., 2015; Malan et al., 2019). Variable upwelling hotspots leads to variable rates of primary productivity, and subsequently variable rates of detrital settling, across the Agulhas Bank (Probyn et al., 1994).

2.1.3.3 Coastal upwelling features of the EAB

Another prominent site for coastal upwelling is divergent upwelling (**Fig. 2.1b**), present between Port Alfred and Port Elizabeth. This upwelling feature is due to the movement of the AC offshore, which induces replacement flow of cold water to the coast (Hutchings et al., 2019). At times this divergent upwelling is clearly evident in remote sensing data (Boyd et al., 1992; Duncan et al., 2019), but at other times the upward doming of the isotherms does not break the surface and therefore is not evident in the remote sensing data (Jury and Goschen, 2020; Malan,

2013). The strength of the AC is thought to influence the prominence of this coastal upwelling feature (Lutjeharms et al., 1989). A stronger AC will induce a stronger Ekman veering response along the landward edge of the AC, favouring the upwelling of cold-nutrient-rich waters to the surface (Lutjeharms 2006).

Due to the variable nature in physiochemical parameters of the EAB, it has been suggested that there is a quasi-permanent upwelling feature in the region of Port Alfred that is crucial for priming the rest of the EAB for increased primary production (Lutjeharms, 2006). This feature was studied further by Malan (2013) using remote sensing techniques in conjunction with *in-situ* observations of ship-borne hydrographic data and deployed current meters near Port Alfred. Malan (2013) showed that IOCW was present on the Agulhas Bank for 85 % of the 2-year study period between 2009 – 2011. However, most interesting is that this upwelled water signature was not present in remote sensing sea surface temperature (SST) data. Furthermore, the strength of the upwelling cell in Port Alfred consistently influences the cold-subsurface temperature variability downstream (Malan, 2013). The quasi-permanent upwelling cell off Port Alfred primes the rest of the Agulhas Bank, particularly the oncoming embayment's, for enhanced primary productivity. As a result, Lutjeharms (2006) suggested that this upwelling cell acts as an essential secondary biological pump for the Agulhas Bank.

The Agulhas Bank on the east coast is in general less productive than the Benguela Upwelling system on the west coast. The rates of primary productivity are variable and follow the same east-to-west trend evident for the thermocline (Probyn et al., 1994). The upper water column of the Agulhas Bank is characterized by lower mean chlorophyll-a concentrations (~ 1.48 $mg.m^{-3}$) compared to the southern Benguela region (> 3.0 $mg.m^{-3}$) (Probyn et al., 1994). On the EAB, increased rates of primary productivity (> 2.0 $mg.m^{-3}$) can be seen in the region of coastal upwelling within the bays, e.g., Algoa Bay & St Francis Bay (Probyn et al., 1994). The increased coastal upwelling suggests that the EAB may be more productive regarding phytoplankton biomass than other western boundary current systems.

Owing to the importance of the Agulhas Bank to a host of commercially important marine species, several studies have focused on the productivity of the Agulhas Bank (Hutchings et al., 2002; Lamont et al., 2018; Lutjeharms et al., 2007; Probyn et al., 1994; Rouault et al., 2000). In a 5-year study from 1997 – 2002, Demarcq et al. (2003) observed a distinct seasonal surface signal in chlorophyll-a, with the highest concentrations observed in February, March, and April. Through studies on the spatial distribution of chlorophyll-a concentrations, a proxy for the rate of primary productivity in the water column, Shannon et al. (1984) and Probyn et al. (1994) showed that primary productivity increased towards the coast and attributed this to summer wind-driven upwelling (Jackson et al. 2012). A sub-surface chlorophyll maximum typically exists between 20 – 55 m in summer when nitrate concentrations in the surface mixed layer become limiting (Carter et al., 1987, Probyn et al., 1994). Carter et al. (1987) noticed that this subsurface chlorophyll maximum appears to be light limiting, which may have profound consequences for chokka catch due to the disruption to chokka aggregations, although this has never been tested.

The relationship between primary productivity and variable nearshore coastal temperatures provides an appropriate backdrop to understanding the drivers of coastal benthic turbidity events on the EAB. Turbidity and the resultant Benthic Nepheloid Layer (BNL) are closely linked to the hydrography of the area where it occurs (McCave, 2019). The rates of primary productivity are enhanced in coastal upwelling regions (Duncan et al., 2019). Therefore, it is essential to understand that the dynamics of variability in the AC interactions with the coastal environment are likely to control the expression of the BNL on the Agulhas Bank.

2.2 Nepheloid Layers

2.2.1 Definitions

First observed in water mediums by Kalle (1939) and Jerlov (1953), and later described in detail by Ewing and Thorndike (1965), the term nepheloid layer (derived from the Greek work 'nephos' meaning cloud) has long been used to describe the phenomenon of a water mass feature exhibiting high concentrations of SPM. A nepheloid layer is typically measured as a function of increased particle concentrations that distort, scatter, reflect and attenuate light characteristics within a water medium. The dynamics of nepheloid layers are at best complex, and many individual parameters or events may influence the characteristics of a nepheloid layer (Gardner et al., 2018, 1984). As a result, this section will provide only a brief introduction to the study of nepheloid layers and SPM in the ocean relevant to understanding the broader themes of this thesis.

Nepheloid layers are synonymous with increased turbidity. Perhaps the best definition of turbidity is given by Boss et al. (2015), who suggested that "turbidity is a property commonly used to describe water clarity in both marine and freshwater environments, providing a gross assessment of light attenuation; due to the presence of suspended material." However, it is essential to note that measurements of turbidity are highly subjective. It does not offer a direct measure of the quantity of interest (i.e., particulate matter concentration) but rather an indirect measure of the effect of the SPM on the optical properties of the water column (Boss et al., 2015; Hollister and McCave, 1984; McCave, 2009). More accurately, measurements depend on the make and configuration of the instrument used to confer turbidity. Furthermore, the components of the nepheloid layer are as crucial in obtaining the appropriate response from the optical instrument as the appropriate selection of the instrument itself (McCave, 2019).

A nepheloid layer contains both organic and inorganic components (Zoutendyk & Duvenage, 1989). The particulate matter found within nepheloid layers comprises primarily of "marine snow" which are aggregates of detritus, phytoplankton, and inorganic material which move

passively down the water column (Stukel et al., 2014). Detritus can be broadly defined as non-living organic particulate matter, comprising of but not limited to dead phytoplankton, fecal pellets, molts and other dead organisms, terrigenous material, and aggregates of all of the above (Stukel et al., 2014). Phytoplankton is often the dominant component of sinking particles (Stukel et al., 2014). The most common inorganic component within nepheloid layers comprises terrestrial and marine sediments that are either sourced locally through mechanisms such as rivers or wind erosion or are passively advected long distances due to currents.

Further definitions of nepheloid layer characteristics depend on the distinctive layers' spatial and temporal extent and wherein the water column is being measured. Typically, three types of nepheloid layers have been described and studied in oceanic basins and continental shelves around the world, namely, Surface Nepheloid Layers (SNL), Intermediate Nepheloid Layers (INL), and Benthic Nepheloid Layers (BNL). These are so described based on the distribution in the water column.

2.2.1.1 Surface Nepheloid Layers

Surface nepheloid layers (SNL) are synonymous with increased primary production and phytoplankton concentration in the upper layer of the water column, usually restricted to the euphotic zone above the thermocline (Gardner, 2018).

2.2.1.2 Intermediate Nepheloid Layers

There are various reasons for the formation of Intermediate Nepheloid Layers (INL's) in different oceans of the world. However, it is widely accepted that INL's are closely related to the detachment of particulate matter concentrations from the seabed at the shelf break or on the upper continental shelf (e.g., Hollister and McCave, 1984; Pak and Zaneveld, 1983) and around

submarine canyons (Gardner, 1989). Furthermore, INLs are critical to the transport of matter and energy from the continental shelves and pelagic environment to the deep ocean (Pak et al.,1980).

2.2.1.3 Benthic Nepheloid Layers

In general, the oceans benthic environment contains a higher load of SPM than any other intermediate depth of the water column (Biscaye and Eittreim, 1974). This Benthic Nepheloid Layer (BNL) may extend anywhere from 10 m above the seabed (Zoutendyk and Duvenage, 1989) to several hundreds of meters above the seafloor (Rutgers Van Der Loeff et al., 2002). The maintenance of BNLs within the water column depends on two main features. Firstly, local resuspension of particulate matter into the water column provides the BNL with most of its components. Secondly, settling particles are kept in suspension in the water column as a result of enhanced turbulence and shear stress at the seafloor (e.g., McCave, 2019, 1986).

It has long been accepted that BNLs result primarily from resuspension of bottom sediment either locally or through advective mechanisms due to the interplay between currents and bathymetry and topography (Gardner et al., 2018). However, other sources of BNL drivers in deep oceans include cascading of dense shelf waters or coastal fronts (Puig et al., 2013) and around hydrothermal vents (Beaulieu et al., 2013). Koa et al. (2010) reported a rare event where a strong turbidity current, derived from torrential rain and erosion, can drive hyperphysical flow down a canyon to depths > 3500 m. Furthermore, bottom trawling may contribute to nepheloid layer dynamics on continental shelves through the anthropogenically forced resuspension of sediments (Palanques et al., 2006).

A theory on the resuspension of local sediments was described by Graf et al. (1997) that portrayed resuspension events as a non-closed-looping mechanism that includes settling of fresh particles through the water column (Billet et al., 1983), followed by resuspension as a result of increased shear stress on the bottom boundary layer (Lampitt, 1985), and then differentiation by

aggregation and disaggregation (McCave, 1984; Mikkelsen et al., 2006) before passive settling to the seafloor (Gardner et al., 1990). The dynamic local resuspension loop suggests that resuspension in an area will continue if there is a constant supply of source particles in conjunction with adequate bottom boundary stresses to generate resuspension (Graf et al., 1997). Furthermore, the resuspension loop is influenced by both the benthic fauna (e.g., reefs, Graff and Menden-Deuer, 2016; Graf and Rosenberg, 1997) and the substrate (Palanques et al., 2006). Evidence of increased bacterial activity following resuspension events (Wainright, 1987) highlights the multitude of factors that influence BNL dynamics.

Following ~ 60 years of erratic descriptions of the phenomenon (McCave, 2019), Agrawal (2004) proposed that a BNL must exhibit the following four basic properties: Firstly, the thickness of the nepheloid layer is greater than the mixed layer depth. Thus, the scale and intensity of the layer are a function of the strength of the bottom currents, water density, and Coriolis parameters (Agrawal, 2004). Secondly, the layer is distinctive in its characteristics and decreases in intensity as it clears the bottom boundary layer and moves further up the water column (Agrawal, 2004). Thirdly, the BNL exhibits a balance between gravitational settling of source particles and counteracting vertical turbulent diffusion, maintaining the SPM within the distinctive layer giving the layer its light scattering characteristics (Agrawal, 2004). Lastly, there is a transparent vertical gradient in the concentration of particles of any size. The heaviest and largest particles sink first, and the smaller, less dense particles make up the upper layers of the feature (Agrawal, 2004). When these four basic properties are applied to the historical analysis of benthic turbidity on the EAB and in South Africa as a whole, it is clear that the turbid water phenomenon is indeed a BNL.

2.2.2 Ecological impacts of nepheloid layers

In brief, a nepheloid layer is a particle-rich layer, distinct in nature, found in a water medium. However, the interpretation of nepheloid layer dynamics is much more complex (McCave, 1986). Why are these layers studied in the ocean, and what is their importance? The presence of

nepheloid layers has clear ecological consequences in marine and freshwater environments due to a concentration of particles that may deter organisms from that environment (e.g., Karageorgis et al., 2012; Malviya et al., 2016). Alternatively, it has been suggested that these layers may act as important nursery areas for marine nektobenthic species (Puig et al., 2001).

In an attempt to correlate INL detachment to life-histories and spatial distribution of deep-water species, Puig et al. (2001) found a clear link between detachment of an INL on the northwestern Mediterranean continental margin and the population structure of five nektobenthic species of deep-water shrimp. It was suggested that due to the concentration of particulate matter aggregated passively by the overlying hydrographic conditions, the INL serves as an important nursery and feeding ground for these species (Puig et al., 2001). Furthermore, these authors suggested that due to the prevalence of the INL detachments in the area, that the life history characteristics of these benthic shrimp species had evolved to utilize the INL as a feeding ground which offers further protection from potential predators (Puig et al., 2001). Whether or not the life history characteristics of chokka have evolved to utilize BNL events remains to be to be studied.

In South Africa, it has been suggested that the ecological consequences can be as widespread as the phenomenon itself. The presence or absence of a nepheloid layer has been shown to have a distinct effect on the dominant taxa and community structure of two subtidal reefs off the south-east coast of South Africa (Zoutendyk and Duvenage, 1989). These authors found that the presence of increased particulate matter concentrations associated with an intermittent nepheloid layer was a possible cause for the uneven distribution of macrophytes and filter-feeders (Zoutendyk and Duvenage, 1989). Due to the proximity to coastal mud-plains, the presence of the nepheloid layer limits light availability and, therefore, the distribution of filter feeders. The increased particulate matter load may also deter organisms that cannot rid themselves of this unwanted SPM. The second reef is less adversely affected by the bottom associated nepheloid layer due to its position, south of the coastal mud-plains on a rocky-outcrop higher up the water column. As a result, the second reef had a greater diversity of filter-feeders. The reversal in dominant taxa between these two subtidal reefs may be attributed directly to the presence and

persistence of nepheloid layers (Zoutendyk and Duvenage, 1989), suggesting that turbid water masses could have a greater ecological impact far exceeds the deterrent of squid spawning behaviour on the EAB.

2.2.3 Global distribution of nepheloid layers

Nepheloid layers are highly dynamic features, and the distinct characteristics are localized to environmental forcing mechanisms acting on them (Shideler, 1981). The aspect of nepheloid layer distribution and the ecological consequences thereof are receiving increased attention in the literature in recent years as the ability to measure the phenomenon improves (Gardner et al., 2018; McCave, 2019). The most extensive multi-decadal synthesis of nepheloid layer research was conducted by Gardner et al. (2018). The authors coupled nephelometer and transmissometer measurements from a multitude of studies to provide a review on 52 years of BNL research in different oceans across the globe. It is important to note that this review focused only on the BNL in deep oceans at depths > 2000 m, as the instrumentation used in the study was limited by the presence of natural lighting. Gardner et al. (2018) noted that BNL's had received far greater attention in the scientific community than INL or SNL, likely owing to the importance of cross-shelf sediment transport and the movement of energy and carbon to the deeper oceans. For example, in the Bay of Biscay, studies have shown that the BNL plays an integral role in the lateral, off-slope transport of suspended organic and inorganic particulate matter (Antia et al., 2001; McCave, 1984). The importance of BNL dynamics to cross-self sediment transport was also demonstrated in the North Atlantic (Schaeffer et al., 2013)

Following this review of 52 years of nepheloid layer research in the deep oceans worldwide, BNLs were found to be most pronounced in oceans with high kinetic energy in overlying waters (Gardner et al., 2018), suggesting that the prevalence of BNL's to be closely associated with resuspension events. Furthermore, BNL intensity was shown to be highly episodic. Western Boundary Currents exhibit BNLs more frequently and at a greater intensity than other oceans worldwide (Gardner et al., 2018). Strong BNLs, described in the study by Gardner et al. (2018)

as exhibiting particulate matter concentrations > 20 µg. l^{-1}, were absent in most Pacific, Indian, and Atlantic basins away from the continental margins.

The abyssal ocean south of the Agulhas Bank in the Southern Ocean exhibited some of the most intense BNL observed in the study. Gardner et al. (2018) attributed the unusually high SPM concentrations in the nepheloid layers around the eastern African continental shelf and the Southern Ocean to the highly dynamic Agulhas Current. The BNL intensity in the Southern Ocean was linked to the retroflection of the Agulhas Current south of the Agulhas Bank (Gardner et al., 2018). Similarly, nepheloid layer thickness was unusually high for areas to the east and south of Madagascar, suggesting that sediment was sourced and laterally advected from the lower continental slope. These regions have strong bottom currents and large meanders, similar to those prevalent in the Gulf Stream (Churchill and Milkowski, 1986). Hollister and McCave (1984) found a global correlation between BNL dynamics and the spreading of cold bottom water and high surface kinetic energy generated by mesoscale features such as the Gulf-stream meanders. This general pattern suggests that sediment may be diffused or mixed upward or advected locally by these processes, enhancing BNL prevalence and intensity (Hollister and McCave, 1984).

Fewer studies have focused on nepheloid layers on the continental shelves than in the deep oceans. However, the importance of sediment transport and the fate of particulate matter on continental shelves is receiving more attention globally due to the links with carbon storage and global climate variability (Bao et al., 2019). Hydrographic analysis on benthic turbidity on a continental shelf of the United States of America found that wave-induced bottom-turbulence linked to migrating shelf water masses may be the dominant mechanism for resuspending and maintaining a nepheloid layer in the water column (Shideler, 1981). Furthermore, local advection of particulate matter in the water column may result from shear bed stress from physical mechanisms such as currents (Lampitt et al., 2000), tidal currents (Belde et al., 2017; Johnson et al., 2001), internal waves (Cacchione and Drake, 1986; Puig et al., 2004), surface waves and benthic storms (Gardner and Sullivan, 1981). These mechanisms act on the bottom boundary layer in the same way by inducing oscillatory motion in the water column, which passively

aggregates SPM concentrations (Stukel et al., 2014). The orbital shear velocity on SPM generates an elliptical motion in both intermediate and shallow water (Komar and Miller, 1973), which generates stress on the bottom boundary layer. If the kinetic energy of this stress overcomes the critical threshold bonding the particulate matter to the substrate, an upward flux of suspended particulate matter occurs in the water column (Komar and Miller, 1973).

The distribution of SPM on the Barcelona continental shelf, northwestern Mediterranean, includes four permanent nepheloid layer features: the SNL, the BNL, the shelf-break INL and the slope INL (Puig and Palanques, 1998). The distribution and description of these features were strongly linked to different hydrographic structures and changes in bottom topography. Puig and Palanques (1998) found that the SNL was more developed near the coast. In contrast, the BNL was more developed over the continental margin (Puig and Palanques, 1998). The formation and persistence of the INL over the continental margin was attributed to a density front that acts as a physiochemical barrier to the movement of particulate matter, resembling an interface that retains SPM.

The thermocline can also be a preferential guide for internal waves propagation, producing an intense sediment resuspension when waves intersect with the seabed in the continental shelf (Gardner et al., 1983; Palanques et al., 2006). Thus, the thermocline can work both focusing energy from dynamic processes towards its intersection with the seabed, producing resuspension and also as a transport surface for both horizontally advected and/or resuspended material. Cacchione and Drake (1986) explained the generation and maintenance of BNL and attached INLs observed over certain continental shelves and slopes by shoaling and breaking of internal waves. Moreover, Gardner (1989) demonstrated that waves breaking at internal tide frequencies along the Baltimore canyon produce periodic sediment resuspension events that generate intermediate nepheloid layers. Furthermore, this author suggested that submarine-canyons focus and intensify the internal wave energy. Palanques et al. (2006) also found a strong relationship between nepheloid layer distribution and the thermocline.

2.2.4 Measuring suspended particulate matter (SPM)

Optical instruments have long been used to determine the occurrence, abundance, and distribution of particles in multiple bodies of water (Gardner et al., 1984), from great lakes (Hawley, 2004) to the deepest oceans in the world (Gardner et al., 2018; Puig et al., 2013). Instruments used to record particles in a water medium include optical back-scatter (OBS) instruments, transmissometers, and nephelometers. Nephelometers measure the forward scattering of light and have been used to estimate particle abundance and distribution for many years (Jerlov, 1953; Biscaye and Eittreim, 1977). The OBS is a type of nephelometer that emits light at a known wavelength and measures the amount of light scattered back to an optical sensor (D&A Engineering, 1991). Transmissometers were developed in the early 1970s and made estimates of particle abundance easier by measuring the attenuation of light along a fixed path length (Baker and Lavelle, 1984). A common theme amongst these instruments is that instrument output is closely correlated to the source of suspended particulate matter they measure. Beam attenuation due to particles is linearly correlated to particle concentration when the size and the distribution of the particles are relatively uniform (Baker and Lavelle, 1984).

Accurate and reliable measurements of SPM are restricted in natural environments by the need for the instrumentation to be calibrated for a specific particle size distribution which is endemic to the area of study (Agrawal, 2004, 2005; McCave, 2019; Philpot et al., 2004; Richardson, 1987; Zhang et al., 2016). This presents an ostensible restriction to the use of optical instruments to determine suspended matter concentrations, as sediment and organic particle size distributions are known to change in the natural environment (Pedocchi and García, 2006). Estuarine and inshore marine particles are described by Fugate (2002) as ‘complicated aggregates of minerals and organic materials of different size classes, densities, porosities and degree of stickiness’ (Eisma et al., 1991, Fettweiss et al., 1998, Jago & Bull, 2000). For aggregates, the settling velocity cannot be derived from the size of the particles alone (Pedocchi and Garcia, 2006) since particle density is more than just a function of particle size (e.g., Dyer and Manning, 1999).

Typically, studies on sediment transport in estuarine and or marine environments rely on knowing or estimating the specific size classes or other particle characteristics such as density (Baloyi et al., 2009). Furthermore, fragile flocculants of aggregated particulate matter are known to change over time. SPM is subject to turbulent mixing of the water column on shorter time scales, which alter the physical composition of the aggregate being measured. Two mechanisms that may confound the direct conversion from backscatter or transmissions to suspended sediment concentration are the (i) presence of both rapid and slow settling particulate matter and the (ii) presence of multiple size classes within these two components (Fugate et al., 2002). The improvement on suspended sediment theory (e.g., Agrawal, 2005) has improved the ability of researchers to study both *in-situ* size distribution and particle settling velocity. For example, Gardner et al. (1990) observed that nephelometer measurements were unchanged after the fast-settling particles sank to the bottom of a water bottle, while Boss et al. (2015) noted that particles with mass concentration > 20 µm are underestimated by transmissometers due to variable optical responses of the aggregate.

The analysis of optical measurements in this study is complicated by the myriad of ever-changing conditions of the coastal environment. Gardner et al. (2017) noted that for increased particulate matter concentrations near the seafloor, the more temporarily variable the particulate matter concentrations conferred by nephelometers are likely to be. The optical properties of particles in the water column are subject to variation based on numerous physical and biochemical parameters (e.g., Agrawal, 2005). Firstly, the resultant nephelometric turbidity unit (NTU) value depends not only on the concentration of SPM in the water column but also on the physical colour, size, shape, internal structure, and packing of individual particles (Boss et al., 2015). Conner & De Visser (1992) showed that backscatter from particles is inversely related to the particle's size and mass characteristics. However, it has also been shown (Sutherland and Bryan, 1991) that the effects of colour are just as important in obscuring nephelometer readings.

2.2.5 Nepheloid layer studies in South Africa

In South Africa, a nepheloid layer was first documented by Zoutendyk (1971) off the coast of Mossel Bay (~ 23° E). This author suggested that the dense layer of particulate matter is correlated to the coastal mud-belts present off Mossel Bay (Flemming, 1983). Zoutendyk (1973) and later Zoutendyk and Flemming (1983) reported the occurrence of the phenomenon off the southern coast of South Africa, and later as far north-east as East London (~ 27.5° E), suggesting that the feature is distributed widely across the Agulhas Bank. Zoutendyk (1973) found through hydrographic surveys using a transmissometer that this turbid layer was constrained to the lower 10 m of the water column by the thermocline. The study by Zoutendyk & Flemming (1983) highlighted the sharpness of optical deviation within the bottom boundary associated with the BNL. These authors reported a sudden drop in optical clarity of the water column within this turbid water mass located below the thermocline in summer, with visibility noted to decrease to zero near the seafloor (Zoutendyk & Flemming, 1983).

This led to the study by Zoutendyk and Duvenage (1989), who found that the nepheloid layer had an average concentration of total suspended particulate matter of ~ 19 µg. l^{-1}, ranging between 8.23 – 38.4 µg. l^{-1}, which according to Gardner et al. (2019), defines the BNL as 'strong.' Furthermore, these authors found considerable differences between the percentage fractionality of inorganic and inorganic components within the BNL. Organic matter within the dense particulate matter layer only comprised 7.1 % of the total load, which suggests that the BNL on the EAB is comprised primarily of inorganic components, such as soft sediments and fine muds present around the study site. Zoutendyk & Duvenage (1989) suggested that based on the topography and associated roughness of the seabed, that particles within the size range of 10 – 50 µm would be brought into suspension by all conditions on the southeast coast, while particles within a greater size class would only be resuspended under an increased wave or current activity.

The BNL on the EAB was then observed by Roberts and Sauer (1994) and was postulated as an environmental parameter that may influence the chokka reproductive cycle, and subsequently, chokka catch. This led to the initiation of a 4-year pilot study during which the dynamics of the BNL was assessed using hydrographic surveys across the Agulhas Bank as well as a temporal study of BNL dynamics within an important sub-embayment of the Eastern Agulhas Bank, namely, St Francis Bay (Dorfler, 2002). Benthic turbidity events were found to be a common but variable occurrence across the Agulhas Bank and within the sub-embayment's (Dorfler, 2002). The intensity of the events was linked strongly to wind speed and wave period, suggesting that the role of orbital shear stress in particulate matter resuspension is vital in describing BNL dynamics in South Africa. Furthermore, Dorfler (2002) showed that BNL intensity was most significant within the 100 m isobath and within the sheltered embayment's of the EAB. The BNL was associated with warmer waters > 12°C throughout the sampling period, while a deepening of the thermocline increased the intensity of the BNL in St Francis Bay. Schon et al. (2002) then undertook a model approach on the effects of benthic turbidity on chokka catches. Using a statistical black-box approach, Schon et al. (2002) found turbidity to be the leading environmental parameter affecting catch on the nearshore spawning grounds of the EAB.

BNL studies were taken further by Githaiga-Mwicigi (2012), who assessed the dynamics of nepheloid layers over three years of bi-annual hydrographic surveys on the Agulhas Bank. The was noted to occur in discrete patches across the shelf throughout the year, with the most developed layers inshore on the EAB (Githaiga-Mwicigi, 2012). The main findings from this study suggested that benthic turbidity events were more intense inshore, decreasing in intensity with increasing distance from the coast. Furthermore, the nepheloid intensity was described in relation to temperature and salinity, with these structures associated with the vertical and horizontal distribution of the nepheloid layers. A quantitative study conducted by Githaiga-Mwicigi (2012) on the effect of the BNL on chokka biomass distribution suggested that temperature, salinity, and turbidity were the most significant environmental parameters affecting biomass trawl surveys. Furthermore, the dynamics of the BNL across the Agulhas Bank are associated with a thermohaline gradient, near-bottom current speed, and direction, as well as influx of particulate matter from the surface as a result of increased coastal primary production

(Githaiga-Mwicigi, 2012). This study's surface nepheloid layers comprised primarily of organic matter, i.e., phytoplankton, while the BNL was closely associated with increased bottom boundary stress, including waves and current parameters.

The existence of nepheloid layers around the southern African coast are not limited to the Agulhas Bank. In a study on the environmental impact of diamond mining on the continental shelf sediments of southern Namibia, Rogers and Li (2002) described the frequent presence of suspended silt and clay forming a nepheloid layer. The authors attributed the presence of the nepheloid layer to oscillatory swell-driven and unidirectional wind-driven currents which act upon the upper metre of the benthic substrate, causing frequent and consistent resuspension events. Furthermore, Rogers and Li (2002) suggested that Anthropogenic impacts on the marine sediment, through processes such as dredging and bottom trawling, can significantly impact the ‘patchiness’ of sediment types and therefore resuspension events.

CHAPTER 3
Methods and Materials

3.1 Study Area

3.1.1 The Eastern Agulhas Bank

Chokka are caught mainly on the nearshore spawning grounds of the Eastern Agulhas Bank (EAB), defined in this study as the portion of the southeast coast from 24 – 28 ° E (**Fig 3.1**). The EAB extends to the chokka spawning grounds' outer reach, generally considered to be the 200 m isobath (Roberts et al., 2012), located ~ 50 km off Cape Recife (**CR, Fig 3.1 (A)**). The AC flows in a south-westerly direction, closely following the continental margin until it reaches the Agulhas Bank, which begins to widen south of Port Alfred (~ 27 °E, **Fig 3.1(B)**). In contrast to the non-convoluted coast north of Port Alfred, the inshore spawning grounds of the EAB is characterized by an exposed coastline interspersed with crenulated, log-spiral-shaped embayment's associated with prominent headlands or capes (Birch, 1981).

Climatically, the EAB is defined as a warm temperature climate. This temperate climate generates uniform rainfall throughout the year. The prevailing wind directions on the EAB are orientated parallel to the embayment's, generating complex hydrographic conditions in inner south-west areas of the bay as well as south-west of the prominent headlands. Easterly-component winds drive upwelling on the southern sides of the headlands in all of the sub-embayment's of the EAB (Goschen and Schumann, 1995). The sea surface temperature in the region ranges from 10 – 24 ℃ (Beckley, 1983). The wave climate is characterized predominantly by a seasonal south-westerly swell, with more extreme wave events in winter linked to storm events in the Southern Ocean and strong westerly-component winds. The alternating east-west wind reversals can occur rapidly, but usually last for a few days (Roberts, 2010).

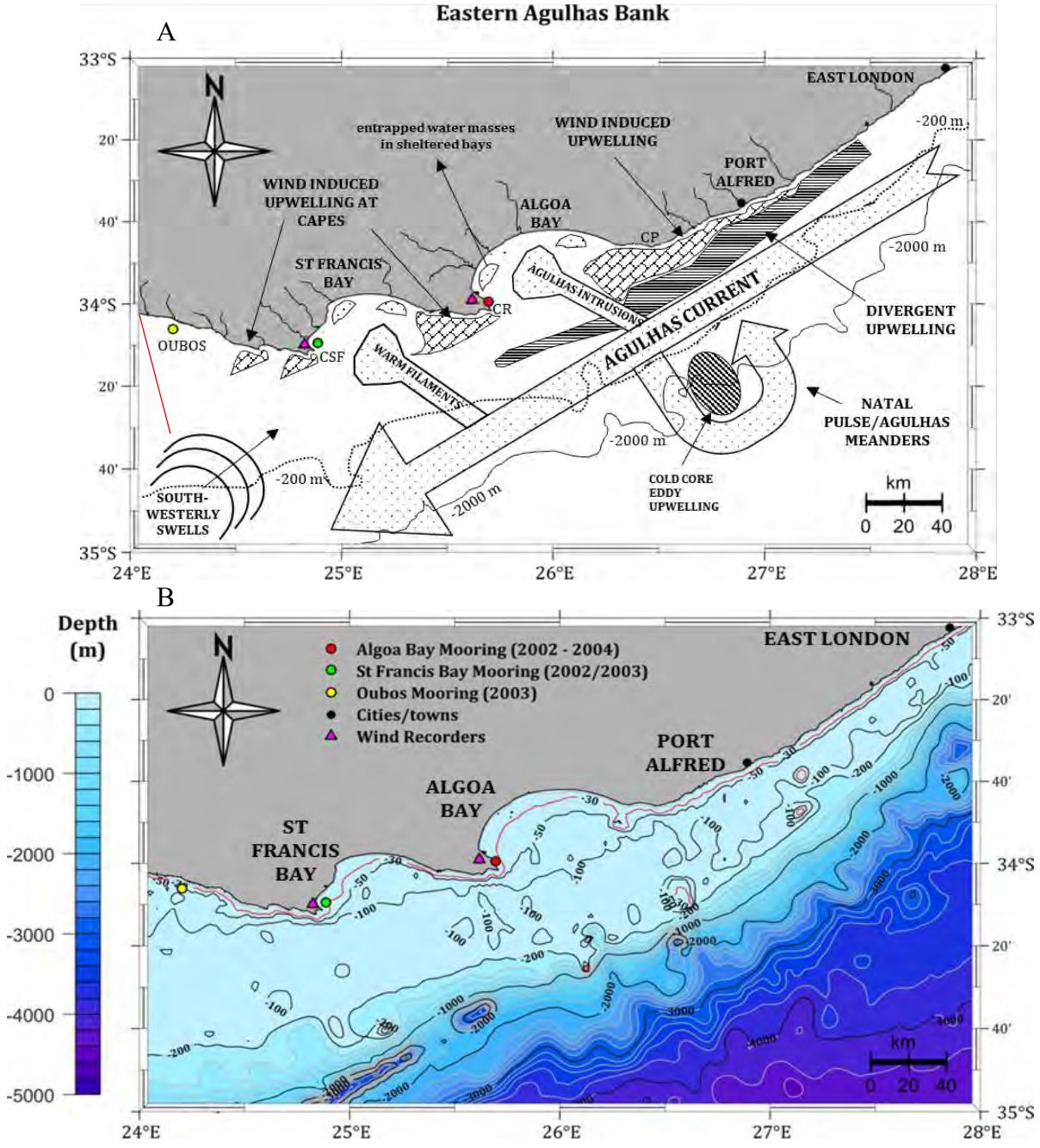

Fig 3.1: Schematic highlighting the variable oceanography of the Eastern Agulhas Bank (A) in comparison to the broadening bathymetry of the Agulhas Bank south-west of Port Alfred (B). The location of Algoa Bay (red), St Francis Bay (green) and Oubos (yellow) mooring locations are evident in both A & B. Schematic A highlights the locations of divergent and wind-induced upwelling hotspots on the EAB in relation to the in-situ instrumentation and weather stations (pink). The dominant south-westerly swells direction is also highlighted in reference to the prominent headlands of the bays on the EAB, namely; Cape St Francis (CSF), Cape Recife (CR) and Cape Padrone (PR). The red line on the left-hand side of **Fig. 3.1 (A)** highlights the location of the hydrographic cruise sampled in November, 2002.

3.1.2 Algoa Bay

Algoa Bay represents the largest of the EAB embayment's, situated between prominent headlands Cape Padrone (**Fig. 3.2**, 33° 46' S, 26° 28' E) and Cape Recife (**Fig. 3.2**, 33° 46' S, 26° 28' E). The current dominates the large-scale oceanography of the area, influenced by the presence of shear-edge eddies and plumes which penetrate over the continental shelf and into the bay during parts of the year (**Fig. 3.1A**; Krug et al., 2014). The coastal city of Port Elizabeth, aptly nicknamed 'The Windy City", is located on the western sector of Algoa Bay near the Cape Recife pinnacle (**Fig. 3.2**). The majority of oceanographic studies have focused on the western sector of the bay (Schumann et al., 2005), or the extended bay itself (Harris 1978, Lutjeharms et al., 1986, Goschen and Schumann 1998, 1994; Boyd et al., 1992, Boyd and Oberholster, 1994). The bay's mouth is ~80 km between the prominent headlands. At the same time, the coastal shelf offshore of Algoa Bay represents the transition between the AC-dominated region to the northeast and the widening Agulhas Bank to the southwest (**Fig. 3.1B**).

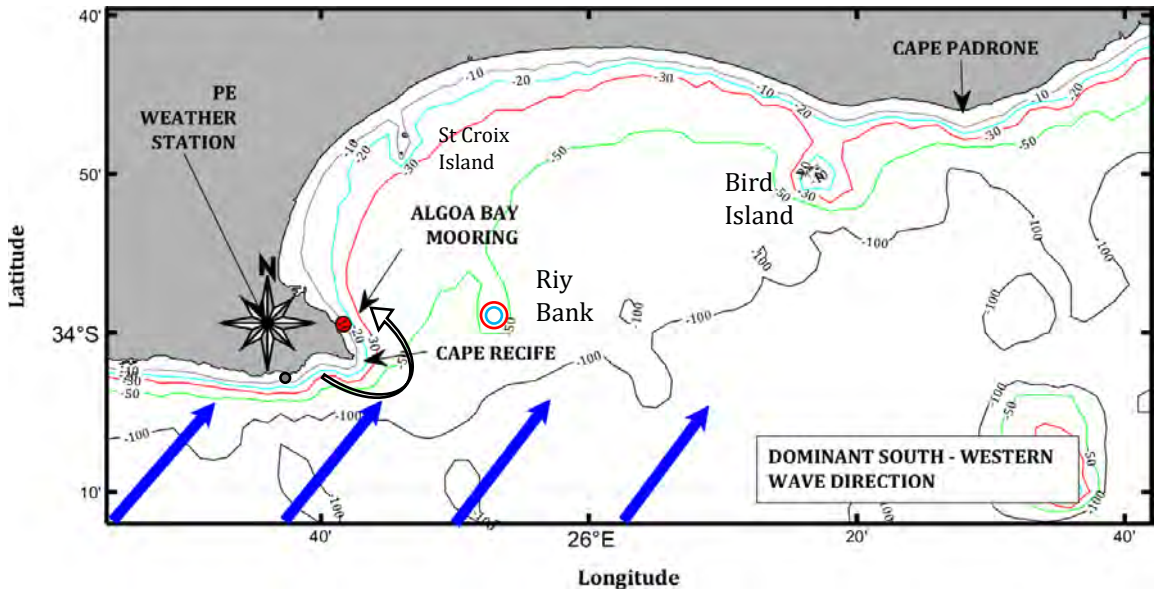

Fig. 3.2: Map showing the position of the Algoa Bay mooring in relation to the prominent headland, Cape Recife, as well as the dominant direction of south-western swell, bathymetry and potential for refraction of swell, wave height and wave period around the point. Other prominent features such as Cape Padrone, Bird Island, Riy Bank and St Croix Island are shown too. Note the convergence of the bathymetric lines near the Cape Recife pinnacle, as well as the position of the Cape Recife temperature recorder (Grey dot).

Algoa Bay is a large, relatively shallow (< 70m), log-spiral-shaped embayment of the EAB. The shape of the bay is due to the intrinsic relationship between the angle of the wave direction (**Fig 3.2**), which shapes the curvature of the shoreline (Bremner, 1983). Riy Bank is a shallow (12 – 15 m) reef situated approximately 2 km east of Port Elizabeth (**Fig. 3.2**; Bremner, 1983). Outside of Riy Bank, the bay contains two groups of islands known as Bird Island (~ 2 km South of Cape Padrone) and St Croix Island, which is found in the center of the bay toward the newly constructed Port of Ngqura (**Fig. 3.2**). Two large permanently open estuaries, namely the Sundays and the Swartkops, open into the western half of the Bay (**Fig. 3.1**).

3.1.3 St Francis Bay

Southwest of Algoa Bay is the prominent chokka spawning ground centered around St Francis Bay. St Francis Bay is often considered the center of the EAB (Jury & Goschen, 2020) and the epicenter of chokka spawning biomass and fishing pressure (Roberts et al., 2012; Sauer et al., 1992). St Francis Bay is the site for the Extended Bay Experiments of 2002 and 2003, respectively (**Fig. 3.1B**). St Francis Bay is a shallow embayment with a gentle sloping seafloor (Birch, 1981) located to the southwest of Algoa Bay (**Fig. 3.1**). Studies have shown there to be complex hydrography in the western sector of St Francis Bay (Dorfler, 2002; Roberts & van den Berg, 2002, Downey et al., 2010), with the presence of an anticyclonic flow pattern isolating the inner hydrography from that of the outer bay. The bottom topography is characterized by a course-to-fine sandy substrate interspersed with rocky patches and low relief reefs (Roberts, 1998). Two primary river systems drain into St Francis Bay, namely the Kromme river and the Gamtoos.

3.1.4 Oubos

Oubos mooring site is located north-east of the Tsitsikamma National Park, a marine protected area on the flatter coast located southwest of St Francis Bay (**Fig. 3.1**). The Oubos mooring differed from the other moorings as it represented the only mooring not within a sheltered

embayment. and therefore, was more exposed to influences of wind-forced upwelling dynamics, as well as Agulhas Current retroflection's in the same way as a bay would.

3.2 Algoa Bay Time-Series Experiment

3.2.1 Relationship between underwater visibility and turbidity

To quantify the optical clarity traversing the spawning grounds of chokka, several scientific dive records were analyzed for occurrences of zero visibility. These historical records, collected between 1992 -1999, were ascertained from logbooks of divers on Self-Contained Underwater Breathing Apparatus (SCUBA) at the DFFE Environmental Monitoring Mooring in St Francis Bay.

In this study, no attempt was made to correlate NTU values directly to particulate matter concentrations as a host of variables, including the constituent particles' physical-chemical and optical properties within the nepheloid layer remain unknown. Therefore, benthic turbidity measurements were correlated to underwater visibility via *in-situ* aquatic visibility assessments conducted by divers. Upon deployment and servicing of the OBS sensors, observers on SCUBA recorded underwater visibility as the distance between a standard Secchi disk placed adjacent to the instrument and the observer at the point at which sight of the Secchi disk becomes distorted. The correlation between NTU values and underwater visibility provides insight into the relationship between particulate matter suspended in the water column and reduction in optical clarity of the water column. The correlation between SPM and NTU is important in this study due to the reliance of visual cues in the reproductive strategy of chokka.

3.2.2 Turbidity

Benthic turbidity was quantitatively measured in hourly intervals over 17 months between 8 November 2002 and 12 March 2003 in Algoa Bay (**Fig 3.1**). The self-contained *OBS 3/OBS-3A* sensors (D&A Instruments & Engineering 1991; U.S. Patent 4,481,157), derive turbidity in the form of Nephelometric Turbidity Units (NTU) by emitting near-infrared light (875 nm) and detecting the backscatter of light off suspended particles in the water column. The backscattered light is measured at different angles and passed through a daylight-rejection filter, with sensor output in NTU dependent on the specific calibration standards suitable for the application of the study (D&A Instruments & Engineering 1991, Boss et al., 2015). Through this measurement method, turbidity is often described as the reduced transmission of light as a result of increased concentrations of particles in a water medium (Sahl et al., 1987).

Due to the neritic spawning habits of chokka squid (Hanlon et al., 1994; Sauer et al., 1997) and the proximity of the nepheloid layer to the seafloor (Zoutendyk and Duvenage, 1989), the instruments were deployed 0.83 m from the seafloor at a depth of ~ 25 m, attached to a sub-surface buoy secured to the substrate by a weighted railway track. The OBS instrument recorded turbidity at hourly intervals at 10 Hz, with NTU measurements an average from 500 readings over 50 seconds.

For the purpose of this study, measurements from the optical sensors are referenced to a turbidity standard, Formazin, and correlated to underwater visibility by divers; as such, the information on the particle's causing backscatter is not essential (Boss et al., 2015, D&A Instruments & Engineering 1991). The instruments were calibrated to a range of 0 – 250 NTU to maintain comparability with previous studies in the region (Dorfler, 2002). The Formazin standards were prepared according to the rigor provided by the "Standard Methods for the Examination of Water and Wastewater" (American Public Health Association 1998), and following procedures in the "D&A Instruments and Engineering" manual (1991).

Biofouling of the instrument sensors resulted in several instances of drift in the data baseline over time. Instrument calibration took place before and after each deployment to assess the NTU baseline shift due to growth on the sensor face. Drift in the NTU baseline was corrected for where evident by linear interpolation of the data. This involved lowering the NTU baseline based on the magnitude of the recorded drift due to biofouling on the optical sensor. In addition, large scale variation in NTU values where data reached saturation point of 250 NTU's, resulting from noise or offset errors, were discarded and replaced with interpolated data.

Optical measurements of benthic turbidity become distorted through the sometimes-rapid growth of algal hydroids on the sensor's face. If left unchecked, algal growth can lead to the habitation of amphipods of increasing size on the sensor face, resulting in the instrument baseline reaching saturation point. In cases where this occurred, data from the study was disregarded. It was noted by observers on SCUBA that many organisms, including basket stars (*Astrocladus euryale*) and Octopus (*Octopus vulgaris*), were often found on and around the mooring. The interference of organisms in front of the lens restricting light attenuation to saturation point may account for the extreme and short (≤ 2 hours) peaks in benthic turbidity sporadically present in the raw data. The data were omitted from the study.

3.2.3 Temperature

Bottom temperature (°C) data were recorded using a linear, solid-state steel-clad thermistor within the self-contained *OBS-3/OBS-3A* (D&A Instruments & Engineering 1991; U.S. Patent 4,481,157) instruments. Temperature was recorded at hourly intervals and coincide with simultaneous measurements of benthic turbidity (**Fig 3.2; red dot)**.

A second source of temperature data involved the deployment of a Star-Oddi Starmon mini underwater temperature recorder (UTR) at a depth of 6 m at Mangolds Pool (34° 2' 17.4012" S, 25° 35' 12.0012" E), southwest of Cape Recife (**Fig 3.2; grey dot**).

3.3 Wind

Prevailing wind conditions are responsible for a large proportion of the small, meso-and-large scale variation in oceanic conditions along the EAB. Hourly data on wind speed and direction obtained from the South African Weather Service (SAWS) for the Port Elizabeth (P.E.) Airport Weather Station (0035209B1). The weather station found at Port Elizabeth International Airport (*Lat: -33.9840; Lon: 35.6100*) is found inland of Cape Recife 63 m above sea level. Wind speed is measured in m/s while wind direction was orientated in degrees from North (DFN). The station, located ~ 3 km from the coast and roughly ~ 5 km from the Algoa Bay Mooring (**Fig 3.1**), ensures locality when viewing the effects of wind on temperature and turbidity within the south-western sector of Algoa Bay. The hourly data on the direction and magnitude for Algoa Bay was converted to its Meridional (-*V, North/South*) and Zonal (-U, *East/West*) components and low-pass filtered to remove wind variability within 36 hours.

3.4 Extended-Bay-Experiments

The results from previous studies on benthic turbidity highlight BNL patches of varying degrees of intensity found across the Agulhas Bank (Dorlfer, 2002; Githaiga-Mwicigi, 2012). However, the largest proportion of turbidity events occur along the nearshore coastal zone and within the EAB's log-spiral-shaped embayment's (Dorlfer, 2002). The EBE was designed to coincide with the October-November annual squid closed season, the bi-annual demersal trawls conducted by the DFFE, and the re-opening of the squid fishery. These sites were selected due to their importance to the commercial squid fishery as common spawning grounds (Sauer et al., 1992), often revisited by spawning cohorts (Oosthuizen and Roberts, 2009; Sauer et al., 1997). Therefore, the Extended-Bay-Experiments (EBE) aimed to determine the spatial-temporal variability in BNL intensity within adjacent embayment traversing the main spawning grounds of chokka

3.4.1 November Closed-Season Study, 2002

In addition to the aforementioned time series experiment, optical instruments (OBS3/OBS3-A) were placed in three locations southwest of Algoa Bay, namely; St Francis Bay (34.08.092 °S, 24.79.75 °E), Oyster Bay (33.11.092 °S, 24.39.765 °E) and Oubos (33.11.092 °S, 24.39.765 °E) (**Fig. 3.1**). The OBS instruments were calibrated according to the methods described in section 3.2.1, deployed at a height of 0.83 m off the seabed at a depth of ~ 25 m at each site.

3.4.2 November Closed-Season Study, 2003

Due to the difficulties associated with the Oubos mooring location in 2002, the site was not revisited for study in 2003. Instead, an additional optical instrument was placed in St Francis Bay (34.08.092 °S, 24.79.75 °E) for 27 days from the 18th of November to the 15th of December (**Fig. 3.1**). The OBS instrument was calibrated according to the methods described in Chapter 3.2.1. The OBS instrument was deployed at a height of 0.83 m off the seabed at a depth of ~ 25 m.

3.5 Hydrographic Survey

A hydrographic survey was carried out by the DFFE in November 2002, using the research vessel FRS AFRICANA cruise number 171. However, due to constraints in the cruise plan, hydrographic sampling of benthic turbidity events on the EAB was restricted to a singular transect (~23.8 °E) to the southeast of the EAB region defined in this study. The transect was selected and plotted using Ocean Data View. A *Sea-Bird Electronics Seacat SBE19* Conductivity, Temperature, and Depth (CTD) profiler was fitted with a *Seapoint turbidity meter* and lowered to within 10 m of the seafloor across 6 stations, from inshore to offshore (**Fig 3.1: red line**). The Seapoint turbidity meter produced an output in Formazin Turbidity Unit (FTU = NTU; D&A Instruments and Engineering 1991). The results from the hydrographic survey of November 2002 are used in conjunction with the 2002 November closed-season study.

A second cruise was conducted by the FRS AFRICANA in November 2003. Unfortunately, the turbidity sensors were left uncalibrated and unused during the cruise and were therefore omitted from this study.

3.6 Remote Sensing Data

The *in-situ* data were further analyzed and contextualized with complementary satellite data. Remote sensing techniques enabled greater volume of environmental data through which the case studies could be explored, and the physical state of the Agulhas Bank could be further examined in an effort to elucidate the intricacies of benthic turbidity events on the EAB.

Satellite observations allow the AC itself to be relatively well monitored. However, the finer spatial scales, faster dynamics, and proximity to the coastline render satellite observations less reliable for the coastal shelf waters inshore of the current (Dohan and Maximenko, 2010; Rouault et al., 2010). Due to the proximity of the *in-situ* moorings with the coastline in conjunction with the significant coastal data drop-out that is synonymous with early remote sensing data, a timeseries of remote sensing data against which to correlate *in-situ* observations proved a challenging task. Therefore, images on sea surface temperature (SST) and ocean colour (Chl-a) provided a means in which further investigation of case studies could be scrutinized. In addition, altimeter-derived measurements of significant wave height facilitate the investigation of the relationship between benthic turbidity and resuspension events, an important component of nepheloid layer dynamics.

3.6.1 Sea Surface Temperature (SST)

The key instrument used in this study was MODIS (*Moderate Resolution Imaging Spectroradiometer*), aboard the Tera and Aqua satellites (NASA). Unfortunately, from a possible 491 days across the study period from November 2002 to March 2004, only 41 cloud-free days

were available for study over the western sector of Algoa Bay. This highlights the difficulty associated with comparing *in-situ* measurements of temperature and satellite-derived measurements of SST (Rouault et al., 2010). Due to the large volume of cloud coverage on the L2P data, the OSTIA (Operational-Sea-Surface-Temperature and Sea-Ice-Analysis system) L4 data product from the ESA CCI project was used to confer the effects of upwelling and downwelling at the study sites (Donlon et al., 2007). However, this proved a cautious approach owing to the overestimation of coastal sea temperatures in reanalysis products.

The SST data was extracted from the Ocean Colour Climate Change Initiative (OC-CCI) developed by the European Space Agency Climate Change Initiative Project (ESA CCI). The OC-SST v3.1 data is freely available online at (cci.esa.int/data, Sathyendranath et al., 2019). For further information on the OC-CCI Project and related documents, please visit esa-oceancolour-cci.org.

3.6.2 Ocean Colour: Chlorophyll-a

Measurements of ocean colour provide indications of the concentration and diversity of phytoplankton. However, the remote observation of ocean colour can be limited in time and space due to numerous confounding factors, including interorbital gaps, aerosols, and clouds that obscure the ocean surface, particularly in coastal regions worldwide (Lamont et al., 2018). This is particularly true of the EAB, where remote sensing of the environment is hindered by the high volume of cloud coverage throughout the year (Lamont et al., 2018).

The ocean colour data was extracted from the Ocean Colour Climate Change Initiative (OC-CCI) developed by the European Space Agency Climate Change Initiative Project (ESA CCI). The OC-CCI v3.1 data is freely available online at (cci.esa.int/data, Sathyendranath et al., 2019). For further information on the OC-CCI Project and related documents, please visit esa-oceancolour-cci.org.

3.6.3 Altimeter-derived significant wave height (Hs)

Due to the lack of *in-situ* observations of wave conditions on the EAB between November 2002 and March 2004, altimeter-derived significant wave height, from here on referred to as Hs (m), is used in this study to infer the effect of wave state on benthic turbidity events in Algoa Bay, EAB.

Satellite altimetry is based on a simple radar principle. A short pulse of radiation with a known power is transmitted from the satellite to the sea surface, which subsequently reflects a portion of this signal back to the satellite. The received signal is a measure of the 'roughness' of the ocean, and considerable noise is associated with the returned satellite signal. Based on the round-trip the pulse takes, the distance from the earth to the satellite instrument can be detected (Schlembach et al., 2020). Scientists use altimeters to measure the ocean surface topography, as well as meaningful estimates of significant wave height, which can be defined as four times the standard deviation from the sea surface elevation (Schlembach et al., 2020). Altimeters measure along a narrow, pencil-beamed swath directly beneath the satellite (~ 10 km wide) in an orbital nature (Ribal and Young, 2019). The resolution of the along-track data is high, with data available at a frequency of 1 Hz, which equates to a measurement every ~ 7 km (Ribal & Young, 2019). The separation of ground tracks depends on the orbital geometry of the satellite, but can extend as far as 400 km between paths at the equator, with a repeat mission time of between 10 and 35 days. This means that certain satellites will only repeat ground-tracks for observations based on the orbital period of the individual satellite, which limits observational capacity to individual satellite missions and ground tracks in order to limit spatial-temporal spurious results.

For this study, measurements of Hs from satellite altimetry were taken from the European Space Agency Climate Change Initiative (ESA CCI). The daily ESA CCI Sea State Daily Multi-Sensor Along-Track L3 Product was downloaded online from the Copernicus online database (https://cds.climate.copernicus.eu/). The level-3 processed data has been calibrated against *in-situ* buoys, cross-validated between satellites, and quality controlled by the Sea State CCI. Validation of the Sea State CCI dataset V1 (January, 2020) is based on comparisons of the

altimeter Hs with *in-situ* buoy-data and numerical wave model results (Dodet et al., 2020). Further information regarding data processing and individual satellite missions can be found in the Product User Guide (Dodet et al., 2020). However, due to the lack of *in-situ* measurements of wave height along this portion of the coast and over the study period, no attempt was made to cross-validate the altimeter-derived wave height data. Therefore, the values presented here provide a gross representation of the wave state of the EAB at the time of the satellite pass and not an accurate reflection of wave state or altimeter precision.

Preliminary analysis on the ESA CCI L3 product showed that it provided calibrated, quality-controlled along-track observations from five satellite missions traversing the EAB. These include TOPEX/POSEIDON, ERS-2, GFO, ENVISAT, and JASON-1 (expressed in ascending order of launch). The 1 Hz along-track altimeter observations are determined as measurements of Hs (m) based on (Quartly and Kurekin, 2020), where Hs represents the median of wave height values within a 50 km radius of the coastally moored *in-situ* instrumentation (Tiemermann et al., 2021, *in press;* Timmermans et al., 2020a; Timmermans et al., 2020b).

Unfortunately, due to the nature of satellite-derived altimeter readings, important wave state variables including wave direction and wave period are not available. The separation of ground tracks depends on the orbital geometry of the satellite, which can extend as far as 400 km between paths at the equator, with a repeat mission time of between 10 and 35 days. This means that certain satellites will only repeat ground tracks for observations based on the orbital period of the individual satellite. The orbital periods of the satellites used in this study vary, with all but one, ENVISAT, following non-sun-synchronous orbits. Satellites JASON-1 and TOPEX/POSEIDON have a 10-day orbital period, whilst GFO has an orbital period of 17 days. Both ERS-2 and ENVISAT, however, represent the most data sparse satellite observers on the EAB, with repeat orbital periods of 35 days, respectively.

Altimeter-derived observations on Hs therefore offers gross assessment of the relative wave state at the time of the satellite pass.

3.7: Data Analysis

All plots were made using MATLAB 2016a. All physical data were tested for normality using a standard probability plot and Shapiro–Wilk test and homogeneity of variance using a Levene's test. The relationship between important variables were assessed using a correlation analysis. The vast number of unknowns associated with both the remote sensing data, the highly modified turbidity data, and large breaks in data acquisition meant that any statistical analysis conducted on these data sets would be confounded by inconsistencies associated with these factors. Therefore, this thesis provides a qualitative analysis of benthic turbidity events in relation to the overlying physical conditions at the time of the event.

CHAPTER 4

Results

4.1 Defining underwater visibility, NTUs, and cleaning the *in-situ* mooring data

4.1.1 Relationship between underwater visibility and turbidity

Analysis of 170 scientific dive records between 1992 – 1999 at the DFFE Environmental Monitoring Mooring site in St Francis Bay showed that visibility near the seabed was ≤ 1 m for 50 % of dives over the course of the decade (**Fig. 4.1**). Underwater visibility was noted to decrease with depth under various overhead conditions, with 18 % of divers reporting visibility of ~ 0 m. In comparison, 39 % of the divers reported having bottom visibility of < 0.5 m (**Fig. 4.1**).

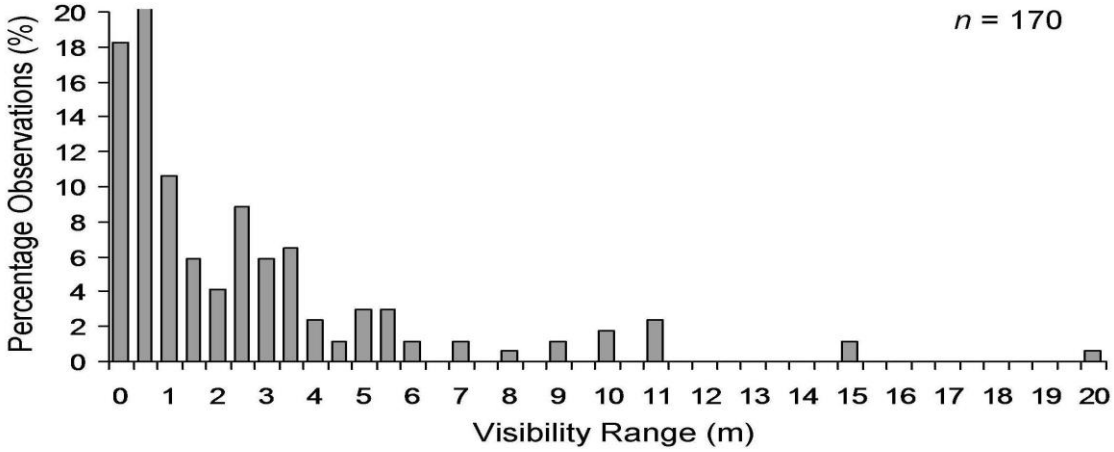

Fig. 4.1: The frequency of occurrence of underwater visibility (m) based on diver observations (n = 170) between 1992-1999 at the DFFE Monitoring Mooring in St Francis Bay, an important chokka squid spawning ground.

Before further examining the results, the relationship between turbidity (NTUs) and actual underwater visibility (m) must be understood.

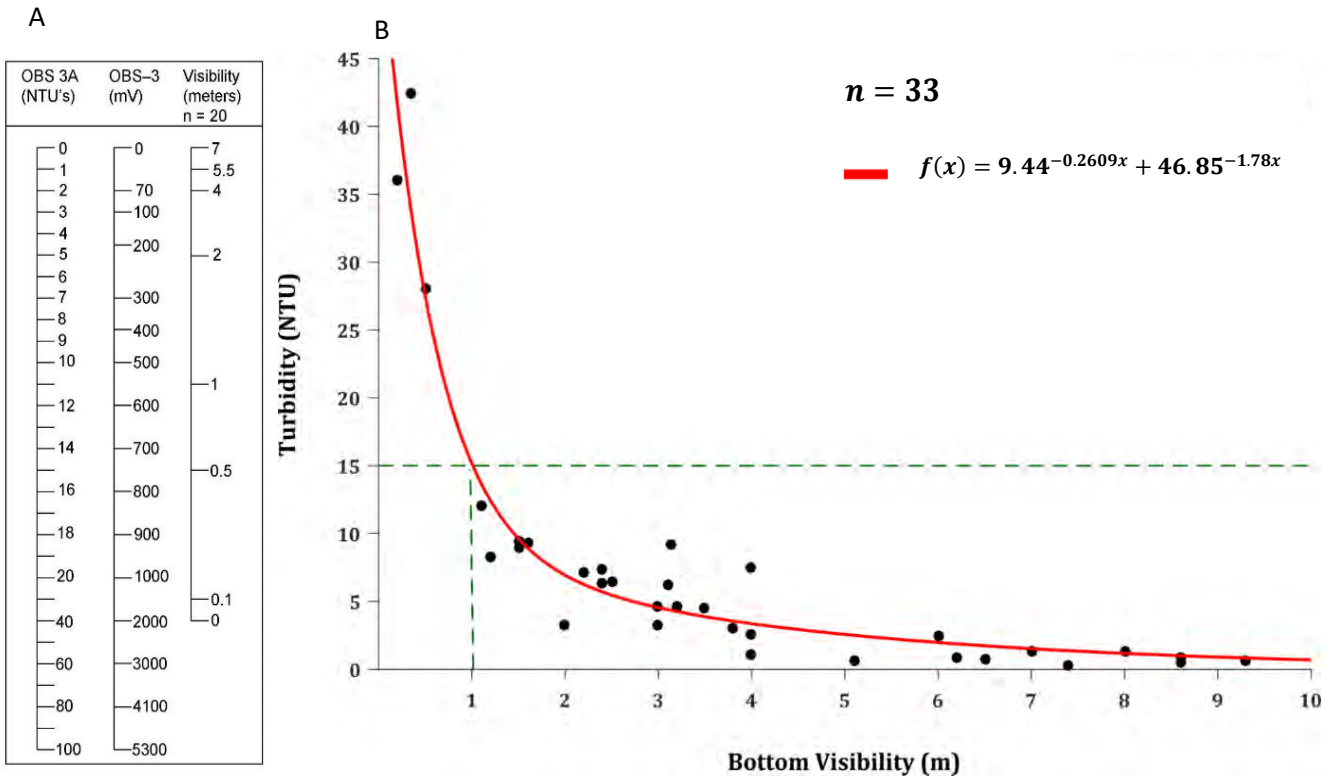

Fig. 4.2: Relationship between benthic turbidity (NTU) and underwater visibility (m) as ascertained through *in-situ* observations by divers. The non-linear relationship is given by the equation f(x), for n = 33. The left panel (1) highlights the relationship between OBS output in mV, comparative Nephelometric Turbidity Units (NTU), and bottom visibility from the study conducted by Dorfler (2002) on bottom turbidity in St Francis Bay between 1999 - 2001. This was incorporated into this study as the same instruments and techniques were used to analyse benthic turbidity. The right panel (2) highlights the relationship between NTU and bottom visibility as ascertained during the deployment period of this study.

The left panel (**Fig. 4.2A**) highlights the relationship between OBS output in mV, comparative Nephelometric Turbidity Units (NTU), and bottom visibility from the study conducted by Dorfler (2002) on benthic turbidity in St Francis Bay between 1999 - 2001. This was incorporated into this study as the same instruments and techniques were used to analyze benthic turbidity in Algoa Bay. The relationship between NTU and bottom visibility as ascertained during the deployment period of this study is evident in the right panel, **Fig 4.2B.** An inversely proportional relationship between benthic visibility (m) and turbidity (NTU) was found from diver observations, i.e., High NTUs = low visibility. The non-linear relationship is given by the

equation $f(x) = 9.44^{-0.2609x} + 46.85^{-1.78x}$ for n = 33. Analysis of both the left (**A**) and right sided (**B**) panel of **Fig 4.2** indicates that for a value of ~ ≥ 15 NTU, benthic visibility conditions are degraded to < 1 m (**Fig. 4.2B**), or less (< 0.5 m, **Fig. 4.2A**).).

Based on the comparison between underwater visibility (m) physically attained by divers and optically derived NTU (**Fig. 4.2B**), turbidity readings were divided into three qualitative brackets that best describe bottom turbidity in terms of visual impairment of the water clarity, namely; (a) *Clear* (< 5 NTU), (b) *Turbid* (5 > – ≤ 15 NTU), and (c) *Black-Out* (> 15 NTU) optical conditions. Sufficiently illuminated waters with little interference to underwater visibility through increased concentrations of SPM are described in this study as '*Clear*' benthic conditions. In contrast, '*Black-Out*' events denote dense SPM concentrations near the seafloor and represent poor visual clarity, as well as a high probability of disruption to squid spawning behaviour. On the other hand, '*Turbid*' conditions, while not dense enough to generate '*Black-Out'* events, signify the presence of elevated particulate matter concentrations that have a negative influence on underwater visibility (**Fig. 4.2B**).

4.1.2 Data quality corrections of benthic turbidity

As mentioned, biofouling also compromised the quality of the optical data evident in the time series. Where evident, drift in the data baseline was corrected for as described in Chapter 3. Instrument retrieval/service/deployment occurred every 6-8 weeks, depending on weather conditions. The extent of biofouling on and around the sensor and underwater visibility (m) was recorded during each dive. Measurements of optical clarity (m) at the time of instrument service/deployment/retrieval were used to generate the relationship between underwater visibility (m) and benthic turbidity (NTU), as seen in **Fig. 4.2B**. This relationship enabled the determination of an endpoint to which linear interpolation of the data took place. From the relationship between benthic turbidity and underwater visibility as ascertained from *in-situ* diver observations, there is an inversely proportional relationship between benthic visibility and turbidity. For the purposes of this study going forward, a value of ≥ 15 NTU highlights poor

visibility conditions on the seafloor, equating to underwater visibility of ≤ 1 m (**Fig. 4.2 (A & B)**).

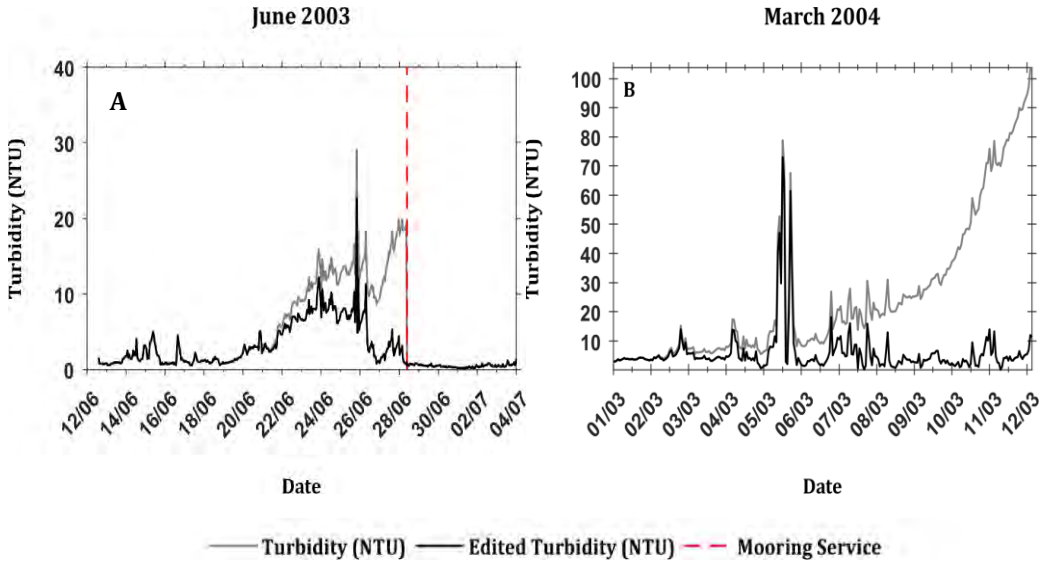

Fig. 4.3: The process of turbidity (NTU) data correction for instances of biofouling during deployment of optical sensors in Algoa Bay, from November 2002 to March 2004. The grey lines demarcate raw bottom turbidity readings, whilst the black lines show corrected bottom turbidity values. The vertical, red-dashed line indicates the date at which a service dive was undertaken.

Fig. 4.3A highlights corrected benthic turbidity following a service conducted by divers on 28 June 2003. The divers noted clear (visibility = 3.2 m) conditions at the time of instrument cleaning, with sporadic albeit minimal algal growth on the edges of the face of the optical sensor. After servicing the instrument, the data were corrected as evident via lowering the NTU baseline via linear interpolation to the end-point correlating to underwater visibility (**Fig. 4.3B**). Similarly, an example of the slow drift of the baseline NTU due to incremental growth on the face of the optical sensor at the end of a 4-week instrument deployment period between February and March 2004 can be seen in **Fig 4.3B**. Here, turbidity was corrected for fouling of the sensor at the end of deployment via linearly interpolated data based on the underwater visibility at the time of retrieval (visibility = 1.4 m; **Fig. 4.3B**).

4.2 The Algoa Bay Time Series Experiment

The hourly measurements of benthic turbidity collected on the inner-eastern side of Cape Refice (Algoa Bay) between 8 November 2002 and 12 March 2004 are shown in **Fig 4.4.** In all, the OBS sensors were deployed for 491 days (17-months). The greatest proportion of data loss occurred over six weeks from 20 December 2003 and 8 February 2004 due to instrument failure. A 10-day break in data from instrument failure occurred in December 2002 and was removed from the data set. Further interruptions, usually only a few days, occurred when the instrument was serviced, or biofouling had compromised the optical sensor; these were omitted from the data set. The loss of continuity due to instrument failure or biofouling meant only 391 days of benthic turbidity data remained.

The 17-month time series of benthic turbidity in relation to overlying physical conditions is illustrated in **Appendix A**. Within **Appendix A1 – A17**, the relationship between benthic turbidity and environmental parameters are combined to highlight the complex interplay between benthic turbidity, bottom temperature, wind, waves and primary productivity. These environmental variables will be further discussed individually in this chapter.

Note:

Appendix nomenclature: Supplementary material in the form of appendices is labelled with letters A – E. In text reference to a specific aspect of the appendices will from here on be referred to as a figure (**Fig.**) followed by the letter of the appendix (e.g., **A**) and then the specific panel or figure number (e.g., **1**). For example, as with Appendix A, the month of November 2002 will be referred to as **Fig. A1**. Similarly, the month of March 2004 will be referenced in text as **Fig. A17**

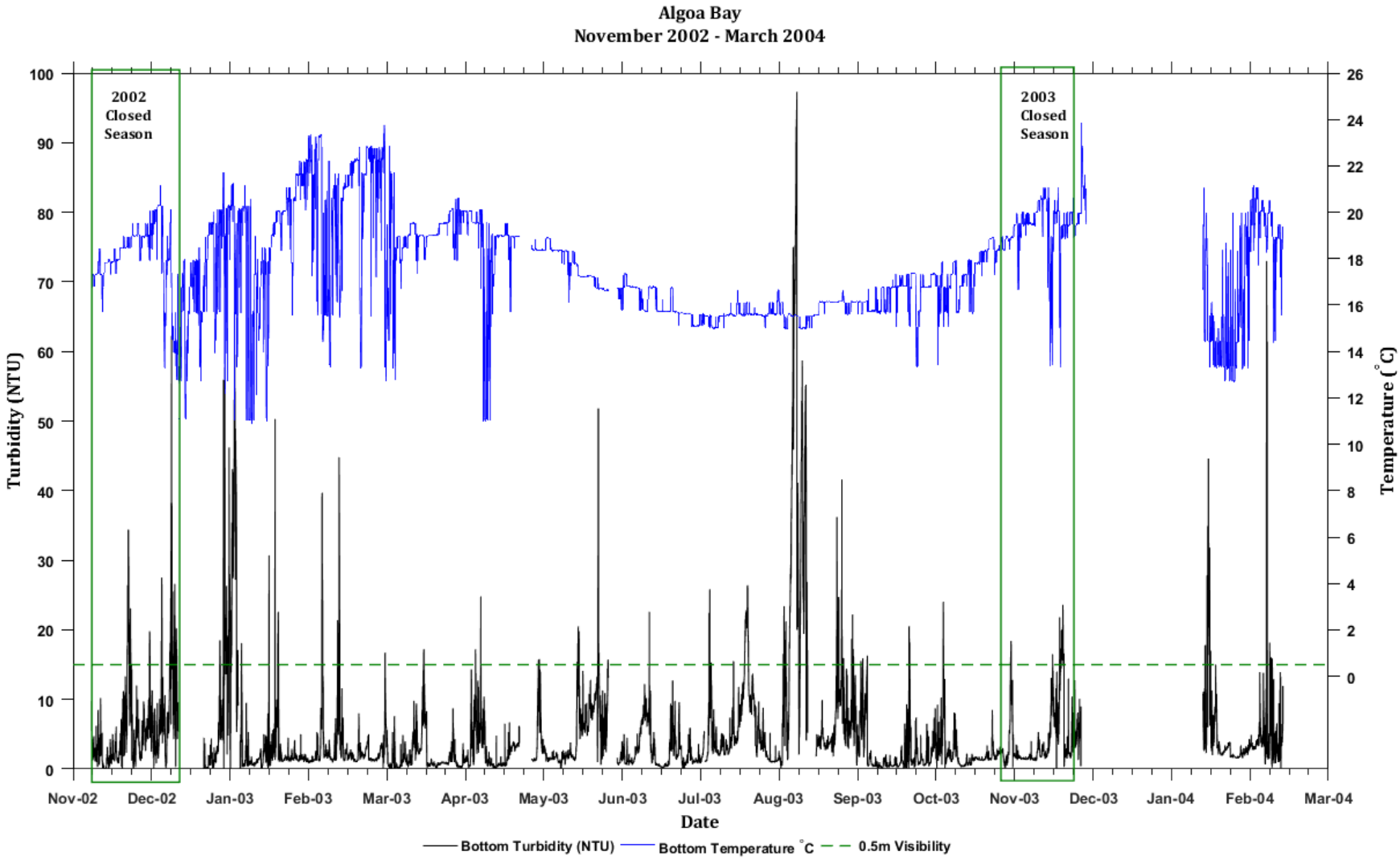

Fig 4.4: Time-series of variables turbidity (NTU) and temperature (°C) collected in Algoa Bay, at a depth of 25 m, throughout the 17-month study period (08/11/2002 - 12/03/2004). The most significant gap in the data between 21/12/2003 - 08/02/2004 occurred as a result of instrument failure. The green dotted line demarcates turbidity values representative of 1 m of visibility or less. Green boxes denote the 3-Bay & 4-Bay studies of 2002 & 2003, respectively.

4.2.1 Benthic Turbidity in Algoa Bay

The Algoa Bay time series indicates that episodic benthic turbidity events were common but highly variable throughout the 17-month sample period (**Fig. 4.4**). Analysis of the data indicates that elevated concentrations of particulate matter existed for ~ 30 % of the sample period. Non-turbid, or '*Clear*' conditions, classified as NTU values < 5 and representative of good underwater visibility, prevailed for ~ 70 % of total readings, or ~ 282 days. Benthic turbidity readings of > 15 NTU correlate to '*Black-Out'* underwater conditions with visibility of ≤ 1 m (green-dotted horizontal line, **Fig. 4.4**), account for ~ 5 % of the total readings, or ~ 27 days. Turbidity values ranging between 5 and 15 NTU are characteristic of elevated concentrations of particulate matter. While not dense enough to produce '*Black-Out*' turbid conditions on the seabed, '*Turbid* ' conditions negatively impact the visual clarity of the water column. These account for ~ 25 % of total readings, or ~ 101 days.

Measurements of benthic turbidity average 4.16 NTU (~ 2 m of underwater visibility, **Fig 4.2B**) throughout the sample period but range from 0 – 96 NTU (**Fig. 4.4**). Monthly plots of bottom temperature (°C) and corrected benthic turbidity (NTU) can be found in **Appendix C**. **Fig. C1 – Fig. C17** illustrate that turbidity events are episodic throughout the sample period, with the intensity and duration of each event highly variable. Both **Fig. 4.4** and **Fig. C1-17** highlight the variability in the duration of turbidity events, with events fluctuating in intensity from hours to several days. Note that there is no data for January 2004 and therefore no **Fig. C15**.

A cumulative frequency histogram highlighting the monthly variability in benthic turbidity based on the three classifications of optical degradation of the water column is presented in **Fig. 4.5**.

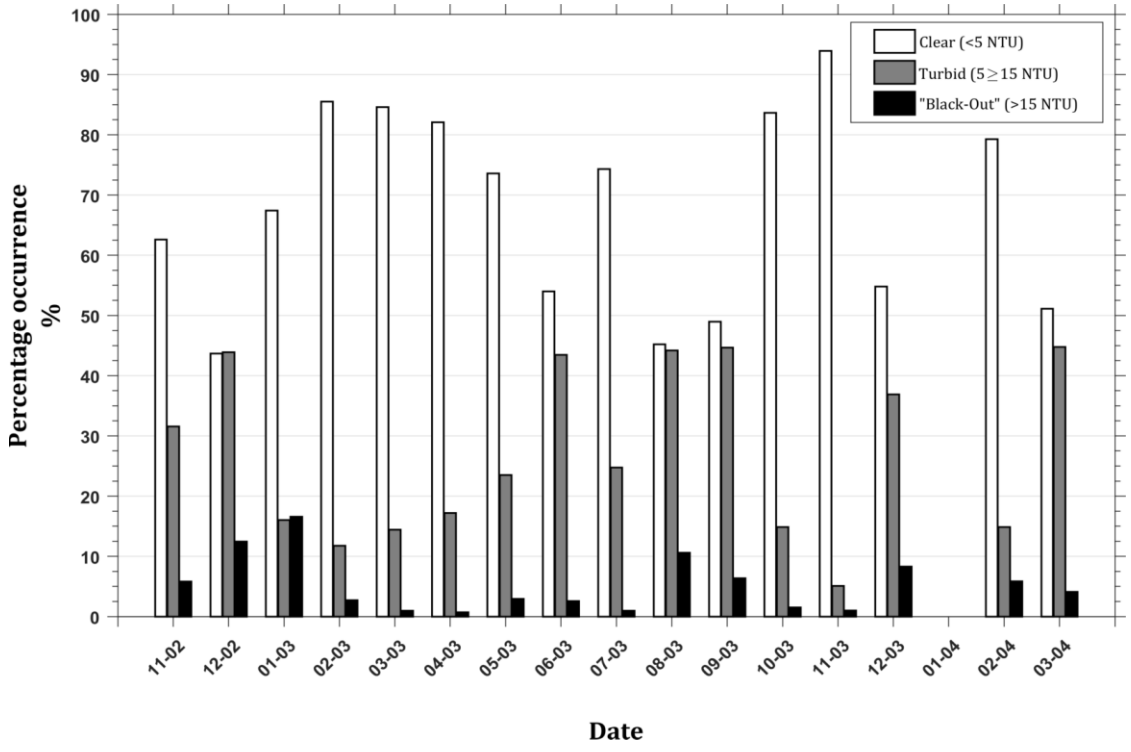

Fig. 4.5: Monthly percentage occurrence of benthic turbidity readings (NTU) in the western sector of Algoa Bay over a 17-month sample period between November 2002 and March 2004. The white bars are representative of good underwater visibility, or '*Clear*' conditions (< 5 NTU). The black bars indicate near- '*Black-Out*' turbid conditions on the seafloor (NTU > 15) whilst the grey bars, denoting NTU values of between 5 – 15 NTU, are expressive of periods of elevated concentrations of particulate matter in suspension within the water column, known as '*Turbid*' conditions.

The most common optical conditions causing '*Black-Out*' events occurred during the summer months of November 2002, December 2002 & 2003, and January 2003. A high proportion of '*Black-Out'* events are also evident in August and September 2003. '*Turbid*' water conditions, represented by the grey bars in **Fig 4.5,** were more prevalent than '*Black-out*' conditions from June 2003 to September 2003, and again in the summer months of November 2002, December 2002 and March 2004.

The seasonal climatology of optical conditions in Algoa Bay is presented in **Fig. 4.6**. Seasonality was determined using three-month austral seasons, namely, summer (December, January, February), autumn (March, April, May), winter (June, July, August), and spring (September, October, November).

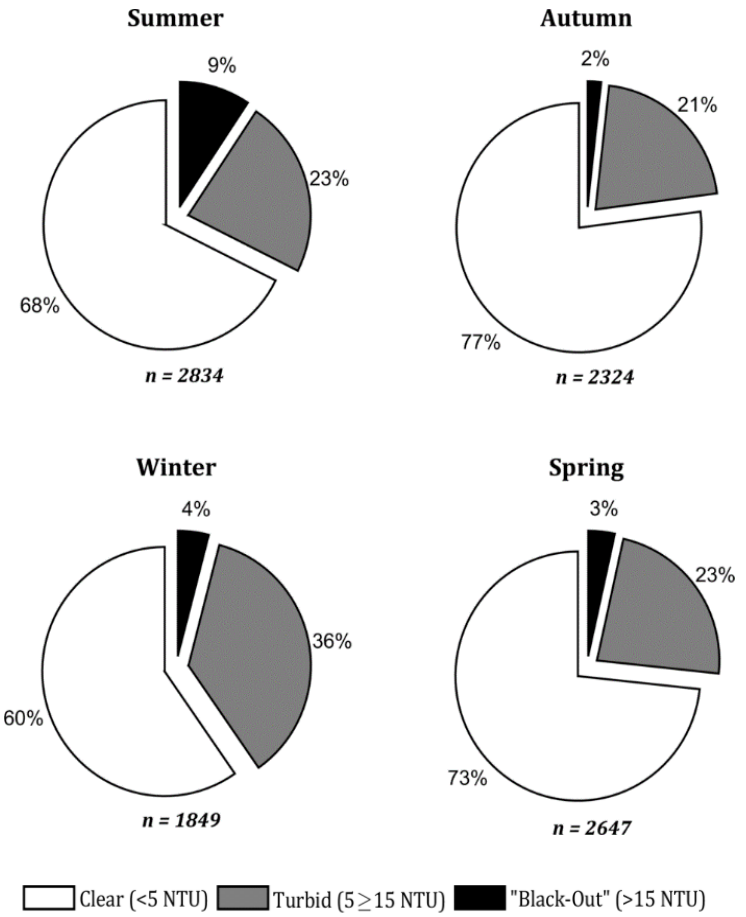

Fig. 4.6: Climatology of benthic turbidity (NTU) in the western sector of Algoa Bay throughout the 17-month sampling period (November 2002 - March 2004). The pie charts indicate the percentage occurrence of turbidity readings. The seasonal sample size (n) is given below each seasonal chart. The white segments are representative of good underwater visibility, or '*Clear'* conditions (< 5 NTU). The black segments indicate '*Black-Out'* turbid conditions on the seafloor (NTU > 15) whilst the grey segments, denoting NTU values of between 5 – 15 NTU, are expressive of periods of elevated concentrations of particulate matter in suspension within the water column, known as '*Turbid*' conditions.

Analysis of these data shows that benthic turbidity readings were on average higher during the months of summer ($x = 5.33$, $std = 7.58$, $n = 2834$), compared to winter ($x = 4.67$, $std = 4.83$, $n = 1849$). The months of spring ($x = 3.50$, $std = 4.21$, $n = 2647$) and autumn ($x = 3.10$, $std = 4.13$, $n = 2324$) hold similar trends in benthic turbidity. The months of autumn and spring had less variability in the intensity of turbidity events than summer, whose standard deviation of 7.58 NTU establishes the summer season as the season with the greatest variability in turbid conditions. Definitive understanding of the seasonal nature of these turbidity events is hindered

by the short duration of the study and sampling of the summer season twice. Furthermore, variable growth on and around the sensor presents a risk when drawing correlations between other environmental variables, e.g., temperature, as data correction procedures may confound the results.

The winter months experience the largest proportion of '*Turbid* ' water conditions compared to any other season, with a total of 40 % of the sample period in winter resembling turbid bottom conditions and subsequently, low visibility, i.e., the greatest deterrent to chokka visibility and resultant dissolution of spawning aggregates (**Fig. 4.6**). The summer season, where low visibility conditions account for 32 % of the sampled period, has the second-highest proportion of '*Turbid*' water conditions, followed by spring and autumn with 26 % and 23 %, respectively.

The most extreme benthic turbidity events generating near-zero visibility on the seafloor were found in the summer months (**Fig. 4.5 and Fig. 4.6**). In summer, '*Black-Out*' turbid conditions account for 9 % of the total readings compared to only 2 %, 3 %, and 4 % of readings in autumn, spring, and winter, respectively (**Fig. 4.6**). The frequency of '*Black-Out*' turbidity events increased throughout the summer months, ranging from 5 % in November 2002 to 16 % in January 2003 (**Fig. 4.5**). The increasing frequency of more densely concentrated turbid waters is seen again in the summer months of November 2003 – March 2004, albeit without any data from January 2004 (**Fig. 4.5**).

A drop-off follows summer in the frequency of '*Black-Out*' turbid conditions leading into autumn and winter (**Fig. 4.5 & Fig. 4.6**). Conditions classified as '*Turbid* ' are more prevalent out of the summer months, increasing in frequency of occurrence between March and June 2003 (**Fig. 4.5**). The highest monthly average of ~16 NTU was recorded in August 2003, due mainly to the high turbidity readings from 22 August to 30 August (**Appendix B**).

4.2.2 Bottom Temperature in Algoa Bay

The OBS instrument recorded simultaneous measurements of temperature and turbidity. The daily bottom temperatures from November 2002 to March 2004 at a depth of ~25 m is shown in **Fig. 4.7**. The values and seasonal trends are similar to those found elsewhere in the nearshore environment on the EAB (e.g., see Downey, 2002; Oosthuizen & Roberts, 2009). The bottom temperature ranged between 10.90 and 24.38°C, with an average of 17.64 ± 2.78 °C.

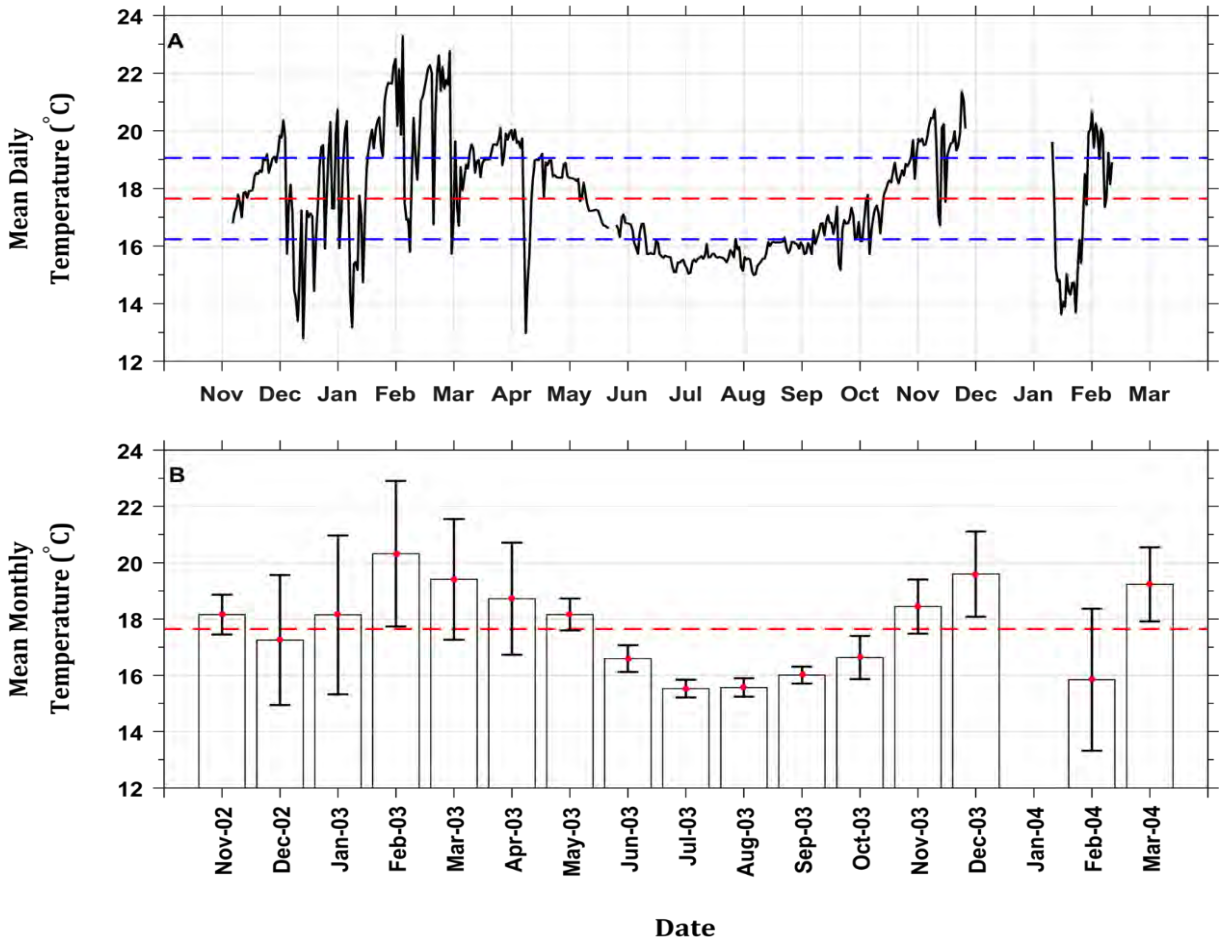

Fig. 4.7: Average daily bottom temperature (A) and monthly averages of bottom temperature in Algoa Bay. The red-dotted line in A and B denote the average bottom temperature over the time-series of 17.64 °C. The blue-dotted lines in (A) indicate standard deviation from the mean, equal to ± 2.78 °C. The error bars in (B) show monthly variation from the mean.

Temperature changes recorded in this study of + 6.27 °C/h^{-1} and - 7.33 °C/h^{-1} illustrate the extent to which temperature influences the benthic environment in Algoa Bay. Furthermore, the temperature regime evident in **Fig. 4.4** and **Fig 4.7** highlights the speed at which variability in bottom temperature occur on the nearshore coastal zone of the EAB. Seasonal climatology of temperature readings, presented in **Fig. 4.8** below, highlight that the temperature was on average higher during the months of autumn (*x = 18.85, std = 1.79, n = 2324*), compared to summer (*x = 18.25, std = 2.88, n = 3143*), spring (*x = 17.24, std = 1.23, n = 2682*) and winter (*x = 15.86, std = 0.61, n = 2091*).

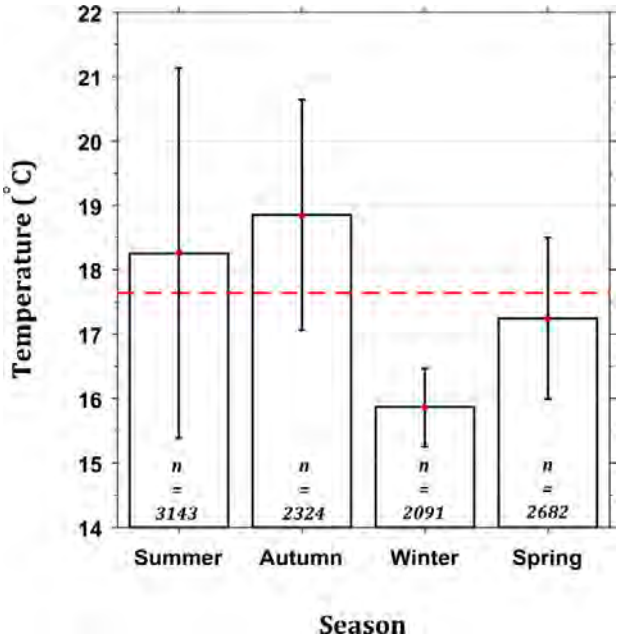

Fig. 4.8: Seasonal average in bottom temperatures (°C) recorded in Algoa Bay between November 2002 and March 2004. Error-bars denote standard deviation from the mean whilst the number of samples (n) are provided in each bar. Red dotted-line shows average bottom temperature throughout the sample period, *17.64 ± 2.78 °C.*

The temperature fluctuates to a much greater extent in the summer months than the more stable temperature regime in winter. The error bars in **Fig 4.7B** and **Fig 4.8** further highlight the variability in bottom temperatures in summer in comparison to the other seasons. The top panel of **Fig. 4.9** highlights the spread of bottom temperature readings throughout the 17-month deployment period, with over 25 % of all readings found within 16.1 – 17 °C. Only 9 % of all readings were found below 16 °C. The bottom panel of **Fig. 4.9** highlights the seasonal variation

in the bottom temperature structure in Algoa Bay. In summer, bottom temperatures ranged from 10.1 – 25 °C, while in spring, bottom temperatures did not exceed 19 °C. The temperature regime shown for autumn explains the higher autumn temperature average as there is a higher seasonal percentage occurrence of temperatures between 17.1 and 22 °C for autumn compared to other seasons (**Fig. 4.9**).

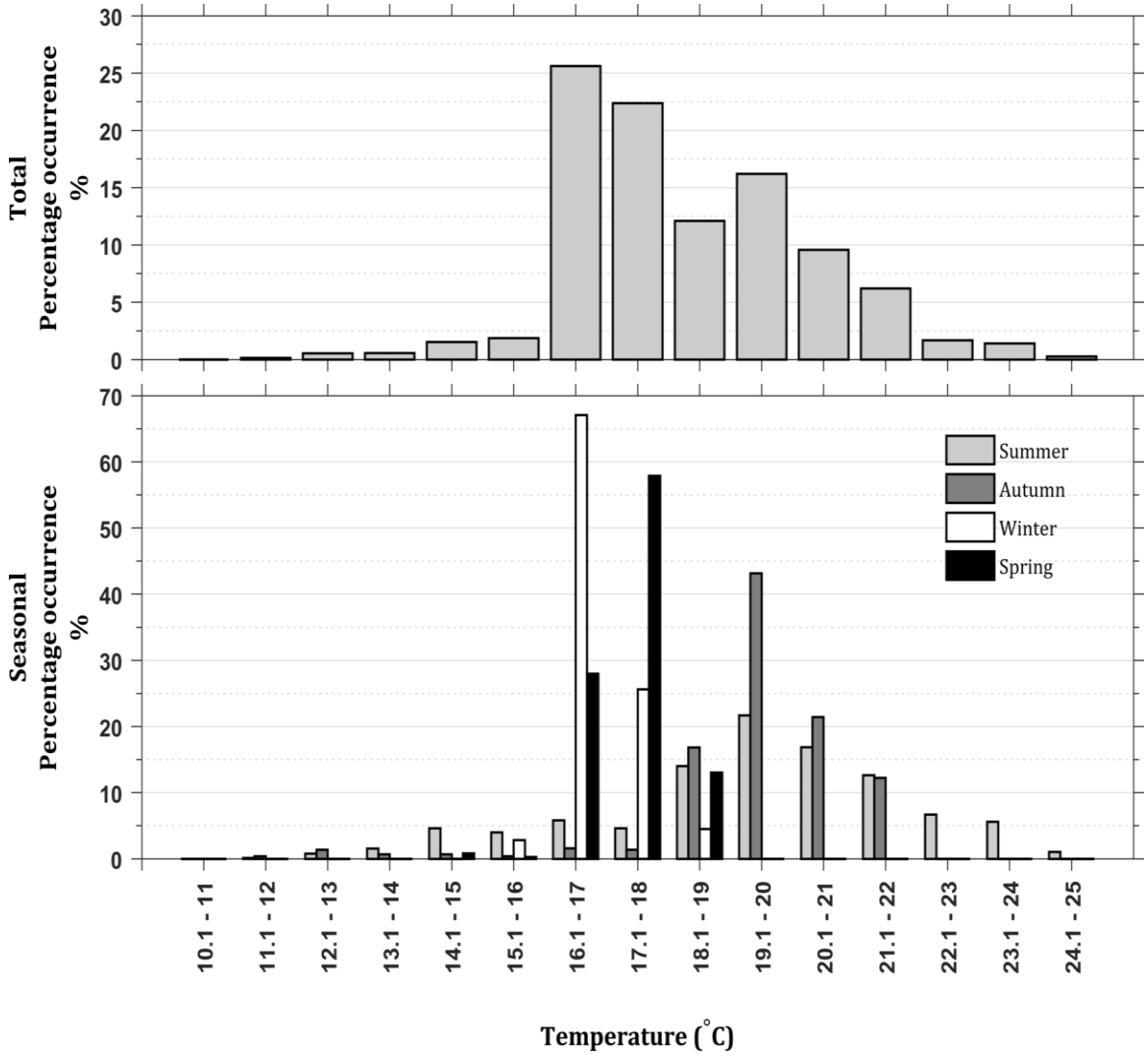

Fig. 4.9: Total percentage occurrence and monthly percentage occurrence of benthic temperatures found in Algoa Bay over the course of 17-months from November 2002 – March 2004. Seasonal percentage occurrence is calculated from 10 238 hourly measurements of bottom temperature (°C).

4.2.3 Relationship Between Bottom Temperature and Turbidity

While temperature and benthic turbidity are analyzed independently above, combined, they show a complicated relationship as seen in **Fig. 4.4** and **Appendix A**. At times, elevations in benthic turbidity coincide with changes in bottom temperature, while in others, they occur in the absence of a change in bottom temperature. Furthermore, there are occasions when optical conditions remained unchanged on the seafloor during temperature changes. A few examples of this duality are exhibited in **Fig. 4.10**.

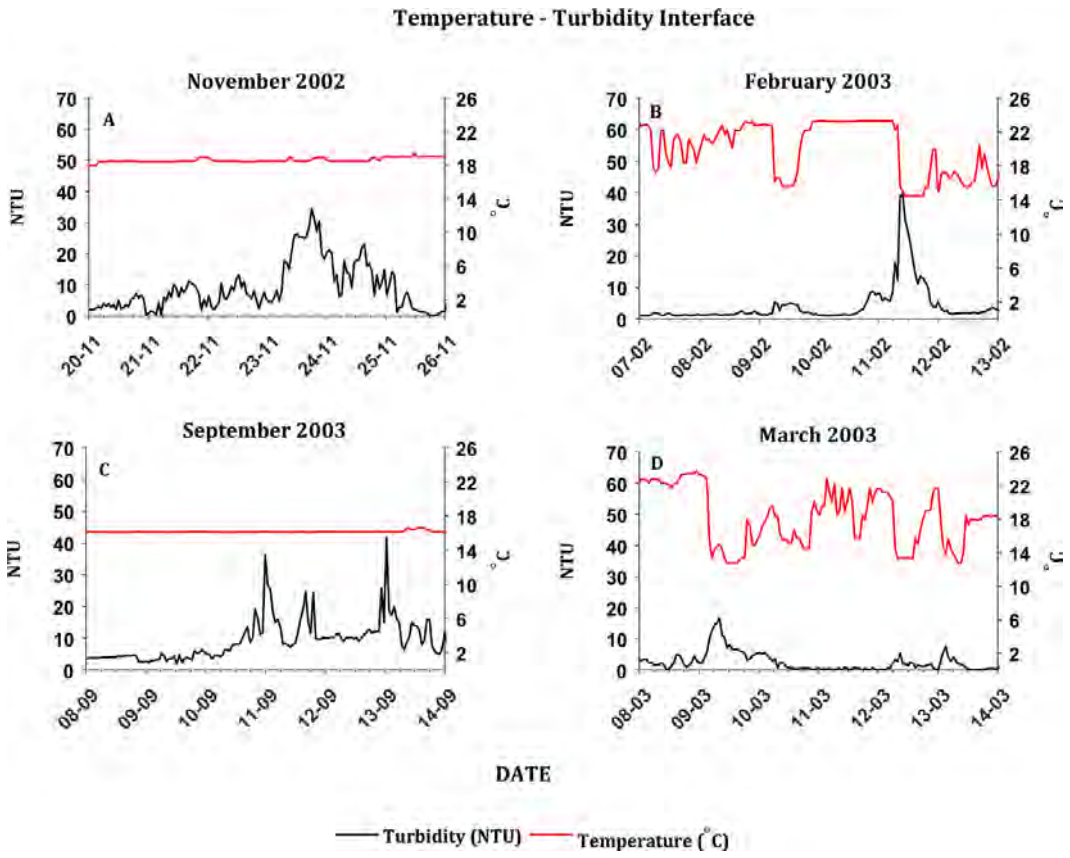

Fig. 4.10: The relationship between bottom temperature (°C) and episodic benthic turbidity events (NTU) in Algoa Bay. The left-sided panels (A & C) highlight incidents where bottom turbidity events occur in the absence of temperature fluctuations (i.e., upwelling). The right-sided panels (B) highlight occurrences of benthic turbidity events coinciding with the phenomenon of upwelling and when upwelling occurs without a subsequent increase in benthic turbidity (D). The above figures were extracted from **Fig. C1**, **Fig. C3**, **Fig. C11** and **Fig. C5**.

The greatest monthly variability in bottom temperature and turbidity co-occurred in January 2003. Measurements of benthic turbidity in January 2003 average 7.15 ± 8 NTU, suggesting that the optical conditions in Algoa Bay fluctuated between '*Clear*' and '*Black-Out*' conditions throughout the month. From the error bars on monthly turbidity present in **Fig 4.11**, it is clear that the variability is greater intra-annually within austral summer than austral winter. The month of February 2003 shows high variability in benthic turbidity and a less variable bottom temperature structure than January 2003.

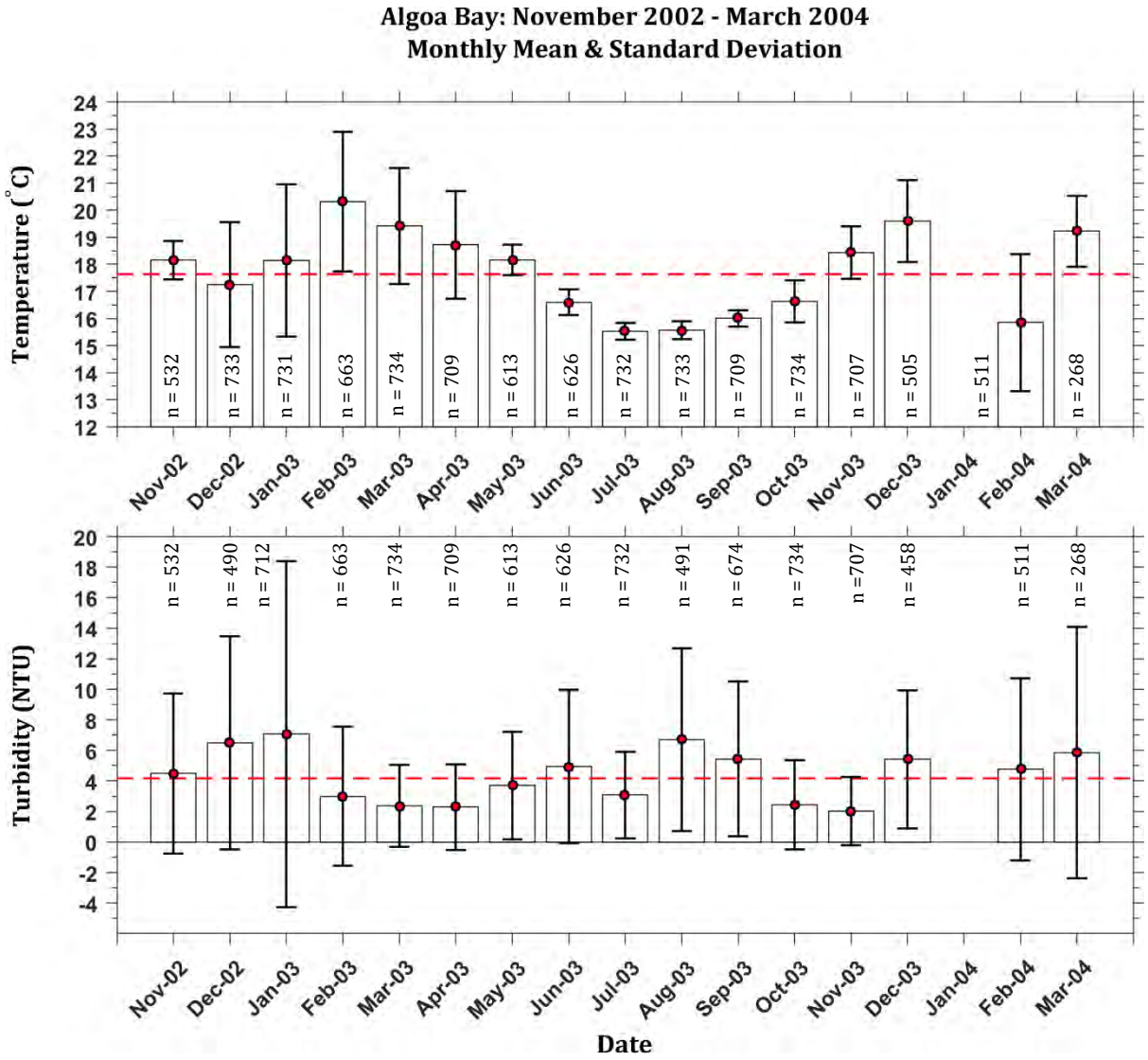

Fig. 4.11: Monthly mean of bottom temperature (°C) and turbidity (NTU) collected over 17-months from November 2002 - March 2004. Error bars represent standard deviation from the monthly mean. Monthly sample size (n) is apparent above the respective monthly bar. Red-dotted lines denote the average across the timeseries, 17.64 °C and 4.16 NTU, respectively.

The lowest monthly variability in bottom temperature between June and September 2003 coincides with a variable benthic turbidity regime in those months (**Fig 4.11**). In terms of benthic turbidity, March, April, October, and November resemble the months with the least variable optical conditions in Algoa Bay. This coincides with a decrease in temperature variability coming out of austral summer and then again linked to increased temperatures in austral spring, 2003. It is clear from this figure that the relationship between benthic turbidity and bottom temperature on the western sector of Algoa Bay is complex.

4.3 Wind

Wind forms an important factor in controlling the spatial and temporal variability in oceanographic conditions in Algoa Bay (Schumann et al., 1982, 2005). From a possible 12408 measurements of wind speed and direction, 12075 Observations were analyzed with a total of 333 missing values. The missing data constitutes less than three percent of the total data, and the remaining data is considered to be valid. Hourly data on wind speed ($m.s^{-1}$) and wind direction (Direction from North) were converted to Zonal (East-West) and Meridional (North-South) velocity components (**Fig 4.12**). A seven-day running mean, used to assess the long-term trend in the wind field at the Port Elizabeth Airport Weather Station, is plotted in red and highlights the dominance of the South-Westerly wind components throughout the sample period. Intermittent North-Easterly component winds, which drive nearshore variability in environmental forcing on the EAB, occur in periods less than one week (**Fig 4.12**; Schumann et al., 2005) and are more prevalent in summer.

The seasonal nature of the wind field across Port Elizabeth, western Algoa Bay, is highlighted in **Fig. 4.13**. A west-south-westerly (WSW) wind predominated throughout the 17-month time series, encompassing 22 % of all measurements on wind direction, while 17 % of the sampled data was orientated in the East-South-Easterly (ESE) direction (**Fig 4.13A**).

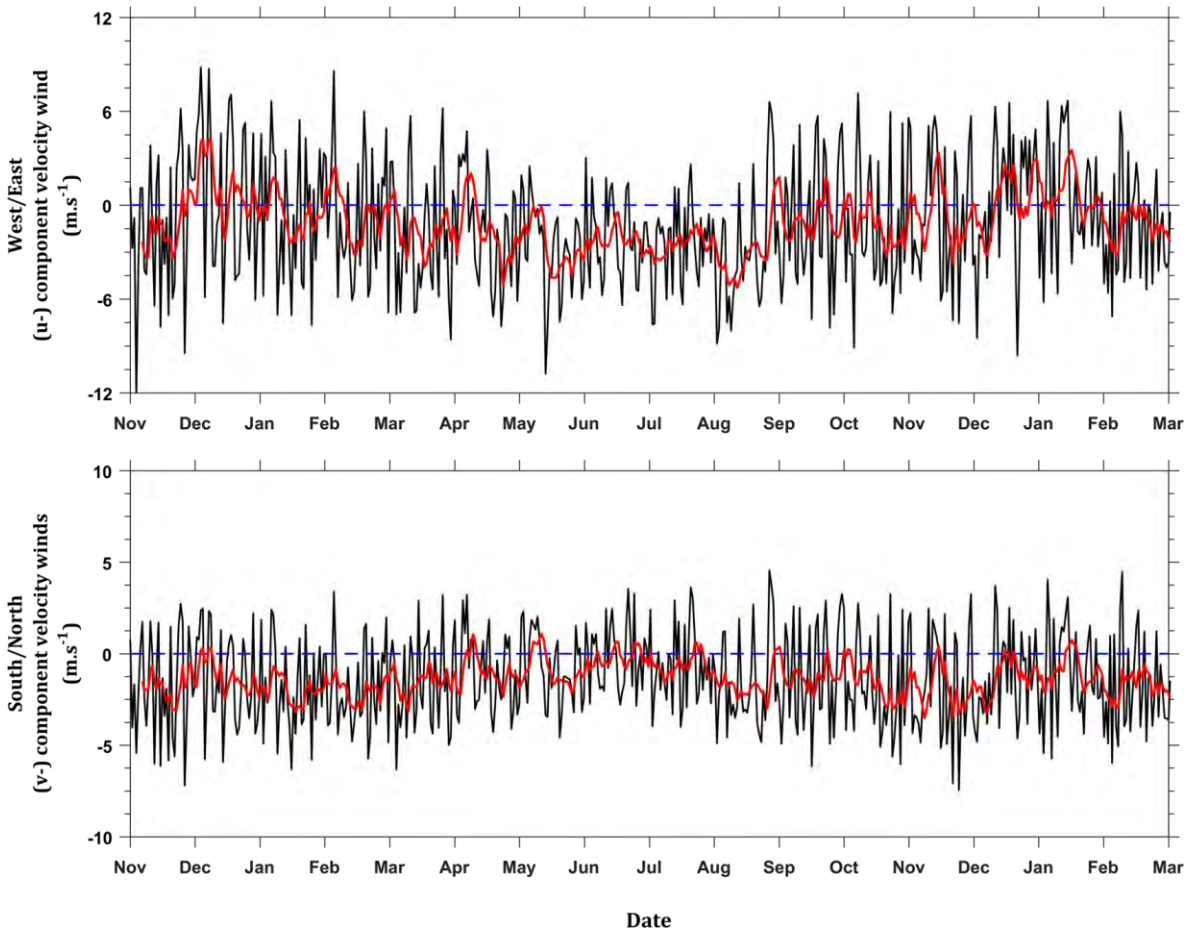

Fig. 4.12: Daily averages of Meridional (North/South, V) and Zonal (West/East, U) velocity components over a 17-month time frame from November 2002 - March 2004 at PE International Airport. A seven-day running mean is plotted in red.

In summer, the frequency and intensity of easterly-component winds increase, promoting upwelling at prominent capes along the EAB. Of notable interest here is that the strongest and most intense winds occur in a North-Easterly (NE) direction (**Fig. 4.13**). While westerly-component winds dominate throughout the year, easterly-component winds are an essential factor in driving offshore Ekman surface transport resulting in frequent yet short-term (3-7 days) upwelling during summer months (**Fig. 4.12** and **Fig 4.13**). A comprehensive set of monthly wind roses can be found in **Appendix D**. **Fig. 4.13A** highlights the principal wind axis for PE Airport across the duration of the study period and the seasonal variation in wind regime on the coast (**Fig 4.13 B – E**).

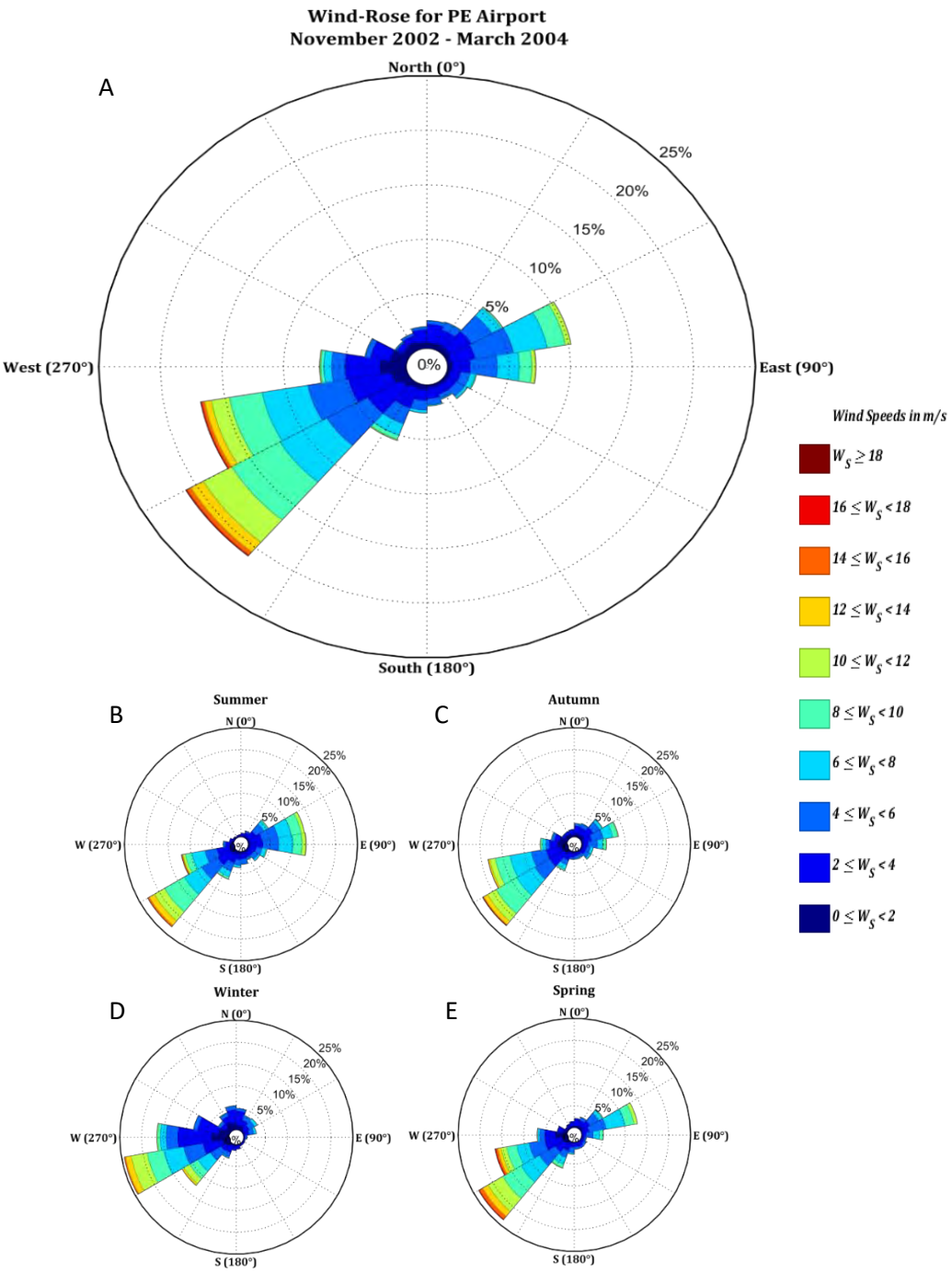

Fig. 4.13: Wind Rose highlights wind speed and direction from Port Elizabeth Weather Station (*0035209B1, 63 m above sea level*) between November 2002 and March 2004 (A). Seasonal wind roses are given in B – E. Colour bands indicate wind speed ranges in $m.s^{-1}$. Values around the concentric circles show the percentage of time wind is blowing towards a particular direction, with the longest spikes highlighting the wind direction with the greatest frequency. Wind direction is measured relative to true north.

4.4 Altimeter-derived Significant Wave Height (Hs) and Benthic Turbidity Events on the EAB

The results presented here indicate that SPM resuspension influences the intensity, prevalence, and longevity of benthic turbidity events on the EAB. A linear regression analysis ($r = 0.38$, $p = 0.0028$, $n = 61$) highlights a statistically significant ($p < 0.05$), positive correlation between altimeter-based significant wave height (Hs; m) and benthic turbidity (NTU) in Algoa Bay (**Fig. 4.14F**).

Individual satellite altimeter missions were assimilated based on the ground tracks' geographical proximity to one another, traversing locations on the Eastern Agulhas Bank (24 – 28 ° E). The geographical locations with corresponding satellite missions and ground tracks are presented in **Fig. 4.14**, namely; **(A)** Algoa Bay, **(B)** Cape Padrone, **(C)** Cape Recife, **(D)** St Francis Bay, and **(E)** Oubos. A total of four satellites (TOPEX/POSEIDON, ENVISAT, GFO & JASON-1) tallying 15 individual passes were used in the spatial analysis. ENVISAT, delineated by dark blue in **Fig. 4.14**, had the most satellite passes over the EAB with seven (986, 973, 528, 515, 442, 70 & 57). GFO passes demarcated as yellow (**Fig. 4.14**), was represented on the EAB with a total of four passes (29, 115, 328, and 414). Both satellites JASON-1 (light blue, 20 & 183) and TOPEX/POSEIDON (green, 96 & 183) were represented by two passes each (**Fig. 4.14**).

As the altimeter-derived measurement of Hs provides only an indication of the wave state at the time of the pass, hourly optical measurements of benthic turbidity (NTU) were compared with Hs (m) measurements based on various constraints of time around the satellite pass. Regression analysis was performed between the spatially aggregated satellite passes (**Fig 4.14, A – E**) and four classifications of temporal means of benthic turbidity encompassing the timing of the individual satellite pass. Time-dependent means of turbidity were generated based on the amount of time either side of the satellite pass from which the NTU is averaged — i.e., Hourly, 6-Hour Mean, 12-Hour Mean, and 24-Hour Mean. The results of the spatial-temporal correlation analysis are shown in **Table 1**. The results of the spatial-temporal regression analysis indicate

that the relationship between Hs and NTU increases with increasing time around the satellite pass and decreasing distance from the mooring.

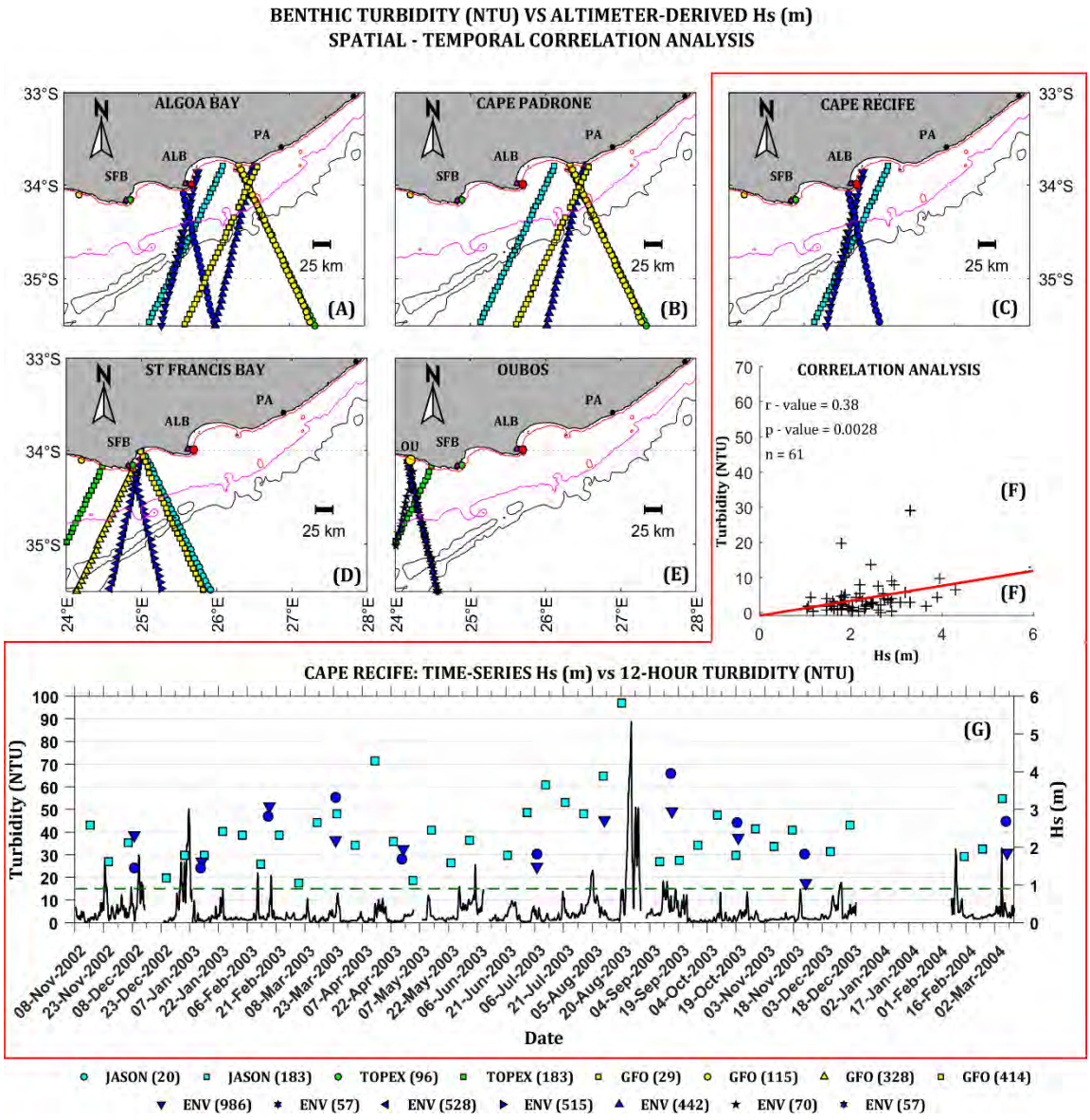

Fig. 4.14: Spatial - temporal regression analysis between geographically assimilated observations of Hs (m) and benthic turbidity (NTU on the Eastern Agulhas Bank (24 – 28 °E). The geographically partitioned satellite passes are shown in A – E, namely; (A) Algoa Bay, (B) Cape Padrone, (C) Cape Recife, (D) St Francis Bay and (E) Oubos. The results from the regression analysis for Cape Recife as well as the timeseries of Hs recorded for the Cape Recife location are seen at (F) and (G), respectively. Coastal bathymetry is represented by the red, magenta and black lines, denoting the 30 m, 200 m and 2000m isobaths, respectively. Port Alfred (PA), Algoa Bay (ALB, red dot), St Francis Bay (SFB, green dot) and Oubos (OU, yellow dot) are shown.

Table 1: Summary of spatial-temporal linear regression analysis between altimeter-derived measurements of significant wave height (Hs) and optically-derived measurements of benthic turbidity (NTU). Individual satellite altimeter missions were assimilated based on the ground tracks geographical proximity to one another and the specific sites of interest traversing the Eastern Agulhas Bank (24 – 28 ° E). Regression analysis was performed between spatially aggregated satellite passes and four classifications of temporal means of benthic turbidity surrounding the timing of the satellite pass, namely, Hourly, 6-Hour Mean, 12-Hour Mean, and 24-Hour Mean. The Cape Recife 12-hour NTU mean, highlighted in bold, is used in this study.

Benthic Turbidity (NTU) vs. Altimeter-Derived Hs (m)

Geographical location	Hourly NTU			6 - Hour NTU Mean			12 - Hour NTU Mean			24 – Hour NTU Mean		
	r	p	n	r	p	n	r	p	n	r	p	n
All Passes	0.09	0.1000	314	0.18	0.0017	316	0.20	0.0003	319	0.16	0.0034	329
Algoa Bay	0.16	0.0590	142	0.24	0.0032	144	0.29	0.0003	146	0.25	0.0021	150
Cape Padrone	0.14	0.1200	121	0.23	0.0111	123	0.28	0.0014	125	0.25	0.0051	128
Cape Recife	0.12	0.3602	71	0.29	0.0240	61	**0.38**	**0.0028**	**61**	0.38	0.0017	64
St Francis Bay	-0.00*	1.0000	139	0.08	0.3800	139	0.10	0.2200	141	0.09	0.2703	147
Oubos	0.24	0.0670	61	0.37	0.0032	62	0.41	0.0010	62	0.30	0.0017	64

* The actual value is equal to -7.1e-04

The strongest correlation that suited the need to reduce spatial-temporal variability was found between passes over the geographical location in closest proximity to the *in-situ* mooring at (**Fig. 4.14C**) Cape Recife with a 12 – hour temporal NTU mean. The monthly (**Fig. 4.15**) and seasonal (**Fig. 4.16**) climatology indicate the average wave state across the EAB to resemble Hs > 2 m throughout the year. This is in agreement with previous studies suggesting that Hs conditions greater than 2 m exist on the EAB for 70 % of the year (McLachlen, 1983; CSIR, 1981, 1987).

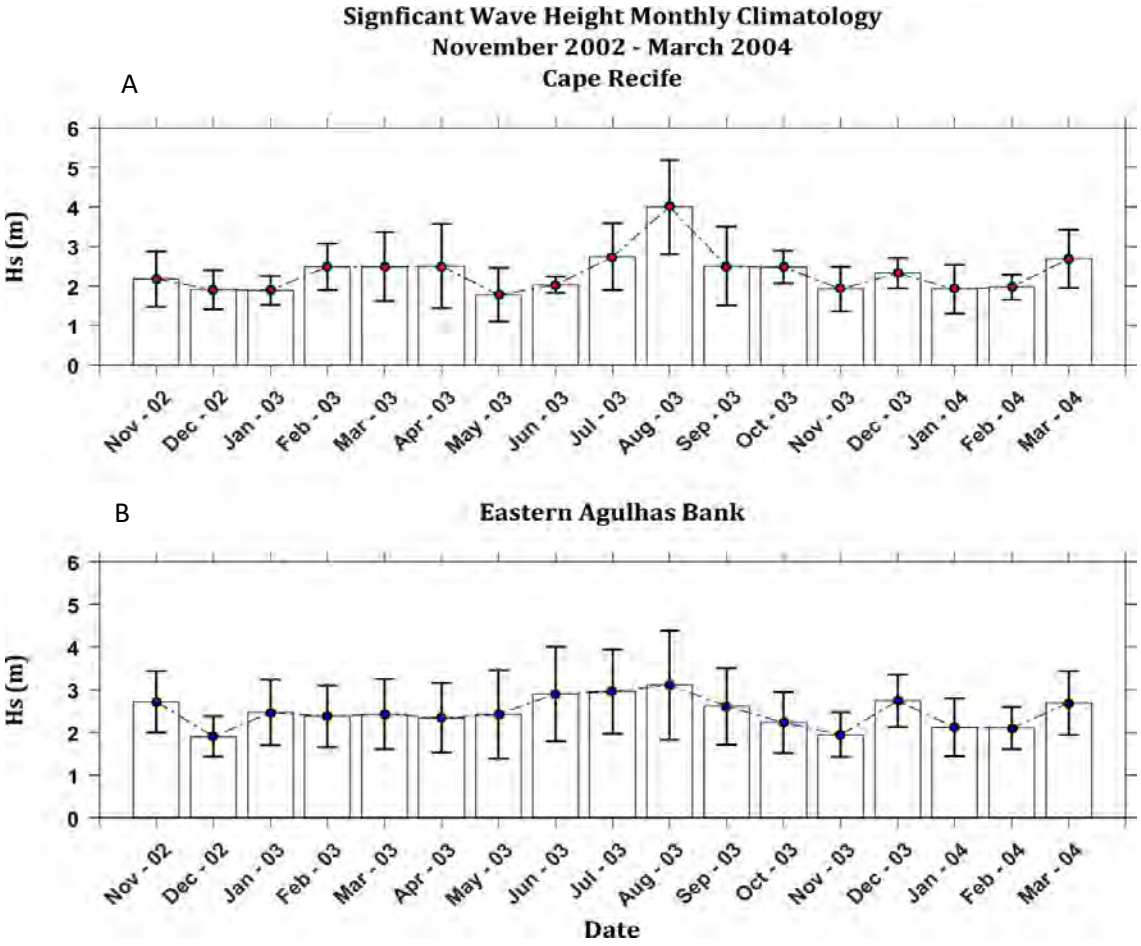

Fig. 4.15: Monthly climatology of altimeter-derived significant wave height (Hs; m) for Cape Recife (A) and the greater Eastern Agulhas Bank (B). Error bars denote standard deviation from the mean whilst the values within the bars highlight the number of Hs counts per month.

The most variable wave states occur in the winter months compared to those in summer and autumn (**Fig. 4.16B**). Furthermore, the seasonal comparison between measurements at Cape Recife and the greater EAB highlights minimal deviation in terms of the general seasonal trend of altimeter-derived Hs (**Fig. 4.16**). It is important to note that the volume of satellite missions and passes are greater for the EAB (4 satellites, 15 passes) than Cape Recife (2 satellites, 3 passes). However, it remains clear that winter experiences the highest average and variability in Hs compared with other seasons.

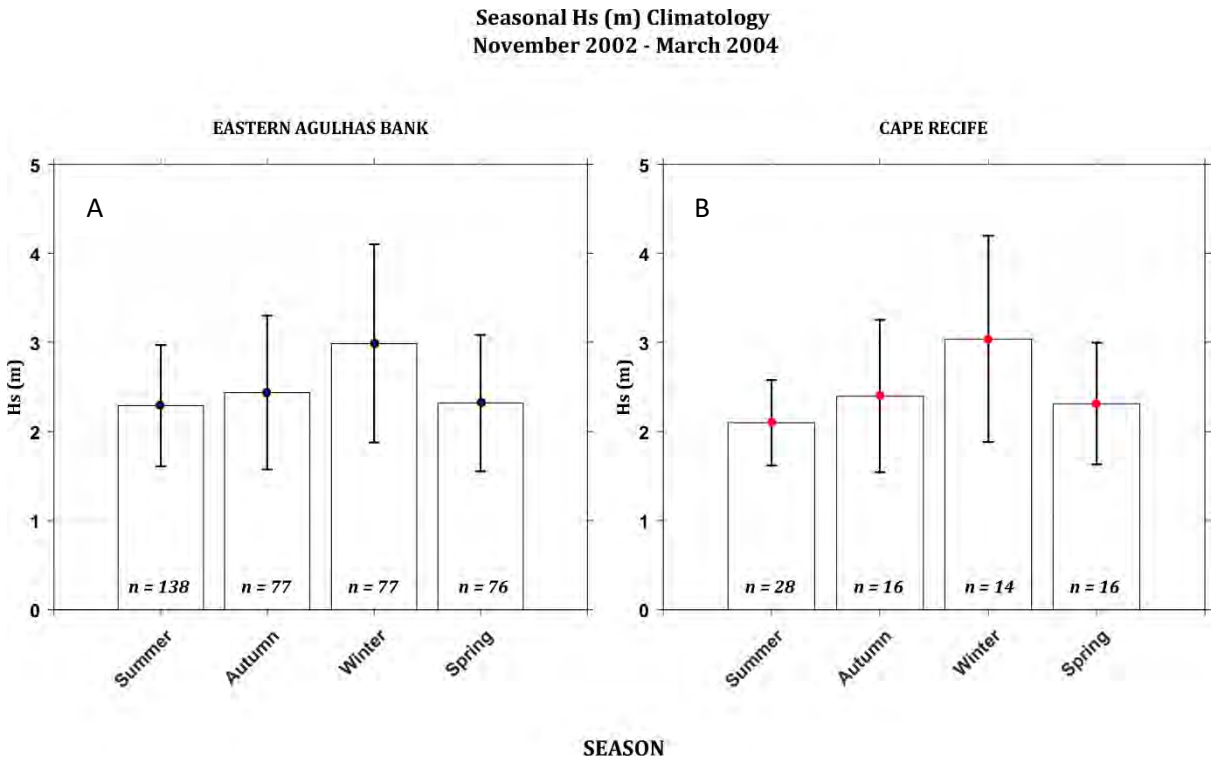

Fig. 4.16: Seasonal climatology of altimeter-derived significant wave height (Hs) for Cape Recife (A) and the entire Eastern Agulhas Bank (B). Error bars denote standard deviation from the mean whilst the values within the bars highlight the number of Hs counts per season.

Measurements of Hs and the variability from these measurements are greater in winter, with increases in Hs (m) variability in both autumn and spring compared to summer (**Fig. 4.16**). This suggests spatial homogeneity in wave state on a seasonal scale at different locations across the EAB (**Fig. 4.15 & Fig. 4.16**). The seasonal figure (**Fig. 4.16**) shows that a similar temporal structure exists for the altimeter-derived measurements of Hs across the EAB.

In comparison, the results from the spatial-temporal correlation analysis suggest that spatial variability in sea state exists within the seasons and even across the same day (**Fig 4.14**). It must be emphasized that there is high uncertainty related to Hs (m) altimeter measurements, particularly in the early years of satellite deployment. In fact, in this study, preliminary data analysis highlighted an anomalously high rejection rate of data associated with ERS-1 & 2 close to the coastline and were subsequently omitted from the analysis.

As shown in **Fig. 4.15A** and **Fig. 4.15B** the percentage occurrence of Hs measurements between the coastal zone (< 10 km from shore) and the Agulhas Bank (AB) mid-shelf (43 – 50 km from shore) highlights how the abundance and quality of the 1 Hz altimeter measurements are influenced by proximity to the coastline. The coastal zone was sampled less than the AB mid-shelf, i.e., 189 measurements versus 393, respectively. Due to the rejection flags associated with data close to the coastline (Timmermans et al., 2020), it is likely that the sizeable coastal data dropout results from pre-processing techniques and not due to proportionately erroneous data between the coastal zone and the mid-shelf. The Agulhas Bank Coastal Shelf, defined as the area between 0 and 50 km from the coastline (**Fig. 4.15B**), showed that while being sampled to a much greater extent, the wave state on the EAB has a median Hs of 2.1 m throughout the sample period. The more consistent proportion of accurate, quality-controlled measurements in the coastal shelf (< 50 km) compared to the coastal zone (< 10 km) justifies the use of the coastal shelf to resemble the dynamics of the wave state on the EAB.

Interestingly, the geographical location of Oubos means that the wave state experienced at the Oubos mooring will be different from that experienced on the narrower part of the bank east towards Algoa Bay and Cape Padrone. Correlation analysis between Hs readings in the proximity of Oubos gave rise to a stronger, more significant correlation between NTU and Hs as depicted in **Table 1**. However, due to the spatial and temporal variability associated with altimeter-derived readings of Hs, it cannot be assumed that the wave state experienced at Oubos will be representative of the wave state experienced on the lee-ward side of Cape Recife. Therefore, although the correlation is stronger in Oubos, the paths closest to the in-situ mooring reduce the impacts of spatial and temporal variability on the relationship between the two variables, which is why the Cape Recife mooring was selected. Furthermore, Oubos is located on a more exposed coastline. Therefore, wave refraction and changes in wave period will be minimal compared to the more sheltered Algoa Bay site.

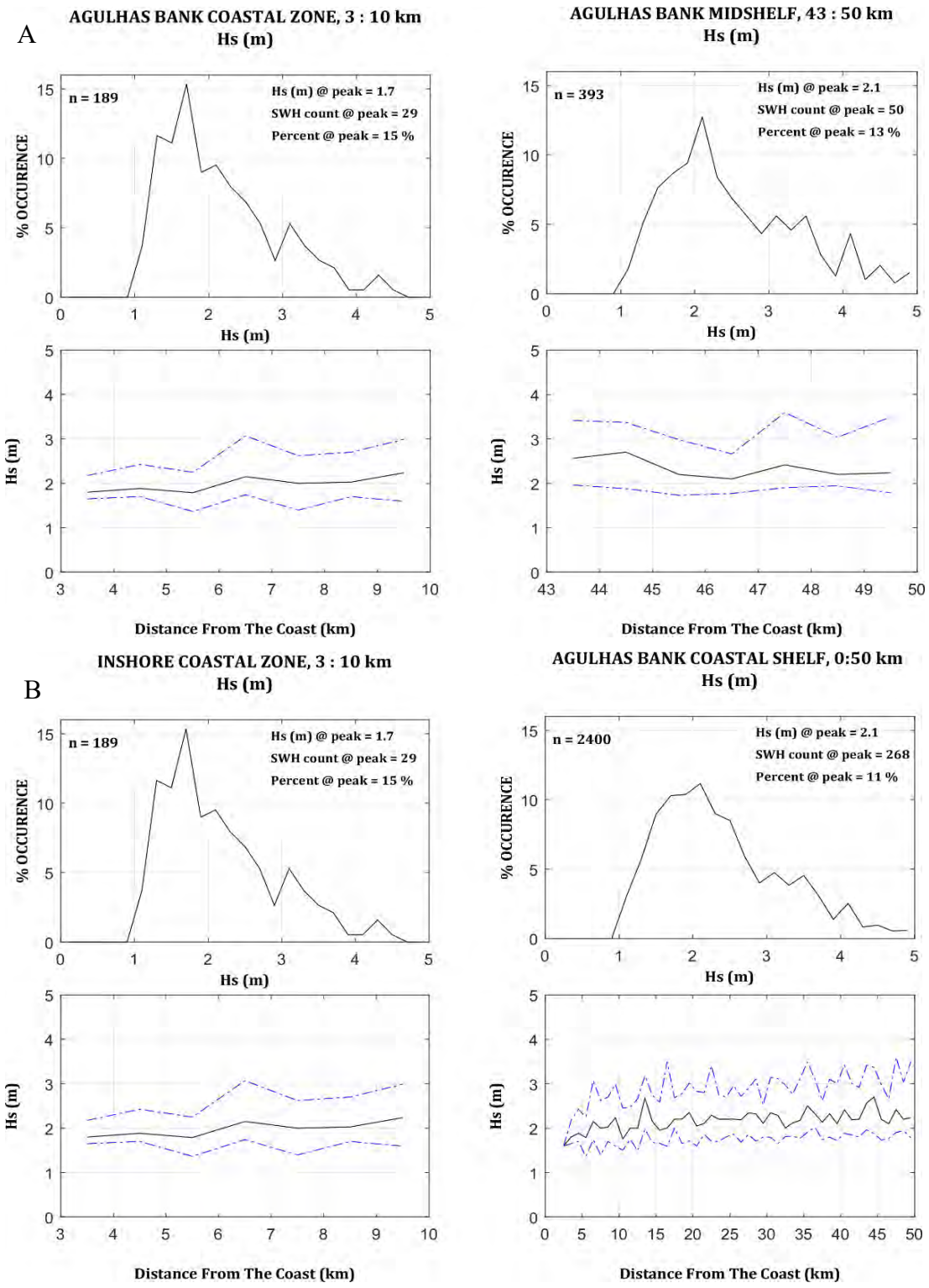

Fig. 4.17: Representation of the overall wave state as measurements of significant wave height (Hs) on the Eastern Agulhas Bank from data taken from the ESA CCI Sea State L3 Altimetry Product. The data was aggregated into 0.2 km bins and all passes were sampled to highlight the variability of wave conditions experienced on the Agulhas Bank. The inshore coastal zone (3 – 10 km) was compared to the mid-shelf (43 – 50km) as well as the coastal shelf (0 -50km). Distances (km) represent the proximity of the measurement to the coast.

4.5 Extended-Bay-Experiments (EBE)

4.5.1 Extended-Bay-Experiment, November 2002

4.5.1.1 Data quality

The Algoa Bay OBS deployment lasted for 77 days, between 8 November 2002, and 24 January 2003. Operational servicing of the instrument took place on 24 November, 24 December and 10 January. As described in Chapter 3.2.1 and illustrated in Chapter 4.1 above, turbidity data were edited to remove erroneous data periods as a result of biofouling, as well as instances where the instrument reached saturation point. During the Algoa Bay deployment, the most prolonged data interruption occurred between 14 and 24 December 2002 due to extensive fouling on the sensor face.

The St Francis Bay deployment from 10 November until 19 December 19, 2002, lasted for 39 days. Analysis of the St Francis Bay data showed that the instrument recorded normally until the evening 11 December, 2002, after which it reverted to low-power mode, and data acquisition stopped, resulting in 8 days of data loss from the 11 - 19 of December, 2002. Due to the instrument halting data acquisition early, before the possibility of biofouling-related growth to occur on the sensor's face, no adjustments were made to the St Francis Bay data.

The Oubos mooring site proved difficult to reach. As a result, the instrument remained deployed for longer than anticipated, totalling 69 days between 7 November 2002, and 14 January, 2003. Service dives scheduled on the 24 November 2002 for both the Oyster Bay and Oubos Bay deployments were aborted due to inclement weather. Despite the prolonged deployment period, the optical sensor window was found to be very clean upon retrieval. Subsequently, the data have been included below. However, the period between 15 - 29 December 2002 saw the instrument's output reach saturation point and therefore was omitted from the study. No further adjustments were made to the Oubos benthic turbidity data on account of the cleanliness of the sensor face upon instrument retrieval. However, extreme caution should be undertaken when comparing

Oubos turbidity data to the other deployment sites. The intensity and duration of events in Oubos after the 30 November cannot be assumed to be an accurate representation of actual conditions at the time of measurement. The incremental increase of the turbidity data baseline in Oubos is a 'classic signature' of biofouling-related interference with the optical sensor. However, the data were included to show relative peaks and troughs in benthic turbidity readings in relation to Algoa Bay and St Francis Bay. The events seen at the Oubos mooring site may have been more or less intense than the data presented here.

4.5.1.2 Events

Fig. 4.18 shows four periods of interest highlighted by the blue-dashed-boxes labelled A – D. The green-dotted vertical lines represent breaks in data acquisition and the subsequent removal of data on biofouling (Algoa Bay) and instrument reaching saturation point (Oubos). Event A highlights a period of 11 days from the 19 November to 31 November, 2002. Within this, we see both site specific and concurrent increases in benthic turbidity, as well as variability in bottom temperature structures across the three deployment sites. Event B highlights a peak in bottom turbidity in St Francis Bay on the 4 December 2002 that was at first not present in the other bays. Event C shows a comparatively large increase in bottom turbidity both in Algoa Bay and Oubos between 10 December 2002 and 14 December 2002. Because of instrument failure, this event was not recorded in St Francis Bay. Event D occurred over a seven-day period between 01 – 07 January 2003, highlighting concurrent peaks in bottom turbidity in Algoa Bay and Oubos.

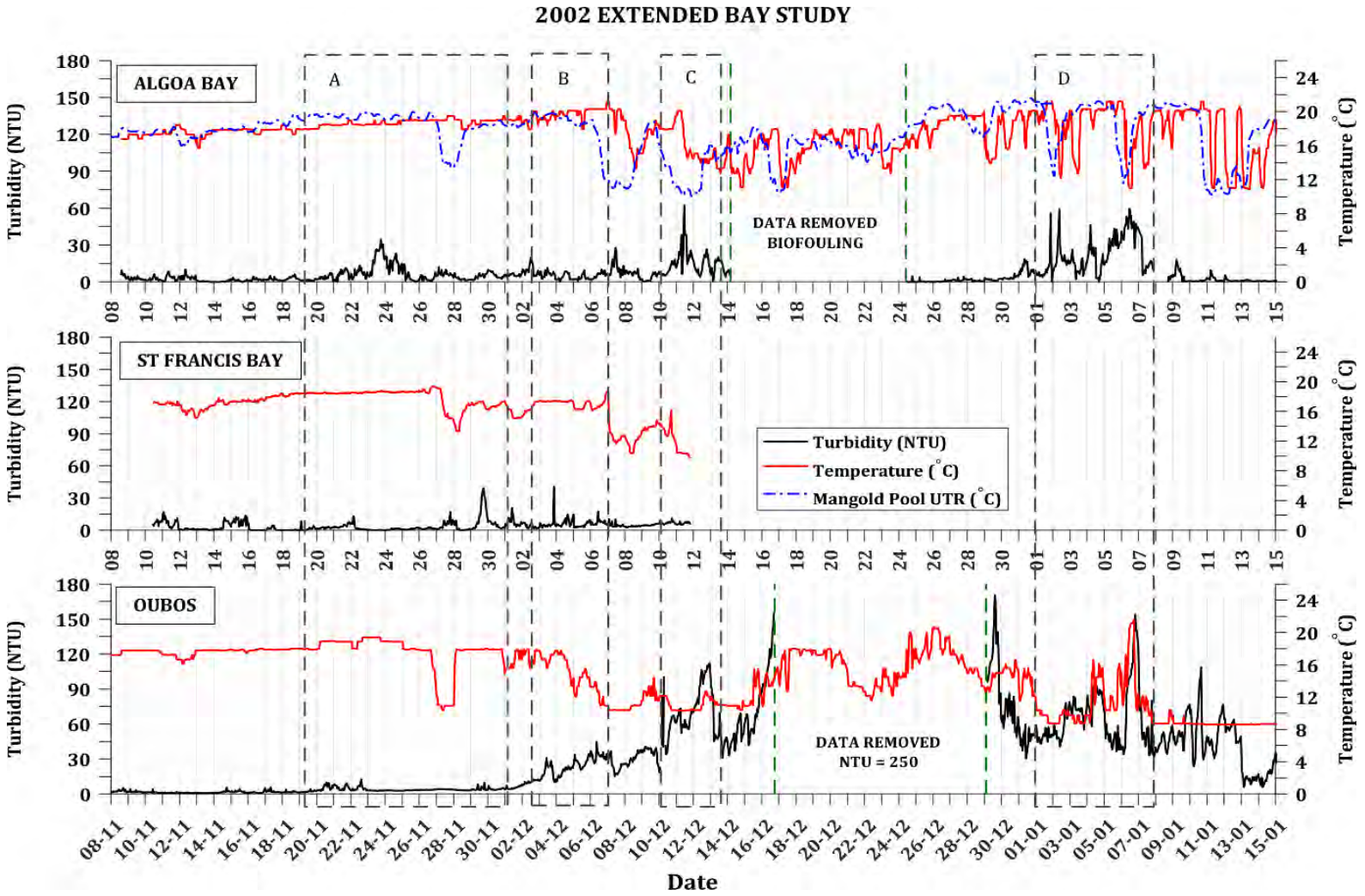

Fig. 4.18: Extended Bay Study of November 2002 displaying hourly observations of bottom temperature (°C, red line) and turbidity (NTU, black line) at three locations traversing the Eastern Agulhas Bank, namely; Algoa Bay (top), St Francis Bay (middle) and Oubos (bottom). Periods of interest discussed in this section are highlighted in the blue dashed-boxes labelled A – D. The green-dashed vertical lines represent dates between which data were omitted from the study due to biofouling (Algoa Bay) and instrument reaching saturation point (Oubos). No measurements of the benthic environment occurred in St Francis Bay after the 11 December 2002. No adjustments were made to the St Francis Bay turbidity data.

The first benthic turbidity event in Algoa Bay from 21 November to 25 November, 2002, was more intense than the concurrent peaks within the other bays (**Fig. 4.18A**). Benthic turbidity is seen to increased gradually from 19 November to reach a maximum of 36 NTU on 23 November, 2002. An increase in benthic turbidity occurred in both St Francis Bay and Oubos from 19 to 23 November, with peaks of 16 NTU in St Francis Bay and 14 NTU at the Oubos mooring. These turbidity values suggest that in all three deployment sites the water clarity was reduced to *'Black-Out'* conditions. The turbidity event depicted in Algoa Bay is brought about following a period of strong south-westerly winds (~ 60 km/h). The event decreases in intensity following a change in the magnitude of the wind strength and direction to wind with a more easterly-component on 24 November (**Fig. E1**).

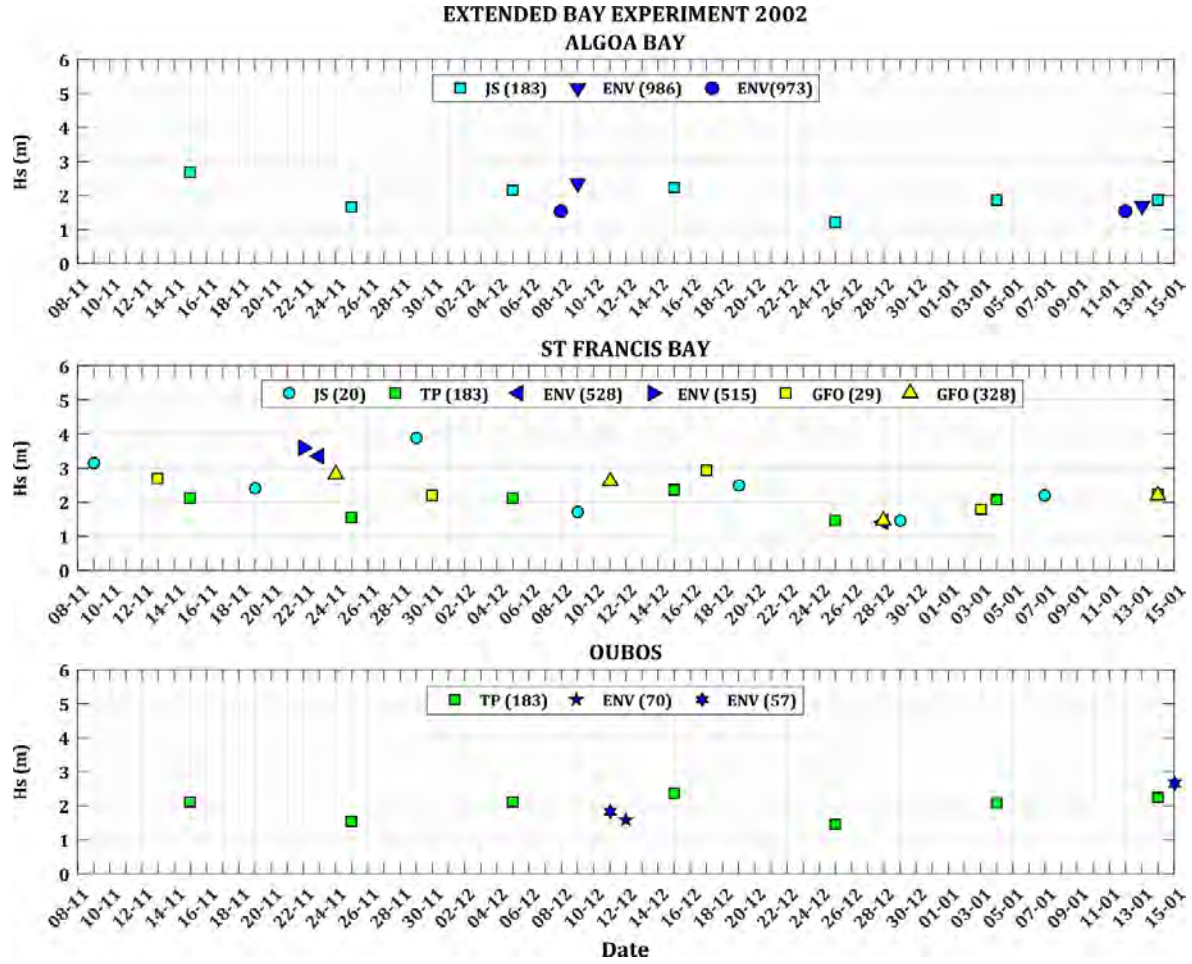

Fig 4.19: Altimeter-derived measurements of significant wave height (Hs, m) for the 2002 Extended-Bay-Experiment. Satellite paths represented here are those closest to the in-situ mooring as described in Chapter 3.

Impact of waves

Altimeter-derived Hs readings show that there were two measurements above 3 m on the 22 November (ENV 528) and 23 November (ENV 515), respectively (**Fig. 4.19**). These readings of Hs coincide with the peaks in benthic turbidity at all three deployment sites. The dissipation of the benthic turbidity during Event A is seen more abruptly in St Francis Bay than in the other two sites. At the St Francis Bay location, benthic turbidity increased gradually from the 19 November to 22 November, after which a peak in bottom turbidity equating to '*Black-Out*' visibility conditions occurred on 23 November. This was followed by a sharp decrease in benthic turbidity following the most intense peak (14 NTU). By mid-day on the 23 November, benthic turbidity readings in St Francis Bay and Oubos had dissipated to resembled '*Clear*' bottom conditions. Comparatively, the optical clarity of benthic environment was still highly disturbed in Algoa Bay for another 36 hours (**Fig. 4.18A**). A further measurement of Hs of 2.9 m was recorded on 24 November (GFO 328), coinciding with the prolonged benthic turbidity event in Algoa Bay (**Fig. 4.18**). The Hs readings obtained by JASON & TOPEX (183) at 15:58 on the 25 November shows the Hs to have dropped below 2 m, by which time the turbidity events in all three locations had dissipated (**Fig. 4.18**).

High productivity levels

Peaks in bottom turbidity also occurred in isolation at each deployment site during Event A. A benthic turbidity event lasting 10 hours occurred in St Francis Bay (17 NTU) and Algoa Bay (13 NTU) on 27 November but was not present at the Oubos mooring. Similarly, the intensity of the event which occurred on the 29 and 30 of November differed in all three sites. In Algoa Bay the benthic turbidity increased to 9 NTU at the same time that benthic turbidity reached 36 NTU in St Francis Bay, whilst a peak in turbidity of 7 NTU was observed in Oubos Bay (**Fig. 4.18A**). Analysis of the remote sensing data shows a high chlorophyll event off Port Alfred between the 16 November to 22 November (**Fig. 4.20**). Of interest is the high chlorophyll-a levels located within Algoa Bay itself in conjunction with highly productive waters off Port Alfred.

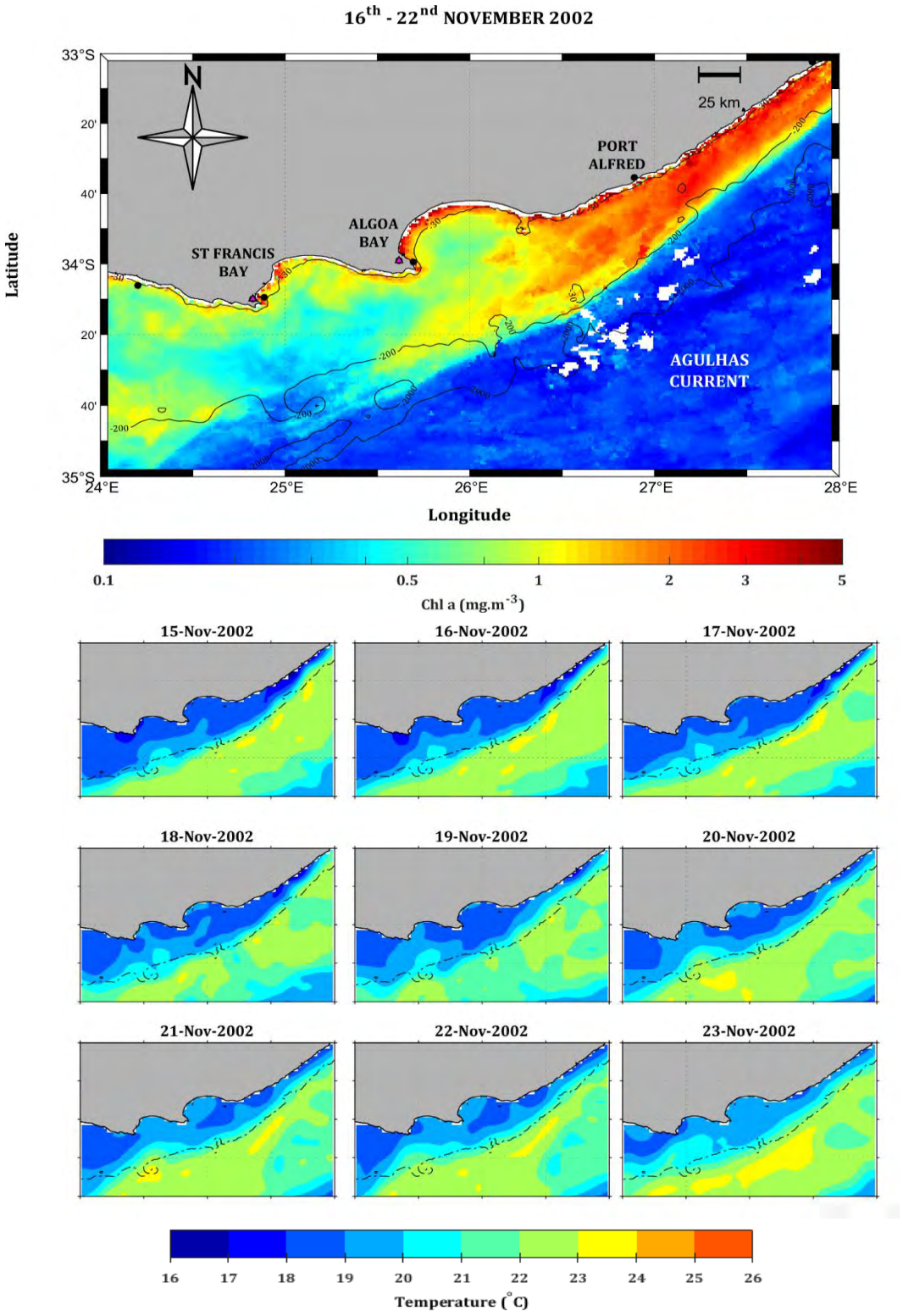

Fig 4.20: Daily OSTIA L3 SST images highlighting the intensity of upwelling on the EAB in the vicinity of the Port Alfred Upwelling Cell (A). A complementary 9-Day composite image of primary productivity (chl-a, mg.m^{-3}) on the EAB from the 16 – 22 November 2002 (B). Note the high productivity emanating from Port Alfred and within Algoa Bay.

The L3 OSTIA SST images in **Fig. 4.20** were selectively enhanced to highlight the presence of cold water emanating from the Port Alfred Upwelling Cell. A persistent westerly-component wind endured from 15 November to 23 November, enhancing the entrainment of particle rich water masses in Algoa Bay (**Fig. 4.20**). Furthermore, the lack of upwelling promoting winds suggests that the upwelling present in the vicinity of Port Alfred is as a result of the interaction of the Agulhas Current and the slope bathymetry, causing divergent upwelling.

Upwelling and downwelling

Of particular interest in the 2002 EBS study is the difference in temperature structure and upwelling intensity experienced at the three different mooring locations. Upwelling events during demarcated periods A – D were observed to varying degrees of intensity between the three deployment locations. The Oubos location experienced the most intense bottom temperature variability, with temperature on average cooler than the temperature in Algoa Bay. The Algoa Bay bottom temperatures fluctuated rapidly between warm-and-cold-water intrusions, highlighting a more variable coastal temperature structure when compared to the Oubos location. The dichotomy between the temperature profiles is principally evident through analysis of the upwelling event on 27 November, 2002 (**Fig. 4.18A**). During this time period, upwelling signatures in the form of reduction of bottom temperature, were present in St Francis Bay and Oubos Bay, but were not evident in the Algoa Bay data.

Winds with a dominant easterly-component, which favour coastal upwelling, persist for a number of days from the 24 November to 28 November, 2002 (**Fig. E1**). The persistent North-Easterly winds from 24 November to 27 November resulted in a period of upwelling most intensely observed in Oubos Bay compared to St Francis Bay. The peak in easterly wind speed (39 km/h) occurred over a 24-hour period from midday 26 November to midday 27 November. During this period of strong Easterly-component winds, bottom temperatures at the Oubos mooring site dropped from 20.12 °C to 10.68 °C. Similarly, thermal signatures in St Francis Bay showed a change in temperature of ± 6.78 °C, with temperature dropping from 19.98 - 13.2 °C

during the upwelling event. The UTR at Mangolds' Pool on the western side of Cape Recife also picks up this upwelling event from the 26 November to 28 November. The Mangold's Pool UTR shows a reduction in bottom temperature over a 2-day period equal to 6.86 °C, from 20.36 – 13.5 °C (**Fig. 4.18A**).

Following this upwelling event, a reversal in wind direction to a strong south-westerly wind (54 km/h) resulted in the rapid downwelling of warmer water at the Oubos mooring location on 28 November. The intensity of the temperature change experienced at Oubos was different to that experienced in Algoa Bay and St Francis Bay. St Francis Bay experienced a slightly delayed and less intense upwelling event in comparison to Oubos Bay, with a temperature change of ~ 4 °C at its most intense. However, following the same period of strong westerly winds, the benthic temperature regime in St Francis Bay never recovered from the first initial influx of colder upwelled water, with water temperatures remaining a few degrees lower throughout the rest of the deployment. During the strong-westerly component winds, the Algoa Bay mooring experienced a slight (< 0.5 °C) drop in bottom temperature whilst bottom temperatures increased in both St Francis Bay and Oubos

A westerly wind then endures for two days from 28 November to 30 November before easterly-component winds dominate throughout the first week of December 2002 (**Fig. E2**). The temperature profiles show that from the 1 December to 7 December, persistent winds with an upwelling favourable easterly had a greater effect on the bottom temperature in Oubos compared to Algoa Bay and St Francis. Bottom temperatures began to drop on 3 December in Oubos and this was not mirrored at the other two mooring locations. The persistent easterly-component winds reach a peak on the 6 December and 7 December, whereby bottom temperatures in both the St Francis Bay and Oubos moorings had dropped while there was no change to the bottom temperature in Algoa Bay.

A third event, highlighted by blue-box C in **Fig. 4.18**, extends from 10 December to 14 December, 2002, and is evident in Algoa Bay and Oubos Bay. This period of increased benthic

turbidity occurs at a time of strong winds, alternating between the upwelling favourable North-Easterly and downwelling favourable South-Westerly (**Fig. E2**). The peak of the turbidity event in Algoa Bay occurs at the onset of upwelling, as evident by the change in water temperatures and increased benthic turbidity. Turbidity readings on 11 December reached a maximum of 62 NTU in Algoa Bay, while the data collected from Oubos shows a similar increase in bottom turbidity during this time. Wind direction alternated from upwelling favourable easterlies to downwelling favourable westerlies on 11 December, coinciding with a drop in bottom temperature in Algoa Bay and St Francis Bay but not at the Oubos deployment site (**Fig. E2**). Analysis of the chlorophyll-a data suggests that a period of high productivity occurred between the 06 and 13 December, 2002 (**Fig 4.19**).

The dynamic of alternating wind-driven up-and-downwelling bringing about an increase in benthic turbidity is again evident in **Fig. 4.18D**, where benthic turbidity increases in both Algoa Bay and Oubos simultaneously following dynamic changes in the bottom temperature at each site (**Fig. E3**). A double spike in benthic turbidity in Algoa Bay on 1 January and 2 January, 2003, coincides with the change of wind direction from easterly-component to a strong westerly-component wind (**Fig. E3**). This brought about the first initial peak on 1 January in the absence of a fluctuation in bottom temperature whilst the second peak on the 2 January coincided with a decrease in bottom temperatures in Algoa Bay (from 20.13 °C to 10.82 °C). An increase in benthic turbidity is again observed in Algoa Bay on the 4 January which correlates to a small (~ 1 °C) decrease in bottom temperature during a westerly-component wind. A concurrent peak in benthic turbidity occurs at the same time at the Oubos mooring location on 4 January, instead correlating to an increase in bottom temperatures during the event as a result of warmer water brought to the coast via downwelling promoting westerly-component winds (**Fig. E3**).

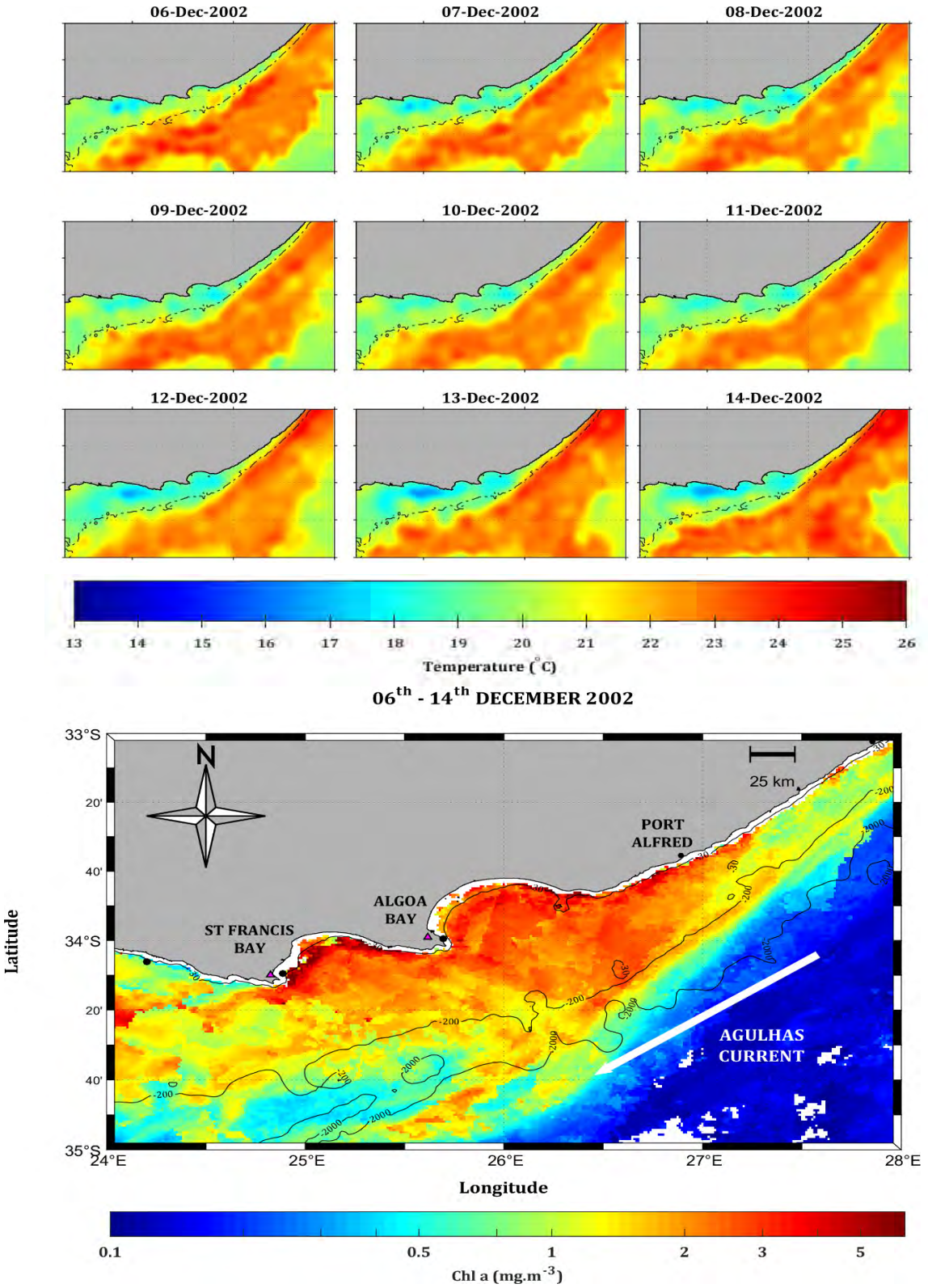

Fig 4.21: Daily OSTIA L3 SST images highlighting the intensity of upwelling on the EAB (A). (B) a complementary 9-Day composite image of primary productivity (chl-a, mg.m^{-3}) on the EAB from the 06 – 14 December 2002 (B). Note the high productivity (as a result of upwelling) in Algoa Bay and St Francis.

4.5.1.3 Supplementary Cruise Data, 28 November 2002

An opportunity for greater shelf data arose during my investigation when the FRS AFRICANA (cruise #171) was in the vicinity of one of the moorings, ~ 23.8 °E.

An OBS 3 turbidity sensor, attached to a CTD and lowered to within 10 m of the seafloor, was used during this cruise. A total of six Stations (A212541 – A21258) were analyzed for benthic turbidity concerning other environmental parameters, including turbidity, temperature, oxygen, fluorescence, and salinity. On 28 November, the wind field around Algoa Bay saw a wind-reversal from a westerly-to-easterly, promoting upwelling on the western side of Cape Recife. This upwelling was first recorded by the Mangold's Pool UTR and corresponds with an increase in bottom turbidity ('*Turbid*' conditions). A well-defined thermocline is clearly evident in **Fig. 4.22**, with a temperature minimum of 9.3 °C located ~ 50 km offshore, where the 'Cold-Ridge' is evident. The upward doming of the thermocline at the fourth furthers transect from the coast, evident by the close grouping of the isotherms, is an unmistakable feature of the 'Cold-Ridge' (Roberts, 2005). Of particular interest in relation to the Temperature-Turbidity Interface is the horizontal and vertical temperature distribution across the shelf (**Fig. 4.22**).

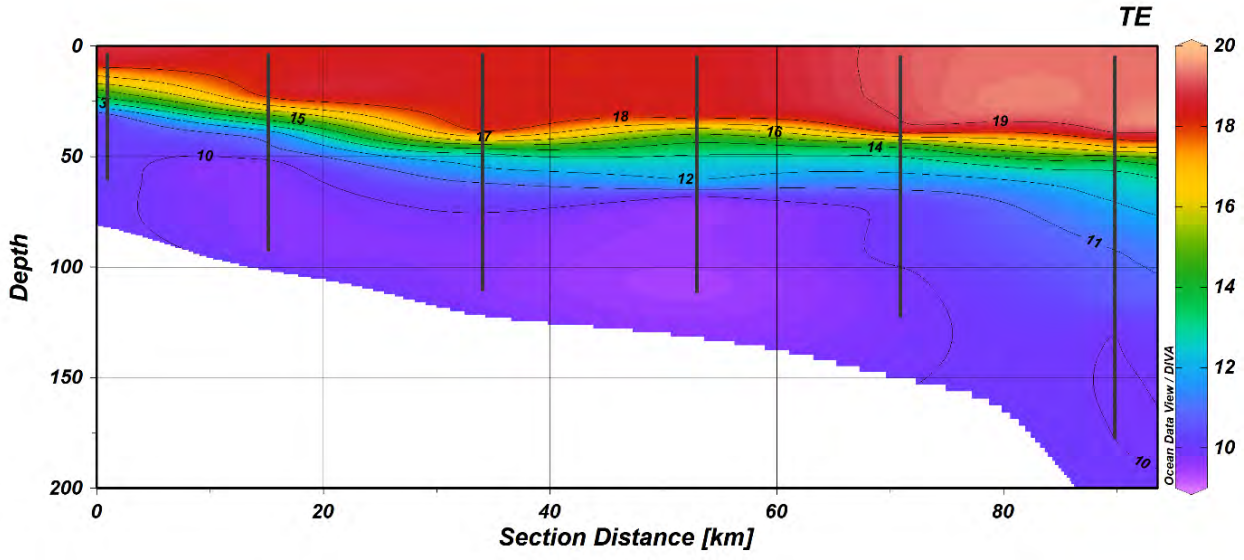

Fig. 4.22: Transect of surface to bottom temperature (°C) at six sampling stations during the bi-annual demersal surveys conducted by DFFE on board the 'FRS AFRICANA,' cruise #171, between October – November 2002. This transect was sampled on the 28th of November, 2002.

Turbidity in the transect is markedly inshore **Fig. 4.23**, with the highest turbidity values of 1.2 NTU present at the coastal station and decreasing with distance from the shore. The nepheloid layer is most intense below the thermocline, absent within the closely formed isotherms, and then again marginally present in the surface layer, forming a Surface Nepheloid Layer (SNL). The SNL is weakest closest to the coast and increases with distance from the coast, reaching a maximum over the 'Cold-Ridge.' The intensity of the BNL is confined to the coastal zone, decreasing with distance away from the coast. An increase in benthic turbidity readings on the third transect, ~35 km from the coast, suggests that the turbidity sensor recorded the upper reach of a BNL on the Agulhas Bank mid-shelf (**Fig. 4.23**).

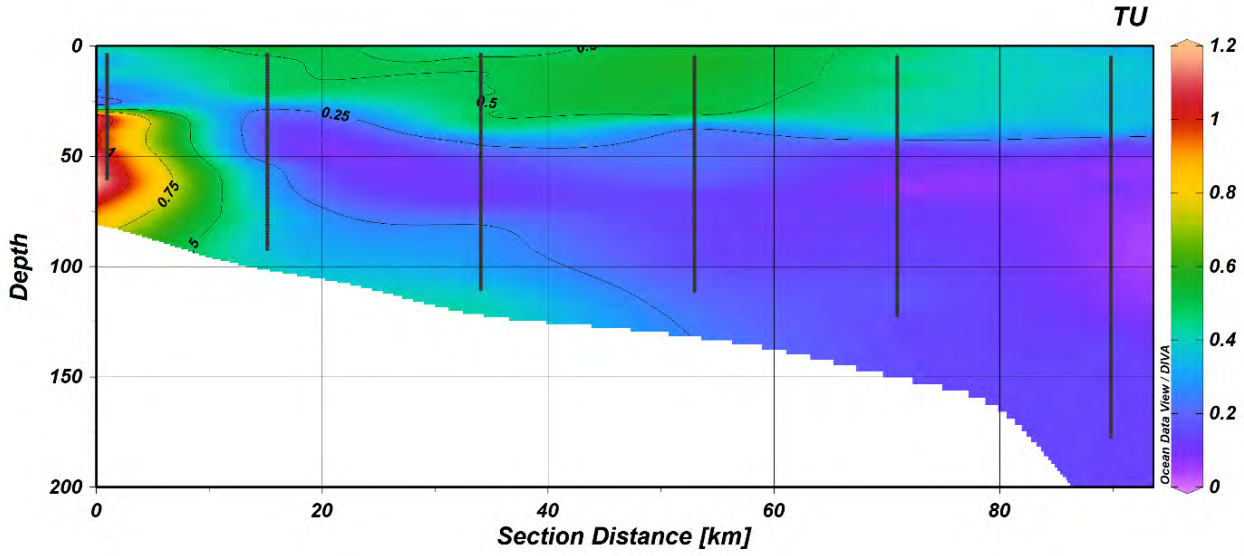

Fig. 4.23: Transect of surface to bottom turbidity (NTU) at six sampling stations during the bi-annual demersal surveys conducted by DFFE on board the 'FRS AFRICANA,' cruise #171, between October – November 2002. This transect was sampled on the 28th of November, 2002. Note that the CTD stopped ~10 m from the benthos.

Measurements of fluorescence (**Fig. 4.24**) follow the same west-east pattern associated with the SNL, with fluorescence increasing in strength further away from the coast, between 50 – 80 km offshore, located in the vicinity of the 'Cold-Ridge.' Oxygen readings within the BNL (**Fig. 4.25**) are also of interest, as the lowest oxygen values are located directly within the BNL.

Measurements of salinity (Fig. 4.26) are highest within the area of the warmest temperature (Fig. 4.22) and greatest fluorescence signature (Fig. 4.24).

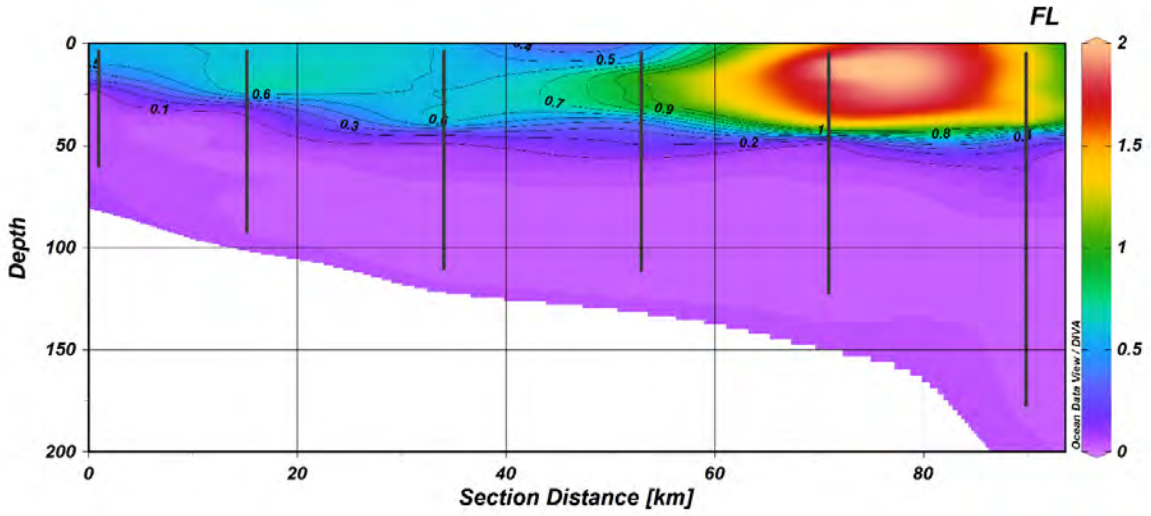

Fig. 4.24: Transect of surface to bottom fluorescence at six sampling stations during the bi-annual demersal surveys conducted by DFFE on board the 'FRS AFRICANA,' cruise #171, between October – November 2002. This transect was sampled on the 28th of November, 2002. Note that the lowest values for fluorescence are located inshore near the most intense BNL expression. In contrast, the highest fluorescent values are located further offshore.

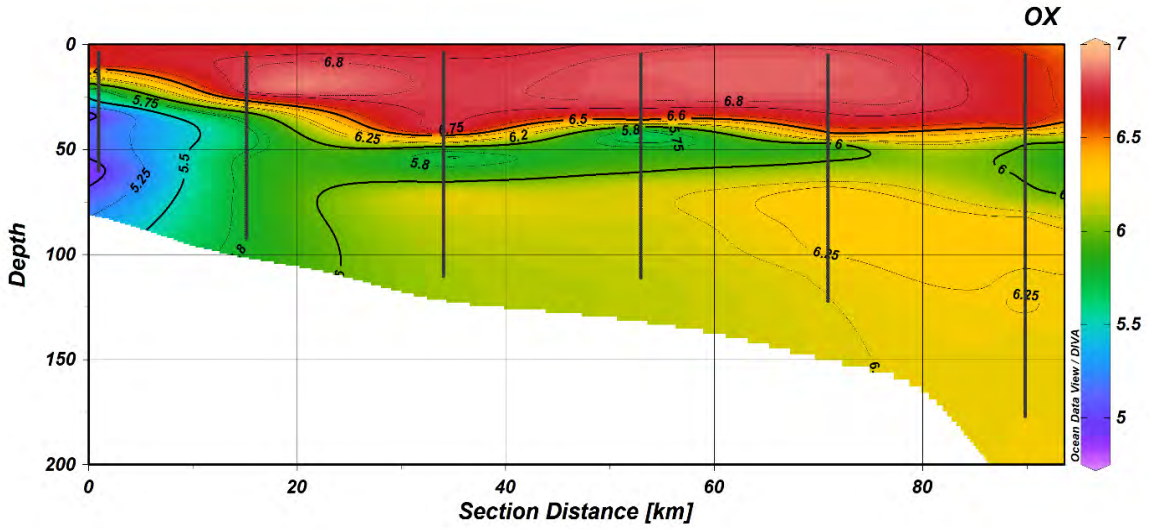

Fig. 4.25: Transect of surface to bottom oxygen at six sampling stations during the bi-annual demersal surveys conducted by DFFE on board the 'FRS AFRICANA,' cruise #171, between October – November 2002. This transect was sampled on the 28th of November, 2002. Note that the lowest values for oxygen are located inshore near the most intense BNL expression.

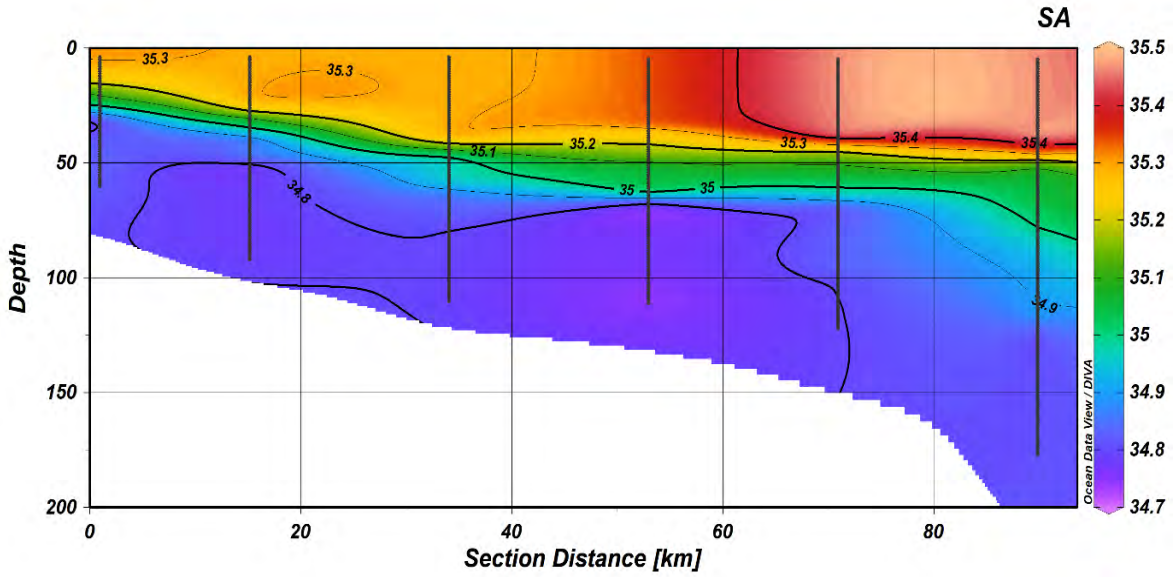

Fig. 4.26: Transect of surface to bottom salinity at six sampling stations during the bi-annual demersal surveys conducted by DFFE on board the 'FRS AFRICANA,' cruise #171, between October – November 2002. This transect was sampled on the 28th of November, 2002.

4.5.2 Extended-Bay-Experiment, November 2003

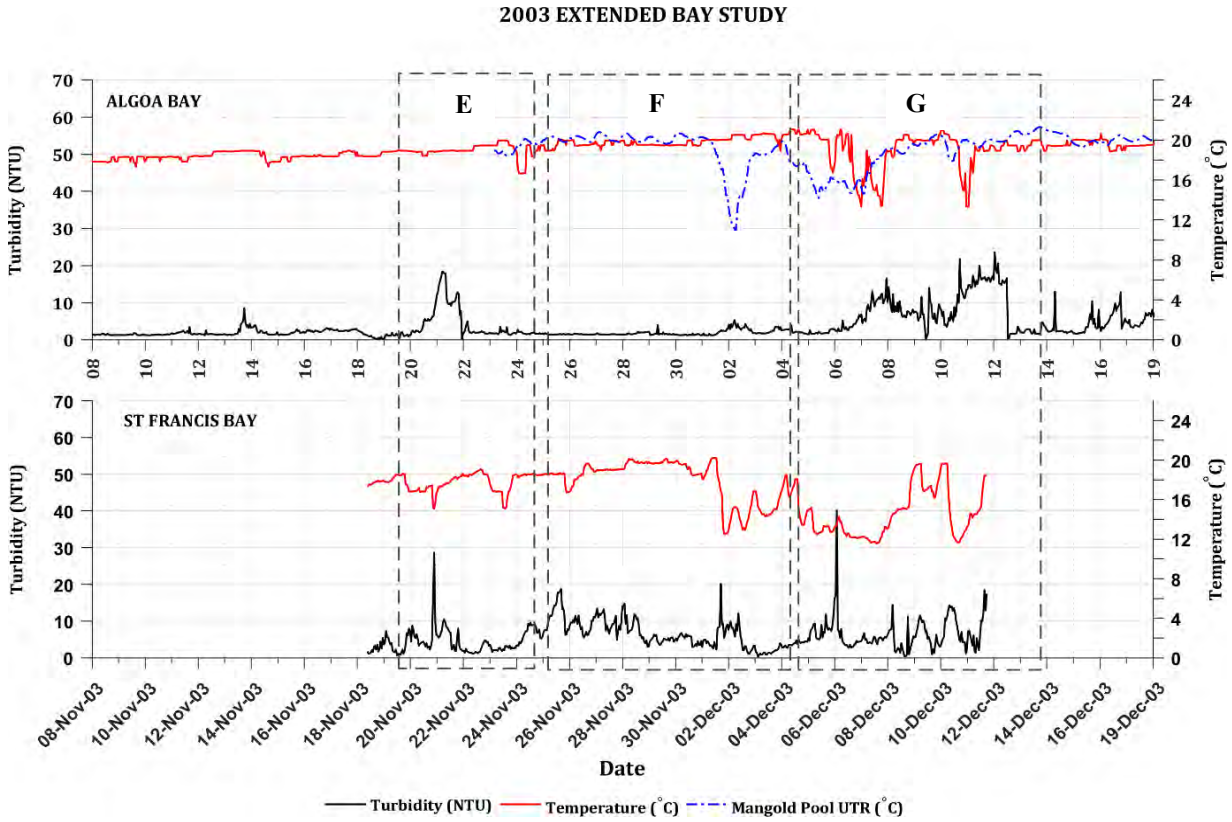

Fig. 4.27: Extended Bay Experiment of November 2003 displaying hourly observations of bottom temperature (°C, red line), surface temperature at Mangold's Pool (°C, blue dotted line), and turbidity (NTU, black line) at Algoa Bay (top), St Francis Bay (bottom). Periods of interest discussed in this section are highlighted in the grey dashed-boxes labelled E – G.

4.4.2.1 Data quality

As with the first EBS, the data collected for this experiment in November-December 2003 are shown in similar format (**Fig. 4.27**). Here the OBS mooring in Algoa Bay was complemented with a 26-day OBS deployment in St Francis Bay from 18 November, 2003, to 12 December, 2003. Due to the short deployment period for the St Francis Bay sensor, no adjustments were made to the data on account of lack of biofouling interference. The Algoa Bay mooring was serviced on 12 December, 2003. Divers noted a thin film of algal hydroids on the optical sensor window, and the instrument was cleaned and data corrected for as described in Chapter 3. The

visibility at the time of instrument servicing was 3.2 m. In contrast, the St Francis Bay mooring was removed the previous day and divers noted underwater visibility of < 0.5 m.

4.4.2.2 Events

Turbidity averaged 4.6 NTUs in Algoa Bay during the deployment period, compared to 7.9 NTU during the St Francis Bay deployment. Variability in bottom conditions is evident in the average bottom temperatures, 19.1 ℃ in Algoa Bay and 17.2 ℃ in St Francis Bay, respectively.

The OBS instruments recorded similar turbidity values in both bays at the start of the St Francis Bay 17.2 ℃ deployment period (2.3 NTU vs 2.1 NTU, respectively). Therefore, it is of considerable interest that the benthic turbidity structure in St Francis Bay was so variable compared to the Algoa Bay mooring. The three events, labelled E – G, were selected to bring to light the variability in these two contrasting environmental variables across two adjacent embayment's of the EAB.

Event E

In Event E (**Fig. 4.27**), it is clear that there are both concurrent and site-specific turbidity events in both Algoa Bay and St Francis Bay. At the start of the event, on 19 November 2003, the similarities in site-specific benthic turbidity are evident in both Algoa Bay and St Francis Bay where NTU < 2. This suggests that conditions were '*Clear*' in both bays simultaneously. From the 20 November to 22 November, 2003, a westerly wind swept through both bays (**Fig. E13**), resulting in a continuation of the bottom temperature structure in Algoa Bay but a change in bottom temperature in St Francis Bay (**Fig. 4.27A**). At first, the bottom temperature rises at the onset of the westerly winds before the bottom temperature drops, resulting in a concurrent increase in benthic turbidity throughout. The largest peak in benthic turbidity during these events occurs in St Francis Bay on the 20 November, 2003, coinciding with a small drop in bottom temperature (~ 2℃). This peak was equal to 28 NTU (UWV ≤ 0.5 m), compared to only 10 NTU in Algoa Bay, and lasted for a period of two hours only. The largest peak in the Algoa Bay NTU

occurred during the reversal of wind direction from downwelling (westerly) to upwelling (easterly) several hours later, on 21 November, 2002 (**Fig. E13**). At this stage, the benthic turbidity event in St Francis Bay decreased from 28 – 18 NTU, and the corresponding increase in NTU in Algoa Bay saw a peak at 18 NTU (**Fig. 4.27A**).

On 22 November, the wind field in Algoa Bay reversed again inducing upwelling and the turbidity event rapidly dissipated in Algoa Bay (**Fig. 4.27E**). Comparatively, the drop in NTU as a result of the onset of easterly saw an initial increase in bottom temperature in St Francis Bay. The easterly persisted for two days before a reversal in wind direction resulting in a drop in bottom temperature coincided with a very small increase in benthic turbidity in Algoa Bay (**Fig. E13**). In St Francis Bay, the easterly wind brought a decrease in bottom temperature at the mooring and a delayed response in benthic turbidity, reaching a peak of 10 NTU at the end of event A, compared to 2.3 NTU in Algoa Bay. Altimeter-derived measurements of Hs (m) suggest that these peaks and troughs in benthic turbidity during Event E are as a result of the interaction between temperature and wind-components, and are not a result of wave induced resuspension as the GFO (29) measurement shows Hs < 2 m during this period (**Fig 4.28**).

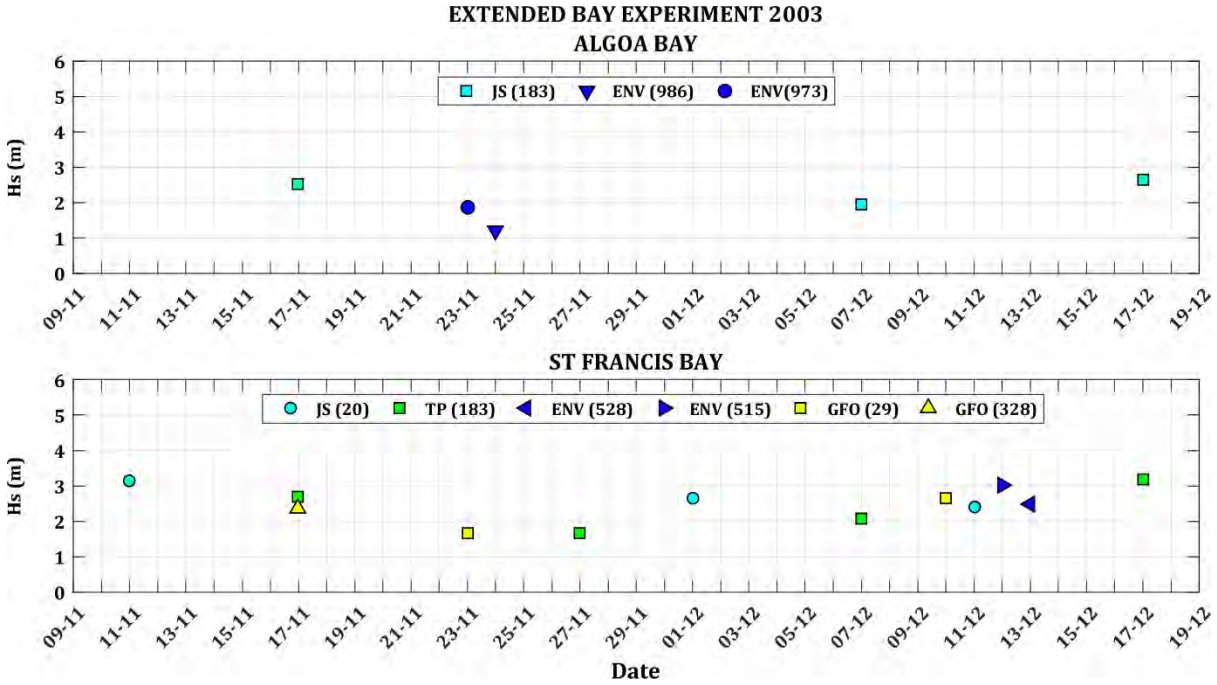

Fig 4.28: Altimeter-derived measurements of significant wave height (Hs, m) for the 2003 Extended-Bay-Experiment. The figure is divided geographically into satellite paths which are closest to the in-situ mooring using the methods described in Chapter 3

Event F

The second event of the EBE 2003 study occurs between 25 November and the 5 December. During this ~ 11-day period, benthic turbidity in Algoa Bay was considerably less than benthic turbidity levels in St Francis Bay (**Fig. 4.27F**). A strong westerly wind dominates the first 6 days of the event, from 25 November to 1 December (**Fig. E13**), whereby the wind direction reverses to a strong and prominent easterly-component wind from 01 December to 08 December (**Fig. E14**). However, a period of intermittent westerly (3 December - 4 December) breaks up the week-long prominent easterly component wind (**Fig. E14**). In terms of benthic turbidity, the Algoa Bay mooring remained very stable in optical clarity until the onset of the strong-easterly component winds on 01 December. These easterly winds resulted in rapid upwelling of colder water evident in both the St Francis Bay and the Mangold's Pool UTR data. The upwelling was not felt at the Algoa Bay mooring until well over a week later (**Fig. 4.27F**). However, a slight increase in benthic turbidity in Algoa Bay coincided with the change in wind direction (2 December).

The St Francis Bay turbidity structure was markedly different during compared to Algoa Bay during Event F (**Fig. 4.27**). The onset of strong-westerly component winds resulting in an increase in benthic turbidity in St Francis Bay, with a peak of 19.1 NTU on the afternoon of the 25 November shortly after the strong-westerly wind started to blow (**Fig. E13**). A small wind-reversal the following day (26 November) resulted in the movement of some of this upwelled water from outside to the inside of the bay. The benthic turbidity conditions persisted with the westerly component wind, with peaks and troughs in benthic turbidity correlated to wind speed from the 26 November to 1 December. At the onset of the strong-easterly component wind in Algoa Bay, the St Francis Bay mooring saw an initial reduction in benthic turbidity before reaching a peak of 20.2 NTU. This peak in benthic turbidity coincided with a drop in temperature from 20.2 ℃ to 13.4 ℃ (**Fig. 4.27F**). The easterly-component winds fluctuate in speed over the next four days, which is evident in the temperature regime of St Francis Bay toward the end of Event F.

Event G

The third and final event encompasses the last days of the St Francis Bay mooring deployment, from 04 December to 12 December 2003 (**Fig. 4.27G**). During this period, an intense 'Black-Out' event lasted only a few hours on the 06 December 2003 that was much more intense in St Francis Bay than in Algoa Bay. A slight wind-reversal from easterly to westerly winds brought about this turbidity increase in St Francis Bay. Due to the persistence of the easterly-component winds for a number of days (**Fig. E14**), upwelling became evident in the bottom mooring in Algoa Bay on 06 December owing to the easterly-westerly wind reversal (**Fig. E14**). A westerly-component wind is then prevalent from 08 December to 10 December, during which the turbidity profiles in both bays exhibited temporal variability. The relationship between temperature and turbidity is evident again during the last peak and trough in benthic turbidity and temperature in St Francis Bay on 10 December and 11 December.

4.5.3 Highlights of the Extended-Bay-Experiments

The Extended-Bay-Experiments of 2002 and 2003 demonstrate the variability in both benthic turbidity (NTU) and temperature (°C) structures traversing the main spawning grounds for *L. reynaudii*. More importantly, the exhaustive descriptions of the events listed above provide an important backdrop to understanding the dynamics of benthic turbidity within Algoa Bay, and the greater EAB itself. It is clear from both the 2002 and 2003 EBE that the Algoa Bay mooring location differs in the response of benthic turbidity to environmental forcing mechanisms compared to St Francis Bay and Oubos. Easterly-component winds induce upwelling on the western side of Cape Recife, and only wind-reversals to the downwelling favourable westerly winds result in a delayed temperature and subsequent turbidity response at the Algoa Bay mooring (e.g., Event A, 2002; Event G, 2003). Furthermore, the impact of wind-induced water turbulence, and subsequently wave events, is more intense in St Francis Bay (Event A, 2002) than in Algoa Bay.

The EBE showed that the alternation of the wind regime between upwelling favourable easterlies and downwelling favourable westerlies are responsible for a significant proportion of peaks in benthic turbidity in Algoa Bay. The wind-driven movement of particulate-matter-rich water masses around the Cape Recife pinnacle inducing and dissipating turbidity events described in the EBE above are seen throughout the 17-month time-series of benthic turbidity in Algoa Bay (**Fig. A1 – Fig. A17**). A black dashed-box demarcates examples of these events in **Fig. A1** to **Fig. A17**. Furthermore, high primary production in the area further abets the formation of the BNL through the sinking of organic particulate matter (Event B & D, 2002). However, the relationship between productivity in the euphotic zone and benthic visibility is hampered by a host of unknowns, such as current speed and direction at the mooring locations. Green dashed-boxes highlight examples of possible organic matter-rich nepheloid layers in **Fig. A1** to **Fig. A17**. Resuspension events in the Algoa Bay time-series experiment, as a result of strong winds or waves, are highlighted in red-dashed boxes in **Fig. A1** to **Fig. A17**. There is considerable overlap between these mechanisms and benthic turbidity events across the 17-month time series in Algoa Bay.

CHAPTER 5

Discussion and Conclusions

Due to the importance of visual stimuli in the reproductive process of chokka, the primary aim of this study was to investigate the relationship between turbidity events and environmental parameters on the EAB. While the intention was to pursue an uninterrupted time-series of benthic turbidity within Algoa Bay and comparable data sets from the Extended-Bay-Experiments, this proved a challenging task. Several breaks in *in-situ* data acquisition occurred due to instrument failure, servicing of instruments, and biofouling on the optical sensor itself. Despite these challenges, the results presented in this thesis show that periods of increased particulate matter concentrations, and the resultant BNL, are common but variable occurrences traversing the commercially important nearshore spawning grounds of *L. reynaudii*.

Despite benthic turbidity averaging 4.16 NTU (~ 2 m of underwater visibility, **Fig 4.2B**) throughout the sampling period, it is clear that the dynamics of benthic turbidity are not consigned to one season or time of year (**Fig 4.4**). Instead, the dynamics of benthic turbidity in Algoa Bay are primarily influenced by local environmental factors which impact turbidity at different time scales (**Fig. A1 – A17**). Therefore, a vastly improved time series encompassing all seasons equally with minimal data loss and correction is required for more robust statistical analysis of inter- and intra-seasonal variation in benthic turbidity in Algoa Bay and the EAB at large. Furthermore, turbidity events are observed in patches across the EAB (Dorfler, 2002; Downey, 2009; Githaiga-Mwicigi, 2012). Therefore, it should be noted that the time series here is specific to the mooring location and does not account for spatial and temporal variability within Algoa Bay and across the EAB itself. Robust statistical analysis of the relationship between turbidity and catch rates were found to be confounded by the unique hydrography around the location of the mooring in Algoa Bay Time-series Experiment and the extensive coverage of commercial fishing hotspots on the EAB.

Algoa Bay Time-series Experiment

(i) Benthic Turbidity

The 17-month time-series experiment in Algoa Bay highlights the variability of benthic turbidity events on a localized spatial and temporal scale. These results point to the studies conducted by Dorfler (2002) in South Africa and the study conducted by Palanques and Biscaye (1992) off New England, USA. The results of this study compare well with those of Palanques and Biscaye (1992), who found that benthic turbidity was not a continuous feature across the shelf but occurred in varying degrees of intensity (for detailed review, see McCave, 2019). Furthermore, turbidity exhibited higher concentrations inshore decreasing with distance offshore. Similarly, in South Africa, Dorfler (2002) and Githaiga-Mwicigi (2012) found that benthic turbidity events decrease in intensity further offshore. Thus, this study reinforces the notion that benthic turbidity is concentrated in the nearshore environment, particularly the nearshore coastal zone, and is linked to nearshore coastal shelf processes.

Turbidity readings were divided into three qualitative brackets that best describe bottom turbidity in terms of visual impairment of the water clarity, namely; (a) '*Clear'* (> 5 NTU), (b) '*Turbid'* (5 < – ≥ 15 NTU), and (c) '*Black-Out' (> 15 NTU)*. The results highlight that turbid water conditions existed for a significant proportion (~ 30 %) of the sample period between November 2002 and March 2004. Optical conditions described as '*Clear* ' predominated throughout the 17-month time series, prevailing for ~ 70 % of total readings, or ~ 282 days. In contrast, '*Black-Out'* benthic conditions are characterized by a high potential for inhibiting nearshore squid spawning aggregations (Roberts, 1998) and account for ~ 5 % of the total readings or ~ 27 days. Turbidity values ranging between 5 and 15 NTU are characteristic of elevated concentrations of particulate matter. While not dense enough to produce '*Black-Out'* turbid conditions on the seabed, '*Turbid'* conditions negatively impact the visual clarity of the water column (**Fig. 4.6**). These conditions account for ~ 25 % of total readings or ~ 101 days. The higher percentage of '*Clear*' optical conditions throughout the sampling period, in conjunction with increased annual chokka catches during the period 2002 – 2004 (**Fig. 1.1**), suggests that the frequency and

intensity of BNL events on the EAB may have been more optimal for the fishery than in 2000 – 2001, with catches improving significantly during the study period.

The results in this study highlight the unpredictability in the intensity of turbidity events found within Algoa Bay, even at a very localized scale. Furthermore, the degree to which sharp fluctuations in optical clarity influence the coastal benthic environment is highlighted in this thesis, as turbidity levels can change from '*Clear*' to '*Black-Out'* in a matter of hours or even, in some cases, almost instantaneously (**Fig. 4.4**). The "patchiness" characteristic of BNLs on the EAB, coupled with the intensity of optical degradation, highlights the degree to which spawning aggregations of chokka are influenced by this phenomenon. As these BNL events move passively with the hydrography of the area, aggregations of chokka will actively move into areas with more favourable light to continue spawning. Due to the nature of the fishery, i.e., hand-jigs from small fishing vessels, the unpredictable movement of aggregations due to turbidity induced disruption leads to inconsistent and variable rates of catch. However, re-use of communal spawning sites suggests that these disruptions may occur on short time scales or that the aggregation may not have to move too far to 'escape' the turbid water.

The time-series experiment on benthic turbidity in Algoa Bay highlight events with greater intensity in summer than in winter. Based on the percentage occurrence of '*Black-Out*' conditions (**Fig. 4.6**), the austral summer season (9 %) experienced the greatest proportion of near-zero bottom visibility conditions compared to winter (4 %). However, the winter months (40 %) were more '*Turbid'* than the summer months (31 %) (**Fig. 4.5**). A caveat to any seasonal determination is that the austral summer season was sampled twice compared to winter, autumn, and spring. Furthermore, the dominant source type and composition of particles being detected by the OBS can change over various time scales, ensuring caution when evaluating seasonal and interannual variability in sediment and marine snow constituents (Stukel et al., 2014). Without information on the dominant source particles present in the nepheloid layer in this study, a cautious approach to understanding the nature of seasonality is needed here.

Despite these limitations, inferences on seasonality in BNL dynamics can be ascertained from the collected data. The largest proportion of favourable '*Clear*' conditions, resembling sufficiently illuminated waters suitable for chokka spawning, occur in the autumn and spring months, with 77 % and 73 %, respectively. This correlates well with the peak of chokka spawning found in early summer and autumn leading into winter (Melo and Sauer, 1999; Sauer et al., 1999). The peaks in spawning correlate to the months which demonstrate the highest proportion of '*clear*' water conditions (**Fig. 4.5**). Despite the reduction in the frequency of '*Black-Out*' conditions in the winter months, except for August 2003, it is clear that conditions distorting optical clarity of the water column in winter are as prevalent but to a lesser degree as intense as those present in summer (**Fig. 4.6**).

The relationship between SPM, turbidity and underwater visibility as undertaken in this study highlights the difficulty associated with understanding the dynamics of these events on the EAB. The data presented in **Fig 4.2B**, collected between 2002 – 2004, is selectively biased towards favourable weather conditions needed for instrument deployment, retrieval, and servicing. The bias associated with fair-weather diving accounts for the larger proportion of underwater visibility records showing favourable diving conditions than the more unfavourable low-visibility conditions (**Fig. 4.2B**). However, the inversely proportionate relationship demonstrates that high NTU values represent low optical clarity at the benthos. To further understand the nature of turbidity throughout the water column, optical and temperature sensors would need to be deployed simultaneously throughout the water column. However, due to the expensive nature of these instruments, this was not possible in this study but may be possible for studies like this in the future.

(ii) Bottom Temperature

The time-series of bottom temperature recorded in Algoa Bay (**Fig. 4.4**) from November 2002 to March 2004 is representative of the typical bottom temperatures found along the EAB (Downey, 2002; Goschen and Schumann, 1988a; Oosthuizen and Roberts, 2009; Roberts, 2010; Roberts

and Sauer, 1994; Schumann et al., 1995). Underlined by a trend of seasonal warming and cooling, the dynamic temperature regime in Algoa Bay is influenced mainly by periodic episodes of wind-driven up-and-downwelling, particularly in summer, where easterly-component winds are more prevalent than in winter (**Fig. 4.7. & Fig 4.13**; Beckley, 1983). The dynamic wind-driven movement of water around the mooring in Algoa Bay accounts for a large amount of variability in both bottom temperature and turbidity. In the summer months, the increased photoperiod, in conjunction with various drivers of upwelling, facilitates the formation and maintenance of a two-tiered thermal structure evident in Algoa Bay throughout the time series (Lutjeharms, 2006; Swart and Largier, 1987). Similarly, warm water intrusions and retroflection's to-and-from the bay, influenced by hydrographic features such as the Natal Pulse, also contribute to the wide range of benthic temperatures seen within this study (**Fig. 4.4 & Fig 4.9**; Goschen et al., 2015, 2012; Goschen and Schumann, 1988a).

A temperature range of ~ ± 5 °C, as evident in this study, is not uncommon for this coastal region (Schumann et al., 1982, 2005, Goschen & Schumann 2011, Goschen et al., 2012, 2015). The austral summer season exhibited the greatest variability in bottom temperature structures due to the dynamic wind regime which governs the process of upwelling near Cape Recife (**Fig. 4.4 & Fig. 4.10**; Goschen and Schumann, 1995). Subsequently, isothermal conditions were prevalent in winter, with fewer warm and cold-water intrusions. Temperature changes recorded in this study of + 6.27 °C/h^{-1} & - 7.33 °C/h^{-1} illustrate the extent to which temperature fluctuations influence the benthic environment in Algoa Bay. The study period, 2002 -2004, fit into a period of unusually warm summers on the EAB between 2001 and 2005 owing to the prevalence of an El-Nino event in the Pacific Ocean (Duncan et al., 2019). Despite the proposed reduction in the strength of easterly-component winds, upwelling resulting from wind forcing was still an essential component to benthic turbidity in Algoa Bay (**Fig. 4.11 & Fig. 4.13**). Goschen et al. (2012) suggested that wind-driven processes act on temperature structures that already exist on the Agulhas Bank. Therefore, coastal upwelling mechanisms not linked to wind-driven upwelling were responsible for the movement of cold Indian Ocean Central Waters onto the Agulhas bank north-east of Algoa Bay, priming the EAB for further upwelling events (Goschen et al., 2015; Goschen and Schumann, 1988; Jackson et al., 2012).

Satellite imagery on sea surface temperature (SST) throughout the sample period highlights the degree to which mesoscale variability in the Agulhas Current is responsible for the inconstant temperature regime (Jackson et al., 2012; Lutjeharms, 1981). Divergent upwelling as a result of the deviation of the Agulhas Current from the coast in the vicinity of Port Alfred (Lutjeharms, 1981) was evident in the thermal signatures of the EAB for most of the study period. This suggests that the upwelling cell near Port Alfred was responsible for 'preparing' the Agulhas Bank for wind-induced upwelling through the advection of Indian Ocean Central Water (< 10 °C) onto the shelf, where it is carried south-westwards with the prevailing current (Lutjeharms, 2006). The rapid changes in temperature evident in the western sector of Algoa Bay are a result of the movement of different water masses into the region and around the Cape Recife pinnacle (Goschen and Schumann, 1988a; Lutjeharms et al., 2000; Schumann et al., 2005b).

(iii) Wind

As mentioned previously, the study period falls within the larger environmental forcing mechanism of the El-Nino-Southern-Oscillation (Duncan et al., 2019). During an El-Nino event, westerly-component winds dominate the Eastern Agulhas Bank leading to less frequent easterly component winds, and the results presented in this thesis follow this general trend. As reported by the Port Elizabeth Airport Weather Station, the coastal wind-field in Algoa Bay is positioned parallel to the largescale orientation of the log-spiral-shaped Algoa Bay. The predominant wind direction throughout the study was west-south-west, with easterly-component winds more prevalent in summer than in winter (**Fig. 4.12 & Fig. 4.13**). Wind systems are known to pass through Algoa Bay in periods of 2.6 – 7 days (**Fig.4.12**; Schumann, 1999; Schumann et al., 1991, 1982). The reaction of waters at the coast to strong winds from the east has been shown to be very rapid (e.g., Beckley, 1983; Lutjeharms, 1998) and can have an important influence on the ecology of the adjacent coastline (Schumann et al., 1998).

Considerable variability in oceanographic and meteorological forcing exists between Algoa Bay's eastern and western sides (Roberts et al., 2012). Algoa Bay is characterized by strong West-East seasonal variability in sea temperature structure due to changing seasonal upwelling centers from west-east within the bay (Roberts et al., 2010). The prevailing wind directions in Algoa Bay are parallel to the orientation of the coastline, and the dynamic nature of the wind regime on the EAB generates complex hydrography, particularly across the western sector of Algoa Bay (Roberts, 1990). Strong south-westerly winds prevail throughout the year in the bay (Schumann et al., 1991) but become dominant in the winter (**Fig 4.13**). In summer, easterly winds become equally influential, resulting in a typical pattern of alternating easterly and westerly winds, usually lasting a few days (Roberts 2010). Swell is consequently predominantly from the southwest, but an easterly component becomes important during summer (Grundlingh and Rossouw, 1995).

The delayed response of bottom temperature measurements to upwelling events at the Algoa Bay mooring is a result of an interesting dynamic between alternating upwelling promoting easterly winds and downwelling promoting westerly winds. Following a period of strong easterly component winds, upwelling is evident in SST data on the south-west of Cape Recife, but the temperature remained stable at the mooring location. This is because the warmer water on the western side of Algoa Bay is forced passed the mooring by the wind-driven currents, and then may be driven back into the bay as a result of strong intermittent westerly component winds (Roberts, 1990; Roberts et al., 2010). If the westerly component winds increase in intensity or duration following a distinct upwelling event, then the colder water is brought north-east around the Cape Recife pinnacle and across the mooring. At times, the temperature at the Algoa Bay mooring was opposite of what would be expected based on the predominant wind direction. The temperature at the Mangold's Pool UTR showed a stronger correlation to wind direction than the Algoa Bay mooring, likely due it's location on the more exposed coastline south-west of Cape Recife. The upwelling signatures present in the Mangolds Pool UTR were not present in Algoa Bay at the same time. Without accurate data on wind direction, many instances of "upwelling" in Algoa Bay would have been falsely identified based solely on dynamic temperature changes.

Extended-Bay-Experiments (EBE)

The aim of the Extended-Bay-Experiments (EBE) was to determine the spatial extent of turbidity events in adjacent embayment's traversing important spawning sites on the EAB. Initiated during the annual squid industry closed-season in November 2002 & 2003, the EBE results give further weight to the notion that the spatial-temporal extent of turbidity events along the EAB occurs not in isolation but at varying degrees of intensity along the coast. Furthermore, the presence of both concurrent and site-specific turbidity events within these studies suggests that the drivers of turbidity events in adjacent embayment's are a factor of both large-scale and local forcing mechanisms.

It is clear from both the EBE that benthic turbidity conditions in Algoa Bay are less intense than those prevalent in St Francis Bay. The difference in bottom temperature regime, altimeter-derived significant wave height, and wind patterns between Algoa Bay and St Francis Bay, and more specifically between the two mooring locations, are as a result of the degree of exposure at each mooring location (Pattrick and Strydom, 2014; Rautenbach et al., 2019; Swart et al., 2015; Swart and Largier, 1987). The St Francis Bay mooring location is less protected from incident swell and wind conditions than the Algoa Bay mooring (Dorfler, 2002; Downey-Breedt et al., 2016). This degree of exposure is the resultant for the differences in environmental parameters seen at each site (Patrick and Strydom, 2014). Furthermore, the Oubos mooring in the 2002 EBE study was by far the most variable in terms of temperature and turbidity, which may also be correlated to the degree of exposure (Pattrick and Strydom, 2014), in particular to variables such as wind speed, wind direction, wave direction and wave period.

The difference between the St Francis Bay and Algoa Bay turbidity measurements in the EBE can also result from complex hydrography in the vicinity of the St Francis Bay mooring. Hydrographic studies in the western sector of St Francis Bay demonstrate the presence of an anticyclonic flow pattern (Dorfler, 2002; Roberts and van den Berg, 2002; Downey et al., 2010). This anticyclonic flow pattern may isolate the hydrography of the western sector of St Francis Bay from the rest of the bank (Roberts and van den Berg, 2002). The entrainment of particles

within the anticyclonic flow pattern may result in the increased intensity of turbidity events in St Francis Bay compared to Algoa Bay. As a result, the contribution of organic matter to the intensity of BNL dynamics in St Francis Bay may be greater than Algoa Bay. The temperature regime in Algoa Bay, influenced by the complex hydrography around Cape Recife, may result in more rapid movements of water masses, preventing detrital settling to the benthos.

As per Malan (2013), upwelling is not always present in the thermal imagery in the vicinity of the Port Alfred Upwelling Cell. The fact that there is not a 'clear' picture of upwelling from remote sensing SST, but a clear indication of enhanced primary production in the area, is typical of the role of the Port Alfred Upwelling Cell in acting as a secondary biological pump for the EAB (Lutjeharms, 2006).

Mechanisms responsible for BNL dynamics

In conjunction with previous studies on benthic turbidity dynamics, the results from this study suggest that some degree of uniformity exists amongst the chaotic processes that govern BNL intensity on the Agulhas Bank (Dorfler, 2002; Downey, 2009; Oosthuizen et al., 2009; Githaiga-Mwicigi, 2012). When looking at the environmental factors in isolation, it is difficult to understand the processes which form and modulate BNL dynamics. Due to the complex nature of the events coupled with a lack of essential environmental variables, such as currents and optical responses of source particles, the mechanisms responsible for BNL dynamics were qualitatively examined for recurring drivers and themes. The results presented in this study elucidated the intricacies of these events, and the nature of the events can be bracketed into one of three primary mechanisms responsible for the dynamics of benthic turbidity on the EAB, namely; (i) fragmentation of BNL into 'patches,' (ii) resuspension events/wave-induced turbidity, and (iii) Temperature-Turbidity Interface.

(i) Fragmentation of BNL into 'patches'

It is important to remember that the benthic nepheloid layer has both organic and inorganic components (Zoutendyk & Duvenage, 1989). Several studies have highlighted the 'patchiness' of nepheloid layers across the Agulhas Bank, and several reasons exist for the fragmentation of turbidity events into patches. Firstly, coastal upwelling zones and hence nutrient concentrations are not uniformly distributed across the bank. The uneven distribution of coastal upwelling centers on the EAB (Schumann et al., 1982; Walker, 1986) leads to the uneven distribution of areas of primary production, and subsequently, the settling of phytodetrital material throughout the water column (Stukel et al., 2014).

In conjunction with the uneven distribution of primary production in the euphotic zone of the EAB (Barlow et al., 2010, Lamont et al., 2018) are irregularities in the coastline that includes the sheltered bays of Algoa Bay and St Francis Bay. Under the right conditions, entrainment of phytoplankton rich waters in the bays as a result of physical forcing mechanisms of wind (Schumann, 1999) or the Agulhas Current (Goschen et al., 2015; Russo et al., 2019) lead to proportionately higher rates of productivity within the embayment's and, consequently, a greater proportion of detrital settling compared to more exposed areas of the coastline (Barlow et al., 2020). As phytoplankton blooms emerge in patches along the coast, the resultant detrital fallout will result in areas of increased concentrations of SPM compared to areas adjacent to or above it (Gardner et al., 1983; Gardner and Sullivan, 1981; Richardson, 1987). Turbidity levels at a fixed location will rise and fall as SPM is advected and distributed by the overlying physical conditions of the Agulhas Current (Jackson et al., 2012).

The role of the oceans biological pump and the subsequent fate of organic matter in the ocean has been studied exhaustively in oceans around the world (see Turner (2015) for a detailed review), however, the variable flux rates are very understudied on the EAB. Organic and inorganic particles settling from surface waters are subjected to the physical, biological, and chemical processes of aggregation, disaggregation, decomposition and dissolution (Turner,

2015), adding to the variable rates of detrital settling and therefore SPM distribution on the seafloor (Biscaye and Eittreim, 1974; Gardner et al., 2018).

The role of the Agulhas Current on passive particle movement on the EAB has been primarily focused on the nearshore retention of commercially important larvae (e.g., Jackson et al., 2012b; Lutjeharms and Da Silva, 2019; Roberts, 2010, 2009; Weidberg et al., 2015). The key findings from these studies suggest that larvae that are advected seawards are unlikely to be returned to the continental shelf and are therefore lost to the nearshore (< 70 m) coastal system (Weidberg et al., 2015). The same principle of advection-driven-loss of particulate rich water masses may also act on the prevalence and longevity of the nepheloid layers found on the EAB, and account for the 'patchiness' reported in this study and previous studies (e.g., Dorfler, 2002; Githaiga-Mwicigi, 2012). Further fragmentation of the phytoplankton blooms and the resultant marine snow environment may occur as a result of alternating prevailing wind conditions (Roberts, 2010), reverse alongshore currents (Roberts and van den Berg, 2002; Roberts, 2010), wave action (Johnson et al., 2001; Puig et al., 2004; Roberts et al., 2010; Roberts and Van Den Berg, 2002), mesoscale features of the Agulhas Current (Goschen et al., 2015; Jackson et al., 2012; Malan et al., 2019, 2018), and bathymetry (Boyd et al., 1992; Goschen et al., 2012b; Le Clus et al., 1996; Naveira Garabato et al., 2004).

As these patches of SPM move passively with the hydrography of the area, chokka are likely to actively move to areas with favourable light to continue spawning. In terms of the fishery itself, inconsistent catches over a similar geographical area are a result of the movement of targeted spawning aggregations away from BNL "patches" that are synonymous with the EAB.

(ii) Resuspension events/Wave-induced turbidity

Easterly-component winds drive upwelling at the capes (Boyd and Shillington, 1994; Russo et al., 2019; Schumann et al., 1982; Walker, 1986), which through Ekman veering/pumping brings cold, nutrient-rich waters from the outer shelf to the nearshore spawning grounds (Roberts, 1998b; Roberts et al., 2010). Here, where conditions are optimal for primary production followed by secondary enhancement (Probyn et al., 1994; Stukel et al., 2014), the coastal zone is enriched with phytodetrital material, which makes up the marine snow environment, and critically, the organic component of the nepheloid layer (Zoutendyk & Duvenage, 1989).

During quiescent oceanic conditions (Pasqual et al., 2010; Puig et al., 2013; Ribó et al., 2013), the settling of the phytodetrital material from the euphotic zone to the benthos clears the water column's upper reaches while generating a dense layer of suspended particulate matter near the seafloor (e.g., hydrographic transect; **Fig. 4.22 & Fig. 4.23**). Depending on the strength of the thermocline and the proximity of the thermocline to the seafloor, the dense layer of particulate matter is limited and regulated in its upward/downward rate of flux by the strength of the thermocline/pycnocline (Carter et al., 1987).

In summer, coastal upwelling and increased photoperiod combine to develop a well-stratified water column on the Agulhas Bank (Larger and Swart, 1987). Dorfler (2002) showed that benthic turbidity increased in intensity below the thermocline when the thermocline moved closer to the seafloor. Westerly component winds, particularly in summer, push warm surface waters from the outer reach of the bay into the bay itself (Lutjeharms 2006). Further mesoscale variability in the Agulhas Current trajectory is then responsible for entraining or expelling these water masses from the bays (Jackson et al., 2012). In winter, the westerly component winds and increased wave activity induce vertical mixing of the water column (Probyn et al., 1994). This vertical mixing is further enhanced during large swell or storm activity, particularly in winter. It is well accepted that kinetic energy as a result of strong waves and currents are the principle components responsible for resuspension of particulate matter from the seafloor (Gardner et al., 2018; Gardner and Sullivan, 1981). The wave period, not measured here due to constraints in

remote sensing data, is an essential aspect in maintaining the particulate matter in suspension (Gardner et al., 2018). The results from this study suggests that resuspension events as a result of orbital shear stress on the benthic substrate due to increased wave height to be the most important and significant factor influencing turbidity events on the EAB. This study highlighted the average wave height as ~ 2 m, which was suggested as the threshold as to which small inorganic particles as well as the lighter, organic particles would be resuspended (Zoutendyk & Duvenage, 1989). This study correlates to previous studies on wave height in the area, where wave height conditions greater than 2 m were present for 70 % of the year, while wave periods exceeding 8s exist for 95 % of the year (CSIR 1986, 1992). Based on the annual averages of wave height and period, there is a consistently high potential for sediment resuspension throughout the year (Zoutendyk & Duvenage, 1989).

Depending on the timing of the algal bloom in relation to the strength of the thermocline, sinking particulate matter may remain in suspension above the pycnocline or have the upward flux of SPM restricted by the presence of the thermocline/pycnocline barrier (Carter et al., 1987). The physiochemical and density barrier that is created by intense thermoclines lead to the generation of Intermediate Nepheloid layers and Surface Nepheloid layers such as those present in the hydrographic surveys in EBE-2002 (**Fig. 4.22 & Fig. 4.23**). Therefore, primary and secondary production in the euphotic zone over the inshore spawning grounds is vital to predicting benthic turbidity events, taking into account Agulhas Current variability on water masses within the bays (Roberts, 2010). Furthermore, in conjunction with the phytodetrital settling from periods of elevated primary production, resuspended sediment or previously deposited organic particulate matter due to wave-related orbital shear stress contributes to the density of the nepheloid layer found on or directly above the seabed (Biscaye and Eittreim, 1974; Brewer et al., 1976; Gardner et al., 2018; Masunaga et al., 2017; McCave, 1986; Puig et al., 2013; Salat et al., 2010).

(iii) Temperature-Turbidity Interface

The relationship between benthic turbidity and bottom temperature is, at best, complex and is not discussed here in detail, with further research required (**Fig 4.10**). At times there is a clear increase in bottom turbidity, which coincides with a change in bottom temperature, either through the movement of colder, nutrient-rich bottom water onto the shelf or via physical processes of warm water expulsion from the inner shelf (Roberts, 2010; Roberts and Nieuwenhuys, 2016). It appears that during instances such as these, that the Temperature-Turbidity Interface governs the dynamics of benthic turbidity. The Temperature-Turbidity Interface can also be considered to be density dependent (Pasqual et al., 2010; Puig et al., 2013; Salat et al., 2010), whereby the vertical and horizontal flux of sediment and organic matter is controlled by the restrictive temperature boundary (Carter et al. 1987). However, benthic turbidity events are also known to occur in more isothermal conditions, i.e., in the absence of this density-controlled Temperature-Turbidity Interface. Primary production on the outer Agulhas Bank was thought to be hindered by the lack of a stable thermocline (Hidalgo et al., 2012; Probyn et al., 1994; Swart and Largier, 1987).

Interestingly, Townsend et al. (1992) showed that phytoplankton blooms are possible in the absence of vertical stratification of the water column. These authors suggest that water column stability is not a prerequisite for phytoplankton blooms to develop and for phytoplankton cells to remain above critical depth. The deepening penetration of light in the clear waters during increased solar radiation, in conjunction with the absent, or weak, vertical wind mixing, could maintain cell growth rates that overcome the vertical excursion rates in the neutrally stable water column thus leading to a bloom. Once begun, the bloom may enhance the warming of the surface waters by virtue of light scattering and absorption properties of the phytoplankton particles. Thus, in some instances, the development of the thermocline may be initiated by, rather than serve as a prerequisite for, the initiation of an algal bloom. Further research is required to fully understand the dynamics between particle flux rates and the transient thermocline on the EAB.

Climate change and fisheries management

In light of the unprecedented and unpredictable climatic changes expected in the Anthropocene, modern scientific discourse on fisheries management has emphasized the need to take an ecosystem approach to the governance of marine resources (Cowan et al., 2012; Hilborn, 2004; Hilborn et al., 2003). Furthermore, a holistic understanding of the environment in which commercially viable marine resources reside is increasingly essential, owing to the global demise in traditional fin-fish which has accelerated targeted cephalopod fisheries throughout the globe (Caddy and Rodhouse, 1998; FAO, 2012; Mullon et al., 2005; Paterson et al., 2010). Perhaps most importantly, moving towards a greater understanding of the relationship between resource abundance and environmental variability is pertinent to implementing effective management strategies (FAO, 2012; Rice, 2011). Therefore, the need to further explore the fundamental relationships between stock and recruitment, and the distribution of species based on both biotic and abiotic factors, will contribute to the global resilience of our declining marine resources (Côté and Darling, 2010; Hodgson et al., 2015).

The results presented in this thesis exemplify the difficulty associated with understanding the drivers of BNL events on the EAB. Although squid are probably the best placed oceanic organisms to deal with climate change, owing to incredible life-history plasticity across all stages (Pecl and Jackson, 2008), chokka are restricted from extending their home range by the warm Agulhas Current and the cold Benguela current, and may be negatively influenced by changing conditions. For example, severe winter storms along the southern African coast in 1992 resulted in high swells, and beach erosion adjacent to the inshore squid spawning grounds, which may have accounted for exceptionally poor catches that year (Roberts & Sauer, 1994; Roberts et al. 2012). Severe winter storms may be linked to El-Nino conditions, which enhance severe westerly winds on the south coast and longer-term climate change. Extreme weather events are predicted to increase in frequency and intensity in the 21st century, which may affect the spawning process through increased turbidity events because of the increased frequency of wave and storm events (Duncan et al., 2019). Roberts et al. (2012) postulate that higher waves, more storms, and general warming of the water column is likely to see a shift in the reproductive

strategy to the cooler mid-shelf region. This may have consequences for both the fishery and the reproductive success rate.

In terms of nepheloid layer dynamics, climate change is expected to alter the temperature regime of the EAB as a result of the broadening of the Agulhas Current (Malan et al., 2019). As the Agulhas Current decreases in speed as a result of global climatic changes, the frequency and intensity of upwelling is expected to increase on the EAB (Duncan et al., 2019; Malan et al., 2019). The increased frequency in upwelling will result in greater primary and secondary production through increased nutrient availability. Subsequently, this will result in greater volumes of detrital settling which then primes the EAB for resuspension events. Coastal upwelling on the EAB is expected to increase in both intensity and duration in the coming century (Duncan et al., 2019), and it is likely that nepheloid layers on the EAB will also follow this upward trend. Owing to the increased detrital settling as a result of increased upwelling, it may be that the BNL is influenced both spatially, temporally and in intensity. Due to the greater column of detritus on the substrate, and the increased wave activity expected in the area (Duncan et al., 2019), BNL events will increase in intensity across all seasons, but particularly in summer when easterly component winds favour upwelling. The duration of these events may also increase, as the dynamic wind regime is expected to stabilize (Malan et al., 2019).

It is unclear whether the above will have an affect on the “patchiness” of BNL events on the EAB. It may be that due to increased upwelling and marine snow, that BNL events would encompass a greater proportion of the bank and embayment’s as a result of excess settled detritus on the substrate. Alternatively, the increased rate of upwelling and subsequent primary production and settling of marine snow aggregates may increase the “patchiness” characteristic of BNL events due to an even more uneven distribution of settled particles which are then resuspended. The difficulty in predicting the events now ensures that future projections of these events are, currently, unattainable.

If BNL events become a more dominant mode variability on the EAB, it is expected that chokka will move away from the highly variable nearshore coastal zone onto the mid-shelf, where they become largely unavailable to the depth limited hand-jig fishery. This could have profound consequences on the chokka industry as a whole, whose labour is highly dependent on nearshore catches. However, the increased frequency and intensity of upwelling events on the EAB may result in greater movement of water masses enriched with particles, and subsequently, provide a greater proportion of 'clear' conditions optimal for chokka reproduction. Despite the ambiguity here, it is evident that the nature of BNL events is likely to change in conjunction with climate change, and the distribution of chokka will be similarly affected. It is clear from projections that climate change is likely to increase environmental variability in the nearshore coastal zone, and it may be that chokka expand the spawning habitat to encompass the mid-to-deep shelf to avoid the unpredictability of environmental perturbations on the nearshore EAB. With a greater proportion of spawning aggregations occurring further offshore, the reliance of the coastal communities on chokka catch may result in disastrous socio-economic consequences for the industry and communities. However, the plasticity of cephalopods to environmental changes provides the industry with sufficient hope that these consequences can be overcome to continue the sustainable exploitation of our declining marine resources.

Due to the variable life-history traits of *Loliginid* squid (Pecl et al., 2004) and the nature of the fishery itself, i.e., targeting spawning aggregations, the industry is currently controlled through effort limitation. The Total Applied/Allowable Effort (TAE) measures the maximum amount of fishing pressure that can be applied to a single stock species over a specific period (Iwata et al., 2010). A mandatory five-week closed season (19 October – 21 November) during the peak summer spawning period has been in place since 1998 (Roel, 1998). From 2003 to 2013, the fishery was controlled via restrictions on the number of fishers and boats involved in the fishery, with effort level capped at 2422 crew or 136 vessels, whichever occurred first (Cochrane et al., 2014; DFFE, 2020). In 2014, it was decided that a 'floating' closed-season of between three and five months would be implemented to safeguard the fishery, through early detection regarding exceeding the TAE, from future collapses (Cochrane et al., 2014; DFFE, 2020).

In the only quantitative study on benthic turbidity and chokka catch abundance, Schön et al. (2002) found benthic turbidity to be the main influential factor, accounting for 13 % of catch variation. As suggested by Zoutendyk and Duvenage (1989), the ecological consequences of the nepheloid layer may be as widespread as the distribution of the phenomenon itself. A primary motivation behind any fishery related study on the relationship between catch abundance and the environment is to improve the understanding of the relationship and address the management of the fishery accordingly. Evident from this study is that benthic turbidity events are a common, year-round occurrence, traversing the entire primary spawning grounds of chokka. Due to the importance of visual stimuli in the reproductive process, and based on underwater visibility assessments conducted by divers, it has been postulated that the short-term variability in squid catch abundance could be because of nepheloid-layer-driven-termination of the spawning process (Roberts and Sauer, 1994). Due to the highly erratic nature of the hydrography of the EAB, management measures need to dynamic and be introduced and changed annually, as information on the resource becomes available. Current management through effort limitation, with the inclusions of variable closed seasons, appears to be the best management practice for chokka squid (Lipinski et al., 2020) and in fact for cephalopods in general (Arkhipkin et al., 2015; Benson and Craig, 2014; Maxwell et al., 2004).

Conclusions and future research

The study attempted to address four key questions;

- *How does benthic turbidity relate to underwater visibility?*

From the relationship between benthic turbidity and underwater visibility as ascertained from in-situ diver observations (**Fig. 42**), it is clear that there is an inversely proportional relationship between benthic visibility (m) and turbidity (NTU). Measurements of benthic turbidity were divided into three qualitative brackets that best describe bottom turbidity in terms of visual impairment of the water clarity, namely; (a) *Clear* (> 5 NTU), (b) *Turbid* (5 < – ≥ 15 NTU), and

(c) Black-Out (> 15 NTU) optical conditions. '*Black-Out*' events denote very dense SPM concentrations near the seafloor and represent poor visual clarity, as well as a high probability of disruption to squid spawning behaviour. On the other hand, '*Turbid*' conditions, while not dense enough to generate '*Black-Out*' events, signify the presence of elevated particulate matter concentrations that have a negative influence on underwater visibility.

- *What is the frequency and intensity of benthic turbidity events in Algoa Bay, a sheltered embayment of the EAB?*

The 17-month time-series recorded in Algoa Bay indicates that benthic turbidity events are a common but highly variability occurrence. Based on the qualitative classifications of benthic turbidity concerning the optical clarity of the water column, turbid conditions existed for ~ 30 % of the sample period. Benthic turbidity readings of > 15 NTU correlate to '*Black-Out*' underwater conditions with visibility of ≤ 1 m, accounted for ~ 5 % of the total readings, or ~ 27 days. The seasonality of nepheloid layer influence on the EAB is confounded by the short duration of the study and the fact that the summer season was sampled twice, however, turbidity events were more prevalent in winter (40 %) than in summer (31 %), followed by spring (26 %) and then autumn (23 %). The most extreme (or intense) events were found in summer (9 % of readings resembled '*Black-Out*' conditions) when upwelling and high levels of primary production are most dominant.

- *What is the spatial extent of turbidity events on the EAB?*

The Extended-Bay-Experiment (EBE) conducted in 2002 and 2003 demonstrated that benthic turbidity events do not occur in isolation but vary in degrees of intensity along the coast, suggesting 'patchiness' of the BNL. The occurrence of both site-specific and concurrent turbidity events suggests that both localized and largescale environmental forcing mechanisms are responsible for the variability evident in benthic turbidity structures between geographically

distinct embayment's of the EAB. There were incidences when benthic turbidity events were present in one bay but not in another. The intensity of turbidity events also differed in each embayment (e.g., Event A, EBE 2002). The Hydrographic survey revealed the greatest BNL intensity closest to the coast, decreasing further offshore.

- *What are the environmental drivers of these benthic turbidity events?*

This study revealed a complicated relationship between wind-induced movement of particle rich water masses on the inner-eastern side of Cape Recife, Algoa Bay (mentioned previously when looking at SST by Schumann et al., 1982; Goschen and Schumann, 1988). In general, winds with an easterly-component were not well correlated with increases in benthic turbidity. However, short wind-reversals, which are synonymous with the area (Roberts, 2010), were the principal driver of benthic turbidity events in Algoa Bay (e.g., EBE 2003). Wind-induced movement of water masses, either through upwelling and downwelling, transports the BNL 'patches' with alongshore currents. Furthermore, in conjunction with westerly-component winds, high instances of primary production enabled entrainment of particle-rich water masses in Algoa Bay (e.g., Event A & D, EBE 2002). This enabled higher rates of marine snow to settle toward the benthos, whereby the next wind-driven event would move the further enriched water mass past the mooring, resulting in peaks and troughs of benthic turbidity.

This study found no significant correlation between benthic turbidity events and chlorophyll-a concentrations. This was due mainly to the proximity of the mooring to the coast in conjunction with high cloud-coverage confounding robust statistical analysis. However, the role of the Port Alfred Upwelling Cell on primary production rates within Algoa Bay was evident from remote sensing data throughout the study.

The most significant driver of benthic turbidity events appears to be correlated to wave events. Analysis of altimeter-derived significant wave height indicates that particulate matter

resuspension influences the intensity, prevalence, and longevity of benthic turbidity events on the EAB. A linear regression analysis ($r = 0.38$, $p = 0.0028$, $n = 61$) highlights a statistically significant ($p < 0.05$), positive correlation between altimeter-based significant wave height (Hs; m) and benthic turbidity (NTU) in Algoa Bay. Wave events at the Algoa Bay mooring were not as intense as the more exposed coastline due to refraction around the Cape Recife Pinnacle, a feature that has been observed in other studies (e.g., Patrick and Strydom, 2014). Similarly, resuspension events caused by longshore currents associated with wind-variability were also important components to nepheloid layer dynamics on the EAB. In contrast to the Algoa Bay mooring location, upwelling events in St Francis Bay brings about an increase in benthic turbidity. However, the reverse conditions (where westerly component winds reverse the upwelling process), seem to be drive turbidity events in Algoa Bay (**Fig. A1 – Fig. A17**).

Future research:

The results of this thesis expand on existing knowledge of the dynamics of benthic turbidity on the Eastern Agulhas Bank. Furthermore, the role of this thesis in examining the mechanisms responsible for nepheloid layer dynamics will contribute towards building improved predictive capacity useful to fisheries managers.

There are a host of environmental parameters not covered in this study, which may influence the dynamics of benthic turbidity in Algoa Bay. These include wave period, wave direction, current speed, current direction, irradiance levels, internal waves/Rossby Waves as well as the contribution of riverine and terrestrial sedimentation to the formation and maintenance of the BNL. Future research on the constituents, source particles and concentration of particulate matter within the BNL will advance the ability to model, and therefore predict these water mass features, and subsequently, implications for coastal ecology. A focus of future studies should be on quantifying the relationship between BNL constituents and physical concentrations of particulate matter ($\mu g.l^{-1}$), including variables such as density, porosity and variability of both organic and inorganic matter which make up the BNL.

Finally, by incorporating the qualitative analysis of the dynamics of nepheloid layers on the EAB into Regional Oceanographic Models (ROMS), General Linear Models (GLM) and particle distribution models such as DELFT-3D, it is possible to move toward predicting the timing and intensity of these events. For example, including turbidity in the model approach conducted by Joyner (2016) will help fine-tune the relationship between chokka catch abundance on the nearshore spawning grounds and environmental variability.

List of References:

Agnew, D.J., Beddington, J.R., Hill, S.L., 2002. The potential use of environmental information to manage squid stocks. Can. J. Fish. Aquat. Sci. 59, 1851–1857. https://doi.org/10.1139/f02-150

Agrawal, Y., 2004. Bottom Nepheloid Layer. Oceanography 17, 79–79. https://doi.org/10.5670/oceanog.2004.51

Agrawal, Y.C., 2005. The optical volume scattering function: Temporal and vertical variability in the water column off the New Jersey coast. Limnol. Oceanogr. 50, 1787–1794. https://doi.org/10.4319/lo.2005.50.6.1787

Antia, A.N., Koeve, W., Fischer, G., Blanz, T., Schulz-Bull, D., Scholten, J., Neuer, S., Kremling, K., Kuss, J., Peinert, R., Hebbeln, D., Bathmann, U., Conte, M., Fehner, U., Zeitzschel, B., 2001. Basin-wide particulate carbon flux in the Atlantic Ocean: Regional export patterns and potential for atmospheric CO 2 sequestration. Global Biogeochem. Cycles 15, 845–862. https://doi.org/10.1029/2000GB001376

Arkhipkin, A.I., Rodhouse, P.G.K., Pierce, G.J., Sauer, W., Sakai, M., Allcock, L., Arguelles, J., Bower, J.R., Castillo, G., Ceriola, L., Chen, C.S., Chen, X., Diaz-Santana, M., Downey, N., González, A.F., Granados Amores, J., Green, C.P., Guerra, A., Hendrickson, L.C., Ibáñez, C., Ito, K., Jereb, P., Kato, Y., Katugin, O.N., Kawano, M., Kidokoro, H., Kulik, V. V., Laptikhovsky, V. V., Lipinski, M.R., Liu, B., Mariátegui, L., Marin, W., Medina, A., Miki, K., Miyahara, K., Moltschaniwskyj, N., Moustahfid, H., Nabhitabhata, J., Nanjo, N., Nigmatullin, C.M., Ohtani, T., Pecl, G., Perez, J.A.A., Piatkowski, U., Saikliang, P., Salinas-Zavala, C.A., Steer, M., Tian, Y., Ueta, Y., Vijai, D., Wakabayashi, T., Yamaguchi, T., Yamashiro, C., Yamashita, N., Zeidberg, L.D., 2015. World squid fisheries. Rev. Fish. Sci. Aquac. 23, 92–252. https://doi.org/10.1080/23308249.2015.1026226

Augustyn, C.J., 1991. The biomass and ecology of chokka squid *Loligo vulgaris reynaudii* off the West Coast of South Africa. South African J. Zool. 26, 164–181. https://doi.org/10.1080/02541858.1991.11448245

Augustyn, C.J., 1990. Biological studies on the chokker squid loligo vulgaris reynaudii (cephalopoda; myopsida) on spawning grounds off the south-east coast of South Africa. South African J. Mar. Sci. 9, 11–26. https://doi.org/10.2989/025776190784378736

Augustyn, C.J., Lipinski, M.R., Sauer, W.H.H., Roberts, M.J., Mitchell-Innes, B.A., 1994. Chokka squid on the Agulhas Bank: life history and ecology. S. Afr. J. Sci. 90, 143–154.

Augustyn, C.J., Llpiński, M.R., Sauer, W.H.H., 1992a. Can the loligo squid fishery be managed effectively? A synthesis of research on loligo vulgaris reynaudii. South African J. Mar. Sci. 12, 903–918. https://doi.org/10.2989/02577619209504751

Augustyn, C.J., Llpiński, M.R., Sauer, W.H.H., 1992b. Can the loligo squid fishery be managed effectively? A synthesis of research on loligo vulgaris reynaudii. South African J. Mar. Sci. 12, 903–918. https://doi.org/10.2989/02577619209504751

Baker, E.T., Lavelle, J.W., 1984. Effect of Particle Size on the Light Attenuation Coefficient of Natural Suspensions. J. Geophys. Res. 89, 8197–8203. https://doi.org/10.1029/JC089iC05p08197

Baloyi, J., Mahlathi, C.D., Wessels, G.J.C., Ubbink, O., Smit, J.E., 2009. Numerical study of the resultant sediment transport near the Port of Ngqura due to the blockage of a sediment bypass, in: 13th International Conference on Heat Transfer, Fluid Mechanics and Thermodynamics. pp. 940-949Baloyi, J., Mahlathi, C.D., Wessels, G.J.C.

Bao, R., Zhao, M., McNichol, A., Galy, V., McIntyre, C., Haghipour, N., Eglinton, T.I., 2019. Temporal constraints on lateral organic matter transport along a coastal mud belt. Org. Geochem. 128, 86–93. https://doi.org/10.1016/j.orggeochem.2019.01.007

Barlow, R., Lamont, T., Gibberd, M.J., Russo, C., Airs, R., Tutt, G., Britz, K., van den Berg, M., 2020. Phytoplankton adaptation and absorption properties in an Agulhas Current ecosystem. Deep. Res. Part I Oceanogr. Res. Pap. 157, 103209. https://doi.org/10.1016/j.dsr.2019.103209

Barlow, R., Lamont, T., Kyewalyanga, M., Sessions, H., Morris, T., 2010. Phytoplankton production and physiological adaptation on the southeastern shelf of the Agulhas ecosystem. Cont. Shelf Res. 30, 1472–1486. https://doi.org/10.1016/j.csr.2010.05.007

Beal, L.M., Elipot, S., 2016. Broadening not strengthening of the Agulhas Current since the early 1990s. Nature 540, 570–573. https://doi.org/10.1038/nature19853

Beaulieu, S.E., Baker, E.T., German, C.R., Maffei, A., 2013. An authoritative global database for active submarine hydrothermal vent fields. Geochemistry, Geophys. Geosystems 14, 4892–4905. https://doi.org/10.1002/2013GC004998

Beckley, L.E., 1983. Sea-surface Temperature Variability around Cape Recife, South Africa. S. Afr. J. Sci. 79, 436–438.

Belde, J., Reuning, L., Back, S., 2017. Bottom currents and sediment waves on a shallow carbonate shelf, Northern Carnarvon Basin, Australia. Cont. Shelf Res. 138, 142–153. https://doi.org/10.1016/j.csr.2017.03.007

Benson, M.H., Craig, R.K., 2014. The End of Sustainability. Soc. Nat. Resour. 27, 777–782. https://doi.org/10.1080/08941920.2014.901467

Biscaye, P.E., Eittreim, S.L., 1977. Suspended Particulate Loads and Transports in the Nepheloid Layer of the Abyssal Atlantic Ocean, Developments in Sedimentology. https://doi.org/10.1016/S0070-4571(08)70556-9

Biscaye, P.E., Eittreim, S.L., 1974. Variations in Benthic Boundary Layer Phenomena: Nepheloid Layer in the North American Basin, in: Suspended Solids in Water. Springer US, pp. 227–260. https://doi.org/10.1007/978-1-4684-8529-5_15

Blackburn, S., Sauer, W.H.H., Lipinski, M.R., 1998. The embryonic development of the Chokka squid loligo vulgaris reynaudii d'Orbigny, 1845. Veliger.

Boletzky, S. V., 1994. Embryonic development of cephalopods at low temperatures. Antarct. Sci. 6, 139–142. https://doi.org/10.1017/S0954102094000210

Boss, E., Guidi, L., Richardson, M.J., Stemmann, L., Gardner, W., Bishop, J.K.B., Anderson, R.F., Sherrell, R.M., 2015. Optical techniques for remote and in-situ characterization of particles pertinent to GEOTRACES. Prog. Oceanogr. 133, 43–54. https://doi.org/10.1016/j.pocean.2014.09.007

Boyd, A.J., Shillington, F.A., 1994. Physical forcing and circulation patterns on the Agulhas Bank. S. Afr. J. Sci. 90, 114–122.

Boyd, A.J., Taunton-Clark, J., Oberholster, G.P.J., 1992. Spatial features of the near-surface and midwater circulation patterns off western and southern South Africa and their role in the life histories of various commercially fished species. South African J. Mar. Sci. 12, 189–206. https://doi.org/10.2989/02577619209504702

Boyle, P.R., Pierce, G.J., Hastie, L.C., 1995. Flexible reproductive strategies in the squid Loligo forbesi. Mar. Biol. 121, 501–508. https://doi.org/10.1007/BF00349459

Bremner, J.M., 1983. Properties of Logarithmic Spiral Beaches with Particular Reference to Algoa Bay. Sandy Beaches as Ecosyst. 97–113. https://doi.org/10.1007/978-94-017-2938-3_6

Brewer, P.G., Spencer, D.W., Biscaye, P.E., Hanley, A., Sachs, P.L., Smith, C.L., Kadar, S., Fredericks, J., 1976. The distribution of particulate matter in the Atlantic Ocean. Earth Planet. Sci. Lett. 32, 393–402. https://doi.org/10.1016/0012-821X(76)90080-7

Brierly, A.S., Thorpe, J.P., Pierce, G.J., Clarke, M.R., Boyle, P.R., 1995. Genetic variation in the neritic squid Loligo forbesi (Myopsida: Loliginidae) in the northeast Atlantic Ocean. Mar. Biol. 79–86.

Cacchione, D.A., Drake, D.E., 1986. Nepheloid layers and internal waves over continental shelves and slopes. Geo-Marine Lett. 6, 147–152. https://doi.org/10.1007/BF02238085

Caddy, J.F., Rodhouse, P.G., 1998. Cephalopod and groundfish landings: Evidence for ecological change in global fisheries? Rev. Fish Biol. Fish. 8, 431–444. https://doi.org/10.1023/A:1008807129366

Campos, E.J.D., Velhote, D., Da Silveira, I.C.A., 2000. Shelf break upwelling driven by Brazil current cyclonic meanders. Geophys. Res. Lett. 27, 751–754. https://doi.org/10.1029/1999GL010502

Carter, R.A., McMurray, H.F., Largier, J.L., 1987. Thermocline characteristics and phytoplankton dynamics in Agulhas Bank waters. South African J. Mar. Sci. 5, 327–336.

Churchill, J.H., Milkowski, G.W., 1986. A cyclonic eddy and shelf-slope water exchange associated with a gulf stream warm core ring. J. Geophys. Res. 91, 9615–9623.

Cochrane, K.L., Augustyn, C.J., Fairweather, T., Japp, D., Kilongo, K., Iitembu, J., Moroff, N., Roux, J.P., Shannon, L., van Zyl, B., vaz Velho, F., 2009. Benguela Current Large Marine Ecosystem-Governance and management for an ecosystem approach to fisheries in the region. Coast. Manag. 37, 235–254. https://doi.org/10.1080/08920750902851187

Cochrane, K.L., Oliver, B., Sauer, W., 2014. An assessment of the current status of the chokka squid fishery in South Africa and an evaluation of alternative allocation strategies. Mar. Policy 43, 149–163. https://doi.org/10.1016/j.marpol.2013.05.006

Côté, I.M., Darling, E.S., 2010. Rethinking ecosystem resilience in the face of climate change. PLoS Biol. 8. https://doi.org/10.1371/journal.pbio.1000438

Cowan, J.H., Rice, J.C., Walters, C.J., Hilborn, R., Essington, T.E., Day, J.W., Boswell, K.M., 2012. Challenges for Implementing an Ecosystem Approach to Fisheries Management. Mar. Coast. Fish. 4, 496–510. https://doi.org/10.1080/19425120.2012.690825

Crookes, D.J., Brenner, L., 2016. Fisheries : Facts and Trends South Africa. WWF Rep. Ser. 112, 1–9.

De Ruijter, W.P.M., Beal, L., Biastoch, A., Zahn, R., 2013. The role of the agulhas system in regional and global climate. Eos (Washington. DC). https://doi.org/10.1002/2013EO100005

DEFF, 2020. Status of the South African Marine Fishery Resources. https://doi.org/10.13140/RG.2.2.30734.48962

Demarcq, H., Barlow, R.G., Shillington, F.A., 2003. Climatology and variability of sea surface temperature and surface chlorophyll in the benguela and agulhas ecosystems as observed by satellite imagery. African J. Mar. Sci. 25, 363–372. https://doi.org/10.2989/18142320309504022

Dencausse, G., Arhan, M., Speich, S., 2010. Spatio-temporal characteristics of the Agulhas Current retroflection. Deep. Res. Part I Oceanogr. Res. Pap. 57, 1392–1405. https://doi.org/10.1016/j.dsr.2010.07.004

Dodet, G., Piolle, J.F., Quilfen, Y., Abdalla, S., Accensi, M., Ardhuin, F., Ash, E., Bidlot, J.R., Gommenginger, C., Marechal, G., Passaro, M., Quartly, G., Stopa, J., Timmermans, B., Young, I., Cipollini, P., Donlon, C., 2020. The Sea State CCI dataset v1: Towards a sea state climate data record based on satellite observations. Earth Syst. Sci. Data 12, 1929–1951. https://doi.org/10.5194/essd-12-1929-2020

Dohan, K., Maximenko, N., 2010. Monitoring ocean currents with satellite sensors. Oceanography 23, 94–103. https://doi.org/10.5670/oceanog.2010.08

Donlon, C., Robinson, I., Casey, K.., Vazquez-Cuervo, J., Armstrong, E., Arino, O., Gentemann, C., Piolle, J.F., Barton, I., Beggs, H., Wick, G., Emery, B., Minnett, P., 2007. The Global Ocean Data Assimilation Experiment High-resolution Sea Surface Temperature Pilot Project. African Meteorogical Soc. 1197–221.

Downey-Breedt, N.J., Roberts, M.J., Sauer, W.H.H., Chang, N., 2016. Modelling transport of inshore and deep-spawned chokka squid (Loligo reynaudi) paralarvae off South Africa: The potential contribution of deep spawning to recruitment. Fish. Oceanogr. 25, 28–43. https://doi.org/10.1111/fog.12132

Downey, N.J., 2009. The effect of temperature and turbidity on spawning chokka squid, loligo reynaudii, in Eastern Cape Waters. Nelson Mandela University.

Downey, N.J., Roberts, M.J., Baird, D., 2010. An investigation of the spawning behaviour of the chokka squid Loligo reynaudii and the potential effects of temperature using acoustic telemetry. ICES J. Mar. Sci. 67, 231–243. https://doi.org/10.1093/icesjms/fsp237

Duncan, M.I., James, N.C., Bates, A.E., Goschen, W.S., Potts, W.M., 2019. Localised intermittent upwelling intensity has increased along South Africa's south coast due to El Niño–Southern Oscillation phase state. African J. Mar. Sci. 41, 325–330. https://doi.org/10.2989/1814232X.2019.1656105

Dyer, K.R., Manning, A.J., 1999. Observation of the size, settling velocity and effective density of flocs, and their fractal dimensions. J. Sea Res. 41, 87–95. https://doi.org/10.1016/S1385-1101(98)00036-7

Elipot, S., Beal, L.M., 2018. Observed Agulhas Current sensitivity to interannual and long-term trend atmospheric forcings. J. Clim. https://doi.org/10.1175/JCLI-D-17-0597.1

Ewing, M., Thorndike, E.M., 1965. Suspended matter in deep ocean water. Science (80-.). 147, 1291–1294. https://doi.org/10.1126/science.147.3663.1291

FAO, 2012. World Fisheries and Aquaculture.

Forsythe, J., Kangas, N., Hanlon, R.T., 2004. Does the California market squid (Loligo opalescens) spawn naturally during the day or at night? A note on the successful use of ROVs to obtain basic fisheries biology data. Fish. Bull. 102, 389–392.

Gardner, W., Richardson, M.J., Walsh, I., Berglund, B., 1990. In-Situ Optical Sensing of Particles for Determination of Oceanic Processes: What Satellites Can't See, But Tranmissometers Can. Oceanography 3, 11–17. https://doi.org/10.5670/oceanog.1990.02

Gardner, W.D., 1989. Baltimore Canyon as a modern conduit of sediment to the deep sea. Deep Sea Res. Part A, Oceanogr. Res. Pap. 36, 323–358. https://doi.org/10.1016/0198-0149(89)90041-1

Gardner, W.D., Richardson, M.J., Hinga, K.R., Biscaye, P.E., 1983. Resuspension measured with sediment traps in a high-energy environment. Earth Planet. Sci. Lett. 66, 262–278. https://doi.org/10.1016/0012-821X(83)90140-1

Gardner, W.D., Richardson, M.J., Mishonov, A. V., 2018. Global assessment of benthic nepheloid layers and linkage with upper ocean dynamics. Earth Planet. Sci. Lett. 482, 126–134. https://doi.org/10.1016/j.epsl.2017.11.008

Gardner, W.D., Sullivan, L.G., 1981. Benthic Storms: Temporal Variability. Science (80-.). 213, 329–332.

Gardner, W.D., Sullivan, L.G., Thorndike, E.M., 1984. Long-term photographic, current, and nephelometer observations of manganese nodule environments in the Pacific. Earth Planet. Sci. Lett. 70, 95–109. https://doi.org/10.1016/0012-821X(84)90212-7

Gardner, W.D., Tucholke, B.E., Richardson, M.J., Biscaye, P.E., 2017. Benthic storms, nepheloid layers, and linkage with upper ocean dynamics in the western North Atlantic. Mar. Geol. 385, 304–327. https://doi.org/10.1016/j.margeo.2016.12.012

Githaiga-Mwicigi, J., 2012. The distribution, formation, origins and constituents of nepheloid layers on the Agulhas Bank, South Africa, and thier implications for chokka (Loligo reynaudii) squid. University of Cape Town.

Glazer, J.P., Butterworth, D.S., 2006. Some refinements of the assessment of the South African squid resource, Loligo vulgaris reynaudii. Fish. Res. 78, 14–25. https://doi.org/10.1016/j.fishres.2005.12.011

Goschen, W.S., Bornman, T.G., Deyzel, S.H.P., Schumann, E.H., 2015. Coastal upwelling on the far eastern Agulhas Bank associated with large meanders in the Agulhas Current. Cont. Shelf Res. 101, 34–46. https://doi.org/10.1016/j.csr.2015.04.004

Goschen, W.S., Schumann, E.H., 2011. The physical oceanographic processes of Algoa Bay, with emphasis on the western coastal region.

Goschen, W.S., Schumann, E.H., 1995. Upwelling and the occurrence of cold water around Cape Recife, Algoa Bay, South Africa. South African J. Mar. Sci. 16, 57–67. https://doi.org/10.2989/025776195784156520

Goschen, W.S., Schumann, E.H., 1988a. Ocean current and temperature structures in algoa bay and beyond in november 1986. South African J. Mar. Sci. 7, 101–116. https://doi.org/10.2989/025776188784379198

Goschen, W.S., Schumann, E.H., 1988b. Ocean current and temperature structures in algoa bay and beyond in november 1986. South African J. Mar. Sci. 7, 101–116. https://doi.org/10.2989/025776188784379198

Goschen, W.S., Schumann, E.H., Bernard, K.S., Bailey, S.E., Deyzel, S.H.P., 2012a. Upwelling and ocean structures off Algoa Bay and the south-east coast of South Africa. African J. Mar. Sci. 34, 525–536. https://doi.org/10.2989/1814232X.2012.749810

Goschen, W.S., Schumann, E.H., Bernard, K.S., Bailey, S.E., Deyzel, S.H.P., 2012b. Upwelling and ocean structures off Algoa Bay and the south-east coast of South Africa. African J. Mar. Sci. 34, 525–536. https://doi.org/10.2989/1814232X.2012.749810

Graff, J.R., Menden-Deuer, S., 2016. Physical and optical properties of phytoplanktonrich layers in a coastal fjord: A step toward prediction and strategic sampling of plankton patchiness. Mar. Ecol. Prog. Ser. https://doi.org/10.3354/meps11601

Grundlingh, M., Rossouw, M., 1995. Wave attenuation in the Agulhas Current. S. Afr. J. Sci. 91, 357–359.

Hanan, D., 1998. Market squid: what we know and what we need to know for effective management. CalCOFI Rep. 39, 53–54.

Hanlon, R.T., 1998. Mating systems and sexual selection in the squid loligo: how might commercial fishing on spawning squids affect them? CalCOFI Rep. 39.

Hanlon, R.T., Messenger, J.B., 1996. Cephalopod behaviour. Oceanogr. Lit. Rev. 11, 1131.

Hanlon, R.T., Smale, M.J., Sauer, W.H.H., 2002. the Mating System of Tbe Squid Loligo Vulgaris Reyna Udii (Cephalopoda , Mollusca) Off South Africa : Fighting , Guarding , Sneaking , Mating Ant Egg Laying Behavior. System 71, 331–345.

Hanlon, R.T., Smale, M.J., Sauer, W.H.H., 1994. An ethogram of body patterning behavior in the squid Loligo vulgaris reynaudii on spawning grounds in South Africa. Biol. Bull. 187, 363–372. https://doi.org/10.2307/1542293

Hara, M., 2009. Crew members in South Africa's squid industry; whether they have benefitted from transformation and governance reforms. Mar. Policy 33, 513–519. https://doi.org/10.1016/j.marpol.2008.11.008

Hawley, N., 2004. Response of the benthic nepheloid layer to near-inertial internal waves in southern Lake Michigan. J. Geophys. Res. C Ocean. 109, 1–14. https://doi.org/10.1029/2003JC002128

Hidalgo, P., Escribano, R., Fuentes, M., Jorquera, E., Vergara, O., 2012. How coastal upwelling influences spatial patterns of size-structured diversity of copepods off central-southern Chile (summer 2009). Prog. Oceanogr. 92–95, 134–145. https://doi.org/10.1016/j.pocean.2011.07.012

Hilborn, R., 2004. Ecosystem-based fisheries management: Mar. Ecol. Prog. Ser. 274, 275–278.

Hilborn, R., Quinn, T.P., Schindler, D.E., Rogers, D.E., 2003. Biocomplexity and fisheries sustainability. Proc. Natl. Acad. Sci. U. S. A. 100, 6564–6568. https://doi.org/10.1073/pnas.1037274100

Hill, S.L., Agnew, D.J., 2002. Optimal harvest strategies for single-cohort squid populations 71, 371–381.

Hobday, A.J., Cochrane, K., Downey-Breedt, N., Howard, J., Aswani, S., Byfield, V., Duggan, G., Duna, E., Dutra, L.X.C., Frusher, S.D., Fulton, E.A., Gammage, L., Gasalla, M.A., Griffiths, C., Guissamulo, A., Haward, M., Jarre, A., Jennings, S.M., Jordan, T., Joyner, J., Ramani, N.K., Shanmugasundaram, S.L.P., Malherbe, W., Cisneros, K.O., Paytan, A., Pecl, G.T., Plagányi, É.E., Popova, E.E., Razafindrainibe, H., Roberts, M., Rohit, P., Sainulabdeen, S.S., Sauer, W., Valappil, S.T., Zacharia, P.U., van Putten, E.I., 2016. Planning adaptation to

climate change in fast-warming marine regions with seafood-dependent coastal communities. Rev. Fish Biol. Fish. 26, 249–264. https://doi.org/10.1007/s11160-016-9419-0

Hodgson, D., McDonald, J.L., Hosken, D.J., 2015. What do you mean, "resilient"? Trends Ecol. Evol. 30, 503–506. https://doi.org/10.1016/j.tree.2015.06.010

Hollister, C.D., McCave, I.N., 1984. Sedimentation under deep-sea storms. Nature 309, 220–225. https://doi.org/10.1038/309220a0

Hutchings, K., Laird, M., Wright, A., Clark, B.M., 2019. Algoa Bay Sea-Based Aquaculture Development Zone.

Hutchings, L., 1994. The Aguhas Bank: a synthesis of available information and a brief comparison with other east-coast shelf regions. S. Afr. J. Sci. 90, 179–185.

Hutchings, L., Beckley, L.E., Griffiths, M.H., Roberts, M.J., Sundby, S., Van der Lingen, C., 2002. Spawning on the edge: Spawning grounds and nursery areas around the southern African coastline, in: Marine and Freshwater Research. https://doi.org/10.1071/MF01147

Iwata, Y., Ito, K., Sakurai, Y., 2010. Is commercial harvesting of spawning aggregations sustainable?-The reproductive status of the squid Loligo bleekeri. Fish. Res. 102, 286–290. https://doi.org/10.1016/j.fishres.2009.12.010

Jackson, G.D., O'Dor, R.K., Andrade, Y., 2005. First tests of hybrid acoustic/archival tags on squid and cuttlefish. Mar. Freshw. Res. 56, 425–430. https://doi.org/10.1071/MF04248

Jackson, J.M., Rainville, L., Roberts, M.J., McQuaid, C.D., Lutjeharms, J.R.E., 2012a. Mesoscale bio-physical interactions between the Agulhas Current and the Agulhas Bank, South Africa. Cont. Shelf Res. 49, 10–24. https://doi.org/10.1016/j.csr.2012.09.005

Jackson, J.M., Rainville, L., Roberts, M.J., McQuaid, C.D., Lutjeharms, J.R.E., 2012b. Mesoscale bio-physical interactions between the Agulhas Current and the Agulhas Bank, South Africa. Cont. Shelf Res. 49, 10–24. https://doi.org/10.1016/j.csr.2012.09.005

Johnson, D.R., Weidemann, A., Pegau, W.S., 2001. Internal tidal bores and bottom nepheloid layers. Cont. Shelf Res. 21, 1473–1484. https://doi.org/10.1016/S0278-4343(00)00109-6

Joyner, J., 2016. The influence of environmental variabilitty on the catch of chokka, Loligo reynaudii, off the coast of South Africa. Rhodes University.

Jury, M.R., Goschen, W.S., 2020. Physical ocean-atmosphere variability over the shelf of South Africa from reanalysis products. Cont. Shelf Res. 202, 104135. https://doi.org/10.1016/j.csr.2020.104135

Kainge, P., Kirkman, S.P., Estevão, V., van der Lingen, C.D., Uanivi, U., Kathena, J.N., van der Plas, A., Githaiga-Mwicigi, J., Makhado, A., Nghimwatya, L., Endjambi, T., Paulus, S., Kalola, M., Antonio, M., Tjizoo, B., Shikongo, T., Nsiangango, S., Uahengo, T., Bartholomae, C., Mqoqi, M., Hamukuaya, H., 2020. Fisheries yields, climate change, and ecosystem-based management of the Benguela Current Large Marine Ecosystem. Environ. Dev. 36, 1–18. https://doi.org/10.1016/j.envdev.2020.100567

Karageorgis, A.P., Georgopoulos, D., Kanellopoulos, T.D., Mikkelsen, O.A., Pagou, K., Kontoyiannis, H., Pavlidou, A., Anagnostou, C., 2012. Spatial and seasonal variability of particulate matter optical and size properties in the Eastern Mediterranean Sea. J. Mar. Syst. 105–108, 123–134. https://doi.org/10.1016/j.jmarsys.2012.07.003

Komar, P.D., Miller, M.C., 1973. The threshold of sediment movement under oscillatory water waves. J. Sediment. Petrol. 43, 1101–1110.

Krug, M., Tournadre, J., Dufois, F., 2014. Interactions between the Agulhas Current and the eastern margin of the Agulhas Bank. Cont. Shelf Res. 81, 67–79. https://doi.org/10.1016/j.csr.2014.02.020

Lamont, T., Brewin, R.J.W., Barlow, R.G., 2018. Seasonal variation in remotely-sensed phytoplankton size structure around southern Africa. Remote Sens. Environ. 204, 617–631. https://doi.org/10.1016/j.rse.2017.09.038

Lampitt, R.S., 1985. Evidence for the seasonal deposition of detritus to the deep-sea floor and its subsequent resuspension. Deep Sea Res. Part A, Oceanogr. Res. Pap. 32, 885–897. https://doi.org/10.1016/0198-0149(85)90034-2

Lampitt, R.S., Newton, P.P., Jickells, T.D., Thomson, J., King, P., 2000. Near-bottom particle flux in the abyssal northeast Atlantic. Deep. Res. Part II Top. Stud. Oceanogr. 47, 2051–2071. https://doi.org/10.1016/S0967-0645(00)00016-3

Largier, J.L., Swart, V.P., 1987. East-west variation in thermocline breakdown on the Agulhas bank. South African J. Mar. Sci. 5, 263–272. https://doi.org/10.2989/025776187784522252

Le Clus, F., Hennig, H.F.K.O., Rogers, J., 1996. Bathymetry and sediment type effects on catch rates of Austroglossus pectoralis (Soleidae) on the inner central agulhas bank. South African J. Mar. Sci. 17, 79–92. https://doi.org/10.2989/025776196784158608

Leber, G.M., Beal, L.M., Elipot, S., 2017. Wind and current forcing combine to drive strong upwelling in the Agulhas Current. J. Phys. Oceanogr. 47, 123–134. https://doi.org/10.1175/JPO-D-16-0079.1

Lipiński, M.R., Mwanangombe, C.H., Durholtz, D., Yemane, D., Githaiga-Mwicigi, J., Sauer, W.H.H., 2020. Age estimates of chokka squid Loligo reynaudii off South Africa and their use to test the effectiveness of a closed season for conserving this resource. African J. Mar. Sci. 42, 461–471. https://doi.org/10.2989/1814232X.2020.1842804

Lipinski, M.R., Soule, M., 2007. Disintegration of a large concentration of loliginid squid as a response to predation. Rev. Fish Biol. Fish. 17, 477–485. https://doi.org/10.1007/s11160-006-9026-6

Lipiński, M.R., van der Vyver, J.S.F., Shaw, P., Sauer, W.H.H., 2016. Life cycle of chokka-squid Loligo reynaudii in South African waters. African J. Mar. Sci. https://doi.org/10.2989/1814232X.2016.1230074

Lutjeharms, J.R.E., 2006. The ocean environment off southeastern Africa: A review. S. Afr. J. Sci. 102, 419–426.

Lutjeharms, J.R.E., 1981. Features of the southern Agulhas Current circulation from satellite remote sensing. S. Afr. J. Sci. 77, 231–236.

Lutjeharms, J.R.E., Catzel, R., Valentine, H.R., 1989. Eddies and other boundary phenomena of the Agulhas Current. Cont. Shelf Res. 9, 597–616.

Lutjeharms, J.R.E., Cooper, J., Roberts, M., 2000. Upwelling at the inshore edge of the Agulhas Current. Cont. Shelf Res. 20, 737–761. https://doi.org/10.1016/S0278-4343(99)00092-8

Lutjeharms, J.R.E., Da Silva, C.E., 2019. Agulhas current, in: Encyclopedia of Ocean Sciences. Elsevier, pp. 236–247. https://doi.org/10.1016/B978-0-12-409548-9.11362-4

Lutjeharms, J.R.E., Durgadoo, J. V., Ansorge, I.J., 2007. Surface drift at the western edge of the Agulhas Bank. S. Afr. J. Sci. 103, 63–67.

Lutjeharms, J.R.E., Roberts, H.R., 1988. The Natal pulse: An extreme transient on the Agulhas Current. J. Geophys. Res. Ocean. 93, 631–645.

Malan, N., Backeberg, B., Biastoch, A., Durgadoo, J. V., Samuelsen, A., Reason, C., Hermes, J., 2018. Agulhas Current Meanders Facilitate Shelf-Slope Exchange on the Eastern Agulhas Bank. J. Geophys. Res. Ocean. 123, 4762–4778. https://doi.org/10.1029/2017JC013602

Malan, N., Durgadoo, J. V., Biastoch, A., Reason, C., Hermes, J., 2019. Multidecadal Wind Variability Drives Temperature Shifts on the Agulhas Bank. J. Geophys. Res. Ocean. 124, 3021–3035. https://doi.org/10.1029/2018JC014614

Malan, N.C., 2013. Driving Mechanisms of the Port Alfred upwelling cell inshore of the Agulhas Current. University of Cape Town.

Malviya, S., Scalco, E., Audic, S., Vincent, F., Veluchamy, A., Poulain, J., Wincker, P., Iudicone, D., de Vargas, C.,

Bittner, L., Zingone, A., Bowler, C., 2016. Insights into global diatom distribution and diversity in the world's ocean. Proc. Natl. Acad. Sci. https://doi.org/10.1073/pnas.1509523113

Martins, R.S., Roberts, M.J., Chang, N., Verley, P., Moloney, C.L., Vidal, E.A.G., 2010a. Effect of yolk utilization on the specific gravity of chokka squid. ICES J. Mar. Sci. 67, 1323–1335.

Martins, R.S., Roberts, M.J., Chang, N., Verley, P., Moloney, C.L., Vidal, E.A.G., 2010b. Effect of yolk utilization on the specific gravity of chokka squid (Loligo reynaudii) paralarvae: Implications for dispersal on the Agulhas Bank, South Africa. ICES J. Mar. Sci. 67, 1323–1335. https://doi.org/10.1093/icesjms/fsq098

Martins, R.S., Roberts, M.J., Vidal, É.A.G., Moloney, C.L., 2010c. Effects of temperature on yolk utilization by chokka squid (Loligo reynaudii d'Orbigny, 1839) paralarvae. J. Exp. Mar. Bio. Ecol. 386, 19–26. https://doi.org/10.1016/j.jembe.2010.02.014

Masunaga, E., Arthur, R.S., Fringer, O.B., Yamazaki, H., 2017. Sediment resuspension and the generation of intermediate nepheloid layers by shoaling internal bores. J. Mar. Syst. 170, 31–41. https://doi.org/10.1016/j.jmarsys.2017.01.017

Maxwell, M.R., Henry, A., Elvidge, C.D., Safran, J., Hobson, V.R., Nelson, I., Tuttle, B.T., Dietz, J.B., Hunter, J.R., 2004. Fishery dynamics of the California market squid (Loligo opalescens), as measured by satellite remote sensing. Fish. Bull. 102, 661–670.

McCave, I.N., 2019. Nepheloid layers, in: Encyclopedia of Ocean Sciences. pp. 170–183. https://doi.org/10.1016/B978-0-12-409548-9.11207-2

McCave, I.N., 2009. Nepheloid Layers, in: Encyclopedia of Ocean Sciences. Elsevier Ltd, pp. 8–18. https://doi.org/10.1016/B978-012374473-9.00671-8

McCave, I.N., 1986. Local and global aspects of the bottom nepheloid layers in the world ocean. Netherlands J. Sea Res. 20, 167–181.

McCave, I.N., 1984. Erosion, transport and deposition of fine-grained marine sediments. Geol. Soc. Spec. Publ. 15, 35–69. https://doi.org/10.1144/GSL.SP.1984.015.01.03

Melo, Y., Sauer, W.H.H., 2007. Determining the daily spawning cycle of the chokka squid, Loligo reynaudii off the South African Coast. Rev. Fish Biol. Fish. 17, 247–257. https://doi.org/10.1007/s11160-006-9034-6

Melo, Y.C., Sauer, W.H.H., 1999. Confirmation of serial spawning in the chokka squid Loligo vulgaris reynaudii off the coast of South Africa. Mar. Biol. 135, 307–313. https://doi.org/10.1007/s002270050628

Mikkelsen, O.A., Hill, P.S., Milligan, T.G., 2006. Single-grain, microfloc and macrofloc volume variations observed with a LISST-100 and a digital floc camera. J. Sea Res. 55, 87–102. https://doi.org/10.1016/j.seares.2005.09.003

Moltschaniwskyj, N.A., Hall, K., Lipinski, M.R., Marian, J.E.A.R., Nishiguchi, M., Sakai, M., Shulman, D.J., Sinclair, B., Sinn, D.L., Staudinger, M., Van Gelderen, R., Villanueva, R., Warnke, K., 2007. Ethical and welfare considerations when using cephalopods as experimental animals. Rev. Fish Biol. Fish. 17, 455–476. https://doi.org/10.1007/s11160-007-9056-8

Mullon, C., Fréon, P., Cury, P., 2005. The dynamics of collapse in world fisheries. Fish Fish. 6, 111–120. https://doi.org/10.1111/j.1467-2979.2005.00181.x

Naud, M.J., Sauer, W.H.H., McKeown, N.J., Shaw, P.W., 2016. Multiple mating, paternity and complex fertilisation patterns in the chokka squid Loligo reynaudii. PLoS One. https://doi.org/10.1371/journal.pone.0146995

Naveira Garabato, A.C., Polzin, K.L., King, B.A., Heywood, K.J., Visbeck, M., 2004. Widespread Intense Turbulent Mixing in the Southern Ocean. Science (80-.). 303, 210–213. https://doi.org/10.1126/science.1090929

Olyott, L.J.H., Sauer, W.H.H., Booth, A.J., 2007. Spatial patterns in the biology of the chokka squid, Loligo reynaudii on the Agulhas Bank, South Africa. Rev. Fish Biol. Fish. 17, 159–172. https://doi.org/10.1007/s11160-006-9027-5

Oosthuizen, A., Roberts, M.J., 2009a. Bottom temperature and in situ development of chokka squid eggs (Loligo vulgaris reynaudii) on mid-shelf spawning grounds, South Africa. ICES J. Mar. Sci. 66, 1967–1971. https://doi.org/10.1093/icesjms/fsp198

Oosthuizen, A., Roberts, M.J., 2009b. Bottom temperature and in situ development of chokka squid eggs (Loligo vulgaris reynaudii) on mid-shelf spawning grounds, South Africa, in: ICES Journal of Marine Science. pp. 1967–1971. https://doi.org/10.1093/icesjms/fsp198

Oosthuizen, Ané, Roberts, M.J., Sauer, W.H.H., 2002. Temperature effects on the embryonic development and hatching success of the squid Loligo vulgaris reynaudii. Bull. Mar. Sci. 71, 619–632.

Oosthuizen, A., Roberts, M.J., Sauer, W.H.H., 2002. Early post-cleavage stages and abnormalities identified in the embryonic development of chokka squid eggs Loligo vulgaris reynaudii. South African J. Mar. Sci. 379–382. https://doi.org/10.2989/025776102784528367

Pak, H.G., Zaneveld, J.R.V., 1983. Temporal variations of beam attenuation coefficient on the Continental Rise off Nova Scotia. J. Geophys. Res. 88, 4427–4432. https://doi.org/10.1029/JC088iC07p04427

Palanques, A., Durrieu de Madron, X., Puig, P., Fabres, J., Guillén, J., Calafat, A., Canals, M., Heussner, S., Bonnin, J., 2006. Suspended sediment fluxes and transport processes in the Gulf of Lions submarine canyons. The role of storms and dense water cascading. Mar. Geol. 234, 43–61. https://doi.org/10.1016/j.margeo.2006.09.002

Pasqual, C., Sanchez-Vidal, A., Zúñiga, D., Calafat, A., Canals, M., Durrieu De Madron, X., Puig, P., Heussner, S., Palanques, A., Delsaut, N., 2010. Flux and composition of settling particles across the continental margin of the Gulf of Lion: The role of dense shelf water cascading. Biogeosciences 7, 217–231. https://doi.org/10.5194/bg-7-217-2010

Paterson, B., Isaacs, M., Hara, M., Jarre, A., Moloney, C.L., 2010. Transdisciplinary co-operation for an ecosystem approach to fisheries: A case study from the South African sardine fishery. Mar. Policy 34, 782–794. https://doi.org/10.1016/j.marpol.2010.01.019

Pattrick, P., Strydom, N.A., 2014. The effects of exposure in sandy beach surf zones on larval fishes. J. Fish Biol. 84, 1354–1376. https://doi.org/10.1111/jfb.12360

Pecl, G.T., 2004. The in situ relationships between season of hatching, growth and condition in the southern calamary, Sepioteuthis australis. Mar. Freshw. Res. 55, 429–438. https://doi.org/10.1071/MF03150

Pecl, G.T., Jackson, G.D., 2008. The potential impacts of climate change on inshore squid: biology, ecology and fisheries. Rev. Fish Biol. Fish. 18, 373–385.

Pedocchi, F., García, M.H., 2006. Evaluation of the LISST-ST instrument for suspended particle size distribution and settling velocity measurements. Cont. Shelf Res. 26, 943–958. https://doi.org/10.1016/j.csr.2006.03.006

Penven, P., Lutjeharms, J.R.E., Marchesiello, P., Roy, C., Weeks, S.J., 2001. Generation of cyclonic eddies by the Agulhas Current in the lee of the Agulhas Bank. Geophys. Res. Lett. 28, 1055–1058. https://doi.org/10.1029/2000GL011760

Peterson, W.T., Hutchings, L., 1995. Distribution, abundance and production of the copepod Calanus agulhensis on the Agulhas Bank in relation to spatial variations in hydrography and chlorophyll concentration. J. Plankton Res. 17, 2275–2294. https://doi.org/10.1093/plankt/17.12.2275

Philpot, W., Davis, C.O., Paul Bissett, W., Mobley, C.D., Kohler, D.D.R., Lee, Z., Bowles, J., Steward, R.G., Agrawal, Y., Trowbridge, J., Gould, R.W., Arnone, R.A., 2004. Bottom characterization from hyperspectral image data. Oceanography 17, 76–85. https://doi.org/10.5670/oceanog.2004.50

Pierce, G., Belcari, P., Bustamante, P., Challier, L., González, Á., Guerra, Á., Jereb, P., Koueta, N., Lefkaditou, E., Moreno, A., Pereira, J., Piatkowski, U., Robin, J.P., Roel, B., Santos, M.B., Santurtun, M., Seixas, S., Shaw, P., Smith, J., Stowasser, G., Villanueva, R., Wang, J., Wangvoralak, S., 2004. Cephalopod biology and fisheries in Europe 86–118.

Pierce, G.J., Hastie, L.C., Guerra, A., Thorpe, R.S., Howard, F.G., Boyle, P.R., 1994. Morphometric variation in

Loligo forbesi and Loligo vulgaris: regional, seasonal, sex, maturity and worker differences. Fish. Res. 21, 127–148. https://doi.org/10.1016/0165-7836(94)90100-7

Pierce, G.J., Valavanis, V.D., Guerra, A., Jereb, P., Orsi-Relini, L., Bellido, J.M., Katara, I., Piatkowski, U., Pereira, J., Balguerias, E., Sobrino, I., Lefkaditou, E., Wang, J., Santurtun, M., Boyle, P.R., Hastie, L.C., MacLeod, C.D., Smith, J.M., Viana, M., González, A.F., Zuur, A.F., 2008. A review of cephalopod-environment interactions in European Seas. Hydrobiologia 612, 49–70. https://doi.org/10.1007/s10750-008-9489-7

Popova, E., Yool, A., Byfield, V., Cochrane, K., Coward, A.C., Salim, S.S., Gasalla, M.A., Henson, S.A., Hobday, A.J., Pecl, G.T., Sauer, W.H., Roberts, M.J., 2016. From global to regional and back again: Common climate stressors of marine ecosystems relevant for adaptation across five ocean warming hotspots. Glob. Chang. Biol. 22, 2038–2053. https://doi.org/10.1111/gcb.13247

Probyn, T. a, Mitchellinnes, B. a, Brown, P.C., Hutchings, L., Carter, R. a, 1994. Review of primary production and related processes on the Agulhas-Bank. S. Afr. J. Sci.

Puig, P., Company, J.B., Sardà, F., Palanques, A., 2001. Responses of deep-water shrimp populations to intermediate nepheloid layer detachments on the Northwestern Mediterranean continental margin. Deep. Res. Part I Oceanogr. Res. Pap. https://doi.org/10.1016/S0967-0637(01)00016-4

Puig, P., Madron, X.D. de, Salat, J., Schroeder, K., Martín, J., Karageorgis, A.P., Palanques, A., Roullier, F., Lopez-Jurado, J.L., Emelianov, M., Moutin, T., Houpert, L., 2013. Thick bottom nepheloid layers in the western Mediterranean generated by deep dense shelf water cascading. Prog. Oceanogr. 111, 1–23. https://doi.org/10.1016/j.pocean.2012.10.003

Puig, P., Palanques, A., Guillén, J., El Khatab, M., 2004. Role of internal waves in the generation of nepheloid layers on the northwestern Alboran slope: Implications for continental margin shaping. J. Geophys. Res. C Ocean. 109, 1–11. https://doi.org/10.1029/2004JC002394

Quartly, G.D., Kurekin, A.A., 2020. Sensitivity of altimeter wave height assessment to data selection. Remote Sens. 12. https://doi.org/10.3390/RS12162608

Rautenbach, C., Barnes, M.A., de Vos, M., 2019. Tidal characteristics of South Africa. Deep. Res. Part I Oceanogr. Res. Pap. 150, 103079. https://doi.org/10.1016/j.dsr.2019.103079

Reason, C.J.C., 2001. Evidence for the influence of the Agulhas Current on regional atmospheric circulation patterns. J. Clim. https://doi.org/10.1175/1520-0442(2001)014<2769:EFTIOT>2.0.CO;2

Ribal, A., Young, I.R., 2019. 33 Years of Globally Calibrated Wave Height and Wind Speed Data Based on Altimeter Observations. Sci. Data 6, 1–15. https://doi.org/10.1038/s41597-019-0083-9

Ribó, M., Puig, P., Salat, J., Palanques, A., 2013. Nepheloid layer distribution in the Gulf of Valencia, northwestern Mediterranean. J. Mar. Syst. 111–112, 130–138. https://doi.org/10.1016/j.jmarsys.2012.10.008

Rice, J., 2011. Managing fisheries well: Delivering the promises of an ecosystem approach. Fish Fish. 12, 209–231. https://doi.org/10.1111/j.1467-2979.2011.00416.x

Richardson, M.J., 1987. Particle size, light scattering and composition of suspended particulate matter in the North Atlantic. Deep Sea Res. Part A, Oceanogr. Res. Pap. 34, 1301–1329. https://doi.org/10.1016/0198-0149(87)90129-4

Roberts, M.J., 2010. Coastal currents and temperatures along the eastern region of Algoa Bay, South Africa, with implications for transport and shelf-bay water exchange. African J. Mar. Sci. 32, 145–161. https://doi.org/10.2989/1814232X.2010.481153

Roberts, M.J., 2009. Recruitment variability of chokka squid (Loligo reynaudii) - the role of the cold ridge, currents and retention on the Agulhas Bank, South Africa.

Roberts, M.J., 2005. Chokka squid (Loligo vulgaris reynaudii) abundance linked to changes in South Africa's Agulhas Bank ecosystem during spawning and the early life cycle. ICES J. Mar. Sci. 62, 33–55. https://doi.org/10.1016/j.icesjms.2004.10.002

Roberts, M.J., 1998a. The influence of the environment on chokka squid *Loligo vulgaris reynaudii* spawning aggregations: steps towards a quantified model. South African J. Mar. Sci. 20, 267–284. https://doi.org/10.2989/025776198784126223

Roberts, M.J., 1998b. The influence of the environment on chokka squid Loligo vulgaris reynaudii spawning aggregations: Steps towards a quantified model. South African J. Mar. Sci. 267–284. https://doi.org/10.2989/025776198784126223

Roberts, M.J., Downey, N.J., Sauer, W.H., 2012a. The relative importance of shallow and deep shelf spawning habitats for the South African chokka squid (Loligo reynaudii). IC 69(4), 563–571. https://doi.org/10.1093/icesjms/fss153

Roberts, M.J., Downey, N.J., Sauer, W.H., 2012b. The relative importance of shallow and deep shelf spawning habitats for the South African chokka squid (Loligo reynaudii). ICES J. Mar. Sci. 69, 563–571. https://doi.org/10.1093/icesjms/fss023

Roberts, M.J., Nieuwenhuys, C., 2016. Observations and mechanisms of upwelling in the northern KwaZulu-Natal Bight, South Africa. African J. Mar. Sci. 38, S43–S63. https://doi.org/10.2989/1814232X.2016.1194319

Roberts, M.J., Sauer, W.H.H., 1994a. Environment : the key to understanding the South African chokka squid (Lolrgo vulgaris reynaudiD life cycle and fishery ? Antarct. Sci. 6, 249–258.

Roberts, M.J., Sauer, W.H.H., 1994b. Environment: The key to understanding the South African chokka squid (Loligo vulgaris reynaudii) life cycle and fishery? Antarct. Sci. 6, 249–258. https://doi.org/10.1017/S0954102094000386

Roberts, M.J., Van Den Berg, M., 2002. Recruitment variability of Chokka squid (*Loligo reynaudii*)- the role of the cold ridge currents and retention on the Agulhas Bank (South Africa). Bull. Mar. Sci. 71, 691–710.

Roberts, M.J., van der Lingen, C.D., Whittle, C., van den Berg, M., 2010. Shelf currents, lee-trapped and transient eddies on the inshore boundary of the agulhas current, South Africa: Their relevance to the kwaZulu-Natal sardine run. African J. Mar. Sci. 32, 423–447. https://doi.org/10.2989/1814232X.2010.512655

Rodhouse, P.G.K., Pierce, G.J., Nichols, O.C., Sauer, W.H.H., Arkhipkin, A.I., Laptikhovsky, V. V., Lipiński, M.R., Ramos, J.E., Gras, M., Kidokoro, H., Sadayasu, K., Pereira, J., Lefkaditou, E., Pita, C., Gasalla, M., Haimovici, M., Sakai, M., Downey, N., 2014. Environmental effects on cephalopod population dynamics: Implications for management of fisheries, Advances in Marine Biology. https://doi.org/10.1016/B978-0-12-800287-2.00002-0

Roel, B.A., 1998. Stock assessment of the chokka squid, Loligo vulgaris reynaudii.

Roel, B.A., Butterworth, D.S., 2000. Assessment of the South African chokka squid Loligo vulgaris reynaudii: Is disturbance of aggregations by the recent jig fishery having a negative impact on recruitment? Fish. Res. 48, 213–228. https://doi.org/10.1016/S0165-7836(00)00186-7

Roel, B.A., Cochrane, K.L., Field, J.G., 2011. Investigation into the declining trend in chokka squid Loligo vulgaris reynaudii Catches made by South African trawlers . South African J. Mar. Sci. https://doi.org/10.2989/025776100784125735

Roel, B.A., Cochrane, K.L., Field, J.G., 2000. Investigation into the declining trend in chokka squid Loligo vulgaris reynaudii Catches made by South African trawlers. South African J. Mar. Sci. 22, 121–135. https://doi.org/10.2989/025776100784125735

Roel, B.A., Cochrane, K.L., S., B.D., 1998. Investigation on the effects of different levels of effort and of the closed season in the jig fishery for chokka squid *Loligo vulgaris reynaudii*. South African J. Mar. Sci. 19, 501–512. https://doi.org/10.2989/025776198784126935

Rogers, J., Li, X.C., 2002. Environmental impact of diamond mining on continental shelf sediments off southern Namibia. Quat. Int. 92, 101–112. https://doi.org/10.1016/S1040-6182(01)00118-5

Rouault, M., Lee-Thorp, A.M., Lutjeharms, J.R.E., 2000. The atmospheric boundary layer above the Agulhas

Current during alongcurrent winds. J. Phys. Oceanogr. 30, 40–50. https://doi.org/10.1175/1520-0485(2000)030<0040:TABLAT>2.0.CO;2

Rouault, M., Pohl, B., Penven, P., 2010a. Coastal oceanic climate change and variability from 1982 to 2009 around South Africa. African J. Mar. Sci. 32, 237–246. https://doi.org/10.2989/1814232x.2010.501563

Rouault, M., Pohl, B., Penven, P., 2010b. Coastal oceanic climate change and variability from 1982 to 2009 around South Africa. African J. Mar. Sci. 32, 237–246. https://doi.org/10.2989/1814232x.2010.501563

Russo, C. S., Lamont, T., Tutt, G.C.O., van den Berg, M.A., Barlow, R.G., 2019a. Hydrography of a shelf ecosystem inshore of a major Western Boundary Current. Estuar. Coast. Shelf Sci. 228. https://doi.org/10.1016/j.ecss.2019.106363

Russo, C. S., Lamont, T., Tutt, G.C.O., van den Berg, M.A., Barlow, R.G., 2019b. Hydrography of a shelf ecosystem inshore of a major Western Boundary Current. Estuar. Coast. Shelf Sci. 228, 106363. https://doi.org/10.1016/j.ecss.2019.106363

Russo, C S, Lamont, T., Tutt, G.C.O., van den Berg, M.A., Barlow, R.G., 2019. Hydrography of a shelf ecosystem inshore of a major Western Boundary Current. Estuar. Coast. Shelf Sci. 228, 106363. https://doi.org/10.1016/j.ecss.2019.106363

Rutgers Van Der Loeff, M.M., Meyer, R., Rudels, B., Rachor, E., 2002. Resuspension and particle transport in the benthic nepheloid layer in and near Fram Strait in relation to faunal abundances and 234Th depletion. Deep. Res. Part I Oceanogr. Res. Pap. 49, 1941–1958. https://doi.org/10.1016/S0967-0637(02)00113-9

Sahl, L.E., Merrell, W.J., McGrail, D.W., Webb, J.A., 1987. Transport of mud on continental shelves: Evidence from the Texas Shelf. Mar. Geol. 76, 33–43. https://doi.org/10.1016/0025-3227(87)90015-6

Salat, J., Puig, P., Latasa, M., 2010. Violent storms within the Sea: Dense water formation episodes in the NW Mediterranean. Adv. Geosci. 26, 53–59. https://doi.org/10.5194/adgeo-26-53-2010

Sathyendranath, S., Brewin, R.J.W., Brockmann, C., Brotas, V., Calton, B., Chuprin, A., Cipollini, P., Couto, A.B., Dingle, J., Doerffer, R., Donlon, C., Dowell, M., Farman, A., Grant, M., Groom, S., Horseman, A., Jackson, T., Krasemann, H., Lavender, S., Martinez-Vicente, V., Mazeran, C., Mélin, F., Moore, T.S., Müller, D., Regner, P., Roy, S., Steele, C.J., Steinmetz, F., Swinton, J., Taberner, M., Thompson, A., Valente, A., Zühlke, M., Brando, V.E., Feng, H., Feldman, G., Franz, B.A., Frouin, R., Gould, R.W., Hooker, S.B., Kahru, M., Kratzer, S., Mitchell, B.G., Muller-Karger, F.E., Sosik, H.M., Voss, K.J., Werdell, J., Platt, T., 2019. An ocean-colour time series for use in climate studies: The experience of the ocean-colour climate change initiative (OC-CCI). Sensors (Switzerland) 19. https://doi.org/10.3390/s19194285

Sato, N., Iwata, Y., Shaw, P.W., Sauer, W.H.H., 2019. Whole spermatangia within the seminal receptacles of female chokka squid (Loligo reynaudii d'Orbigny, 1839-1841). J. Molluscan Stud. 85, 79–91. https://doi.org/10.1093/mollus/eyy059

Sauer, W.H., 1995. South Africa's Tsitsikamma National Park as a protected breeding area for the commercially exploited chokka squid Loligo vulgaris reynaudii. South African J. Mar. Sci. 16, 365–371. https://doi.org/10.2989/025776195784156575

Sauer, W.H., Lipiński, M.R., 1991. Food of squid Loligo vulgaris reynaudii (Cephalopoda: Loliginidae) on their spawning grounds off the Eastern Cape, South Africa. South African J. Mar. Sci. 10, 193–201. https://doi.org/10.2989/02577619109504631

Sauer, W.H.H., Goschen, W.S., Koorts, A.S., 1991a. A Preliminary Investigation of the Effect of Sea Temperature Fluctuations and Wind Direction on Catches of Chokka Squid *Loligo vulgaris reynaudii* Off the Eastern Cape, South Africa. South African J. Mar. Sci. 11, 467–473. https://doi.org/10.2989/025776191784287466

Sauer, W.H.H., Goschen, W.S., Koorts, A.S., 1991b. A Preliminary Investigation of the Effect of Sea Temperature Fluctuations and Wind Direction on Catches of Chokka Squid *Loligo vulgaris reynaudii* Off the Eastern Cape, South Africa. South African J. Mar. Sci. 11, 467–473. https://doi.org/10.2989/025776191784287466

Sauer, W.H.H., Lipinski, M.R., Augustyn, C.J., 2000. Tag recapture studies of the chokka squid Loligo vulgaris reynaudii d'Orbigny, 1845 on inshore spawning grounds on the south-east coast of South Africa. Fish. Res. 45, 283–289. https://doi.org/10.1016/S0165-7836(99)00118-6

Sauer, W.H.H., Melo, Y.C., De Wet, W., 1999. Fecundity of the chokka squid Loligo vulgaris reynaudii on the southeastern coast of South Africa. Mar. Biol. 135, 315–319. https://doi.org/10.1007/s002270050629

Sauer, W.H.H., Roberts, M.J., Lipinski, M.R., Smale, M.J., Hanlon, R.T., Webber, D.M., O'Dor, R.K., 1997a. Choreography of the squid's "nuptial dance." Biol. Bull. 192, 203–207. https://doi.org/10.2307/1542714

Sauer, W.H.H., Roberts, M.J., Lipinski, M.R., Smale, M.J., Hanlon, R.T., Webber, D.M., O'Dor, R.K., 1997b. Choreography of the squid's "nuptial dance." Biol. Bull. 192, 203–207. https://doi.org/10.2307/1542714

Sauer, W.H.H., Smale, M.J., Lipinski, M.R., 1992a. The location of spawning grounds, spawning and schooling behaviour of the squid Loligo vulgaris reynaudii (Cephalopoda: Myopsida) off the Eastern Cape Coast, South Africa. Mar. Biol. 114, 97–107. https://doi.org/10.1007/BF00350859

Sauer, W.H.H., Smale, M.J., Lipinski, M.R., 1992b. The location of spawning grounds, spawning and schooling behaviour of the squid Loligo vulgaris reynaudii (Cephalopoda: Myopsida) off the Eastern Cape Coast, South Africa. Mar. Biol. 114, 97–107. https://doi.org/10.1007/BF00350859

Schaeffer, A., Roughan, M., Morris, B.D., 2013. Cross-shelf dynamics in a western boundary current regime: Implications for upwelling. J. Phys. Oceanogr. 43, 1042–1059. https://doi.org/10.1175/JPO-D-12-0177.1

Schlembach, F., Passaro, M., Quartly, G.D., Kurekin, A., Nencioli, F., Dodet, G., Piollé, J.F., Ardhuin, F., Bidlot, J., Schwatke, C., Seitz, F., Cipollini, P., Donlon, C., 2020. Round robin assessment of radar altimeter low resolution mode and delay-doppler retracking algorithms for significant wave height. Remote Sens. 12. https://doi.org/10.3390/RS12081254

Schön, P.J., Sauer, W.H.H., Roberts, M.J., 2002. Environmental influences on spawning aggregations and jig catches of chokka squid Loligo vulgaris reynaudii: A "black box" approach. Bull. Mar. Sci. 71, 783–800.

Schumann, E., 2016. Cold water events in Algoa Bay and along the Cape south coast , South Africa , in March / April 1987.

Schumann, E., 2015. Surface winds over Algoa Bay , South Africa Surface winds over Algoa Buy , South Africa.

Schumann, E.G., 1987. The coastal ocean off the east coast of South Africa. Trans. R. Soc. South Africa 46, 215–229. https://doi.org/10.1080/00359198709520125

Schumann, E.H., 1999. Wind-driven mixed layer and coastal upwelling processes off the south coast of South Africa. J. Mar. Res. 57, 671–691. https://doi.org/10.1357/002224099321549639

Schumann, E.H., Beekman, L.J., 1984. Ocean temperature structures on the agulhas bank. Trans. R. Soc. South Africa 45, 191–203. https://doi.org/10.1080/00359198409519483

Schumann, E.H., Brink, K.H., 1990. Coastal-Trapped Waves off the Coast of South Africa: Generation, Progagation and Current Structures. J. p 20, 1206–1218.

Schumann, E.H., Churchill, J.R.S., Zaayman, H.J., 2005a. Oceanic variability in the western sector of Algoa Bay, South Africa. African J. Mar. Sci. 27, 65–80. https://doi.org/10.2989/18142320509504069

Schumann, E.H., Churchill, J.R.S., Zaayman, H.J., 2005b. Oceanic variability in the western sector of Algoa Bay, South Africa. African J. Mar. Sci. 27, 65–80. https://doi.org/10.2989/18142320509504069

Schumann, E.H., Cohen, A.L., Jury, M.R., 1995. Coastal sea surface temperature variability along the south coast of South Africa and the relationship to regional and global climate. J. Mar. Res. 53, 231–248. https://doi.org/10.1357/0022240953213205

Schumann, E.H., Illenberger, W.K., Goschen, W.S., 1991. Surface winds over Algoa Bay, South Africa. S. Afr. J. Sci. 87, 202–207.

Schumann, E.H., Perrins, L.-A., Hunter, I.T., 1982. Upwelling along the South Coast of the Cape Province, South Africa. S. Afr. J. Sci. 78, 238–242.

Schumann, E.H., Ross, G.J.B., Goschen, W.S., 1988. Cold water events in Algoa Bay and along the Cape South coast, South-Africa, in March April 1987. S. Afr. J. Sci. 84, 579–584.

Segawa, S., 1995. Effect of Temperature on Oxygen Consumption of Juvenile Oval Squid Sepioteuthis lessoniana. Fish. Sci. 61, 743–746. https://doi.org/10.2331/fishsci.61.743

Shashar, N., Hanlon, R.T., 2013a. Spawning behavior dynamics at communal egg beds in the squid Doryteuthis (Loligo) pealeii. J. Exp. Mar. Bio. Ecol. 447, 65–74. https://doi.org/10.1016/j.jembe.2013.02.011

Shashar, N., Hanlon, R.T., 2013b. Spawning behavior dynamics at communal egg beds in the squid Doryteuthis (Loligo) pealeii. J. Exp. Mar. Bio. Ecol. 447, 65–74. https://doi.org/10.1016/j.jembe.2013.02.011

Shideler, G.L., 1981. Development of the benethic nepheloid layer on the south Texas continental shelf, western Gulf of Mexico. Mar. Geol. 41, 37–61. https://doi.org/10.1016/0025-3227(81)90103-1

Singh, L., Downey, N.J., Roberts, M.J., Webber, D.M., Smale, M.J., van den Berg, M.A., Harding, R.T., Engelbrecht, D.C., Blows, B.M., 2009. Design and calibration of an acoustic telemetry system subject to upwelling events. African J. Mar. Sci. 31, 355–364. https://doi.org/10.2989/AJMS.2009.31.3.8.996

Smale, M., Sauer, W., Roberts, M., 2001. Behavioural interactions of predators and spawning chokka squid off South Africa: Towards quantification. Mar. Biol. 139, 1095–1105. https://doi.org/10.1007/s002270100664

Smith, J.M., Macleod, C.D., Valavanis, V., Hastie, L., Valinassab, T., Bailey, N., Santos, M.B., Pierce, G.J., 2013. Habitat and distribution of post-recruit life stages of the squid Loligo forbesii. Deep. Res. Part II Top. Stud. Oceanogr. 95, 145–159. https://doi.org/10.1016/j.dsr2.2013.03.039

Speich, S., Lutjeharms, J.R.E., Penven, P., Blanke, B., 2006. Role of bathymetry in Agulhas Current configuration and behaviour. Geophys. Res. Lett. 33, 2–6. https://doi.org/10.1029/2006GL027157

Steer, M.A., Moltschaniwskyj, N.A., Gowland, F.C., 2002. Temporal variability in embryonic development and mortality in the southern calamary Sepioteuthis australis: A field assessment. Mar. Ecol. Prog. Ser. 243, 143–150. https://doi.org/10.3354/meps243143

Stukel, M.R., Mislan, K.A.S., Décima, M., Hmelo, L., 2014. Detritus in the pelagic ocean. Eco-DAS IX Symp. Proc. 49–76. https://doi.org/10.4319/ecodas.2014.978-0-9845591-3-8.49

Sutherland, R.A., Bryan, R.B., 1991. Sediment budgeting: A case study in the Katiorin drainage basin, Kenya. Earth Surf. Process. Landforms 16, 383–398. https://doi.org/10.1002/esp.3290160502

Swart, S., Thomalla, S.J., Monteiro, P.M.S., 2015. The seasonal cycle of mixed layer dynamics and phytoplankton biomass in the Sub-Antarctic Zone: A high-resolution glider experiment. J. Mar. Syst. 147, 103–115. https://doi.org/10.1016/j.jmarsys.2014.06.002

Swart, V.P., Largier, J.L., 1987. Thermal structure of Agulhas bank water. South African J. Mar. Sci. 5, 243–252. https://doi.org/10.2989/025776187784522153

Timmermans, B., Shaw, A.G.P., Gommenginger, C., 2020. Reliability of extreme significant wave height estimation from satellite altimetry and in situ measurements in the coastal zone. J. Mar. Sci. Eng. 8, 1–19. https://doi.org/10.3390/jmse8121039

Timmermans, B.W., Gommenginger, C.P., Dodet, G., Bidlot, J.R., 2020. Global Wave Height Trends and Variability from New Multimission Satellite Altimeter Products, Reanalyses, and Wave Buoys. Geophys. Res. Lett. 47. https://doi.org/10.1029/2019GL086880

Townsend, D.W., Mayer, L.M., Dortch, Q., Spinrad, R.W., 1992. Vertical structure and biological activity in the bottom nepheloid layer of the Gulf of Maine. Cont. Shelf Res. 12, 367–387. https://doi.org/10.1016/0278-4343(92)90037-K

Turner, J.T., 2015. Zooplankton fecal pellets, marine snow, phytodetritus and the ocean's biological pump. Prog. Oceanogr. https://doi.org/10.1016/j.pocean.2014.08.005

Van Der Vyver, J.S.F., Sauer, W.H.H., McKeown, N.J., Yemane, D., Shaw, P.W., Lipinski, M.R., 2016. Phenotypic divergence despite high gene flow in chokka squid Loligo reynaudii (Cephalopoda: Loliginidae): implications for fishery management. J. Mar. Biol. Assoc. United Kingdom 96, 1507–1525. https://doi.org/10.1017/S0025315415001794

Vidal, É.A.G., DiMarco, P., Lee, P., 2006. Effects of starvation and recovery on the survival, growth and RNA/DNA ratio in loliginid squid paralarvae. Aquaculture 260, 94–105.

Villanueva, R., 2000. Effect of temperature on statolith growth of the European squid Loligo vulgaris during early life. Mar. Biol. 136, 449–460. https://doi.org/10.1007/s002270050704

Villanueva, R., Arkhipkin, A., Jereb, P., Lefkaditou, E., Lipinski, M.R., Perales-Raya, C., Riba, J., Rocha, F., 2003. Embryonic life of the loliginid squid Loligo vulgaris: Comparison between statoliths of Atlantic and Mediterranean populations. Mar. Ecol. Prog. Ser. 253, 197–208. https://doi.org/10.3354/meps253197

Wainright, S.C., 1987. Stimulation of heterotrophic microplankton production by resuspended marine sediments. Science (80-.). 238, 1710–1712. https://doi.org/10.1126/science.238.4834.1710

Walker, N.D., 1986. Satellite observations of the Agulhas Current and episodic upwelling south of Africa. Deep Sea Res. Part A, Oceanogr. Res. Pap. 33, 1083–1106. https://doi.org/10.1016/0198-0149(86)90032-4

Weidberg, N., Porri, F., Von der Meden, C.E.O., Jackson, J.M., Goschen, W., McQuaid, C.D., 2015. Mechanisms of nearshore retention and offshore export of mussel larvae over the Agulhas Bank. J. Mar. Syst. 144, 70–80. https://doi.org/10.1016/j.jmarsys.2014.11.012

York, C.A., Bartol, I.K., 2016. Anti-predator behavior of squid throughout ontogeny. J. Exp. Mar. Bio. Ecol. 480, 26–35. https://doi.org/10.1016/j.jembe.2016.03.011

Zhang, W., Hanebuth, T.J.J., Stöber, U., 2016. Short-term sediment dynamics on a meso-scale contourite drift (off NW Iberia): Impacts of multi-scale oceanographic processes deduced from the analysis of mooring data and numerical modelling. Mar. Geol. 378, 81–100. https://doi.org/10.1016/j.margeo.2015.12.006

Zoutendyk, P., Duvenage, I., 1989. Composition and biological implications of a nepheloid layer over the inner Agulhas Bank near Mossel Bay, South Africa. Trans. R. Soc. South Africa 47, Part 2, 187–197.

APPENDIX A:

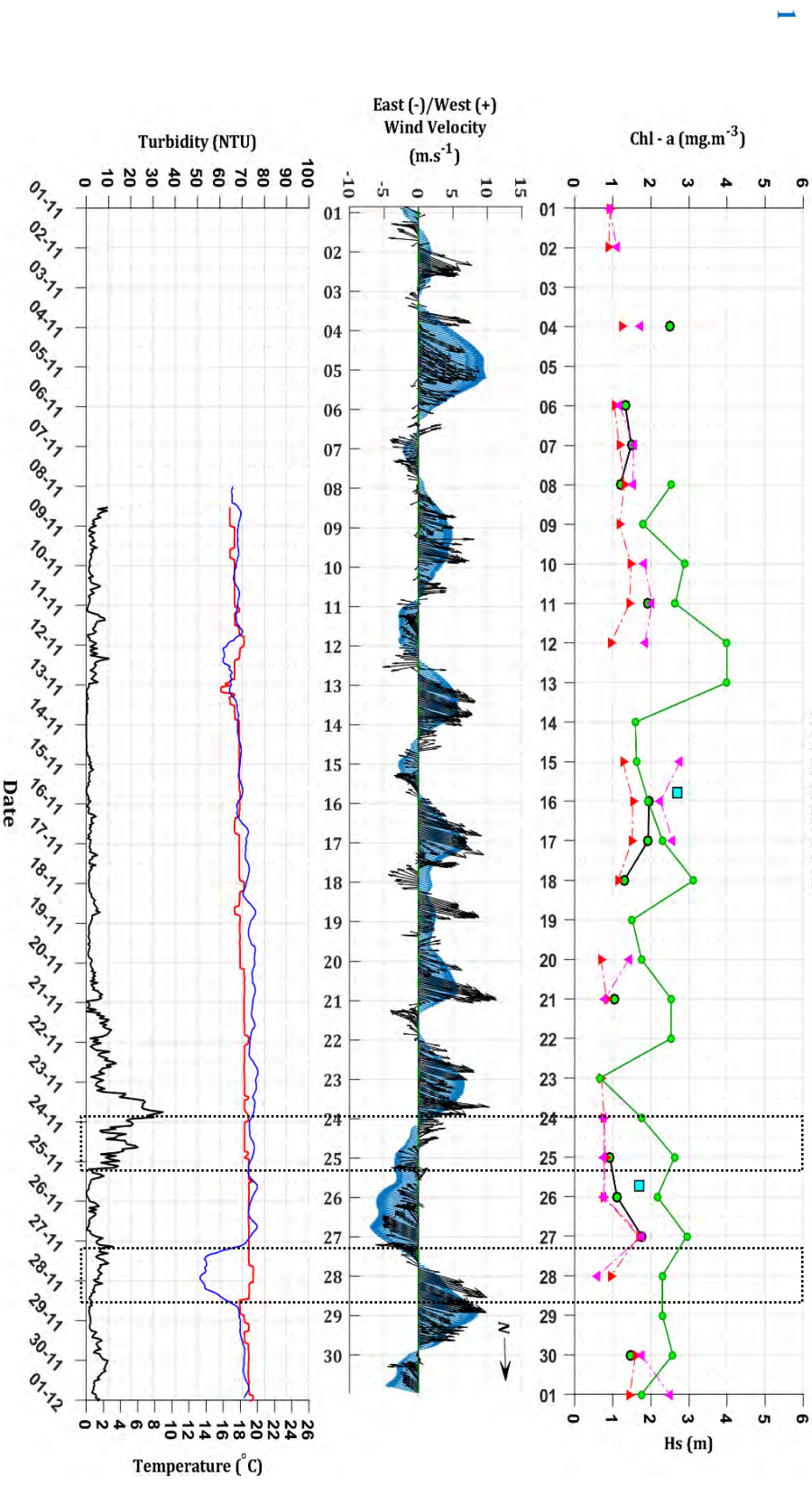

Appendix A: A three-tiered figure of monthly variability in environmental parameters acting on the OBS turbidity sensor in Algoa Bay, a sub-embayment of the Eastern Agulhas Bank. The top panel displays altimeter-derived Hs (m) for the mooring location, and Chlorophyll-A concentrations from L3 and L4 ocean colour products for the mooring location, Algoa Bay and the Port Alfred upwelling cell, respectively. The middle pain denotes a monthly wind vector plot with both raw hourly (black) and low-pass filtered (blue) wind dynamics from the Port Elizabeth International Airport Weather Station. The bottom panel highlights the interplay between benthic turbidity (NTU, black-line), bottom temperature (°C, red-line) and the Mangold's Pool Underwater Temperature Recorder (UTR, blue-line) at Cape Recife. Black-boxes represent wind-reversal induced turbidity events, while red-boxes highlight resuspension events from waves or strong winds. Green-boxes indicate organic matter enrichment of the nepheloid layer.

Appendix A: A three-tiered figure of monthly variability in environmental parameters acting on the OBS turbidity sensor in Algoa Bay, a sub-embayment of the Eastern Agulhas Bank. The top panel displays altimeter-derived Hs (m) for the mooring location, and Chlorophyll-A concentrations from L3 and L4 ocean colour products for the mooring location, Algoa Bay and the Port Alfred upwelling cell, respectively. The middle pain denotes a monthly wind vector plot with both raw hourly (black) and low-pass filtered (blue) wind dynamics from the Port Elizabeth International Airport Weather Station. The bottom panel highlights the interplay between benthic turbidity (NTU, black-line), bottom temperature (°C, red-line) and the Mangold's Pool Underwater Temperature Recorder (UTR, blue-line) at Cape Recife. Black-boxes represent wind-reversal induced turbidity events, while red-boxes highlight resuspension events from waves or strong winds. Green-boxes indicate organic matter enrichment of the nepheloid layer.

2

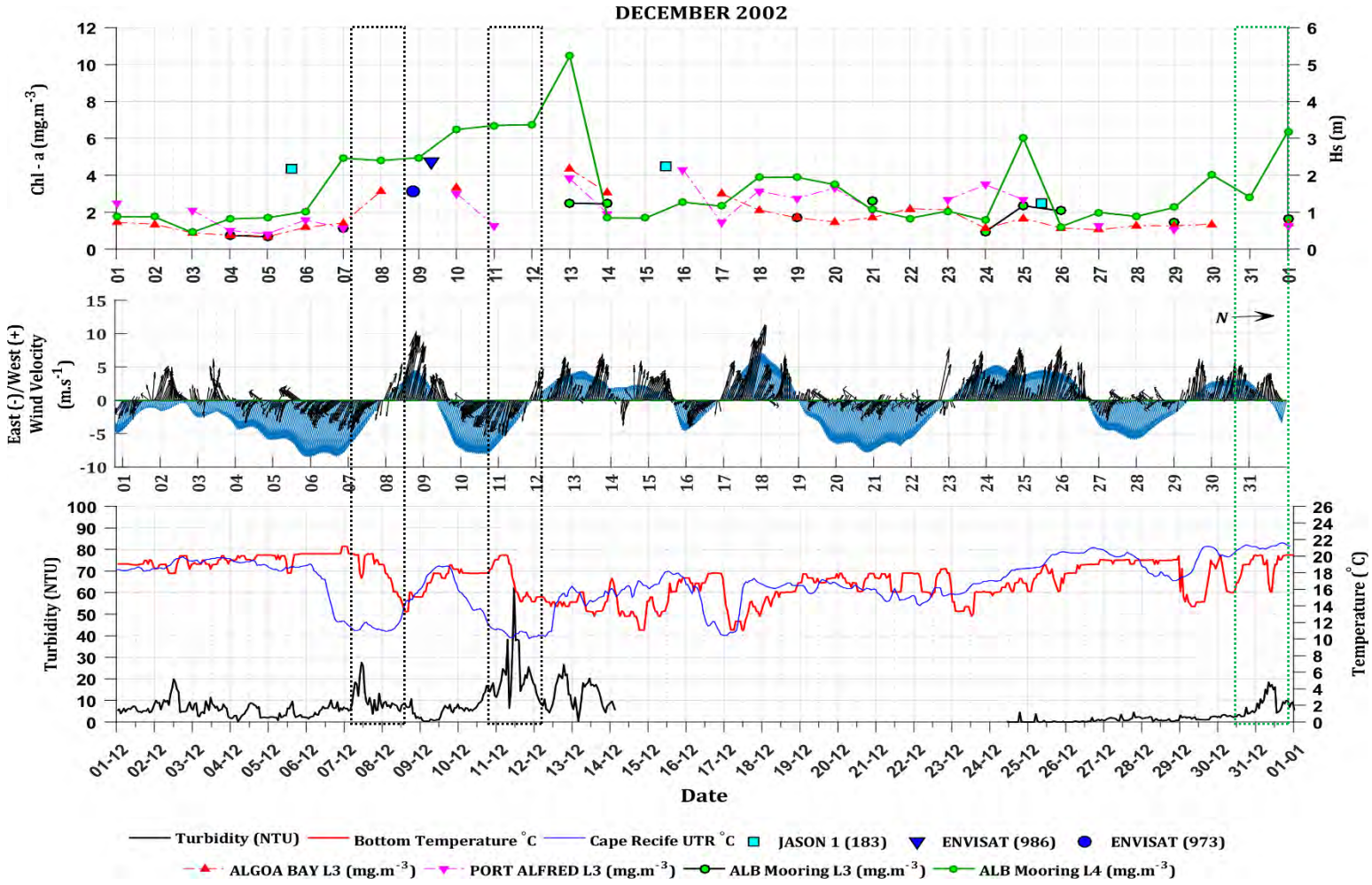

Appendix A: A three-tiered figure of monthly variability in environmental parameters acting on the OBS turbidity sensor in Algoa Bay, a sub-embayment of the Eastern Agulhas Bank. The top panel displays altimeter-derived Hs (m) for the mooring location, and Chlorophyll-A concentrations from L3 and L4 ocean colour products for the mooring location, Algoa Bay and the Port Alfred upwelling cell, respectively. The middle pain denotes a monthly wind vector plot with both raw hourly (black) and low-pass filtered (blue) wind dynamics from the Port Elizabeth International Airport Weather Station. The bottom panel highlights the interplay between benthic turbidity (NTU, black-line), bottom temperature (°C, red-line) and the Mangold's Pool Underwater Temperature Recorder (UTR, blue-line) at Cape Recife. Black-boxes represent wind-reversal induced turbidity events, while red-boxes highlight resuspension events from waves or strong winds. Green-boxes indicate organic matter enrichment of the nepheloid layer.

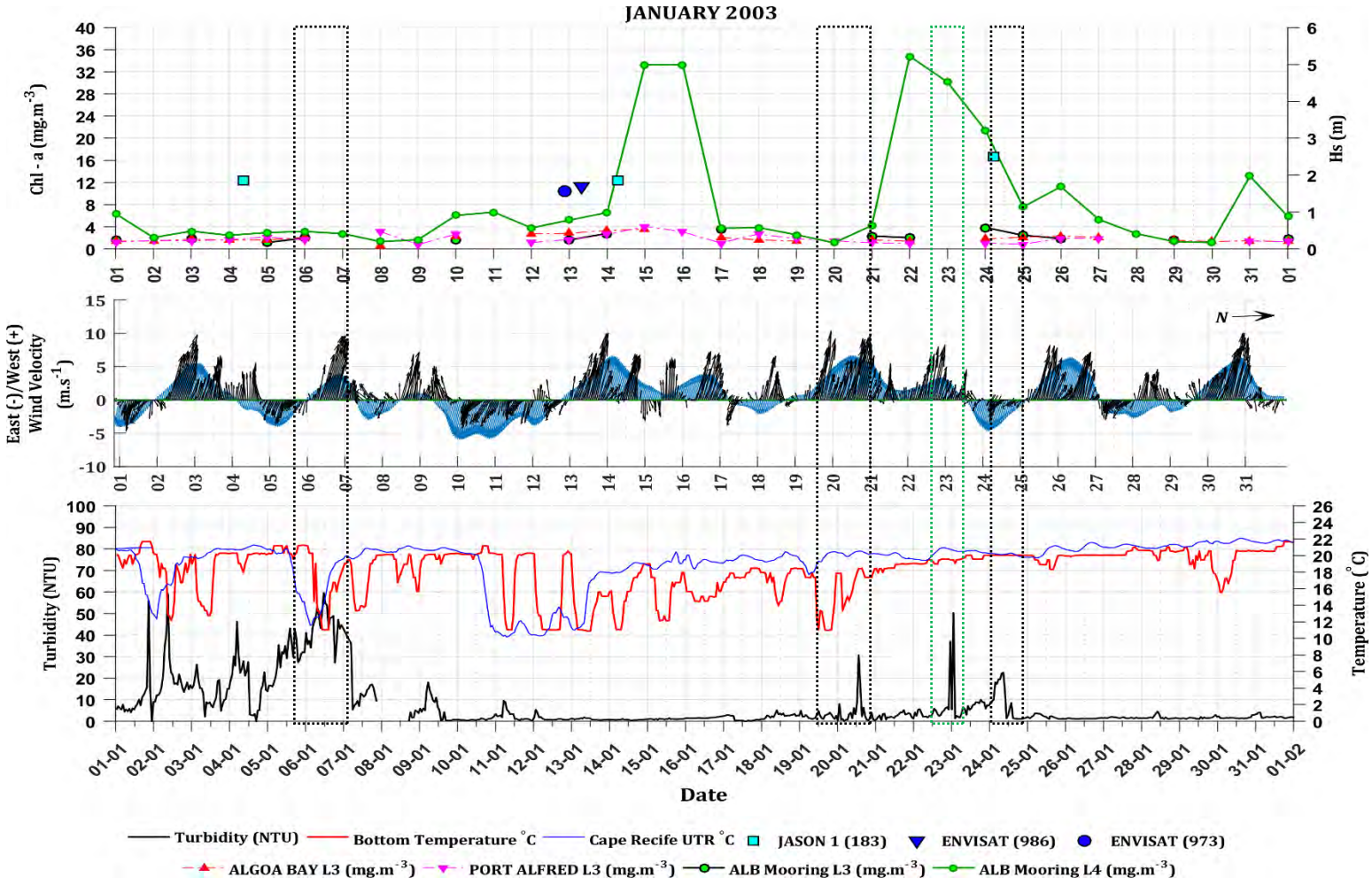

Appendix A: A three-tiered figure of monthly variability in environmental parameters acting on the OBS turbidity sensor in Algoa Bay, a sub-embayment of the Eastern Agulhas Bank. The top panel displays altimeter-derived Hs (m) for the mooring location, and Chlorophyll-A concentrations from L3 and L4 ocean colour products for the mooring location, Algoa Bay and the Port Alfred upwelling cell, respectively. The middle pain denotes a monthly wind vector plot with both raw hourly (black) and low-pass filtered (blue) wind dynamics from the Port Elizabeth International Airport Weather Station. The bottom panel highlights the interplay between benthic turbidity (NTU, black-line), bottom temperature (°C, red-line) and the Mangold's Pool Underwater Temperature Recorder (UTR, blue-line) at Cape Recife. Black-boxes represent wind-reversal induced turbidity events, while red-boxes highlight resuspension events from waves or strong winds. Green-boxes indicate organic matter enrichment of the nepheloid layer.

4

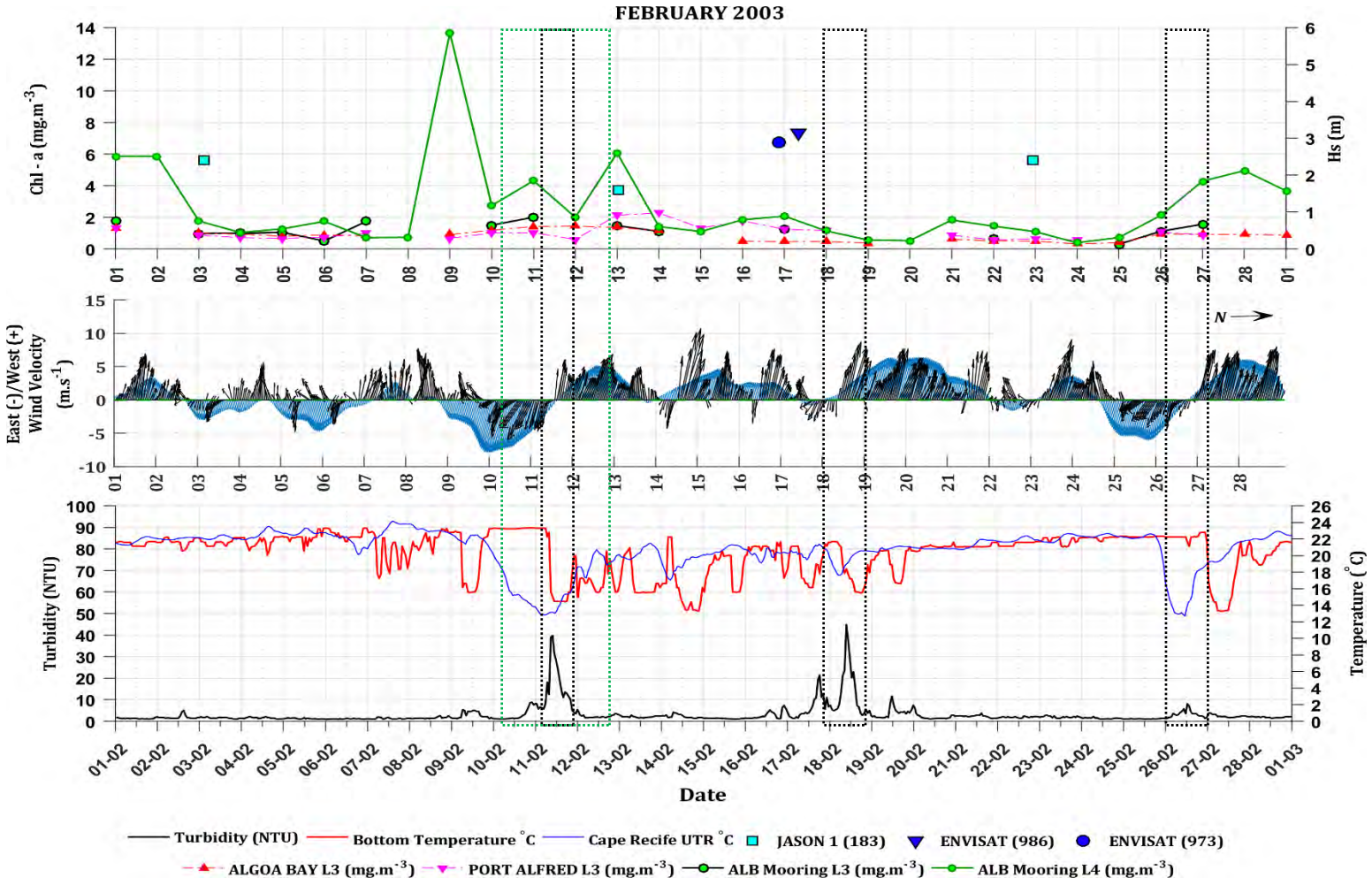

Appendix A: A three-tiered figure of monthly variability in environmental parameters acting on the OBS turbidity sensor in Algoa Bay, a sub-embayment of the Eastern Agulhas Bank. The top panel displays altimeter-derived Hs (m) for the mooring location, and Chlorophyll-A concentrations from L3 and L4 ocean colour products for the mooring location, Algoa Bay and the Port Alfred upwelling cell, respectively. The middle pain denotes a monthly wind vector plot with both raw hourly (black) and low-pass filtered (blue) wind dynamics from the Port Elizabeth International Airport Weather Station. The bottom panel highlights the interplay between benthic turbidity (NTU, black-line), bottom temperature (°C, red-line) and the Mangold's Pool Underwater Temperature Recorder (UTR, blue-line) at Cape Recife. Black-boxes represent wind-reversal induced turbidity events, while red-boxes highlight resuspension events from waves or strong winds. Green-boxes indicate organic matter enrichment of the nepheloid layer.

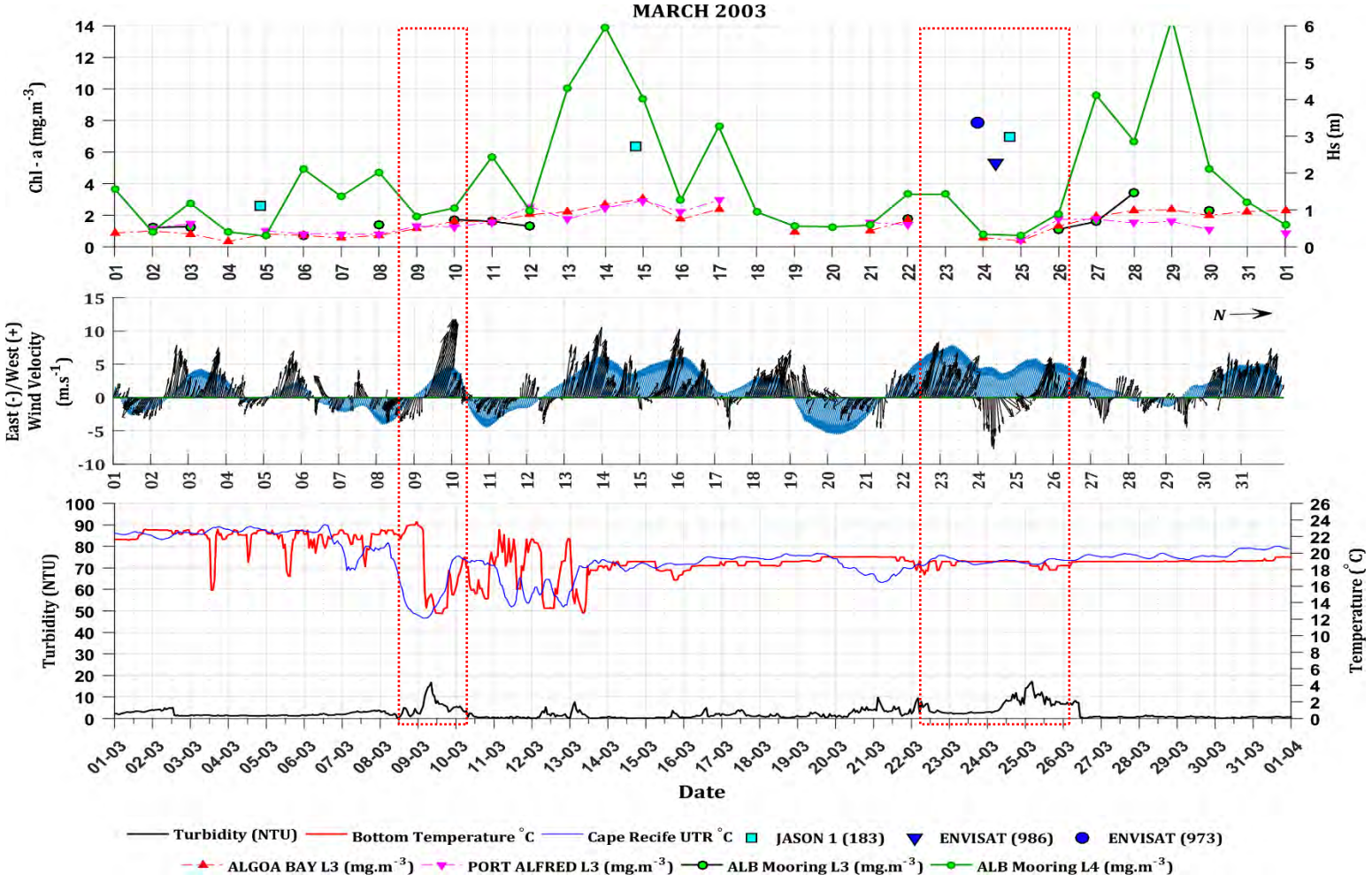

Appendix A: A three-tiered figure of monthly variability in environmental parameters acting on the OBS turbidity sensor in Algoa Bay, a sub-embayment of the Eastern Agulhas Bank. The top panel displays altimeter-derived Hs (m) for the mooring location, and Chlorophyll-A concentrations from L3 and L4 ocean colour products for the mooring location, Algoa Bay and the Port Alfred upwelling cell, respectively. The middle pain denotes a monthly wind vector plot with both raw hourly (black) and low-pass filtered (blue) wind dynamics from the Port Elizabeth International Airport Weather Station. The bottom panel highlights the interplay between benthic turbidity (NTU, black-line), bottom temperature (°C, red-line) and the Mangold's Pool Underwater Temperature Recorder (UTR, blue-line) at Cape Recife. Black-boxes represent wind-reversal induced turbidity events, while red-boxes highlight resuspension events from waves or strong winds. Green-boxes indicate organic matter enrichment of the nepheloid layer.

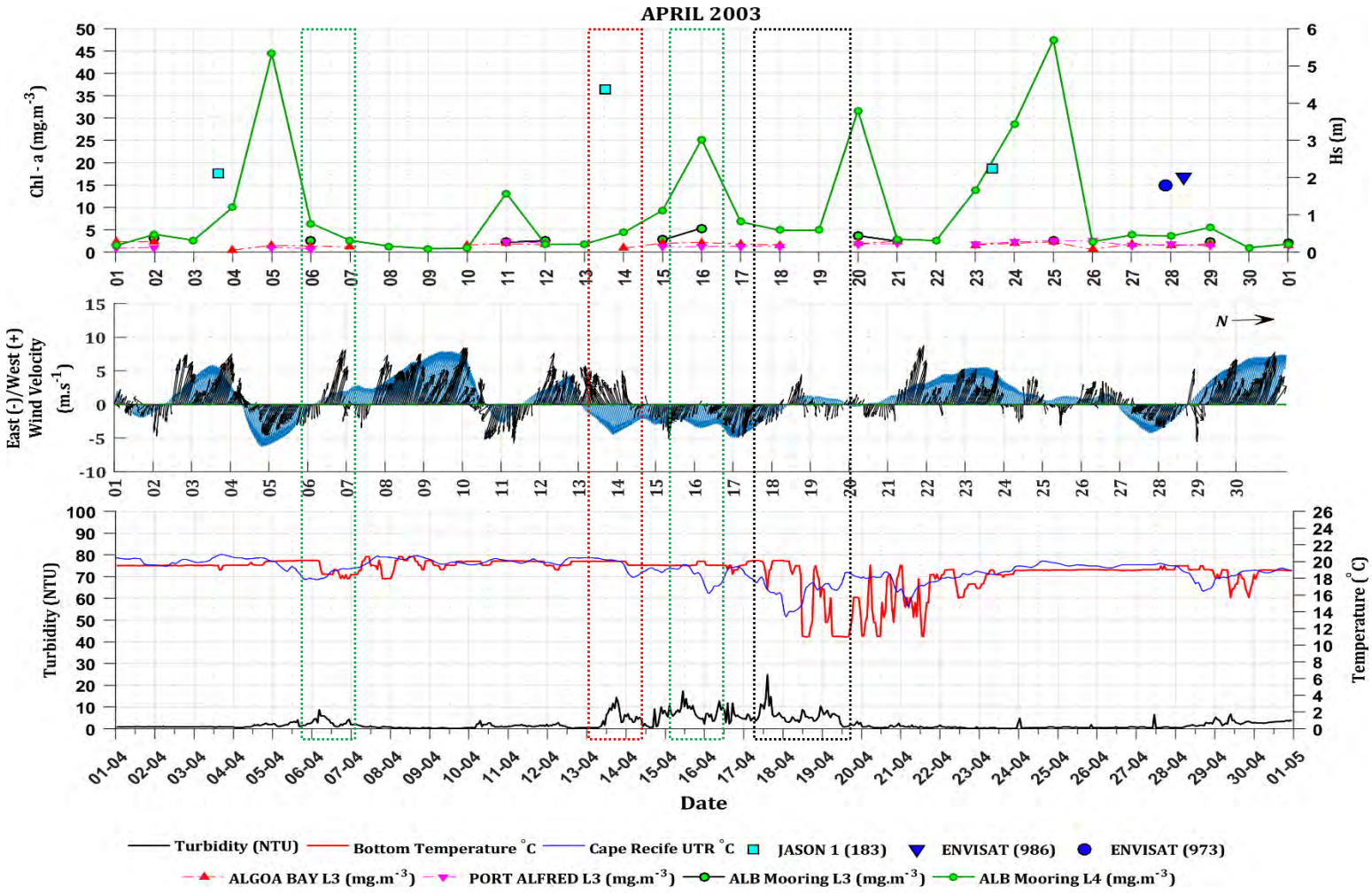

Appendix A: A three-tiered figure of monthly variability in environmental parameters acting on the OBS turbidity sensor in Algoa Bay, a sub-embayment of the Eastern Agulhas Bank. The top panel displays altimeter-derived Hs (m) for the mooring location, and Chlorophyll-A concentrations from L3 and L4 ocean colour products for the mooring location, Algoa Bay and the Port Alfred upwelling cell, respectively. The middle pain denotes a monthly wind vector plot with both raw hourly (black) and low-pass filtered (blue) wind dynamics from the Port Elizabeth International Airport Weather Station. The bottom panel highlights the interplay between benthic turbidity (NTU, black-line), bottom temperature (°C, red-line) and the Mangold's Pool Underwater Temperature Recorder (UTR, blue-line) at Cape Recife. Black-boxes represent wind-reversal induced turbidity events, while red-boxes highlight resuspension events from waves or strong winds. Green-boxes indicate organic matter enrichment of the nepheloid layer.

7

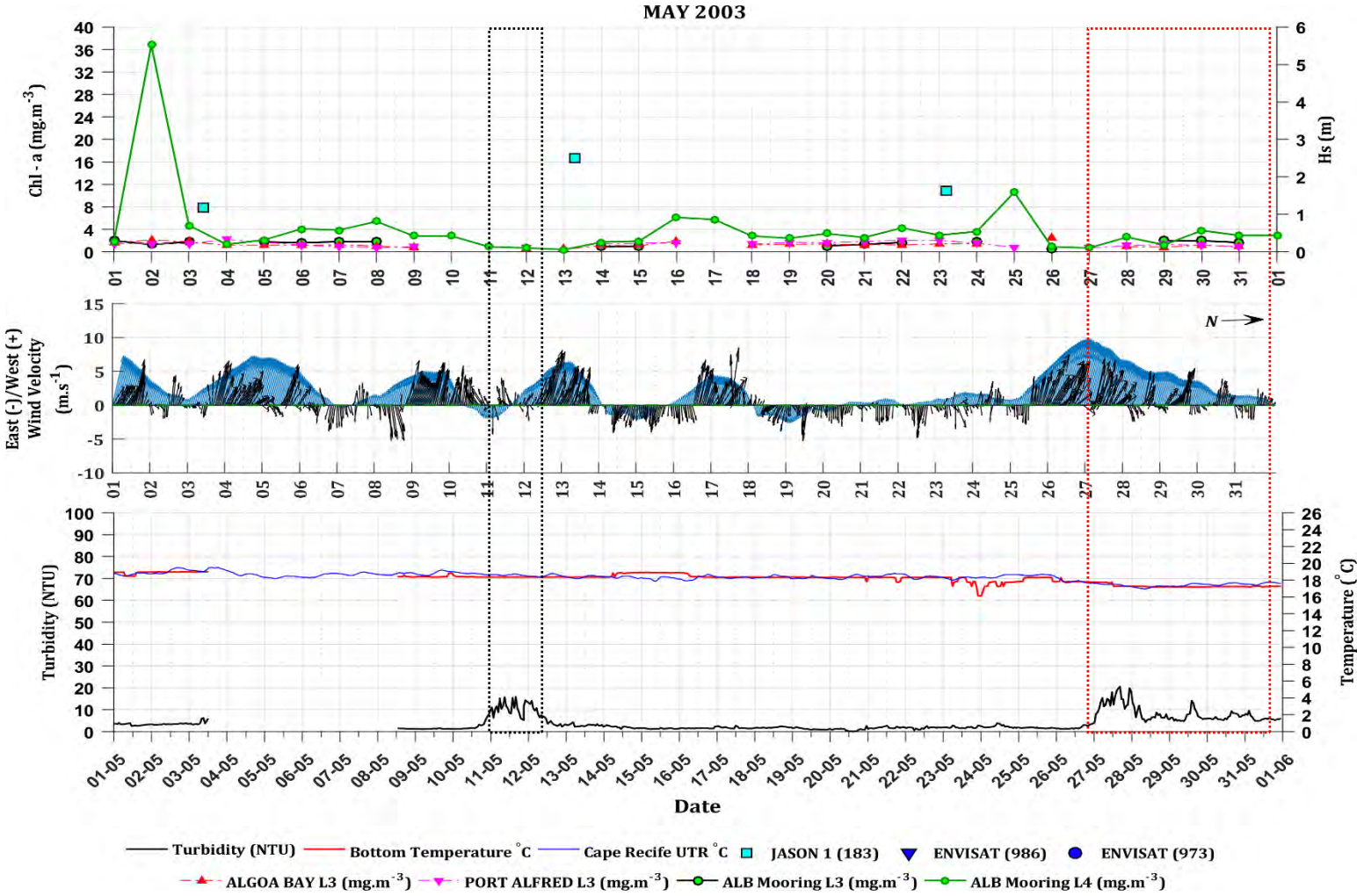

Appendix A: A three-tiered figure of monthly variability in environmental parameters acting on the OBS turbidity sensor in Algoa Bay, a sub-embayment of the Eastern Agulhas Bank. The top panel displays altimeter-derived Hs (m) for the mooring location, and Chlorophyll-A concentrations from L3 and L4 ocean colour products for the mooring location, Algoa Bay and the Port Alfred upwelling cell, respectively. The middle pain denotes a monthly wind vector plot with both raw hourly (black) and low-pass filtered (blue) wind dynamics from the Port Elizabeth International Airport Weather Station. The bottom panel highlights the interplay between benthic turbidity (NTU, black-line), bottom temperature (°C, red-line) and the Mangold's Pool Underwater Temperature Recorder (UTR, blue-line) at Cape Recife. Black-boxes represent wind-reversal induced turbidity events, while red-boxes highlight resuspension events from waves or strong winds. Green-boxes indicate organic matter enrichment of the nepheloid layer.

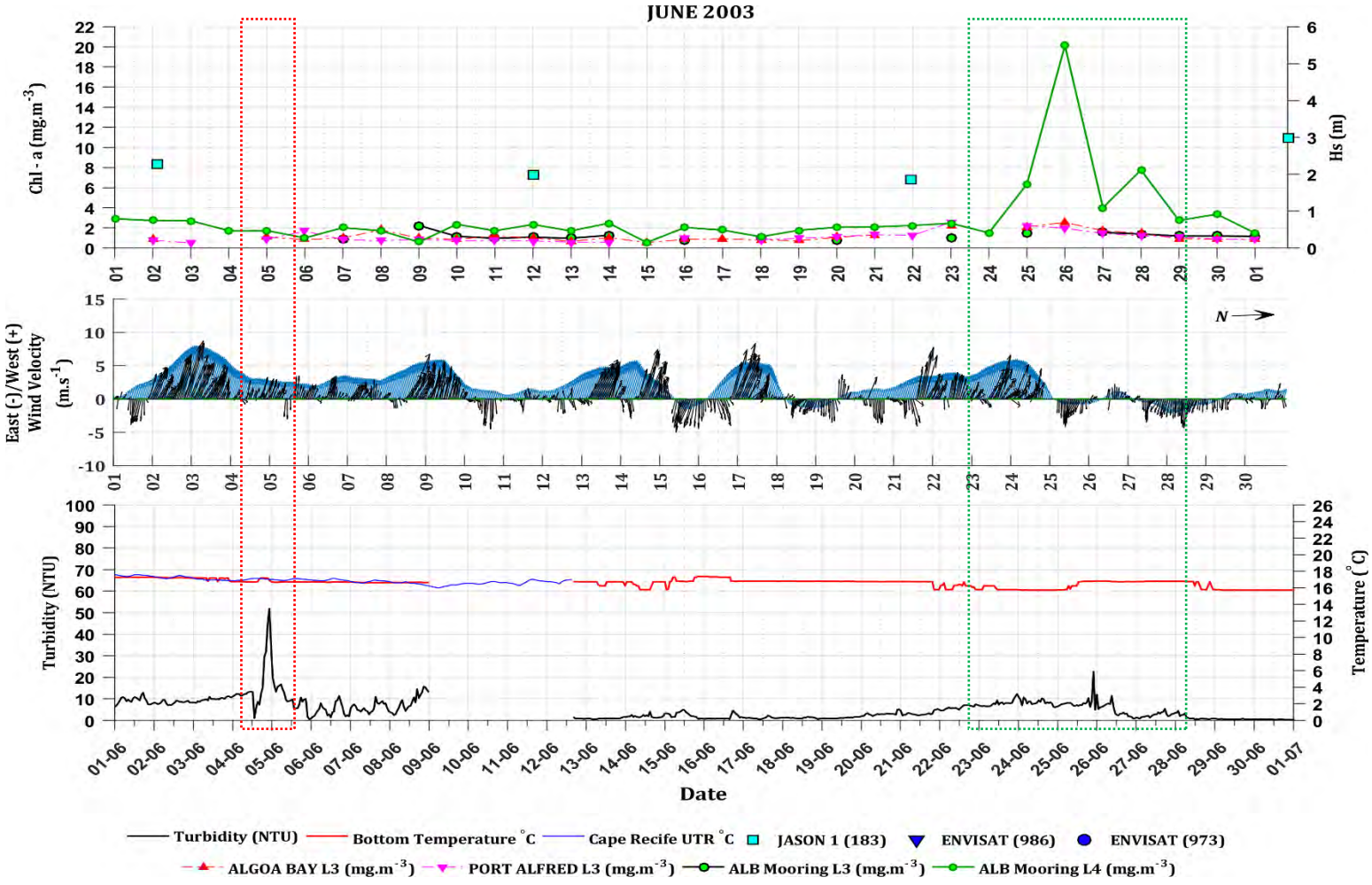

Appendix A: A three-tiered figure of monthly variability in environmental parameters acting on the OBS turbidity sensor in Algoa Bay, a sub-embayment of the Eastern Agulhas Bank. The top panel displays altimeter-derived Hs (m) for the mooring location, and Chlorophyll-A concentrations from L3 and L4 ocean colour products for the mooring location, Algoa Bay and the Port Alfred upwelling cell, respectively. The middle pain denotes a monthly wind vector plot with both raw hourly (black) and low-pass filtered (blue) wind dynamics from the Port Elizabeth International Airport Weather Station. The bottom panel highlights the interplay between benthic turbidity (NTU, black-line), bottom temperature (°C, red-line) and the Mangold's Pool Underwater Temperature Recorder (UTR, blue-line) at Cape Recife. Black-boxes represent wind-reversal induced turbidity events, while red-boxes highlight resuspension events from waves or strong winds. Green-boxes indicate organic matter enrichment of the nepheloid layer.

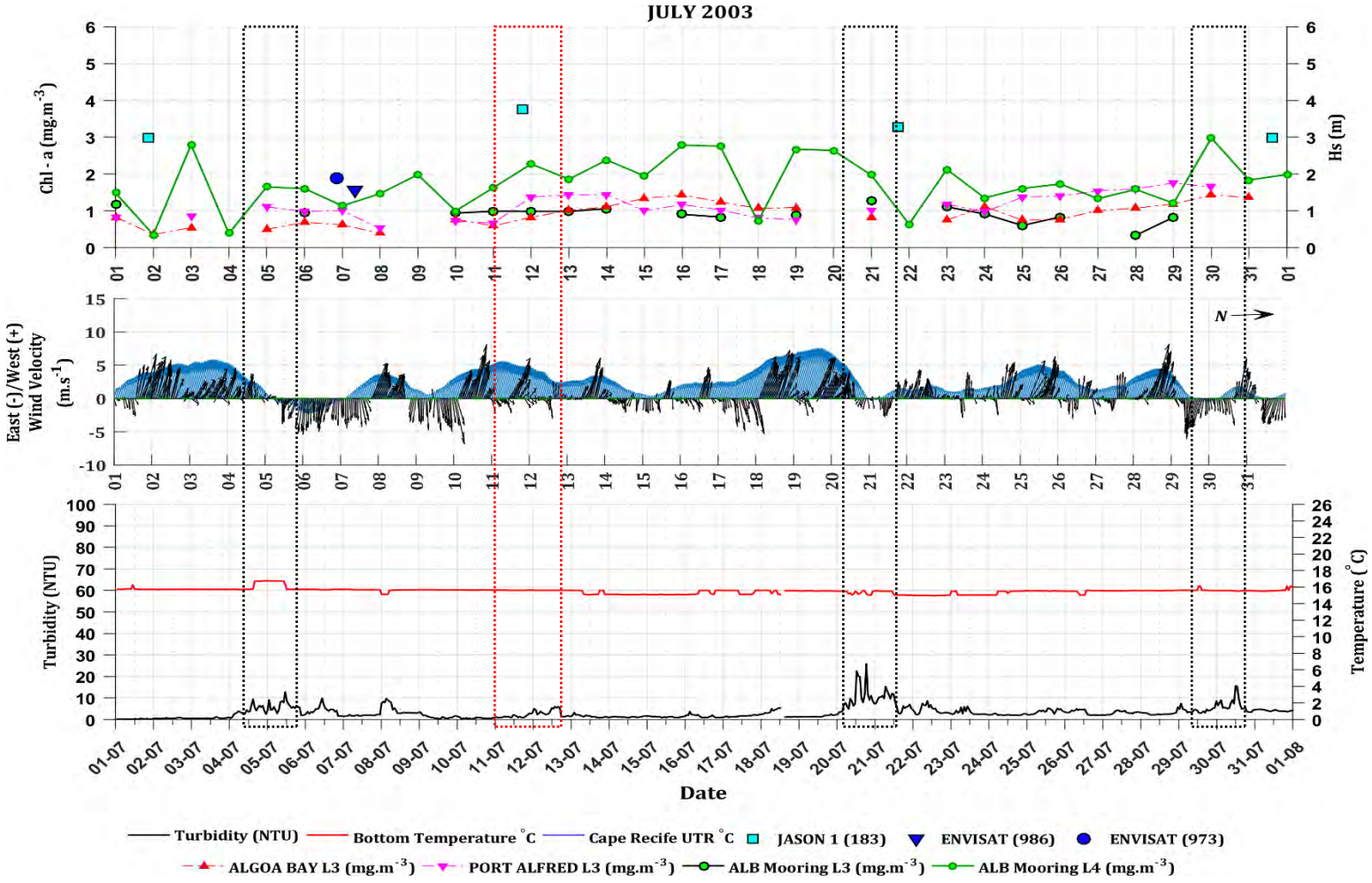

Appendix A: A three-tiered figure of monthly variability in environmental parameters acting on the OBS turbidity sensor in Algoa Bay, a sub-embayment of the Eastern Agulhas Bank. The top panel displays altimeter-derived Hs (m) for the mooring location, and Chlorophyll-A concentrations from L3 and L4 ocean colour products for the mooring location, Algoa Bay and the Port Alfred upwelling cell, respectively. The middle pain denotes a monthly wind vector plot with both raw hourly (black) and low-pass filtered (blue) wind dynamics from the Port Elizabeth International Airport Weather Station. The bottom panel highlights the interplay between benthic turbidity (NTU, black-line), bottom temperature (°C, red-line) and the Mangold's Pool Underwater Temperature Recorder (UTR, blue-line) at Cape Recife. Black-boxes represent wind-reversal induced turbidity events, while red-boxes highlight resuspension events from waves or strong winds. Green-boxes indicate organic matter enrichment of the nepheloid layer.

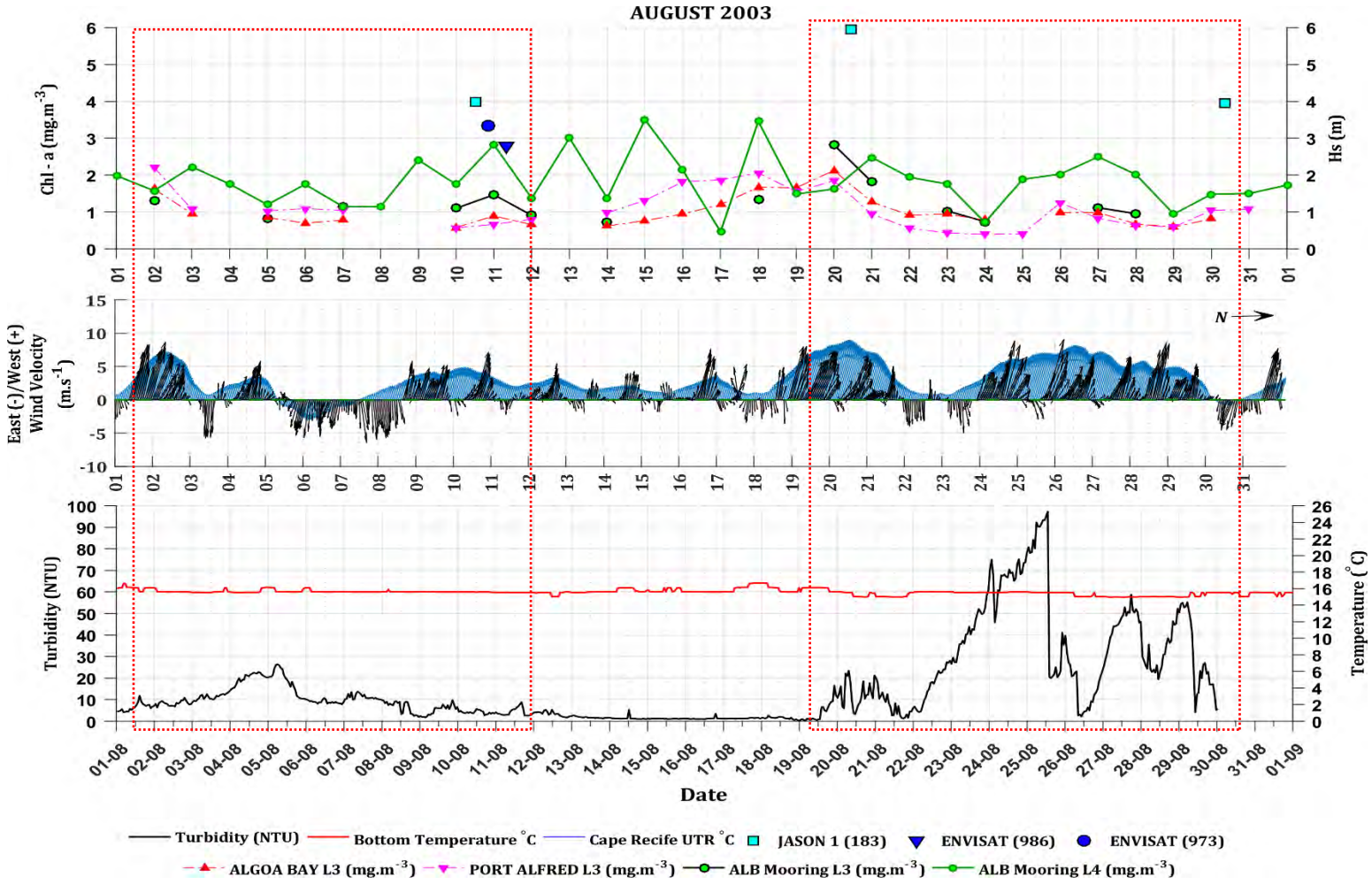

Appendix A: A three-tiered figure of monthly variability in environmental parameters acting on the OBS turbidity sensor in Algoa Bay, a sub-embayment of the Eastern Agulhas Bank. The top panel displays altimeter-derived Hs (m) for the mooring location, and Chlorophyll-A concentrations from L3 and L4 ocean colour products for the mooring location, Algoa Bay and the Port Alfred upwelling cell, respectively. The middle pain denotes a monthly wind vector plot with both raw hourly (black) and low-pass filtered (blue) wind dynamics from the Port Elizabeth International Airport Weather Station. The bottom panel highlights the interplay between benthic turbidity (NTU, black-line), bottom temperature (°C, red-line) and the Mangold's Pool Underwater Temperature Recorder (UTR, blue-line) at Cape Recife. Black-boxes represent wind-reversal induced turbidity events, while red-boxes highlight resuspension events from waves or strong winds. Green-boxes indicate organic matter enrichment of the nepheloid layer.

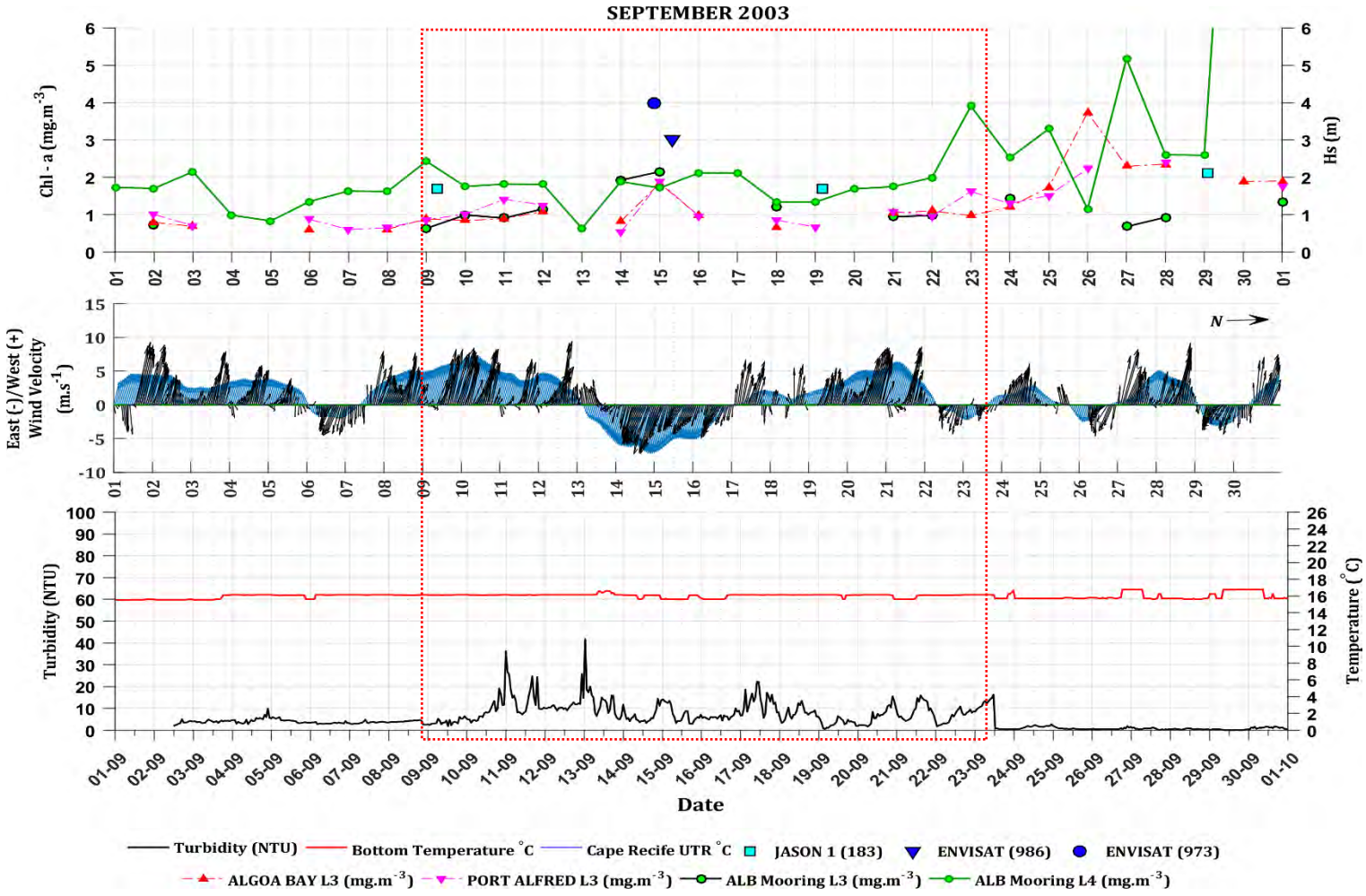

Appendix A: A three-tiered figure of monthly variability in environmental parameters acting on the OBS turbidity sensor in Algoa Bay, a sub-embayment of the Eastern Agulhas Bank. The top panel displays altimeter-derived Hs (m) for the mooring location, and Chlorophyll-A concentrations from L3 and L4 ocean colour products for the mooring location, Algoa Bay and the Port Alfred upwelling cell, respectively. The middle pain denotes a monthly wind vector plot with both raw hourly (black) and low-pass filtered (blue) wind dynamics from the Port Elizabeth International Airport Weather Station. The bottom panel highlights the interplay between benthic turbidity (NTU, black-line), bottom temperature (°C, red-line) and the Mangold's Pool Underwater Temperature Recorder (UTR, blue-line) at Cape Recife. Black-boxes represent wind-reversal induced turbidity events, while red-boxes highlight resuspension events from waves or strong winds. Green-boxes indicate organic matter enrichment of the nepheloid layer.

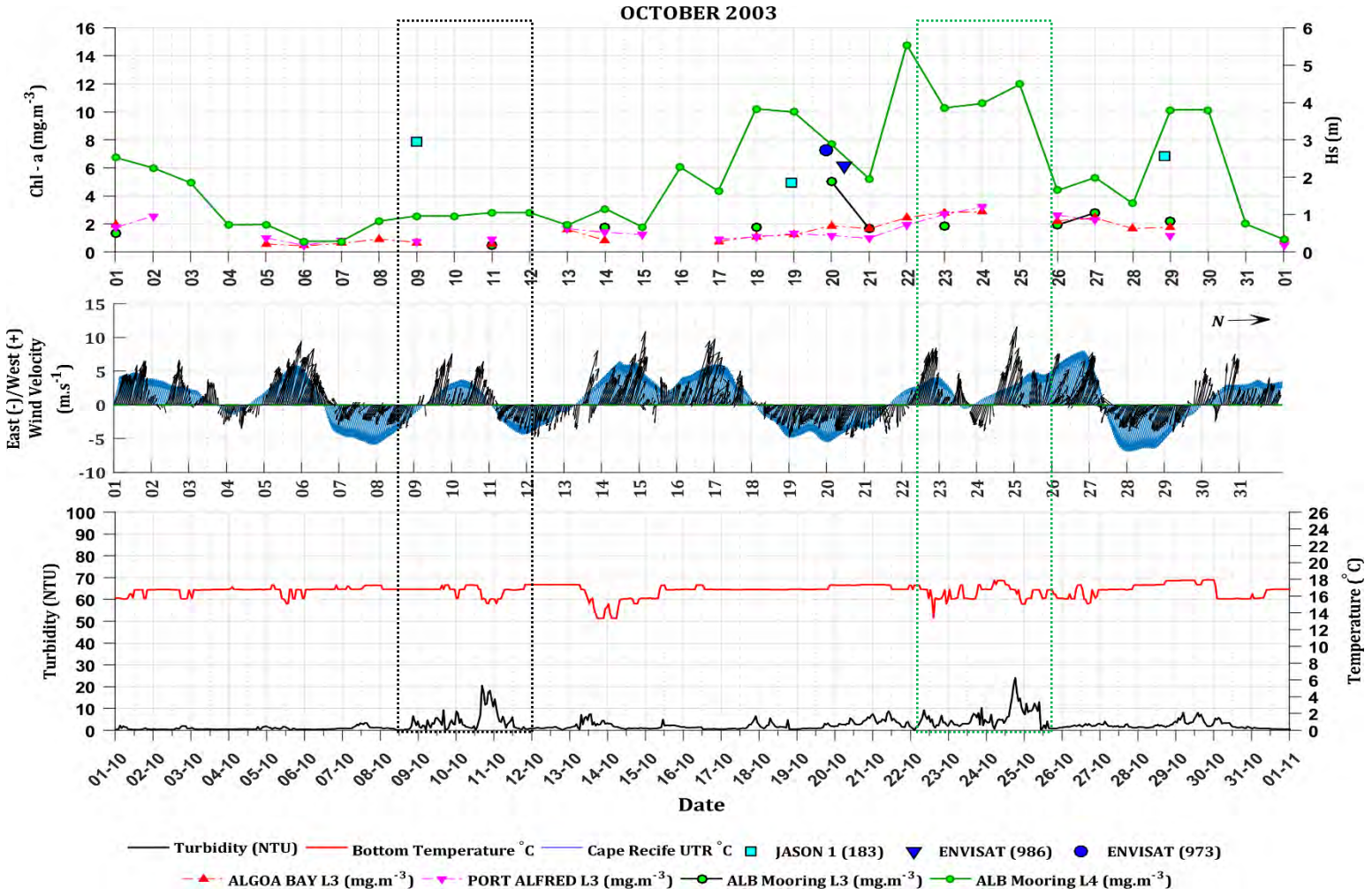

Appendix A: A three-tiered figure of monthly variability in environmental parameters acting on the OBS turbidity sensor in Algoa Bay, a sub-embayment of the Eastern Agulhas Bank. The top panel displays altimeter-derived Hs (m) for the mooring location, and Chlorophyll-A concentrations from L3 and L4 ocean colour products for the mooring location, Algoa Bay and the Port Alfred upwelling cell, respectively. The middle pain denotes a monthly wind vector plot with both raw hourly (black) and low-pass filtered (blue) wind dynamics from the Port Elizabeth International Airport Weather Station. The bottom panel highlights the interplay between benthic turbidity (NTU, black-line), bottom temperature (°C, red-line) and the Mangold's Pool Underwater Temperature Recorder (UTR, blue-line) at Cape Recife. Black-boxes represent wind-reversal induced turbidity events, while red-boxes highlight resuspension events from waves or strong winds. Green-boxes indicate organic matter enrichment of the nepheloid layer.

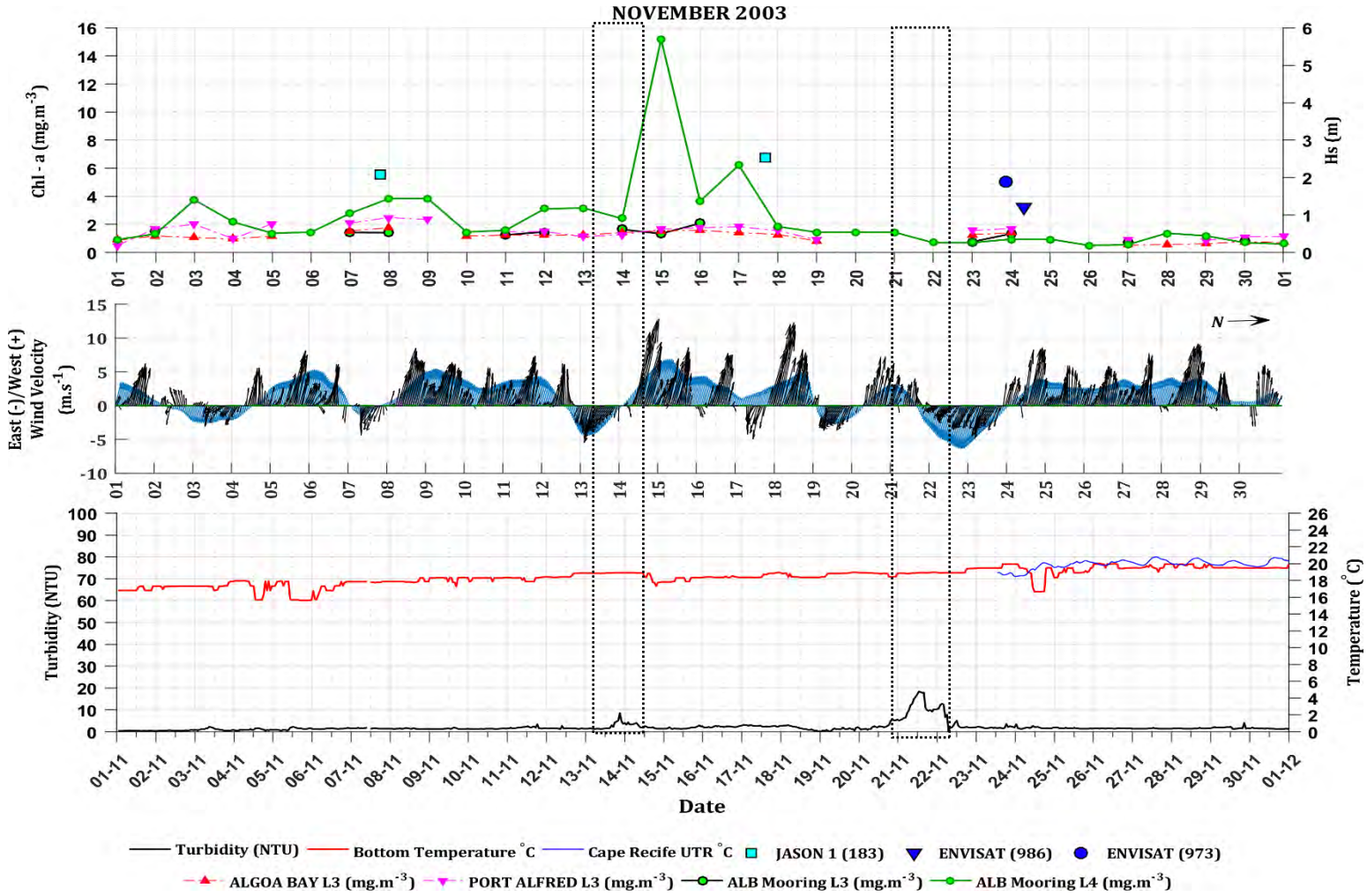

Appendix A: A three-tiered figure of monthly variability in environmental parameters acting on the OBS turbidity sensor in Algoa Bay, a sub-embayment of the Eastern Agulhas Bank. The top panel displays altimeter-derived Hs (m) for the mooring location, and Chlorophyll-A concentrations from L3 and L4 ocean colour products for the mooring location, Algoa Bay and the Port Alfred upwelling cell, respectively. The middle pain denotes a monthly wind vector plot with both raw hourly (black) and low-pass filtered (blue) wind dynamics from the Port Elizabeth International Airport Weather Station. The bottom panel highlights the interplay between benthic turbidity (NTU, black-line), bottom temperature (°C, red-line) and the Mangold's Pool Underwater Temperature Recorder (UTR, blue-line) at Cape Recife. Black-boxes represent wind-reversal induced turbidity events, while red-boxes highlight resuspension events from waves or strong winds. Green-boxes indicate organic matter enrichment of the nepheloid layer.

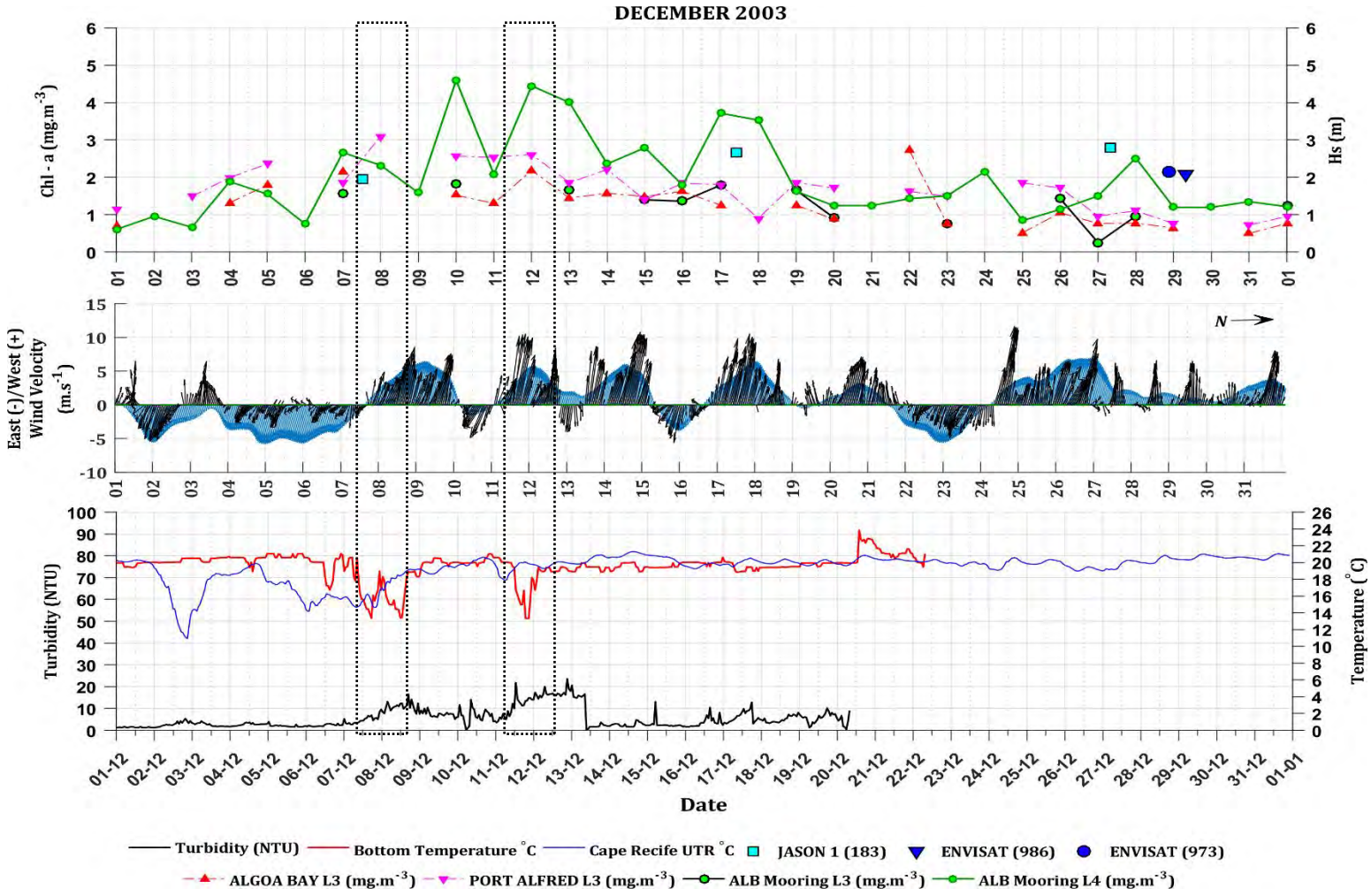

Appendix A: A three-tiered figure of monthly variability in environmental parameters acting on the OBS turbidity sensor in Algoa Bay, a sub-embayment of the Eastern Agulhas Bank. The top panel displays altimeter-derived Hs (m) for the mooring location, and Chlorophyll-A concentrations from L3 and L4 ocean colour products for the mooring location, Algoa Bay and the Port Alfred upwelling cell, respectively. The middle pain denotes a monthly wind vector plot with both raw hourly (black) and low-pass filtered (blue) wind dynamics from the Port Elizabeth International Airport Weather Station. The bottom panel highlights the interplay between benthic turbidity (NTU, black-line), bottom temperature (°C, red-line) and the Mangold's Pool Underwater Temperature Recorder (UTR, blue-line) at Cape Recife. Black-boxes represent wind-reversal induced turbidity events, while red-boxes highlight resuspension events from waves or strong winds. Green-boxes indicate organic matter enrichment of the nepheloid layer.

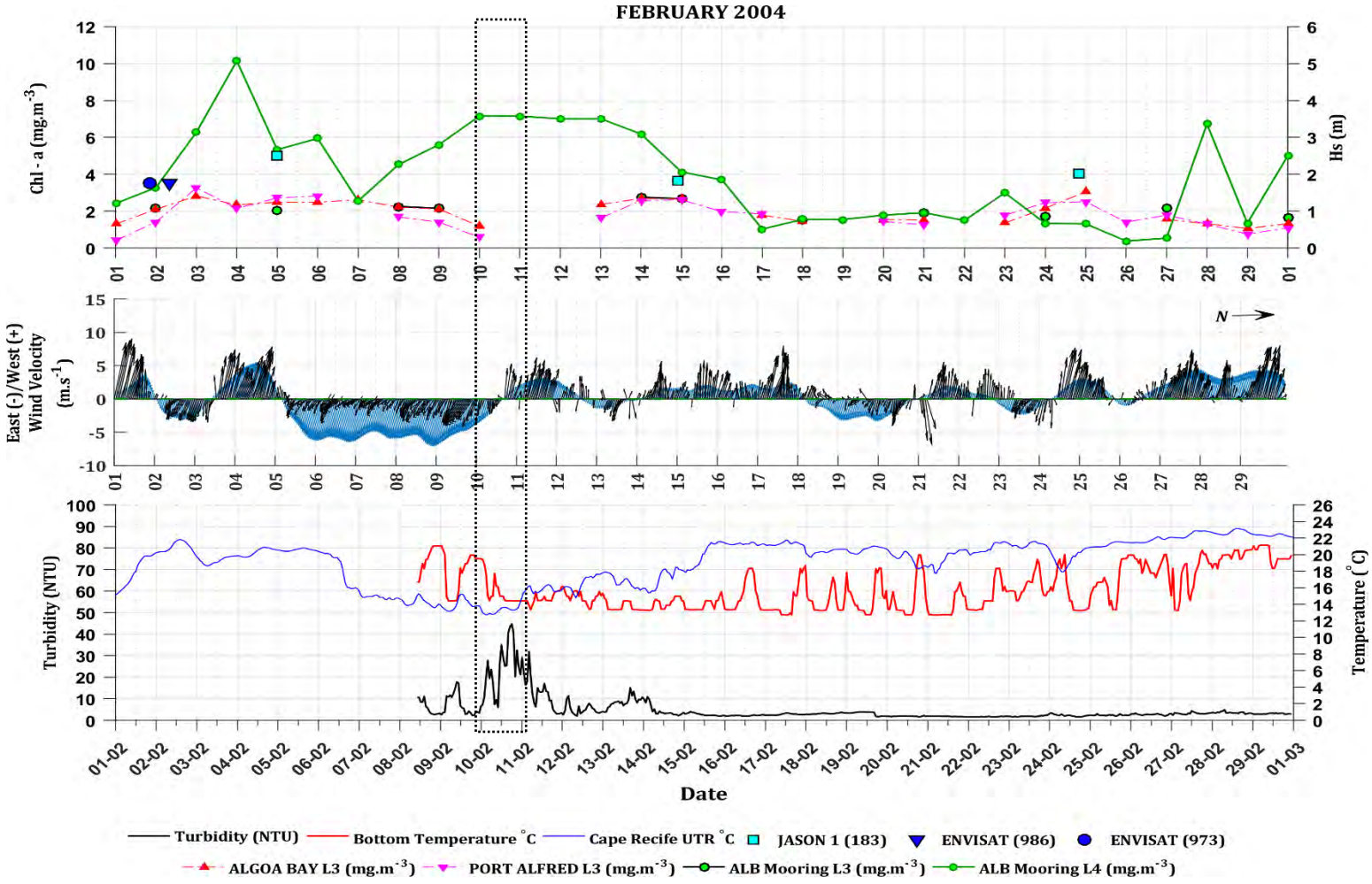

Appendix A: A three-tiered figure of monthly variability in environmental parameters acting on the OBS turbidity sensor in Algoa Bay, a sub-embayment of the Eastern Agulhas Bank. The top panel displays altimeter-derived Hs (m) for the mooring location, and Chlorophyll-A concentrations from L3 and L4 ocean colour products for the mooring location, Algoa Bay and the Port Alfred upwelling cell, respectively. The middle pain denotes a monthly wind vector plot with both raw hourly (black) and low-pass filtered (blue) wind dynamics from the Port Elizabeth International Airport Weather Station. The bottom panel highlights the interplay between benthic turbidity (NTU, black-line), bottom temperature (°C, red-line) and the Mangold's Pool Underwater Temperature Recorder (UTR, blue-line) at Cape Recife. Black-boxes represent wind-reversal induced turbidity events, while red-boxes highlight resuspension events from waves or strong winds. Green-boxes indicate organic matter enrichment of the nepheloid layer.

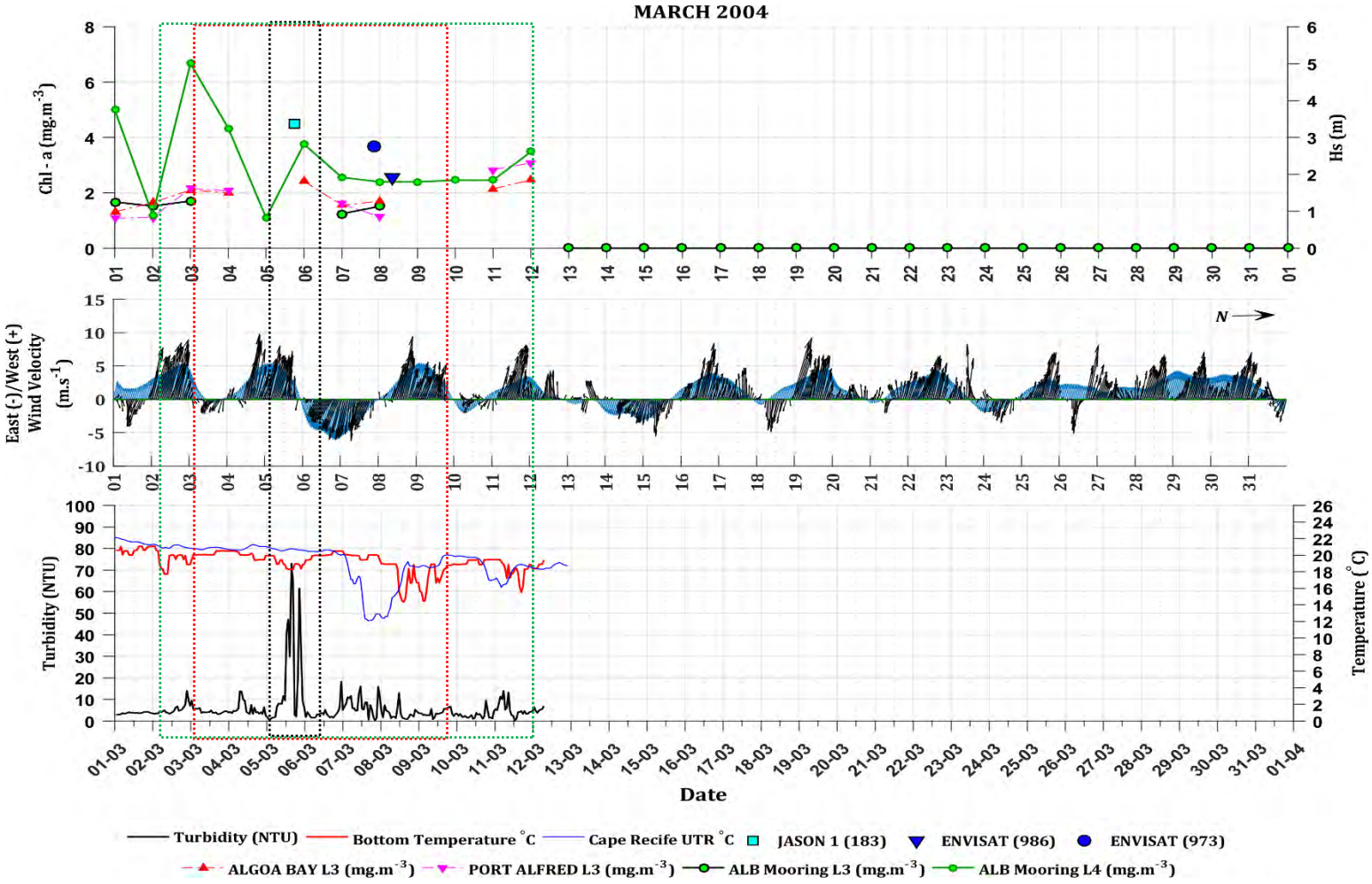

Appendix B: Monthly plots of benthic turbidity (NTU) and temperature (°C) from November 2002 – March 2004 in Algoa Bay, Eastern Agulhas Bank, South Africa.

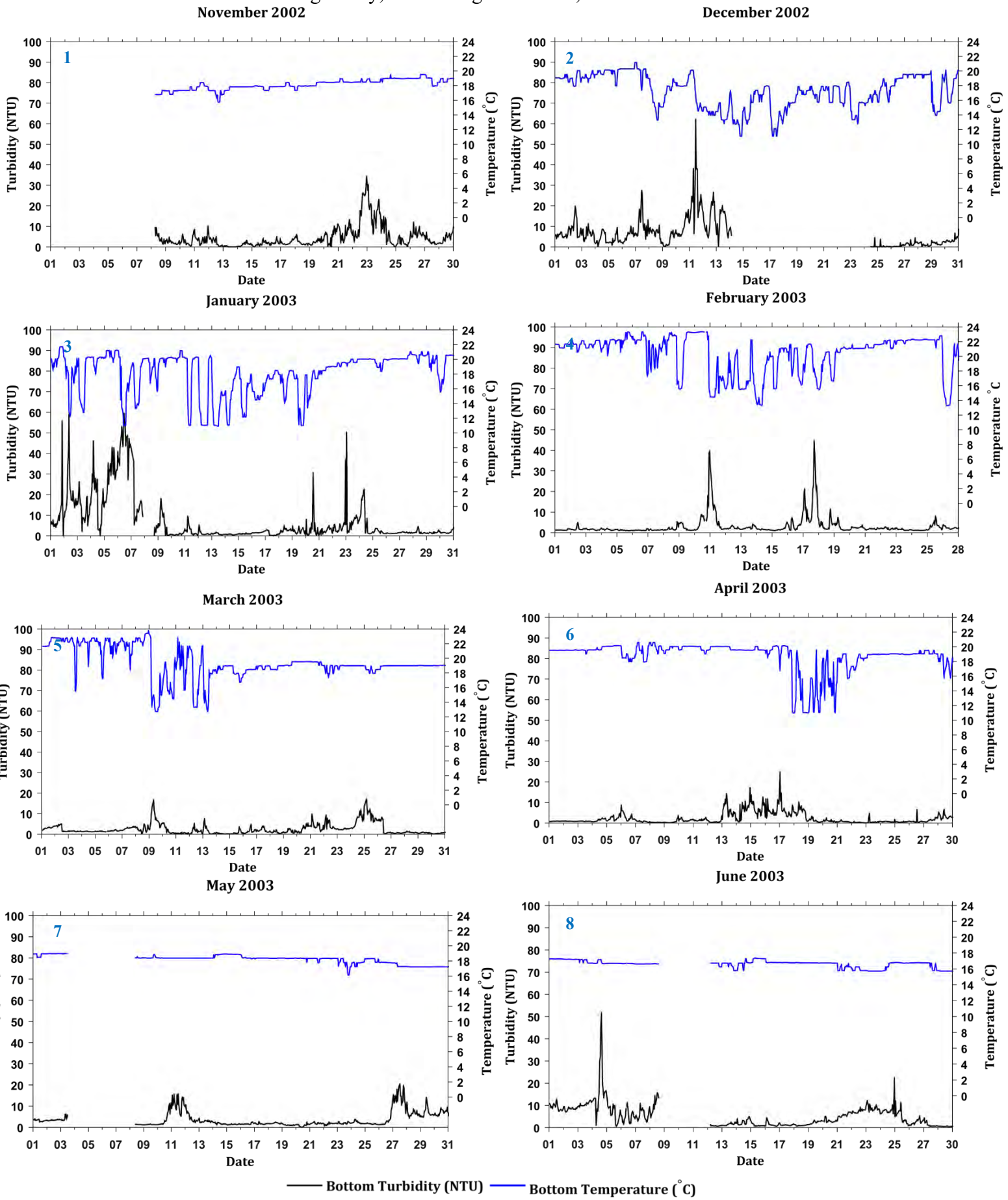

Appendix B: Monthly plots of benthic turbidity (NTU) and temperature (°C) from November 2002 – March 2004 in Algoa Bay, Eastern Agulhas Bank, South Africa.

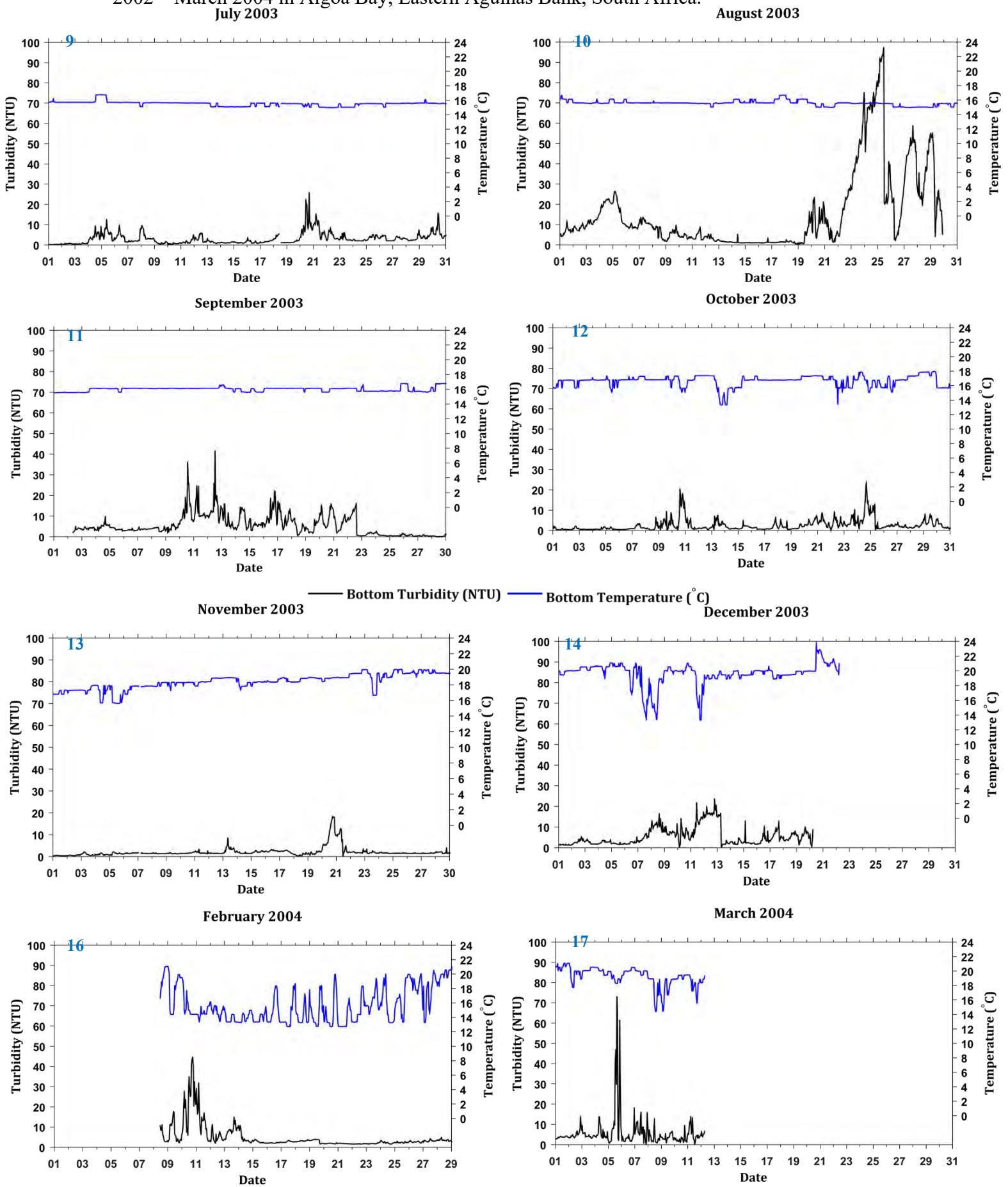

Appendix D: Monthly wind roses highlighting wind speed and direction from Port Elizabeth Weather Station (0035209B1, 63m a.s.l) Colour bands indicate wind speed ranges in $m.s^{-1}$. Values around the concentric circles show the percentage of time wind is blowing towards a particular direction, with the longest spikes highlighting the wind direction with the greatest frequency. Wind direction is measured relative to true north.

1

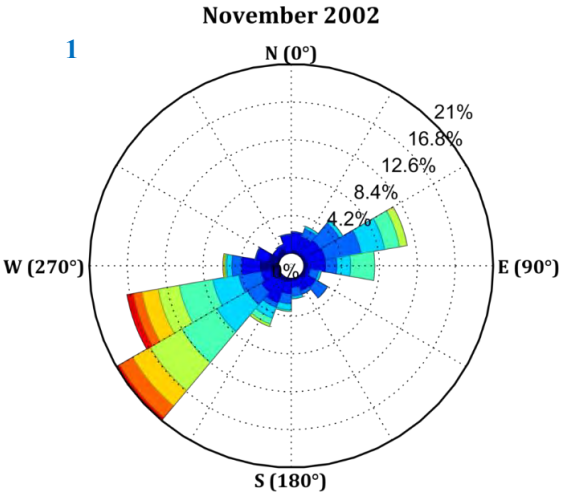

2

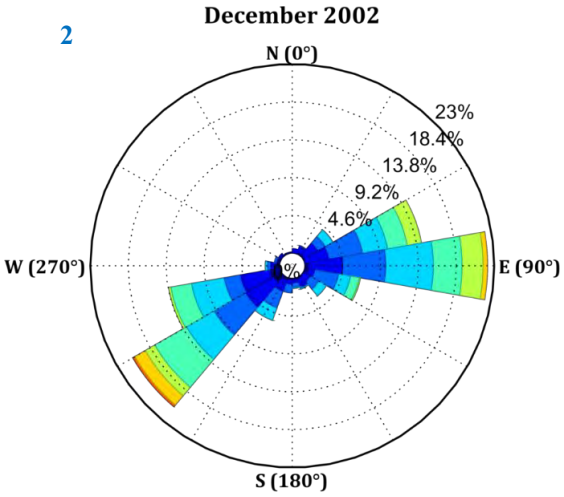

3

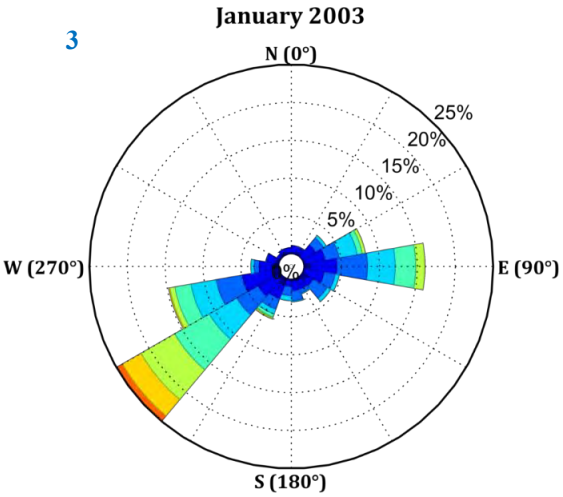

4

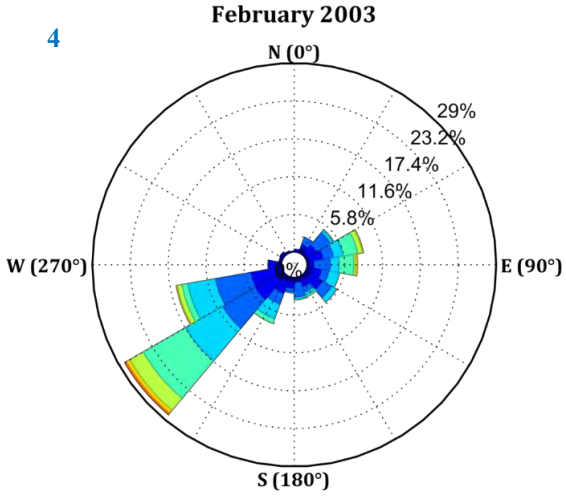

5

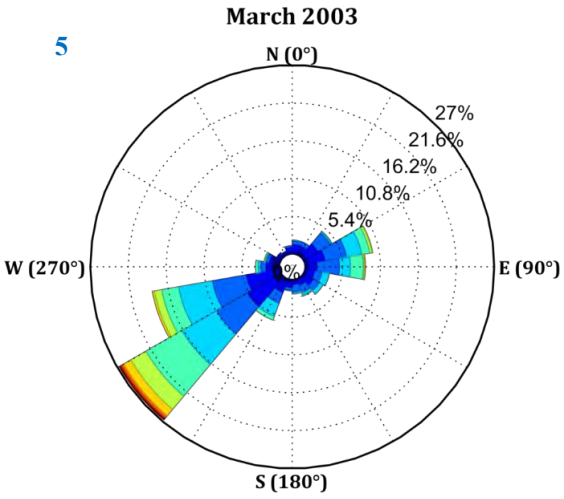

6

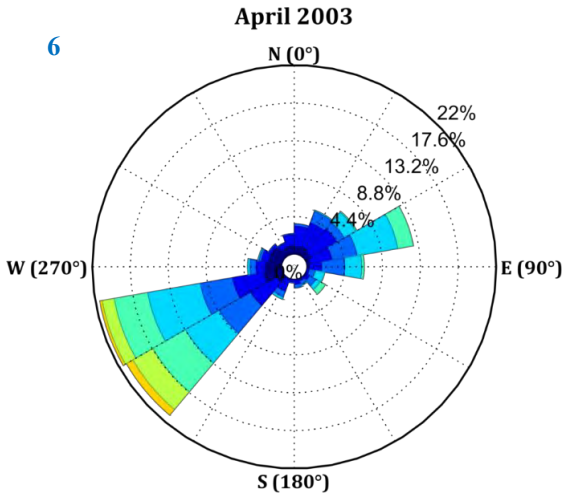

Appendix D: Monthly wind roses highlighting wind speed and direction from Port Elizabeth Weather Station (0035209B1, 63m a.s.l) Colour bands indicate wind speed ranges in $m.s^{-1}$. Values around the concentric circles show the percentage of time wind is blowing towards a particular direction, with the longest spikes highlighting the wind direction with the greatest frequency. Wind direction is measured relative to true north.

7

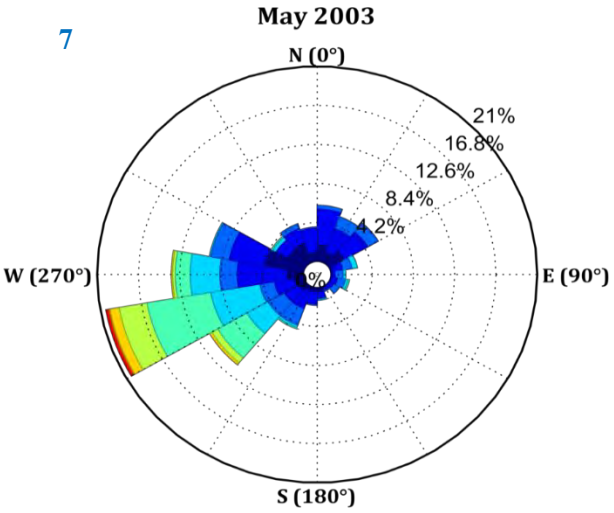

8

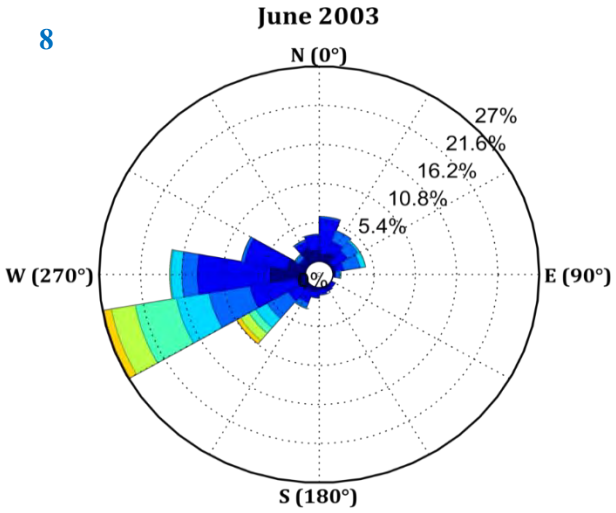

9

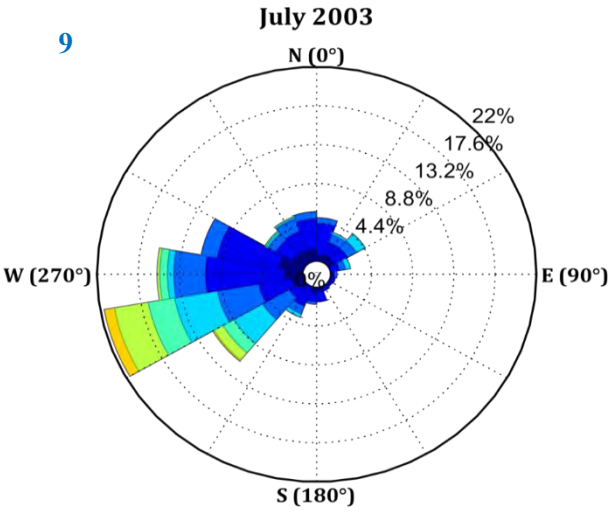

10

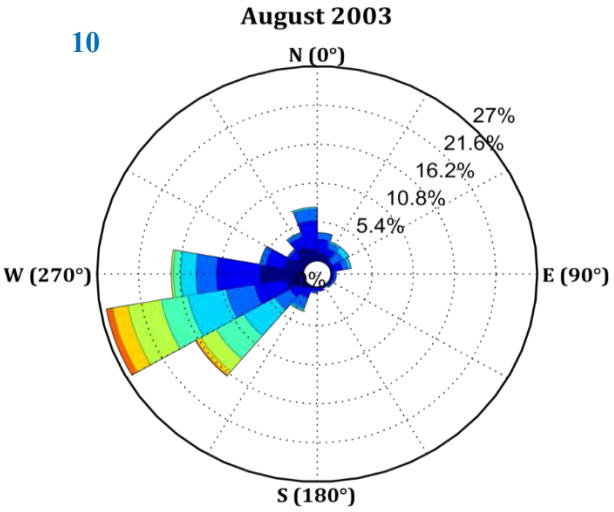

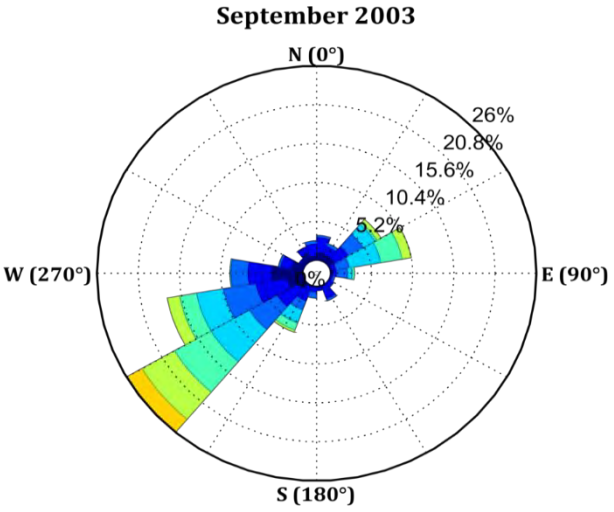

12

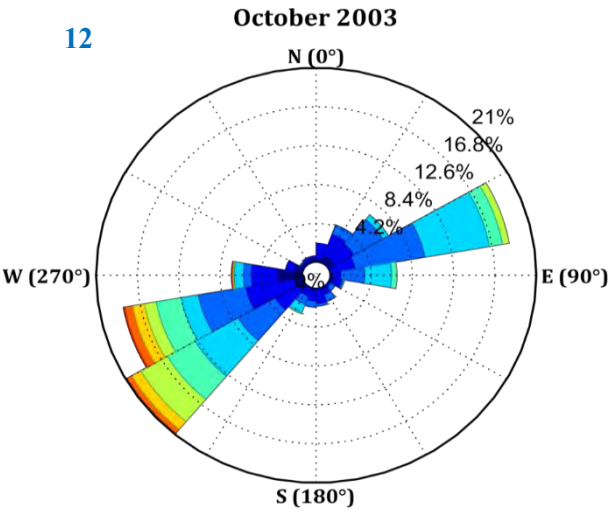

Appendix D: Monthly wind roses highlighting wind speed and direction from Port Elizabeth Weather Station (0035209B1, 63m a.s.l) Colour bands indicate wind speed ranges in $m.s^{-1}$. Values around the concentric circles show the percentage of time wind is blowing towards a particular direction, with the longest spikes highlighting the wind direction with the greatest frequency. Wind direction is measured relative to true north.

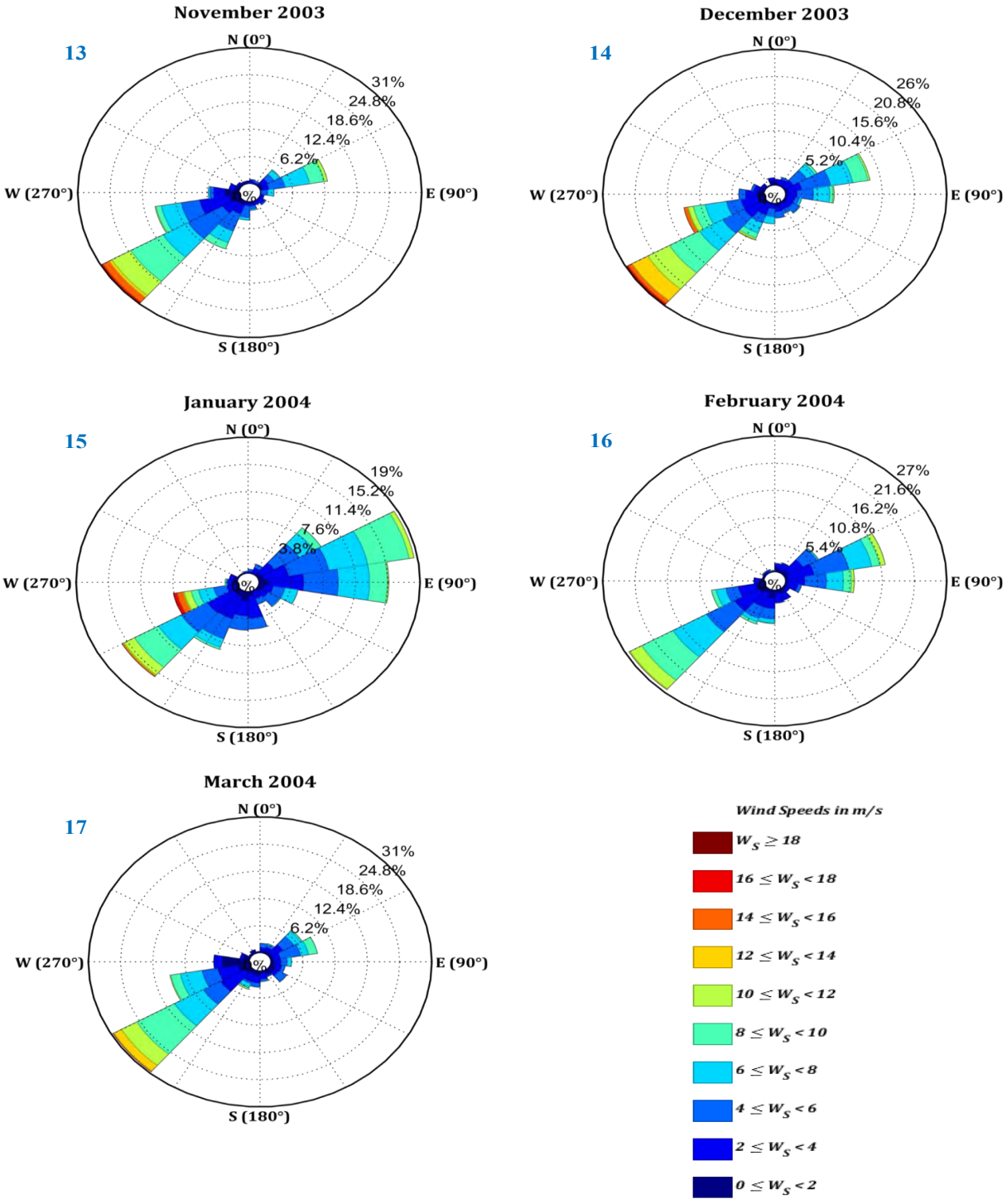

Appendix E: Feather plots depicting wind velocity ($m.s^{-1}$) from Port Elizabeth Airport Weather Station (0035209B1). Hourly wind data was converted to Zonal (-*U*) and Meridional (-V) velocity components and low-pass filtered to remove variance within 36 hours. Positive (+) y-axis values are representative of a westerly wind (Eastward flow; downwelling favourable), while negative (-) y-axis values indicate an easterly wind (Westward flow; upwelling favourable).

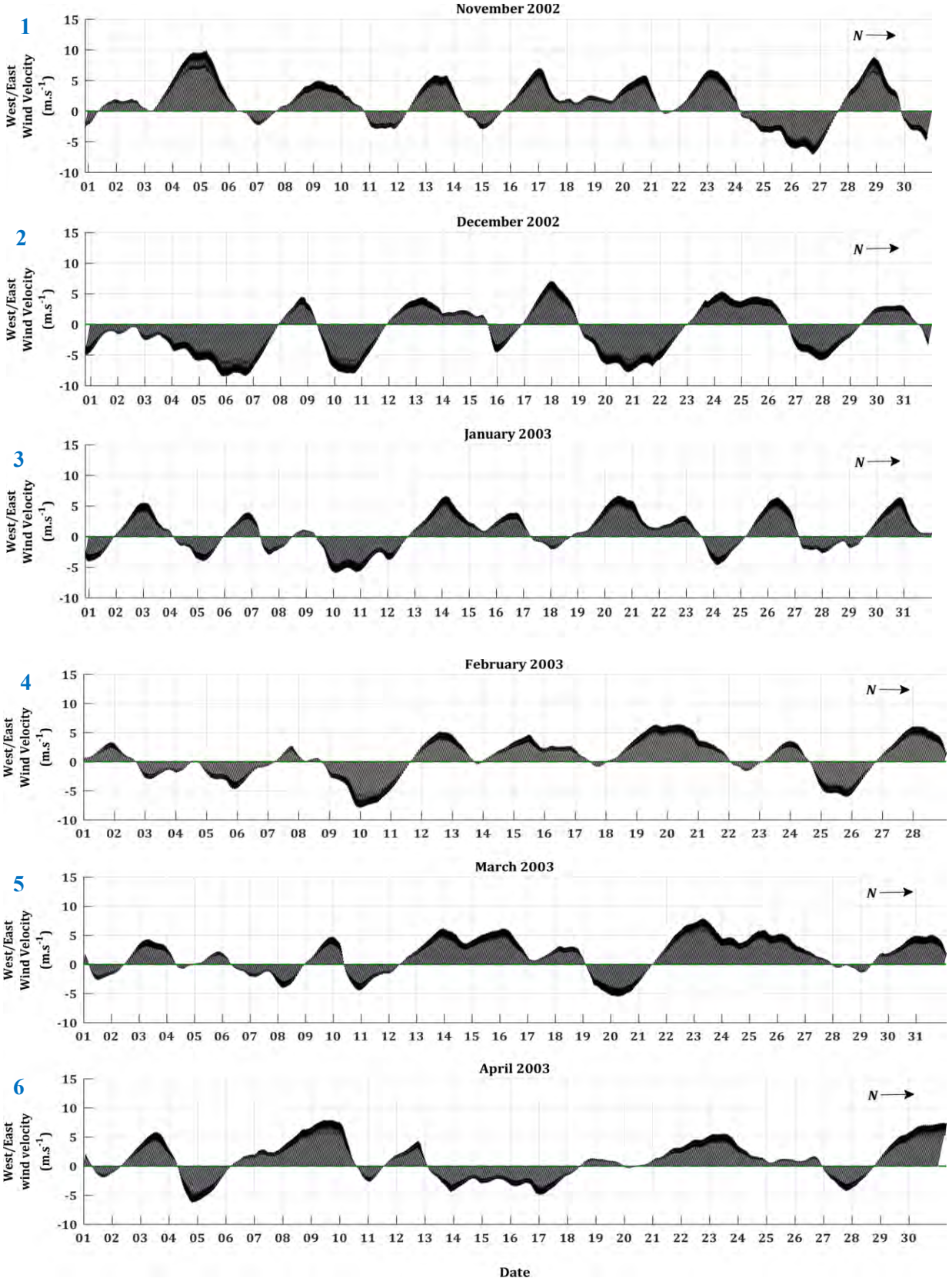

Appendix E: Feather plots depicting wind velocity (m.s^{-1}) from Port Elizabeth Airport Weather Station (0035209B1). Hourly wind data was converted to Zonal (-*U*) and Meridional (-V) velocity components and low-pass filtered to remove variance within 36 hours. Positive (+) y-axis values are representative of a westerly wind (Eastward flow; downwelling favourable), while negative (-) y-axis values indicate an easterly wind (Westward flow; upwelling favourable).

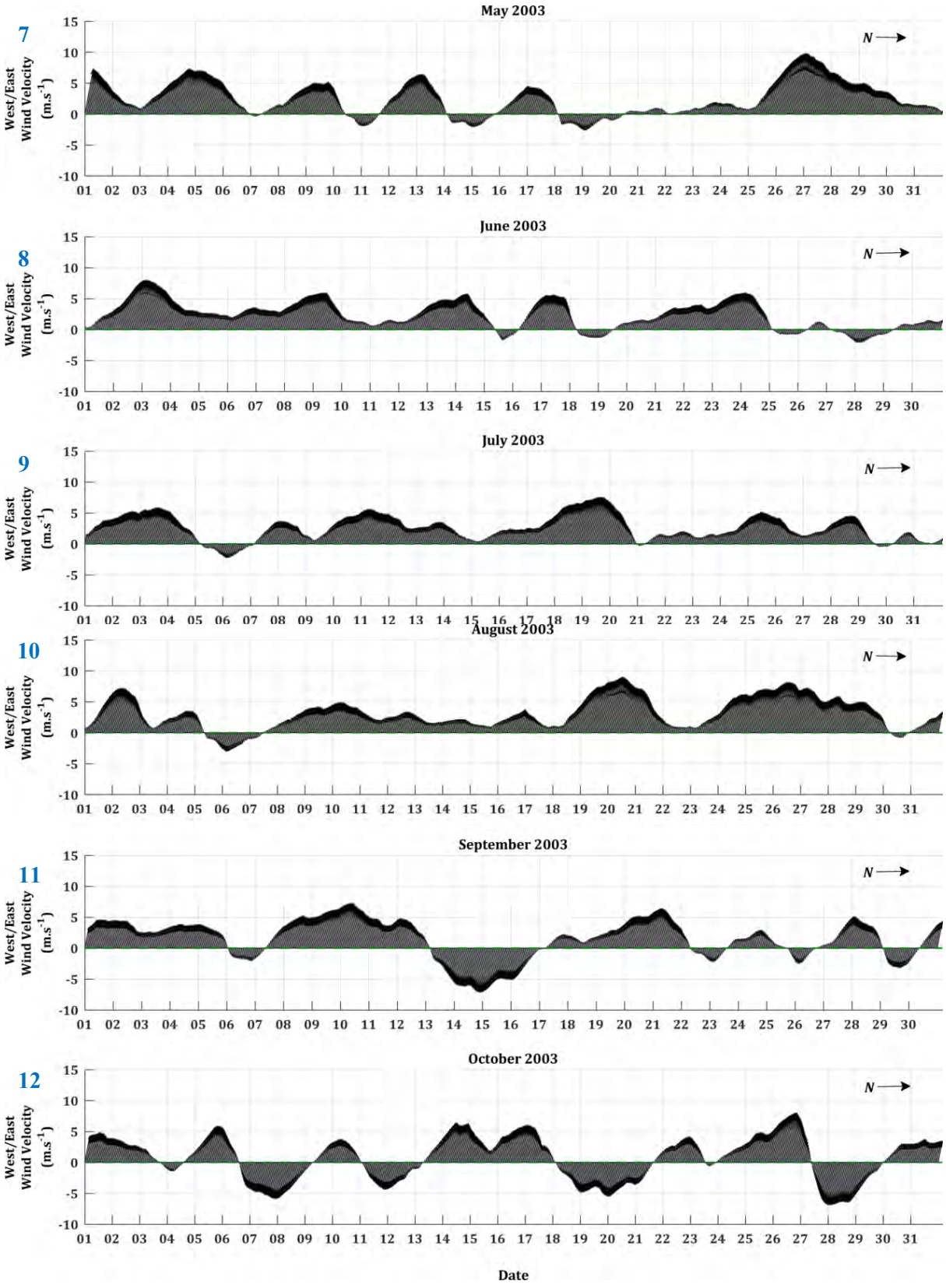

Appendix E: Feather plots depicting wind velocity (m.s^{-1}) from Port Elizabeth Airport Weather Station (0035209B1). Hourly wind data was converted to Zonal (-*U*) and Meridional (-V) velocity components and low-pass filtered to remove variance within 36 hours. Positive (+) y-axis values are representative of a westerly wind (Eastward flow; downwelling favourable), while negative (-) y-axis values indicate an easterly wind (Westward flow; upwelling favourable).